DEVELOPMENT OF RADICAL PROCESSES TRIGGERED BY THE PHOTOCHEMICAL ACTIVITY OF TRANSIENT ORGANIC INTERMEDIATES

Giacomo Filippini

ADVERTIMENT. L'accés als continguts d'aquesta tesi doctoral i la seva utilització ha de respectar els drets de la persona autora. Pot ser utilitzada per a consulta o estudi personal, així com en activitats o materials d'investigació i docència en els termes establerts a l'art. 32 del Text Refós de la Llei de Propietat Intel·lectual (RDL 1/1996). Per altres utilitzacions es requereix l'autorització prèvia i expressa de la persona autora. En qualsevol cas, en la utilització dels seus continguts caldrà indicar de forma clara el nom i cognoms de la persona autora i el títol de la tesi doctoral. No s'autoritza la seva reproducció o altres formes d'explotació efectuades amb finalitats de lucre ni la seva comunicació pública des d'un lloc aliè al servei TDX. Tampoc s'autoritza la presentació del seu contingut en una finestra o marc aliè a TDX (framing). Aquesta reserva de drets afecta tant als continguts de la tesi com als seus resums i índexs.

ADVERTENCIA. El acceso a los contenidos de esta tesis doctoral y su utilización debe respetar los derechos de la persona autora. Puede ser utilizada para consulta o estudio personal, así como en actividades o materiales de investigación y docencia en los términos establecidos en el art. 32 del Texto Refundido de la Ley de Propiedad Intelectual (RDL 1/1996). Para otros usos se requiere la autorización previa y expresa de la persona autora. En cualquier caso, en la utilización de sus contenidos se deberá indicar de forma clara el nombre y apellidos de la persona autora y el título de la tesis doctoral. No se autoriza su reproducción u otras formas de explotación efectuadas con fines lucrativos ni su comunicación pública desde un sitio ajeno al servicio TDR. Tampoco se autoriza la presentación de su contenido en una ventana o marco ajeno a TDR (framing). Esta reserva de derechos afecta tanto al contenido de la tesis como a sus resúmenes e índices.

WARNING. Access to the contents of this doctoral thesis and its use must respect the rights of the author. It can be used for reference or private study, as well as research and learning activities or materials in the terms established by the 32nd article of the Spanish Consolidated Copyright Act (RDL 1/1996). Express and previous authorization of the author is required for any other uses. In any case, when using its content, full name of the author and title of the thesis must be clearly indicated. Reproduction or other forms of for profit use or public communication from outside TDX service is not allowed. Presentation of its content in a window or frame external to TDX (framing) is not authorized either. These rights affect both the content of the thesis and its abstracts and indexes.

UNIVERSITAT ROVIRA I VIRGILI
DEVELOPMENT OF RADICAL PROCESSES TRIGGERED BY THE PHOTOCHEMICAL ACTIVITY OF TRANSIENT ORGANIC INTERMEDIATES
Giacomo Filippini

UNIVERSITAT ROVIRA I VIRGILI
DEVELOPMENT OF RADICAL PROCESSES TRIGGERED BY THE PHOTOCHEMICAL ACTIVITY OF TRANSIENT ORGANIC INTERMEDIATES
Giacomo Filippini

Giacomo Filippini

Development of Radical Processes Triggered by the Photochemical Activity of Transient Organic Intermediates

Doctoral Thesis

Supervised by Prof. Paolo Melchiorre

ICIQ-Institut Català d'Investigació Química

UNIVERSITAT ROVIRA i VIRGILI

Tarragona

2017

UNIVERSITAT ROVIRA I VIRGILI
DEVELOPMENT OF RADICAL PROCESSES TRIGGERED BY THE PHOTOCHEMICAL ACTIVITY OF TRANSIENT ORGANIC INTERMEDIATES
Giacomo Filippini

Prof. Paolo Melchiorre, ICREA Research Professor & ICIQ Group Leader

I STATE that the present study, entitled “Development of Radical Processes Triggered by the Photochemical Activity of Transient Organic Intermediates.” presented by GIACOMO FILIPPINI for the award of the degree of Doctor, has been carried out under my supervision at the Institut Català d'Investigació Química (ICIQ).

Tarragona, August the 10th 2017

Doctoral Thesis Supervisor

Prof. Paolo Melchiorre

UNIVERSITAT ROVIRA I VIRGILI
DEVELOPMENT OF RADICAL PROCESSES TRIGGERED BY THE PHOTOCHEMICAL ACTIVITY OF TRANSIENT ORGANIC INTERMEDIATES
Giacomo Filippini

Acknowledgements

First, I would like to thank *Prof. Paolo Melchiorre* for giving me the opportunity to join his research group. He successfully made me understand the importance of being fully committed to my research and doing everything possible to achieve the best from every single piece of work, from an optimization study to my final thesis. I am grateful to him and I wish the best for his academic career.

Additionally, I would like to thank all the former and current members of the Melchiorre group. In particular, I would like to mention: *Yannick Rey*, *Charlie Verrier*, *Bertrand Schweitzer-Chaput, Luca Buzzetti, Luca Dell'Amico, Giandomenico Magagnano, Daniele Mazzarella, Sara Cuadros, Zhong-Yan Cao, Mauro Moliterno, Giulio Goti, Giacomo Crisenza* and *Eva Raluy*. I want to thank *Dr Lorna Piazzi* and *Maria Checa,* for the administrative support. There are several people that have directly contributed to the revision of this manuscript and I want to thank them for their help: *Bertrand Schweitzer-Chaput*, *Yannick Rey*, *Hamish Hepburn, Giacomo Crisenza* and *Catherine Holden*. I want to thank my old friend *David Savelli,* who made the cover picture of the thesis.

I would like to give the most special acknowledgement to my parents, *Marzio* and *Mafalda,* and to my older brother *Alessandro* for the guidance and support that they constantly provide me.

I must thank my previous scientific mentors, *Luca Bernardi* and *Giorgio Bencivenni* for all they taught me.

I also want to thank my sources of inspiration: *Francesco Guccini*, *Gino Strada*, *Carlo Petrini*, *Roberto Baggio* and "*Via del Pratello"*.

I would like to thank all the research support units at ICIQ, in particular I am thankful to the NMR-staff. I would also like to acknowledge the financial support from the Institute of Chemical Research of Catalonia (ICIQ), MINECO for support through the Severo Ochoa Excellence Accreditation 2014-2018 (SEV-2013-0319) and from the European Research Council for the ERC starting grant (278541-ORGA-NAUT) and ERC consolidator grant (681840-CATA-LUX).

Additionally, I am personally grateful to:

- Ministerio de Economía, Industria y Competitividad of Spain for a Severo Ochoa predoctoral fellowship (SVP-2014-068818)

List of Publications

Some of the results presented in this thesis have been published:

- Filippini, G.; Nappi, M.; Melchiorre P. "Photochemical direct perfluoroalkylation of phenols" *Tetrahedron* **2015**, *71*, 4535.
- Filippini, G.; Silvi, M.; Melchiorre, P. "Enantioselective formal α-methylation and α-benzylation of aldehydes by means of photo-organocatalysis" *Angew. Chem. Int. Ed.* **2017**, *56*, 4447.

UNIVERSITAT ROVIRA I VIRGILI
DEVELOPMENT OF RADICAL PROCESSES TRIGGERED BY THE PHOTOCHEMICAL ACTIVITY OF TRANSIENT ORGANIC INTERMEDIATES
Giacomo Filippini

In memoriam of my beloved grandmother

Erzira Girolomoni

"Trova ciò che sei in ciò che ami,
ubriacati e ucciditi di sogni.
Prepara il tuo bagaglio, preparati a non tornare.
Un vento soffia forte senza risposte,
troppe domande lasciate da parte a riposare.
Perdere tutto, per tutto poi trovare,
dimenticare tutto, senza farsi dimenticare.
Lingue, culture, facce, valori:
la novità si apre in tutti i suoi colori.
Altre storie si mescolano alle mie,
altre persone percorrono le mie vie,
a piedi scalzi mi presento al mondo,
a piedi nudi progetto il mio ritorno,
perché il ritorno dà senso al viaggio,
perché il ritorno è un atto di coraggio"

UNIVERSITAT ROVIRA I VIRGILI
DEVELOPMENT OF RADICAL PROCESSES TRIGGERED BY THE PHOTOCHEMICAL ACTIVITY OF TRANSIENT ORGANIC INTERMEDIATES
Giacomo Filippini

Table of Contents

UNIVERSITAT ROVIRA I VIRGILI
DEVELOPMENT OF RADICAL PROCESSES TRIGGERED BY THE PHOTOCHEMICAL ACTIVITY OF TRANSIENT ORGANIC INTERMEDIATES
Giacomo Filippini

UNIVERSITAT ROVIRA I VIRGILI
DEVELOPMENT OF RADICAL PROCESSES TRIGGERED BY THE PHOTOCHEMICAL ACTIVITY OF TRANSIENT ORGANIC INTERMEDIATES
Giacomo Filippini

Chapter I

General Overview

1.1 Photochemistry Meets Organocatalysis

"*In ordinary chemistry the reactions take place in some definite way, but the photochemical reactions often furnish surprises*"

Giacomo Ciamician

Photochemistry is the branch of chemistry that deals with chemical changes promoted by the absorption of light.[1] In these chemical transformations, the energy required to convert the starting materials into the final products is provided by photons. From this perspective, sunlight is an extraordinary natural source of energy. Indeed, it is inexpensive, non-toxic, abundant, distributed all over the world, and renewable. The necessity of considering alternative energy sources that would allow our generation to move away from the finite fossil fuels is one of the most important issues of the 21st century.[2] One of the earliest scientists that called attention to the energetic problem was Giacomo Ciamician. He pointed out the need for energy transition from fossils to renewables in his seminal paper "The Photochemistry of the Future" published in 1912 (Figure 1.1).[3] One century later, this call is more urgent than ever.

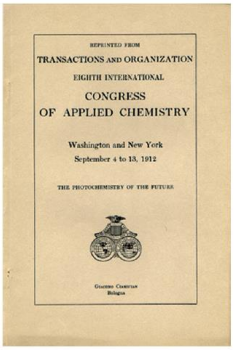
REPRINTED FROM
TRANSACTIONS AND ORGANIZATION
EIGHTH INTERNATIONAL
CONGRESS
OF APPLIED CHEMISTRY
Washington and New York
September 4 to 13, 1912
THE PHOTOCHEMISTRY OF THE FUTURE

Figure 1.1 The famous paper "*The Photochemistry of the future*" by Giacomo Ciamician.

[1] McNaught, A. D. "Compendium of chemical terminology" *The Gold Book. 2nd Ed.* **1997**, Oxford: Blackwell Science.
[2] Armaroli, N.; Balzani, V. "The future of energy supply: challenges and opportunities" *Angew. Chem. Int. Ed.* **2007**, *46*, 52.
[3] Ciamician, G. "The photochemistry of the future" *Science* **1912**, *36*, 385.

Nowadays, photochemistry is an established and broadly used branch of chemistry. Upon light absorption, a chemical species reaches an electronically excited-state, which differs from the corresponding ground-state not only in terms of energy content, but also in the chemical and physical properties.[4] The study of this phenomenon has led to the discovery of a large number of novel reactions and preparative methodologies. A fundamental impediment that has limited the growth of photochemistry and its application on industrial scales, has been the inability of most organic molecules to absorb visible wavelengths of light.[5] For this reason, the typical conditions required for achieving photo-induced reactivity were harsh, involving the use of high-energy UV radiation. In the past decade, the independent efforts of MacMillan,[6] Yoon,[7] and Stephenson,[8] along with other contributors, to solve this problem aroused a renewed interest in photochemical processes driven by visible light within the scientific community. Indeed, these scientific works have paved the way to a new field of research, namely visible-light photoredox catalysis.[9] In general sense, this approach relies on the ability of light-absorbing metal complexes and organic dyes (photocatalysts) to generate, upon direct visible-light excitation, reactive radicals from suitable precursors at ambient temperature. In this method, the radical formation generally proceeds *via* either single-electron transfer (SET) or energy transfer mechanism. The possibility of generating radicals under very mild conditions allowed chemists to achieve unique bond constructions that were not possible using established thermal protocols.[10] This is because traditional radical generation methods typically require forcing reaction conditions, which do not allow the combination of radical chemistry with other efficient tools of organic synthesis. Specifically, enantioselective organocatalysis requires mild conditions for optimal efficiency and stereocontrol.[11] Merging visible-light-triggered photochemistry with organocatalysis provides a unique platform for the development of new methodologies for the efficient synthesis of enantio-

[4] Balzani, V.; Ceroni, P.; Juris, A. "Photochemistry and photophysics: concepts, research, applications" **2014**, Chapter 4, p. 103, Wiley & Sons.
[5] Fagnoni, M.; Dondi, D.; Ravelli, D.; Albini, A. "Photocatalysis for the formation of the C−C bond" *Chem. Rev.* **2007**, *107*, 2725.
[6] Nicewicz, D. A.; MacMillan, D. W. C. "Merging photoredox catalysis with organocatalysis: the direct asymmetric alkylation of aldehydes" *Science* **2008**, *322*, 77.
[7] Ischay, M. A.; Anzovino, M. E.; Du, J.; Yoon, T. P. "Efficient visible light photocatalysis of [2+2] enone cycloadditions" *J. Am. Chem. Soc.* **2008**, *130*, 12886.
[8] Narayanam, J. M.; Tucker, J. W.; Stephenson, C. R. "Electron-transfer photoredox catalysis: development of a tin-free reductive dehalogenation reaction" *J. Am. Chem. Soc.* **2009**, *131*, 8756.
[9] Shaw, M. H.; Twilton, J.; MacMillan, D. W. C. "Photoredox catalysis in organic chemistry" *J. Org. Chem.* **2016**, *81*, 6898.
[10] Prier, C. K.; Rankic, D. A.; MacMillan, D. W. C. "Visible light photoredox catalysis with transition metal complexes: applications in organic synthesis" *Chem. Rev.* **2013**, *113*, 5322.
[11] MacMillan, D. W. C. "The advent and development of organocatalysis" *Nature* **2008**, *455*, 304.

enriched chiral molecules by means of radical reactivity patterns.[12] As early as 2008, David MacMillan exploited the ability of $Ru(bpy)_3^{2+}$ (tris(bipyridine)ruthenium(II)) to function as visible light photocatalyst for the formation of electrophilic radicals **II** from alkyl bromides **2** under mild reaction conditions (Figure 1.2a).[6] These electrophilic radicals could be subsequently trapped by catalytically-generated chiral enamines **I** in an enantioselective fashion. This strategy enabled the development of light-driven stereoselective α-alkylations of aldehydes **1** that could not be realized through ionic pathways (classical S_N2 manifolds).

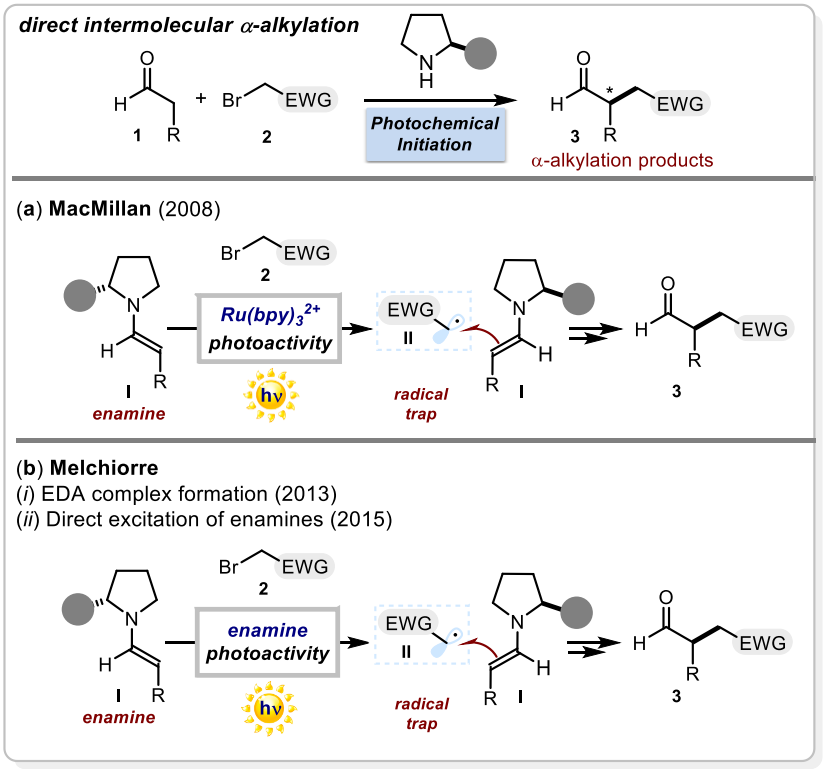

Figure 1.2 Merging photochemistry and enamine-mediated catalysis for the enantioselective α-alkylation of aldehydes: (**a**) the pioneering work by MacMillan. (**b**) Our metal-free approaches to generate radicals: *via* (*i*) EDA complex activation or (*ii*) direct photoexcitation of enamines. EWG: electron-withdrawing group; the grey circle represents the bulky group of the chiral organic catalyst.

[12] Brimioulle, R.; Lenhart, D.; Maturi, M. M.; Bach, T. "Enantioselective catalysis of photochemical reactions" *Angew. Chem. Int. Ed.* **2015**, *54*, 3872.

The reaction mechanism of this transformation will be thoroughly discussed in Chapter II. By exploiting the unique reactivity of photo-catalytically generated open-shell intermediates, this approach greatly expanded the applicability of asymmetric organocatalysis within radical reactivity domains. Inspired by this precedent, our research group has demonstrated that chiral enamines **I**, key intermediates of organocatalytic processes, directly participate in the photoexcitation of suitable substrates (Figure 1.2b). Depending on the nature of the alkyl bromides **2**, it was found that two distinct photochemical pathways are available to enamines for the generation of reactive electrophilic radicals **II**: (*i*) through the formation of photon-absorbing electron donor-acceptor (EDA) complexes, generated upon ground-state association of chiral enamines **I** (donor) with electron-poor alkyl bromides **2** (acceptor);[13] (*ii*) through the direct photoexcitation of the chiral enamines **I**, which can act as photo-reductants when reaching the excited-state.[14] In both cases, the ground-state chiral enamines **I** provide effective stereochemical induction for the ensuing enantioselective radical trap. The photochemical behavior of chiral enamines will be widely discussed in Chapters II and IV. Conceptually, these studies demonstrated that the synthetic potential of organocatalytic intermediates is not limited to the ground-state domain, but could be expanded by exploiting their photochemical activity. Indeed, by bringing an organocatalytic intermediate to an electronically excited-state, light excitation can unlock reaction manifolds that are unavailable to conventional ground-state organocatalytic pathways.

At the outset of my doctoral studies, the activity of the Melchiorre group was mainly centered on the fields of photochemistry and enantioselective organocatalysis. In particular, we learned that the direct excitation of *in situ* formed organocatalytic intermediates can be exploited to generate reactive radicals under mild conditions. The main target of my studies has been to further broaden this reactivity concept while developing new, useful asymmetric transformations that could not be achieved by using classical ground-state reactivity.

---

[13] Arceo, E.; Jurberg, I. D.; Álvarez-Fernández, A.; Melchiorre, P. "Photochemical activity of a key donor-acceptor complex can drive stereoselective catalytic α-alkylation of aldehydes" *Nat. Chem.* **2013**, *5*, 750.

[14] Silvi, M.; Arceo, E.; Jurberg, I. D.; Cassani, C.; Melchiorre, P. "Enantioselective organocatalytic alkylation of aldehydes and enals driven by the direct photoexcitation of enamines" *J. Am. Chem. Soc.* **2015**, *137*, 6120.

1.2. General Objectives and Summary

The main scientific objective of my doctoral research was to employ and combine two powerful fields of molecule activation, photochemistry and organocatalysis, to efficiently realize new carbon-carbon bond forming transformations in an environmentally friendly way. Initially, I focused on the development of a metal-free photochemical strategy for the direct aromatic perfluoroalkylation and trifluoromethylation of substituted phenols (chemistry discussed in Chapter III). In the second part of my PhD work, I was involved in the development of a photochemical enantioselective enamine-mediated α-alkylation of aldehydes with α-iodo sulfones (chemistry discussed in Chapter IV). In both transformations, *in situ* formed intermediates triggered the formation, after light absorption, of reactive electron-poor radicals under mild conditions, and without the need of external photocatalysts.

1.2.1. Photochemical Direct Perfluoroalkylation of Phenols

In Chapter III, the photochemical direct perfluoroalkylation of substituted phenols **5** is discussed (Figure 1.3).[15] The use of simple visible-light, without the need of any photocatalyst or radical initiator, facilitated the aromatic perfluoroalkylation or trifluoromethylation of phenols.

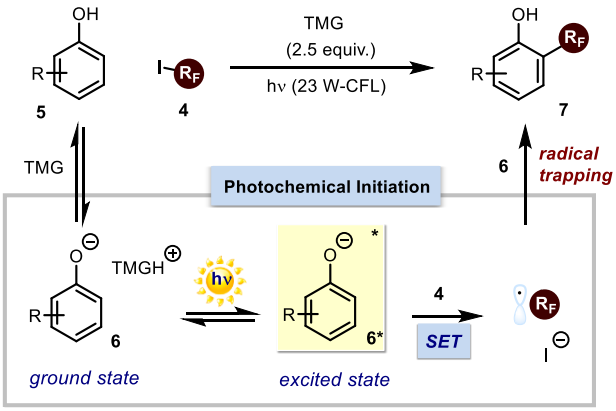

Figure 1.3 Photochemical direct perfluoroalkylation of phenols. SET: single-electron transfer; TMG: 1,1,3,3-tetramethylguanidine; CFL: compact fluorescent light bulb; R_F indicates the perfluoroalkyl fragment.

[15] Filippini, G.; Nappi, M.; Melchiorre, P. "Photochemical direct perfluoroalkylation of phenols" *Tetrahedron* **2015**, *71*, 4535.

Mechanistic studies highlighted the crucial role played by the phenolate anions **6**, transiently generated upon deprotonation of phenols **5**, in initiating the photochemical radical processes. This work was conducted in collaboration with Dr Manuel Nappi, who performed the preliminary experiments.

1.2.2. Enantioselective Formal α-Methylation and α-Benzylation of Aldehydes by Means of Photo-Organocatalysis

Chapter IV discusses the development of the enantioselective formal α-methylation and α-benzylation of aldehydes **1** (Figure 1.4).[16]

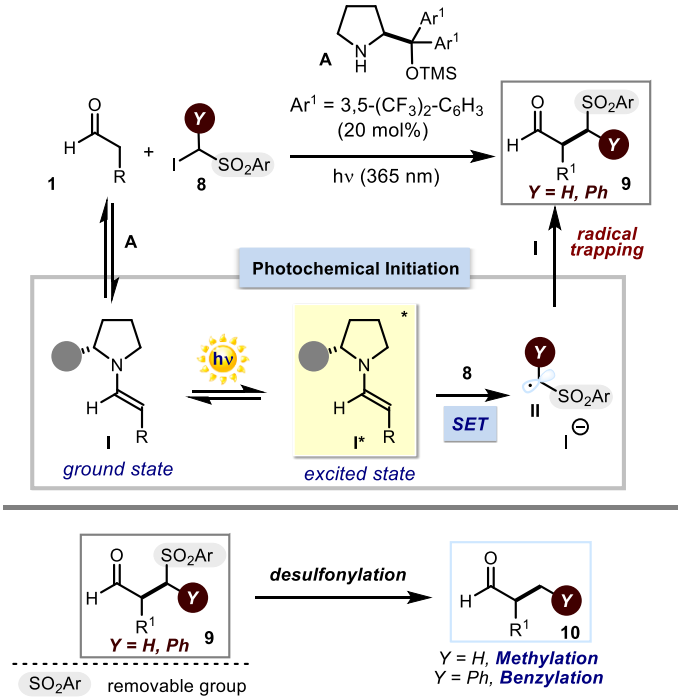

Figure 1.4 Enantioselective formal α-methylation and α-benzylation of aldehydes by means of photo-organocatalysis. SET: single-electron transfer; the grey circle represents the bulky group of the organic catalyst.

[16] Filippini, G.; Silvi, M.; Melchiorre, P. "Enantioselective formal α-methylation and α-benzylation of aldehydes by means of photo-organocatalysis" *Angew. Chem. Int. Ed.* **2017**, *56,* 4447.

The construction of carbonyl α-alkyl stereocenters is an important process in organic synthesis.[17] Despite the importance of these stereogenic units, catalytic protocols for stereoselectively introducing either a methyl or a benzyl group at the α-position of aldehydes remain rare.[18] Our reaction required light in order to proceed, but occurred in the absence of any external photoredox catalyst, which is commonly needed to generate radical intermediates, such as **II**, from electron-poor alkyl halides of type **8**. Mechanistic investigations revealed the direct role of the transiently generated chiral enamine **I** in the photochemical generation of radicals. The desired products **9** were obtained in good isolated yields and with high enantioselectivity. The phenylsulfonyl moiety in products **9** could eventually be removed by simple reductive desulfonylation to reveal methyl and benzyl groups.

This project was conducted in collaboration with Dr Mattia Silvi, who ran the first reactions and was involved in the initial discussion of the optimization studies.

Preliminary experiments on the reaction optimization, conducted during a four-month collaboration with Professor Oliver Kappe (University of Graz, Austria), will be also discussed. During the time in the Kappe group, I tried to develop the photochemical transformation in question under flow conditions. Indeed, the use of flow reactors typically allow for a better irradiation of the reaction mixture compared to that which can be obtained under batch conditions, therefore increasing the productivity of the photochemical process.[19]

[17] a) Modern Carbonyl Chemistry (Ed.; J. Otera), Wiley-WCH, Weinheim, **2000**; b) Principles of Asymmetric Synthesis, 2nd ed. (Eds. R. E. Gawley, J. Aube), Elsevier, Amsterdam, **2012**, chap. 3.

[18] Nagib, D. A. "Catalytic desymmetrization by C-H functionalization as a solution to the chiral methyl problem" *Angew. Chem. Int. Ed.* **2017**, *56*, 7354.

[19] Gutmann, B.; Cantillo, D.; Kappe, C. O. "Continuous-flow technology a tool for the safe manufacturing of active pharmaceutical ingredients" *Angew. Chem. Int. Ed.* **2015**, *54*, 6688.

Chapter II
Introduction

The chemistry developed during this doctoral thesis has largely capitalized upon the ability of electron-rich organic intermediates (*i.e.* phenolate anions and chiral enamines), transiently generated from photochemically inactive precursors (*i.e.* phenols and aldehydes, respectively), to absorb light and reach an electronically excited-state, where the arrangement of the electrons are no longer in the lowest energy combination. From this high energy state, these intermediates can readily engage in an array of single-electron transfer (SET) processes. Specifically, they can give an electron to otherwise inert alkyl iodides thus triggering the formation of reactive radical species. In both transformations, the radicals are generated through the reductive cleavage of the carbon-iodine bond within the alkyl iodide precursor. For this reason, it is important to discuss general aspects regarding intermolecular SET mechanisms, photo-induced SET, and their application in organic synthesis. This is the main aim of the present Chapter.

2.1 Single Electron Transfer

SET is the process whereby an electron moves from an atom or a molecule to another chemical entity. SET is the key concept of redox chemistry, where one reaction partner loses electrons (oxidation) while the other gains electrons (reduction). Electron-transfer reactions are characteristic features of a variety of fundamental biological processes that include energy metabolism (photo-synthesis, respiration and nitrogen fixation), hormone biosynthesis (steroids and prostaglandins), and xenobiotic detoxification.[1] Electron transfer rates (k_{et}, which indicates the electron transfer rate constant) can be estimated according to the Marcus theory.[2] A general simplified representation of this theory is shown in Figure 2.1.[3] The Marcus theory states that the rate at which an electron transfers from a donor (D) to an acceptor (A) is related to two experimental observables: the free energy driving force for the charge-transfer reaction (ΔG^0_{et}) and the reorganization energy

[1] Mauk, A. G. "Biological electron-transfer reactions" *Essays in Biochemistry* **1999**, *34*, 101.
[2] a) Marcus, R. A. "Electron Transfer Reactions in Chemistry: Theory and Experiment (Nobel Lecture)" *Angew. Chem. Int. Ed.* **1993**, *32*, 1111. b) Marcus, R. A.; Sutin, N. "Electron transfers in chemistry and biology" *Biochim. Biophys. Acta* **1985**, *811*, 265.
[3] a) Atkins, P.; de Paula, J. "Physical Chemistry-7th *ed.*" W.H. Freeman and Company, **2002**, New York. b) Stubbe, J.; Nocera, D. G.; Yee, C. S.; Chang, M. C. Y. "Radical initiation in the class I ribonucleotide reductase: long-range proton-coupled electron transfer?" *Chem. Rev.* **2003**, *103*, 2167.

(λ). The last term (λ) is the energy required for all the structural adjustments (in the reactants and in the surrounding solvent molecules) that are needed in order for A and D to assume the conformations required for the SET process. ΔG^0_{et} can be calculated using the standard reduction potentials of A and D (E^0_A and E^0_D, respectively). The term ***A*** is a pre-exponential factor dependent on both the nature of D and A, and the medium through which the electron must travel.

$$D + A \rightleftharpoons D^{\bullet+} + A^{\bullet-}$$

$$k_{et} = \boldsymbol{A} \cdot e^{(-\Delta G/RT)}$$

$$\Delta G = (\Delta G^0_{et} + \lambda)^2/4\lambda$$

$$\Delta G^0_{et} = F\,(E^0_A - E^0_D)$$

Figure 2.1 Marcus theory of electron transfer. F: Faraday constant; T: temperature.

In several chemical systems, the SET causes the cleavage of σ-bonds, therefore leading to a dissociative electron transfer (DET).[4] DETs provide an elegant way to generate reactive species, including radicals. Given a generic chemical species (R-X), which can be either oxidized or reduced, two different DET mechanistic pathways are possible (Figure 2.2): (a) the concerted mechanism, where the R-X bond cleavage and the SET event take place at the same time; (b) the stepwise mechanism, which involves the formation of a radical-ion intermediate. This radical-ion intermediate may undergo either back-electron transfer (BET), returning the starting species, or may undergo fragmentation to afford a neutral radical along with an ionic leaving group.[5]

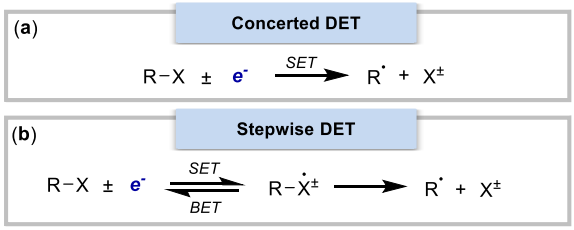

Figure 2.2 Stepwise *vs* concerted DET mechanisms.

[4] Antonello, S.; Maran, F. "Intramolecular dissociative electron transfer" *Chem. Soc. Rev.* **2005**, *34*, 418.
[5] Savéant, J-M. "Electron transfer, bond breaking and bond formation" *Advances in Physical Organic Chemistry* **2000**, *35*, 117.

Both thermodynamic and kinetic factors govern the competition between concerted and stepwise mechanisms.[4] The transition from a stepwise to a concerted mechanism is expected to arise the more the ion-radical is unstable, since its cleavage becomes faster and faster.

2.2 Photo-induced SET

When ground-state molecules absorb visible or ultraviolet (UV) light, electrons in the highest occupied orbitals undergo transitions to unoccupied orbitals lying at higher energies. This means that, by absorbing a photon, the ground-state is converted into an electronically excited-state. The excited-state is an energy-rich species that may release its energy content or undergo chemical modifications. The energy-releasing pathways can be classified as radiative (*i.e.*, transitions to lower states involving light emission) and non-radiative (*i.e.*, transitions involving the release of heat). In addition, the excited-state can participate in numerous inter- and intramolecular processes (Figure 2.3).[6]

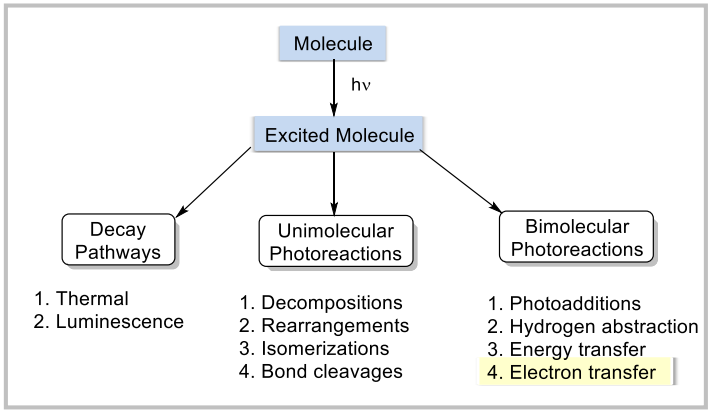

Figure 2.3 A classification of photochemical pathways.

The energy contained in the excited-state has an important effect on its ability to donate or accept electrons (Figure 2.4). In the excited-state, one electron populates an antibonding orbital, which is positioned at a greater separation distance from the nucleus. For this reason, the energy required for a single-electron ejection process (in other words, the ionization potential) is lower with respect to the ground-state species. On the other hand, the presence of a half-filled orbital near the nucleus increases the amount of energy released during a single-electron addition process (in other words, the electron affinity),

[6] Kaoarnos, G. J. "Fundamentals of photoinduced electron transfer." VCH, Weinheim, New York, **1993**, ISBN 3-527-27856-1.

with respect to the ground-state species. This is why a molecule in the excited-state is both a better reductant and a better oxidant than in the ground-state. This aspect is crucial for the work described herein, since it strong reducing agents can be generated by bringing electron-rich chemical species, such as phenolate anions or chiral enamines, to their excited-state.

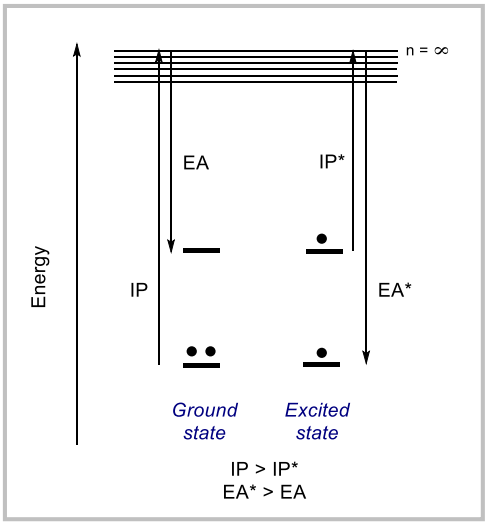

Figure 2.4 The ionization potential (IP) and electron affinity (EA) of an excited-state are decreased and increased, respectively, as compared with the ground-state.

The quantitative formulation of this conclusion is known as the Rehm-Weller equation (Figure 2.5).[7] According to Rehm and Weller, the free-energy change associated to an electron transfer (ΔG^0_{et}) between an excited electron donor (D*) and a ground-state acceptor (A) may be calculated using *eq.* 1 (Figure 2.5).[8] $E^0_{D^+/D^*}$ is the reduction potential of the donor in the excited-state, E^0_{A/A^-} is the reduction potential of the acceptor in the ground-state and ***C*** is a term which takes into account the solvation effects and the coulombic energy variations upon electron transfer. The magnitude of $E^0_{D^+/D^*}$ may be calculated according to *eq. 2* (Figure 2.5), where $E^0_{D^+/D}$ is the reduction potential of the donor in the ground-state and E_{00} is the energetic content of D after one-photon excitation process (excitation energy). $E^0_{D^+/D^*}$ should be smaller than $E^0_{D^+/D}$ implying that the

[7] Rehm, D.; Weller, A. "Kinetics of fluorescence quenching by electron and H-atom transfer." *Isr. J. Chem.* **1970**, *8*, 259.
[8] Farid, S.; Dinnocenzo, J. P.; Merkel, P. B.; Young, R. H.; Shukla, D.; Guirado, G. "Reexamination of the Rehm–Weller data set reveals electron transfer quenching that follows a Sandros–Boltzmann dependence on free energy." *J. Am.Chem. Soc.* **2011***, 133,* 11580.

excited-state is a better electron donor than the ground-state. The excitation energy (E_{00}) may be estimated spectroscopically from the position of the long wavelength tail of the absorption spectrum of the electron donor (D) or, alternatively, from the position of the short wavelength tail of the emission spectrum of D.[9] The combination of *eq*. 1 and *eq*. 2 leads to the Rehm-Weller equation (*eq*. 3). By employing the Rehm-Weller equation, we managed to estimate the reduction potential of excited-state chiral enamines (used as D* in the chemistry discussed in Chapter IV) on the basis of electrochemical and spectroscopic measurements.[10] A similar treatment may be applied to evaluate the free-energy change associated (ΔG^0_{et}) with the electron transfer between an electron acceptor in the excited-state (A*) and a ground-state donor (D).

$$D^* + A \rightarrow D^{\bullet+} + A^{\bullet-}$$

$$\Delta G^0_{et} = (E^0_{D^+/D^*} - E^0_{A/A^-}) - \boldsymbol{C} \qquad (eq.\ 1)$$

$$E^0_{D^+/D^*} = E^0_{D^+/D} - E_{00} \qquad (eq.\ 2)$$

$$\Delta G^0_{et} = (E^0_{D^+/D} - E^0_{A/A^-} - E_{00}) - \boldsymbol{C} \qquad (eq.\ 3)$$

Figure 2.5 Rehm and Weller equation.

2.3 Visible Light Photoredox Catalysis

Photocatalysts (PCs) are chemical species capable of accelerating the rate of a chemical transformation when exposed to light (Figure 2.6).[11]

The photocatalyst (PC) contains a photoactive moiety (chromophore) that absorbs UV-visible light. This event brings the photocatalyst into an electronically excited-state (PC*). A bimolecular process between PC* and a generic compound X could lead to two products: X' and the modified catalyst PC′. Depending on the nature of both the photocatalyst and X, three mechanistic pathways are commonly possible:[12] (a) energy transfer; (b) electron transfer; (c) atom transfer. Subsequently, in order to close the catalytic cycle, PC must then be recovered by reaction of PC′ with another chemical entity

[9] Balzani, V.; Ceroni, P.; Juris, A. "Photochemistry and photophysics: concepts, research, applications" **2014**, Chapter 4, p. 103, Wiley & Sons.

[10] Silvi, M.; Arceo, E.; Jurberg, I. D.; Cassani, C.; Melchiorre, P. "Enantioselective organocatalytic alkylation of aldehydes and enals driven by the direct photoexcitation of enamines" *J. Am. Chem. Soc.* **2015**, *137*, 6120.

[11] König, B. "Chemical photocatalysis" ed. by König Burkhard, 93053 Regensburg (Germany), **2013**, ISBN 978-3-11-026916-1.

[12] Fagnoni, M.; Dondi, D.; Ravelli, D.; Albini, A. "Photocatalysis for the formation of the C−C bond" *Chem. Rev.* **2007,** *107*, 2725.

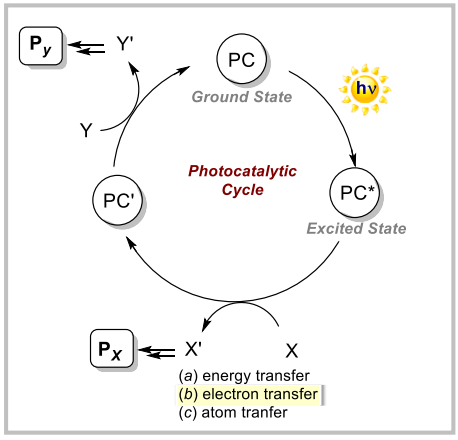

Figure 2.6 General reaction scheme for a photocatalytic reaction promoted by a photocatalyst.

(Y). The reaction products X′ and Y′ are often reactive intermediates in the electronic ground-state that can undergo subsequent transformations, until they form stable products (P_x and P_y). The term "photoredox catalysis" refers to the PC* engaging in SET processes with the substrate (X).[13] In this context, a crucial reactivity concept is the ability of the excited-state photocatalysts PC* to act both as better electron donors and acceptors with respect to the corresponding ground-state. Many of the most commonly employed visible-light photoredox catalysts are polypyridyl complexes of ruthenium and iridium.[13] Specifically, the photochemistry of $Ru(bpy)_3^{2+}$ (tris(bipyridine)ruthenium(II)) and its ability to act as a SET catalyst has been widely documented.[14] In general, $Ru(bpy)_3^{2+}$ absorbs light in the visible region of the electromagnetic spectrum to give stable, long-lived excited-states. Upon absorption of light, the photoexcited state $Ru(bpy)_3^{2+}$* may react both with electron donors (D) and electron acceptors (A), as depicted in Figure 2.7a.[15] Oxidative quenching of $Ru(bpy)_3^{2+}$* with a suitable electron acceptor (A) provides $Ru(bpy)_3^{3+}$ (path a, Figure 2.7a), a strong oxidant, while reductive quenching in the presence of an electron-rich donor (D) provides $Ru(bpy)_3^{+}$, a strong reducing agent (path b, Figure 2.7a).

---

[13] Shaw, M. H.; Twilton, J.; MacMillan, D. W. C. "Photoredox catalysis in organic chemistry" *J. Org. Chem.* **2016**, *81*, 6898.

[14] a) Juris, A.; Gandolfi, M. T.; Manfrin, M. F.; Balzani, V. "Electron and energy Transfer Mechanisms in the quenching of the tris(2,2'-bipyridine)ruthenium(II) luminescence by cyanide complexes." *J. Am. Chem. Soc.* **1976**, *98,* 1047. b) Juris, A.; Balzani, V.; Barigelletti, F.; Campagna, S.; Belser, P.; Von Zelewsky, A. "Ru(II) polypyridine complexes: photophysics, photochemistry, electrochemistry, and chemiluminescence." *Coord. Chem. Rev.* **1988**, *84*, 85.

[15] a) Tucker, J. W.; Stephenson, C. R. J. "Shining light on photoredox catalysis: theory and synthetic applications." *J. Org. Chem.* **2012**, *77*, 1617. b) Yoon, T. P.; Ischay, M. A.; Du, J. "Visible light photocatalysis as a greener approach to photochemical synthesis." *Nat. Chem.* **2010**, *2*, 527.

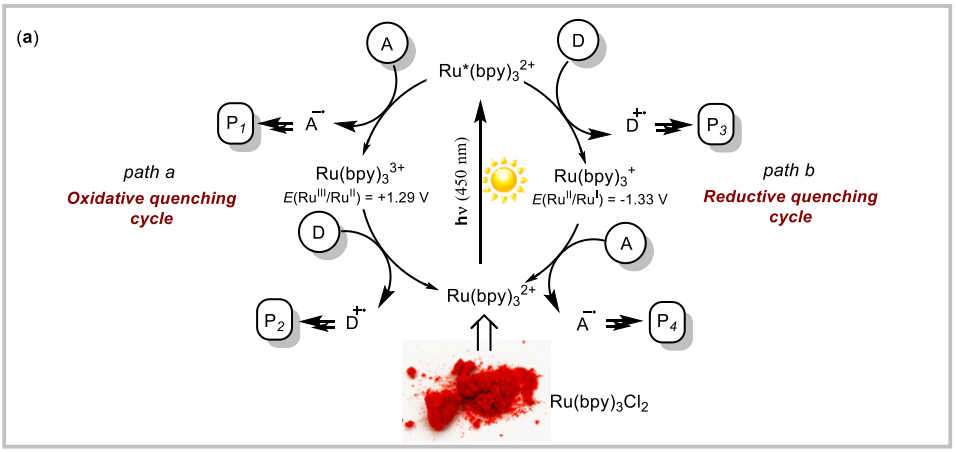

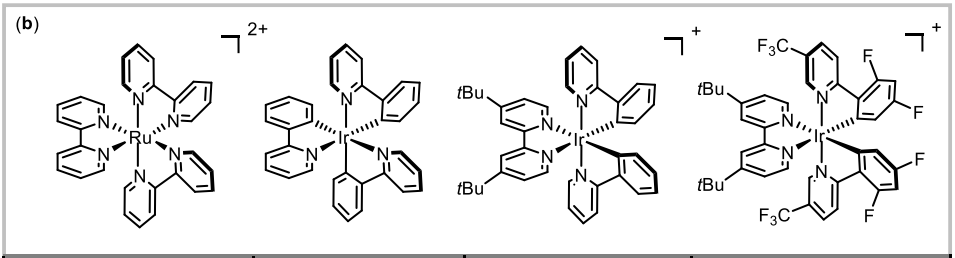

[Ru(bpy)$_3$]$^{2+}$	Ir(III)(ppy)$_3$	[Ir(III)(ppy)$_2$(dtbbpy)]$^+$	Ir(III)[dF(CF3)ppy]$_2$(dtbbpy)$^+$
reduction potential (vs SCE) $E(Ru^{III}/Ru^{*II}) = -0.81$ V	$E(Ir^{IV}/Ir^{*III}) = -1.73$ V	$E(Ir^{IV}/Ir^{*III}) = -0.96$ V	$E(Ir^{IV}/Ir^{*III}) = -0.89$ V
oxidation potential (vs SCE) $E(Ru^{*II}/Ru^{I}) = +0.77$ V	$E(Ir^{*III}/Ir^{II}) = +0.31$ V	$E(Ir^{*III}/Ir^{II}) = +0.66$ V	$E(Ir^{*III}/Ir^{II}) = +1.21$ V
wavelength of maximum absorption $\lambda_{abs} = 452$ nm	$\lambda_{abs} = 375$ nm	$\lambda_{abs} = 410$ nm	$\lambda_{abs} = 380$ nm

Figure 2.7 (**a**) Oxidative and reductive quenching cycles in Ru(bpy)$_3^{2+}$ photochemistry; (**b**) transition-metal photoredox catalysts commonly employed in SET chemistry. SCE: standard calomelan electrode.

Hence, depending upon the conditions employed and the proper selection of the quencher (A or D), Ru(bpy)$_3^{2+}$* can be utilized as a single electron oxidant or reductant. The highly reactive intermediates (radical-anion and radical-cation intermediates, shown in Figure 2.7a), formed upon the SET processes from the photoredox catalyst, can rapidly undergo subsequent transformations to afford the final reaction products ($P_{1\text{-}4}$).

Some common transition metal-based photoredox catalysts and some of their photophysical properties are shown in Figure 2.7b.[13] Ligands play an important role in the redox activity of these species, and they can be finely tuned to infer the desired properties to the photocatalyst. When the electron density of the metal center increases, the oxidative-power of the complex decreases while, its reductive-power simultaneously

increases. This is important because the photocatalyst (metal and ligands) for a particular chemical transformation should be chosen rationally depending upon the redox potentials of the substrates used. (A and D).

2.4 Merging Visible Light Photoredox Catalysis with Aminocatalysis

Ruthenium polypyridyl complexes are well established one-electron photoredox catalysts, that can absorb visible light. These inorganic complexes have found widespread applications in the area of energy storage, hydrogen and oxygen evolution from water and methane production from carbon dioxide.[16] However, until 2008 this class of complexes did not find a substantial application in organic synthesis. A seminal study by the MacMillan group demonstrated the feasibility of merging ruthenium-based photocatalysis with the enamine-mediated catalytic activation of carbonyl compounds (Figure 2.8a).[17] This approach allowed the development of the first direct enantioselective intermolecular α-alkylation of aldehydes **1** with alkyl bromides **2**, a longstanding challenge in organocatalysis that has been considered "the holy grail of organocatalysis".[18] In 1954, the fundamental studies by Gilbert Stork established that preformed enamines can facilitate the S_N2-type α-alkylation of ketones with alkyl halides, therefore affording α-functionalized carbonyl compounds.[19] On the other hand, the development of general aminocatalytic strategies for the stereoselective α-alkylation of carbonyl compounds with simple alkyl halides have not been possible.[20] Indeed, it turned out that addressing this synthetic target was more challenging than expected, mainly because of the modest reactivity of alkyl halides, which complicates the ionic alkylation step while favouring side processes, *e.g. N*-alkylation of the Lewis basic amine catalysts with the alkyl halides and self-aldol condensation. This synthetic problem has been solved utilizing the peculiar reactivity of electron-deficient alkyl radicals, photochemically formed under mild reaction conditions from electron-poor alkyl halides.[17] According to the originally proposed mechanism (Figure 2.8b), the chiral *trans* imidazolidinone organic catalyst **3** condenses with the aldehyde **1** forming the corresponding enamine **5**, while $Ru(bpy)_3^{2+}$ **4** reaches an electronically excited state upon visible light absorption.

---

[16] K.,Kalyanasundaram "Photophysics, photochemistry and solar energy conversion with tris(bipyridyl)ruthenium(II) and its analogues" *Coord. Chem. Rev.* **1982**, *46*, 159.
[17] Nicewicz, D. A.; MacMillan, D. W. C. "Merging photoredox catalysis with organocatalysis: the direct asymmetric alkylation of aldehydes" *Science* **2008**, *322*, 77.
[18] Melchiorre, P. "Light in aminocatalysis: the asymmetric intermolecular α-alkylation of aldehydes" *Angew. Chem. Int. Ed.* **2009**, *48*, 1360.
[19] Stork, G.; Terrell, R.; Szmuszkovicz, J. "A new synthesis of 2-alkyl and 2-acyl ketones" *J. Am. Chem. Soc.* **1954**, *76*, 2029.
[20] Mukherjee, S.; Yang, J. W.; Hoffmann, S.; List, B. "Asymmetric enamine catalysis." *Chem. Rev.* **2007**, *107*, 5471.

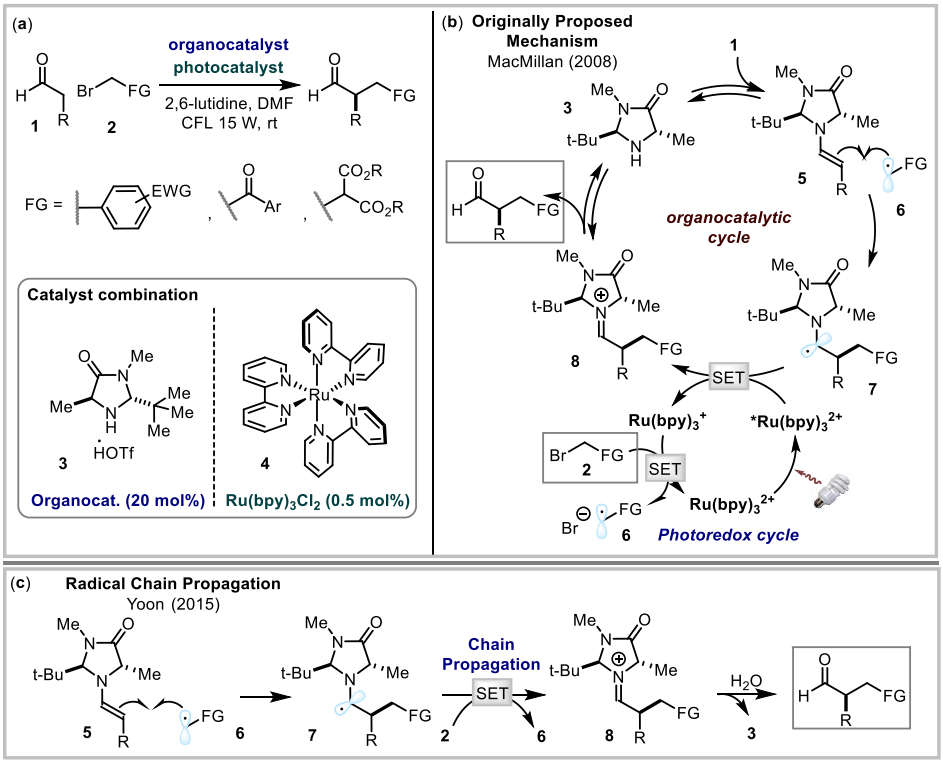

Figure 2.8 (**a**) Asymmetric organocatalytic photoredox α-alkylation of aldehydes, (**b**) reaction mechanism proposed by MacMillan and (**c**) a lately refined mechanistic proposal. CFL: compact fluorescence lamp; SET: single-electron transfer; FG: functional group.

A sacrificial amount of enamine **5** is needed to reduce the excited state photocatalyst Ru* (II) to Ru (I) thereby starting the photoredox cycle. The electron-rich ruthenium (I) photocatalyst gives an electron to **2** via a SET manifold, yielding the original Ru (II) complex and the electron-deficient radical **6**, which is formed *via* DET process. The photoredox cycle is thus closed. The combination of electron-rich enamine **5** with electrophilic radical **6** yields α-amino radical **7**, which is prone to oxidation by the excited Ru (II) photocatalyst. The hydrolysis of the iminium ion **8** provides the desired enantioenriched α-alkylated aldehyde and regenerates the chiral organocatalyst **3**.

In subsequent studies, Yoon and coworkers demonstrated that the reaction actually proceeds through a self-propagating radical chain mechanism initiated by the photochemical activity of the Ru (II) complex (Figure 2.8c).[21] Indeed, a quantum yield

[21] Yoon, T. P.; Cismesia, M. A. "Characterizing chain processes in visible light photoredox catalysis" *Chem. Sci.* **2015**, *6*, 5426.

(Φ (436 nm)) as high as 18 was found for this transformation (diethyl bromomalonate **2** was used as radical precursor). The quantum yield (Φ (λ)) is defined by the IUPAC as the number of events (molecules changed, formed, or destroyed) per number of photons absorbed at a particular wavelength (λ) in the same period of time (*eq.* 4).[22]

$$\Phi(\lambda) = \frac{\text{molecules generated}}{\text{absorbed photons}} \qquad (eq.4)$$

Quantum yield measurements are a convenient method to discriminate whether radical chain mechanisms are taking place. In chain processes initiated by light absorption, one photon can form several molecules of product, resulting in a quantum yield larger than one. Consequently, a quantum yield greater than one can only be explained if a chain pathway initiated by light absorption is present. According to the quantum yield measurement (Φ (436 nm)=18)[21], a more likely product-forming step in the MacMillan chemistry is the chain-propagating reduction of the alkyl bromide **2** by the electron-rich α-amino radical **7**, which can act as a reducing agent.[23] Finally, it is important to underline that the MacMillan study[17] (Figure 2.8) had profound implications on modern organic chemistry. The resulting field of photoredox catalysis provided an effective way of generating radical intermediates from readily available, bench-stable precursors under mild conditions.[13] This meant that enantioselective organocatalysis, which requires mild conditions for optimal efficiency and stereocontrol, could be successfully applied within radical reactivity.

2.5 Generating Radicals *via* the Photochemical Activity of Enamine-based Electron Donor Acceptor (EDA) Complexes

Electron donor acceptor (EDA) complexes were first described by Mulliken, in the middle of last century, as colored molecular association in the ground state of two or more colorless species.[24] EDA complexes are generated through electronic interactions between an electron-rich donor (D) and an electron-poor acceptor (A). The resulting

[22] a) Murov, S. "Handbook of photochemistry" Marcel Dekker, New York, **1973**. b) Kuhn, H. J.; Braslavsky, S. E.; Schmidt, R. "Chemical actinometry" *Pure and App. Chem.* **2004**, *76*, 2105.
[23] a) Ismaili, H.; Pitre, S. P.; Scaiano J. C. "Active participation of amine-derived radicals in photoredox catalysis as exemplified by a reductive cyclization" *Catal. Sci. Technol.* **2013**, *3*, 935. b) Wayner, D. D. M.; Dannenberg, J. J.; Griller, D. "Oxidation potentials of α-aminoalkyl radicals: bond dissociation energies for related radical cations" *Chem. Phys. Lett.* **1986**, *131*, 189.
[24] a) Mulliken, R. S. "Molecular Compounds and their Spectra II" *J. Am. Chem. Soc.* **1952**, *74*, 811; b) Foster, R. "Electron donor–acceptor complexes" *J. Phys. Chem.* **1980**, *84*, 2135.

molecular ground-state association is characterized by a new absorption band that generally lies in the visible range of light. When the EDA complexes are irradiated with light of appropriate wavelength, a single-electron transfer from the HOMO of the electron donor to the LUMO of the acceptor can occur, generating radicals or radical ions (Figure 2.9). The radical ion pair, formed after the first photo-induced electron transfer, may either return to the initial state through a rapid BET process or undergo subsequent transformations. The BETs are generally faster with respect to all other processes that could happen after the SET ($k_{BET} > k_P$). This fact has greatly limited the synthetic utility of EDA complexes in organic synthesis.[25]

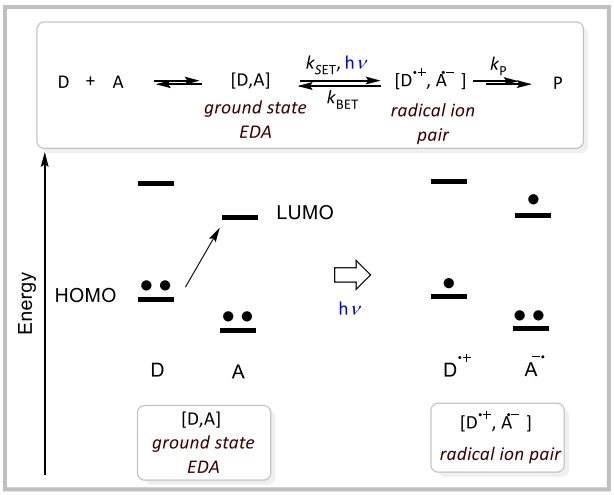

Figure 2.9 Photochemical activity of electron donor acceptor (EDA) complexes.

In 2013, our research group discovered that the photo-activity of EDA complexes generated upon aggregation of an electron-rich enamine **10** and a suitable acceptor (such as **11a**,**b**) could be used to generate reactive radical species under mild reaction conditions, without the need of an external photocatalyst (Figure 2.10).[26] The condensation of aldehydes **1** with the chiral organocatalyst **9** leads to the formation of chiral enamines **10**. Then, the electron-rich intermediate **10** undergoes formation of a colored EDA complex, in the ground state, with the electron-deficient benzyl bromide

[25] Lima, C. G. S.; Lima, T. de M.; Duarte, M.; Jurberg, I. D.; Paixao, M. W. "Organic synthesis enabled by light-irradiation of EDA complexes: theoretical background and synthetic applications" *ACS Catal.* **2016**, *6,* 1389.
[26] Arceo, E.; Jurberg, I. D.; Álvarez-Fernández, A.; Melchiorre, P. "Photochemical activity of a key donor-acceptor complex can drive stereoselective catalytic α-alkylation of aldehydes" *Nat. Chem.* **2013**, *5*, 750.

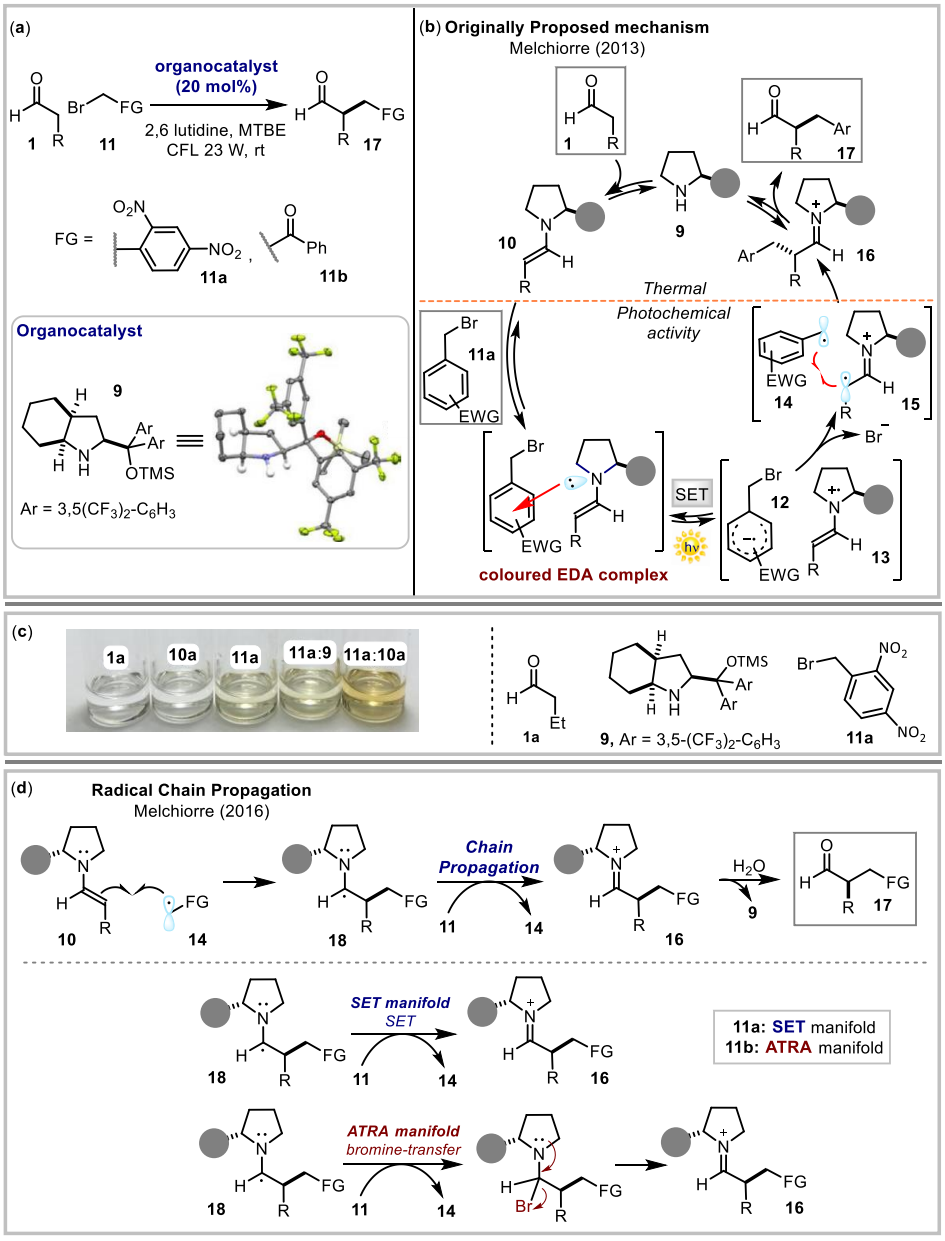

Figure 2.10 (**a**) Photo-organocatalytic asymmetric α-alkylation of aldehydes *via* EDA complex activation; (**b**) the initial proposed mechanism; (**c**) visual appearance of the separate reaction components and of the colored EDA complex in the alkylation of aldehydes with 2,4-dinitrobenzyl bromide **11a**; [**1a**] = 3 M; [**9**] = 0.2 M; [**11a**] = 0.2 M. (**d**) the new proposed mechanism; EWG: electron withdrawing group; SET: single-electron transfer; FG: functional group; ATRA: atom transfer radical addition; the grey circle represents the bulky group of the organic catalyst.

11a (Figure 2.10b). As it is shown in Figure 2.10c, achromatic solutions are obtained from the separate reaction components. However, a marked yellow color can be observed immediately after mixing a methyl *tert*-butyl ether (MTBE) solution of the enamine **10a**, generated *in situ* upon condensation of butanal **1a** (15 equiv.) and the aminocatalyst **9** (1 equiv.), with 2,4-dinitrobenzyl bromide **11a** (1 equiv.).[27]

This color change is characteristic of the formation of an EDA complex. Irradiation with visible light, using a simple 23W-CFL (compact fluorescence light) bulb, promoted a SET from the enamine **10** to the bromo-compound **11a**, providing the two open-shell species **12** and **13**. Crucial for a productive redox process was the high tendency of the radical anion **12** to undergo rapid fragmentation of the carbon-bromide bond ($k_{BET} < k_P$, mesolysis), yielding the leaving group (bromide) and the electrophilic benzyl radical **14**. Originally, it was proposed that the latter open-shell species (**14**) could react in the solvent cage with the chiral radical-cation intermediate **15** to give the enantio-enriched α-alkylated product **17**. The reaction with phenacyl bromide **11b** was proposed to follow a similar pathway. Later, it was demonstrated that the reactions actually proceed through a self-propagating radical chain mechanism, initiated by the photochemical activity of EDA complexes.[27] A quantum yield (Φ (450 nm)) of 25 and 20 were measured for the dinitro-benzyl bromide (**11a**) and phenacyl bromide (**11b**), respectively.[27] This means that, in both cases, the nucleophilic ground-state enamine **10** traps the photochemically generated electrophilic radical **14** to form the corresponding α-amino radical **18** (Figure 2.10d). Two different pathways can be proposed for the propagation step, which would formally oxidize α-aminoalkyl radical **18** to the iminium ion **16**. An electron-transfer from **18** to the electron-poor alkyl halide **11** would regenerate the chain-propagating radical **14** *via* DET, while forming the bromide-iminium ion pair **16**. The feasibility of this step is related to the reduction potential of the alkyl halide **11**, which should match the reduction power of the electron-rich α-aminoalkyl radical **18**. Alternatively, an atom-transfer mechanism can be envisaged, where the α-aminoalkyl radical **18** would abstract a bromine atom from **11**, regenerating the radical **14** while affording an unstable α-bromo amine adduct intermediate, which would eventually evolve to the iminium ion **16**. This pathway would provide a rare example of enantioselective catalytic atom-transfer radical addition (ATRA), a historical methodology for functionalizing olefins with organic

[27] Bahamonde, A.; Melchiorre, P. "Mechanism of the stereoselective α-alkylation of aldehydes driven by the photochemical activity of enamines" *J. Am. Chem. Soc.* **2016**, *138*, 8019.

halides.[28] To discriminate between the two possible propagation manifolds, the reduction potential of **16** (E_p^{red} of **16**) was estimated to be ≈ -0.95 V *vs.* Ag/Ag^+ in CH_3CN (for further details see experimental part within Chapter IV).[27] This value means that the α-aminyl radical of type **18** is incapable of reducing **11b** (E_p^{red} of **11b** = -1.35 V *vs.* Ag/Ag^+ in CH_3CN)[27], indicating that a bromine-transfer mechanism is likely operative with this substrate. On the other hand, a SET reduction is the most likely mechanism when using **11a**, since its potential (E_p^{red} of **11a** = -0.66 V *vs.* Ag/Ag^+ in CH_3CN)[27] makes a SET reduction from intermediate **18** feasible.

2.6 Direct Photoexcitation of Chiral Enamines: a New Approach for Radical Formation

During the investigation of the photochemical asymmetric α-alkylation of aldehydes under enamine-mediated catalysis, our research laboratory found that diethyl bromomalonate **18** can serve as a suitable radical precursor. Indeed, product **19a** was obtained in good yield with high enantioselectivity under the photo-organocatalytic conditions described in Figure 2.11.[10]

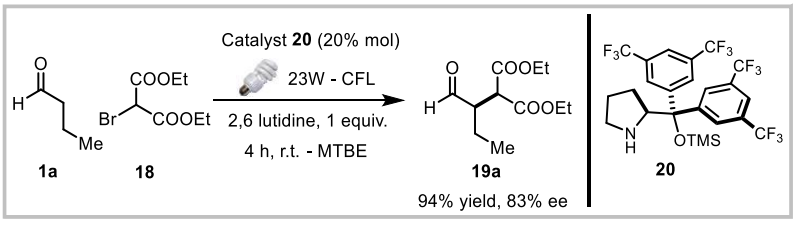

Figure 2.11 Photochemical α-alkylation reaction of butyraldehyde with diethyl bromomalonate; CFL: compact fluorescence lamp.

The reaction is relatively fast (4 hours), requires light in order to proceed, and proceeds without the need of an external photocatalyst. However, no color change was observed during the entire reaction time, qualitatively suggesting that the chemistry is not driven by the formation of an EDA complex in solution. Mechanistic investigations revealed the key role played by the photoexcited enamine **21a**, formed upon condensation of **20** with **1a**, in the photochemical initiation of the reaction. In order to demonstrate this, a series of Stern-Volmer quenching experiments were conducted.[10,27] The emission spectrum of

[28] a) Kharasch, M. S.; Jensen, E. V.; Urry, W. H. "Addition of carbon tetrachloride and chloroform to olefins" *Science* **1945**, *102*, 128. b) Pintauer, T.; Matyjaszewski, K. "Encyclopedia of radicals" **2012**, Volume 4, p. 1851, Wiley.

the stable pre-formed enamine **21b**, prepared by condensation of catalyst **20** and 2-phenylacetaldehyde **1b**, was recorded upon excitation at 365 nm (Figure 2.12a).

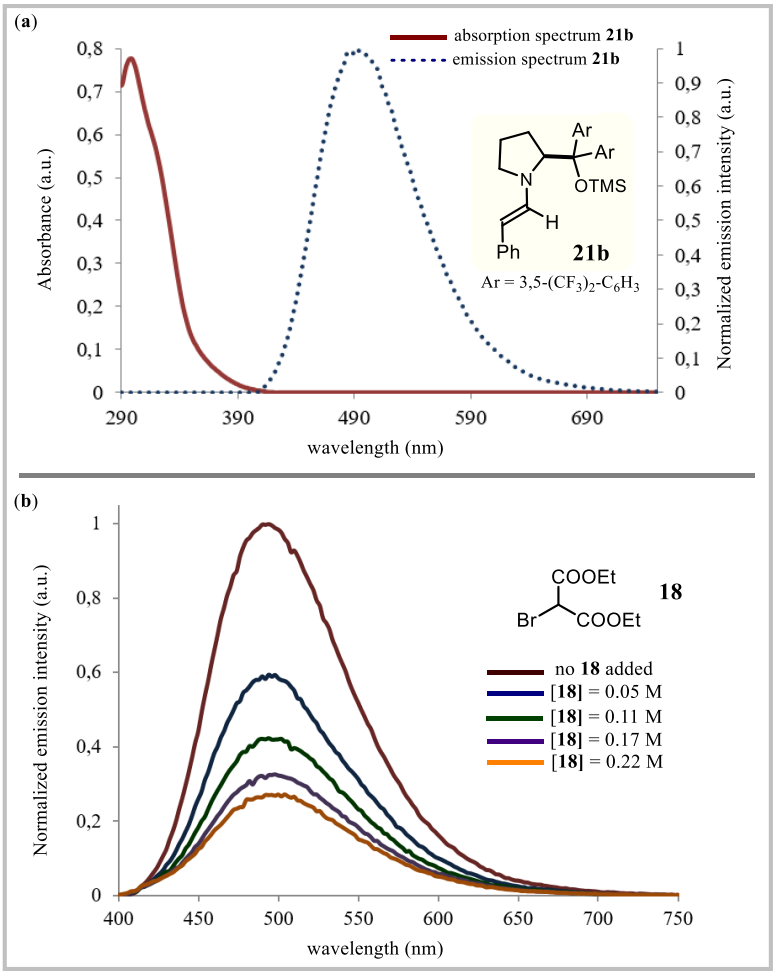

Figure 2.12 (**a**) Absorption and emission spectra of the enamine **21b** (excitation wavelength 365 nm) in toluene. (**b**) Quenching of the enamine **21b** emission ($5 \cdot 10^{-5}$ M in toluene) in the presence of increasing amounts of bromomalonate **18**.

The excited state of this enamine and its emission were effectively quenched by the addition of bromomalonate **18** (Figure 2.12b). This quenching study demonstrated that the excited state enamine (**21b***) can interact with the ground-state **18**, most likely through a SET mechanism. Indeed, the chiral enamine **21b** can directly reach an electronically excited state (**21b***), upon light absorption, becoming a strong reducing

agent, as implied by its reduction potential, which was estimated as ≈ -2.0 V (*vs* Ag/Ag^+ in CH_3CN) employing the Rehm-Weller equation (see section 2.2 within this Chapter). As a consequence, excited enamine **21a*** may trigger the formation of the electrophilic carbon centered radical **23** through the reductive cleavage of **18** *via* SET mechanism (Figure 2.13).

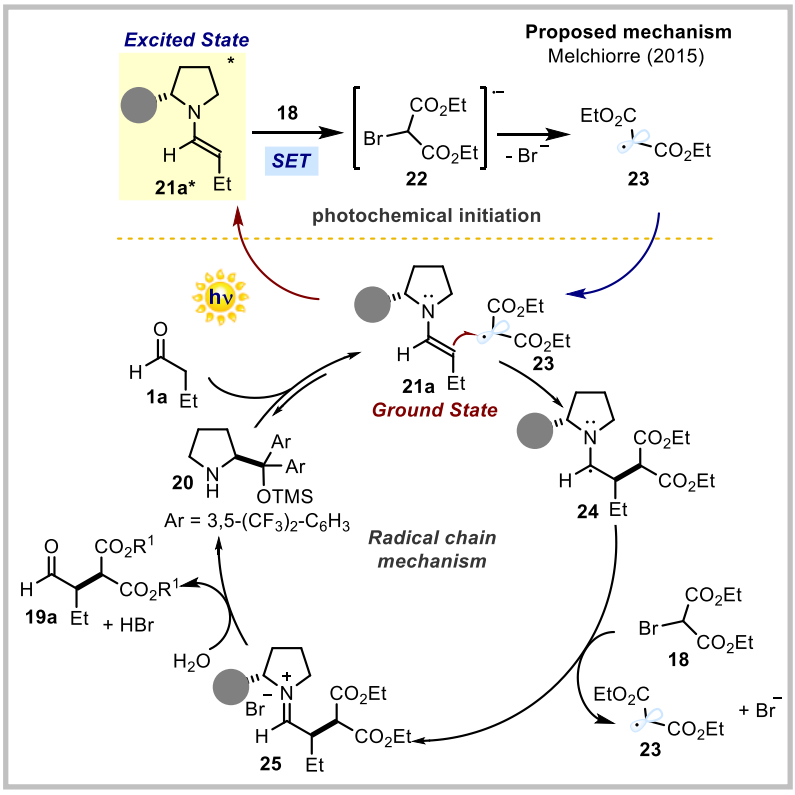

Figure 2.13 Proposed catalytic cycle for the photochemical α-alkylation reaction of butanal with diethyl bromomalonate; SET: single electron transfer; the grey circle represents the bulky group of the organic catalyst.

This electron-poor radical (**23**) can react with a chiral enamine (**21a**) in the ground state providing the corresponding chiral α-amino radical **24**. Indeed, a quantum yield (Φ (400nm)) of 20 was determined for the reaction depicted in Figure 2.11, demonstrating that a propagating radical chain mechanism is operative.[27] This implies that the direct excitation of enamines serves as an initiation to sustain a chain process. In this case, in agreement with the reductive potentials of **25** (E_p^{red} of **25** ≈ -0.95 V *vs.* Ag/Ag^+ in CH_3CN)[27] and **18** (E_p^{red} of **18** = -1.69 V *vs.* Ag/Ag^+ in CH_3CN)[27], the propagation step

proceeds through an ATRA type mechanism. Therefore, the α-aminoalkyl radical **24** abstracts a bromine atom from **18**, regenerating the radical **23** while affording an unstable α-bromo amine adduct, which evolves to the iminium ion pair **25** (Figure 2.13). The hydrolysis of the iminium ion **25** provides the desired enantioenriched α-alkylated aldehyde **19a** and the chiral organocatalyst **20**. These studies demonstrated that light excitation can turn enamines, which behave as nucleophiles in the ground-state, into reductants and trigger the formation of radicals. At the same time, ground-state enamines control the stereochemical course of the radical trapping event. This strategy was used in this thesis for the development of a new synthetically useful light-triggered enantioselective radical transformation.

Chapter III

Photochemical Direct Perfluoroalkylation of Substituted Phenols

Target

Developing a metal-free photochemical strategy for the synthesis of valuable perfluorinated substituted phenols **3** under mild reaction conditions.

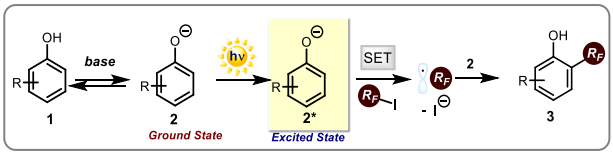

Tool

Use of the photochemical properties of visible light-absorbing, transiently generated phenolate anions **2** to initiate a radical chain perfluoroalkylation process.[1]

3.1 Introduction

The discovery that transiently generated chiral electron-rich enamines **1** can form light absorbing electron donor-acceptor (EDA) complexes upon aggregation with alkyl bromides,[2] and that the photochemical activity of these molecular aggregations can trigger radical transformations under mild conditions, motivated us to expand this synthetic approach. In particular, given the electronic similarities with enamines **1**, in situ formed enolates **2** have been evaluated as potential electron-donors in EDA complex formation (Figure 3.1a). It was found that enolate **4**, formed upon facile deprotonation of the corresponding ethyl α-cyano arylacetate **3**, generates a colored EDA complex upon aggregation with perfluorohexyl iodide (indicated as R_FI in Figure 3.1b).[3] Visible light irradiation of this complex induces a single electron transfer (SET) from the donor to the antibonding orbital-σ* of the acceptor (R_FI), leading, upon rapid and irreversible

[1] The work discussed in this Chapter has been published, see: Filippini, G.; Nappi, M.; Melchiorre P. "Photochemical direct perfluoroalkylation of phenols" *Tetrahedron* **2015**, *71*, 4535.

[2] Arceo, E.; Jurberg, I. D.; Álvarez-Fernández, A.; Melchiorre, P. "Photochemical activity of a key donor-acceptor complex can drive stereoselective catalytic α-alkylation of aldehydes" *Nat. Chem.* **2013**, *5*, 750.

[3] Nappi, M.; Bergonzini, G.; Melchiorre, P. "Metal-free photochemical aromatic perfluoroalkylation of α-cyano arylacetates" *Angew. Chem. Int. Ed.* **2014**, *53*, 4921.

fragmentation of the carbon-iodide bond, to the formation of an electrophilic perfluorohexyl radical (R_F• in Figure 3.1b).

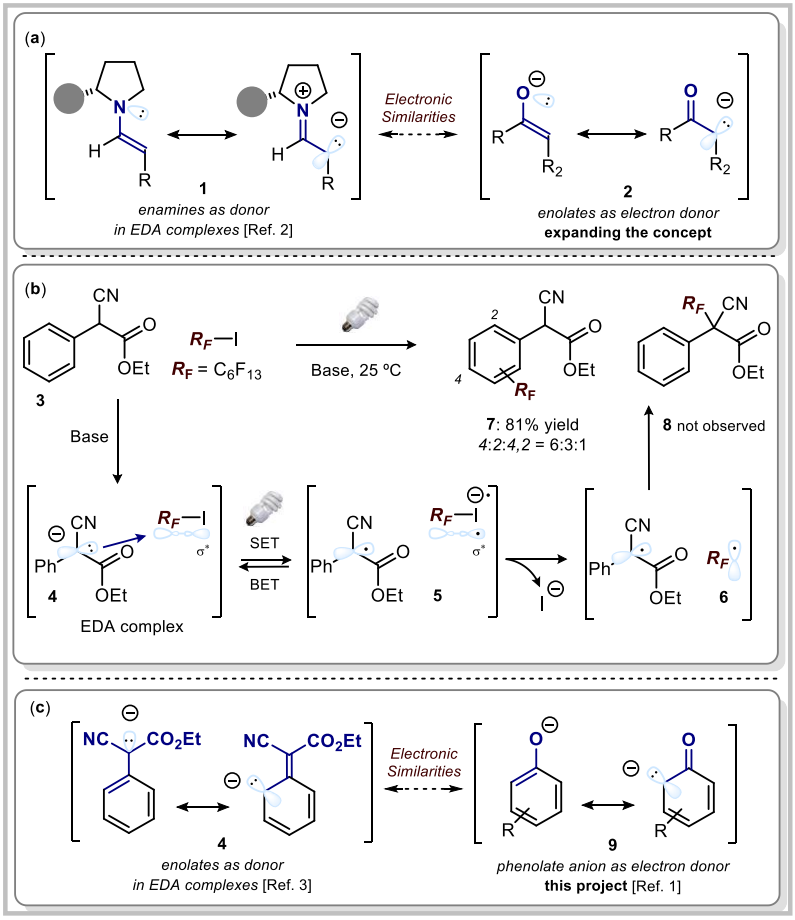

Figure 3.1 (**a**) Expanding the EDA complex activation strategy to other donors than enamines: enolates as suitable electron-donors in EDA complex formation. (**b**) Photochemical aromatic perfluoroalkylation of α-cyano arylacetates triggered by the photoactivity of an enolate-based EDA complex. (**c**) The main idea pursued in the present project: phenolate anions as suitable donor in EDA complex formation. TMG: 1,1,3,3-tetramethylguanidine; R_F indicates the perfluoroalkyl fragment; SET: single-electron transfer; BET: back-electron transfer.

In analogy to our enantioselective α-alkylation of aldehydes[2], it was anticipated the formation of the α-carbonyl perfluroalkylated adduct **8** to be favored, by means of a radical–radical combination or a radical trap by the enolate **4**. On the contrary, only a mixture of arene-perfluoroalkylation products **7** was obtained in good yield (81%), albeit

with poor regioselectivity. Studies carried out by our research group supported a reaction mechanism based on a homolytic aromatic substitution (HAS) pathway, which is generally characterized by a low level of regioselectivity.[4] The reaction mechanism of this photochemical aromatic perfluoroalkylation will be carefully discussed in section 3.4 within this chapter.

Expanding upon this precedent, we initially wondered if in situ generated phenolate anions of type **9**, formed upon deprotonation of the corresponding phenols, could be employed as suitable electron-donors in EDA complex formation with perfluoroalkyl iodides in order to develop a photochemical method for the perfluoroalkylation of substituted phenols (Figure 3.1c). Following this idea, we have been able to develop an operationally simple methodology, which occurs at ambient temperature and under illumination by a fluorescent light bulb, for the synthesis of relevant perfluorinated substituted phenols. During our studies, we found that the chemistry does not rely on the use of any external photoredox catalyst, nor on the formation of ground-state EDA complexes to access radical reactivity patterns. Instead, the process is driven by the ability of phenolate anions **9**, generated upon deprotonation of substituted phenols, to directly reach an electronically excited state by light absorption, while successively triggering the formation of the perfluoroalkyl radicals from R_FI *via* a SET mechanism.[1]

3.2 The Importance of Fluorine Containing Groups

Fluorinated compounds are the least abundant organic halides in nature.[5] Additionally, the vast majority of the terrestrial fluorine is bound in insoluble forms (chemical forms which are poorly accessible for bio-organisms), thereby reducing uptake by bio-organisms. Despite this, fluorine-containing compounds play an increasingly important role in medicinal chemistry, agriculture chemistry, and materials science.[6] In particular, incorporating perfluoroalkyl groups into organic scaffolds is a chemical strategy often employed in medicinal chemistry to modulate the biological activity of drug candidates. The strong electronegativity of fluorine atoms increases the polarization of organic molecules, therefore their ability to form non covalent interactions within the active sites

[4] a) Bowman, W. R.; Storey, J. M. D. "Synthesis using aromatic homolytic substitution-recent advances" *Chem. Soc. Rev.* **2007**, *36*, 1803. b) Gurry, M.; Aldabbagh, F. "A new era for homolytic aromatic substitution: replacing Bu_3SnH with efficient light-induced chain reactions" *Org. Biomol. Chem.* **2016**, *14*, 3849. c) Bolton, R.; Williams, G. H. "Homolytic arylation of aromatic and polyfluoroaromatic compounds" *Chem. Soc. Rev.* **1986**, *15*, 261.

[5] Harper, D. B.; O'Hagan, D.; Murphy, C. D. "The Handbook of Environmental Chemistry" vol.3P, **2003**, G. W. Gribble, Ed. (Springer, Heidelberg, Germany).

[6] Lewandowski, G.; Meissner, E.; Milchert, E. "Special applications of fluorinated organic compounds" *J. Hazard. Mater.* **2006**, *136*, 385.

of enzymes, improving the binding affinity of the drug candidate.[7] In addition, the activity of a drug is closely related to its metabolic stability. Rapid oxidative metabolism by the liver enzymes, in particular the P450 cytochromes, is often found to limit bioavailability, therefore also the activity of the drug.[7c] A frequently employed strategy to circumvent this problem is to increase the ionization potential of the drug and its resistance toward oxidation by introducing a fluorine atom. Moreover, fluorinated groups can alter many other physiochemical properties of organic compounds such as solubility, lipophilicity, acidity, etc.[8] For all these reasons, many commercially available drugs contain aromatic moieties decorated with fluorinated groups (Figure 3.2).[7] Hence, there is a need for the development of new effective synthetic methodologies for the formation of fluorine containing aromatic rings.

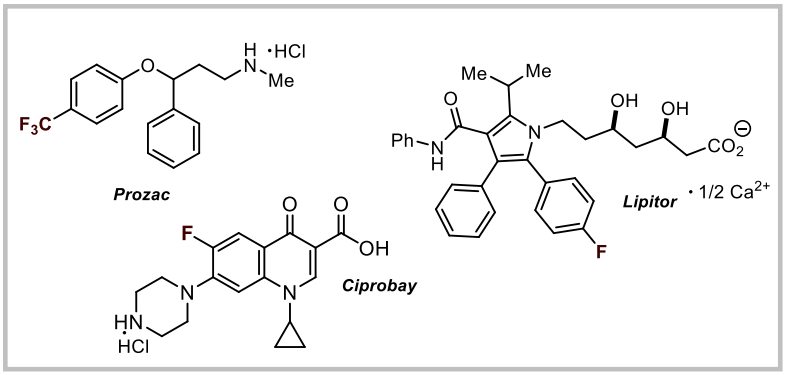

Figure 3.2 Examples of major fluorinated drugs.

To achieve this synthetic objective, cross-coupling methodologies that involve the use of stoichiometric amounts of metals have been developed.[9] This strategy requires the use of pre-functionalized arenes, and the fluorinated fragments are typically installed in place of halides or boronic acid derivatives. More recently, catalytic variants based on transition

[7] a) Purser, S.; Moore, P. R.; Swallow, S.; Gouverneur, V. "Fluorine in medicinal chemistry" *Chem. Soc. Rev.* **2008**, *37*, 320. b) Isanbor, C.; O'Hagan, D. "Fluorine in medicinal chemistry: a review of anti-cancer agents" *J. Fluor. Chem.* **2006**, *127*, 303. c) Bohm, H.-J.; Banner, D.; Bendels, S.; Kansy, M.; Kuhn, D.; Muller, K.; Obst-Sander, U.; Stahl, M. "Fluorine in medicinal chemistry" *ChemBioChem.* **2004**, *5*, 637.

[8] Müller, K.; Faeh, C.; Diederich, F. "Fluorine in pharmaceuticals: looking beyond intuition" *Science* **2007**, *317*, 1881.

[9] a) Tomashenko, O. A.; Grushin, V. V. "Aromatic trifluoromethylation with metal complexes" *Chem. Rev.* **2011**, *111*, 4475. b) McClinton, M. A.; McClinton D. A. "Trifluoromethylations and related reactions in organic chemistry" *Tetrahedron,* **1992**, *32*, 6555.

metals (especially copper and palladium) have been successfully realized.[10] On the other hand, the direct carbon–hydrogen (C-H) bond functionalization of simple arenes provides a more straightforward approach, avoiding the need for the pre-installation of a leaving group on the aromatics. Typically, direct functionalization methodologies rely on radical chemistry and the strongly electrophilic nature of perfluoroalkyl radicals (R_F•).[11] The formation of such fluorinated open-shell species may be achieved through two general activation modes, starting from suitable radical precursors, for instance perfluoroalkyl halides (Figure 3.3a)[12]: (*i*) thermal activation, which generally requires harsh reaction conditions including high temperature, the use of a radical initiator and/or metals, and potentially explosive oxidants; (*ii*) photochemical activation, which enables the formation of R_F• under milder conditions.

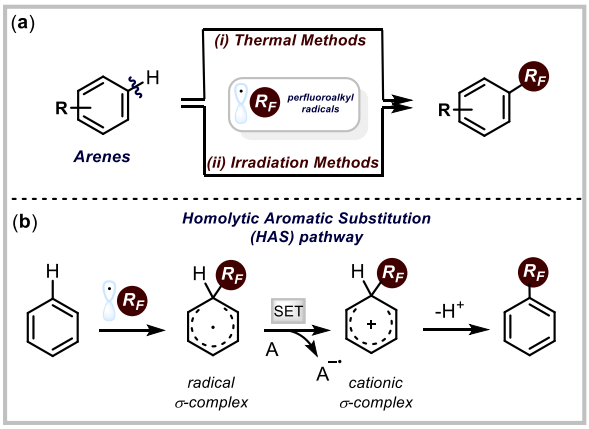

Figure 3.3 (**a**) General methods for the formation of fluorinated radicals and (**b**) mechanism for C-H radical perfluoroalkylation of arenes; SET: single-electron transfer; A: electron-acceptor species.

[10] a) Furuya, T.; Kamlet, A. S.; Ritter, T. "Catalysis for fluorination and trifluoromethylation" *Nature* **2010**, *473,* 470; b) Oishi, M.; Kondo, H.; Amii, H. "Aromatic trifluoromethylation catalytic in copper" *Chem. Commun.* **2009**, 1909; c) Cho, E. J.; Senecal, T. D.; Kinze, T.; Zhang, Y.; Watson, D. A.; Buchwald, S. L. "The palladium-catalyzed trifluoromethylation of aryl chlorides" *Science* **2010**, *328*, 1679; d) Tomashenko, O. A.; Escudero, E. C.; Belmonte, M. M.; Grushin, V. V. "Simple, stable, and easily accessible well-defined $CuCF_3$ aromatic trifluoromethylating agents" *Angew. Chem., Int. Ed.* **2011**, *50*, 7655; e) Litvinas, N. D.; Fier, P. S.; Hartwig, J. F. "A general strategy for the perfluoroalkylation of arenes and arylbromides by using arylboronate esters and [(phen)CuR^F]" *Angew. Chem. Int. Ed.* **2012**, *51*, 536.

[11] Dolbier, W. R., Jr. "Structure, reactivity, and chemistry of fluoroalkyl radicals" *Chem. Rev.* **1996**, *96*, 1557.

[12] Barata-Vallejo, S.; Bonesi, S. M.; Postigo, A. "Perfluoroalkylation reactions of (hetero)arenes" *RSC Adv.* **2015**, *5*, 62498.

These electron-poor radicals (R_F•) can react with arenes through a classical HAS pathway forming a radical σ-complex (Figure 3.3b).[4a] Many reactions defined as homolytic aromatic substitution involve an oxidative step to convert the radical σ-complex into a cationic σ-complex, followed by the rapid loss of a proton to restore aromaticity.

When perfluoroalkyl halides (R_FX) are used as radical precursors, these electron-poor species themselves can often oxidize the radical σ-complexes to the corresponding cationic σ-complex (R_FX = A in Figure 3.3b). Subsequently, the mesolytic cleavage of the C-X bond, within the resulting radical anion, leads to the formation of a new fluorinated radical, which can react with another electron-rich arene molecule, thus starting a self-propagating radical chain process.

3.3 Thermal Radical Perfluoroalkylation of Arenes

Perfluoroalkyl halides (R_FX, X = Cl, Br, and I) are fundamental building blocks in organofluorine chemistry. Indeed, this class of compounds is widely used as a source of perfluoroalkyl radicals (R_F•) in organic synthesis. In 1960, Tiers reported the first efficient protocol for the direct radical perfluoroalkylation of benzene using perfluoroalkyl iodides. The electrophilic perfluoroheptyl radicals were obtained by thermolysis of the starting material ($C_7F_{15}I$) at 250 ºC (Figure 3.4).[13] The fluorinated radical was then trapped by benzene through a HAS mechanism, affording the desired product in good isolated yield (62%).

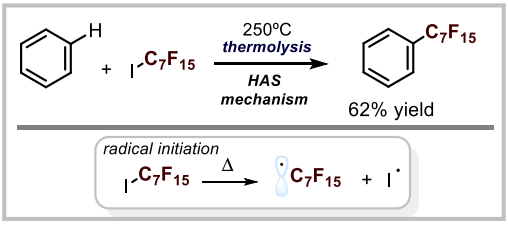

Figure 3.4 Perfluoroalkylation of arenes by thermolysis.

In 1997, Minisci and co-workers developed four alternative methodologies for the direct perfluoroalkylation of aromatic and heteroaromatic compounds **10** employing C_4F_9I as the radical precursor (Figure 3.5).[14] The electrophilic radicals (•C_4F_9) were generated in

[13] Tiers, G. V. D. "Perfluoroalkylation of aromatic compounds" *J. Am. Chem. Soc.* **1960**, *82*, 5513.

[14] Bravo, A.; Bjørsvik, H. R.; Fontana, F.; Liguori, L.; Mele, A.; Minisci, F. "New methods of free-radical perfluoroalkylation of aromatics and alkenes. Absolute rate constants and partial rate factors for the homolytic aromatic substitution by *n*-perfluorobutyl radical" *J. Org. Chem.* **1997**, *62*, 7128.

solution through an iodine atom abstraction mechanism triggered by *in situ* formed phenyl or methyl radicals. As described in Figure 3.5, the four methods are equivalent in terms of reactivity, and the desired product (**11**, X = H) was isolated in high yields in all cases.

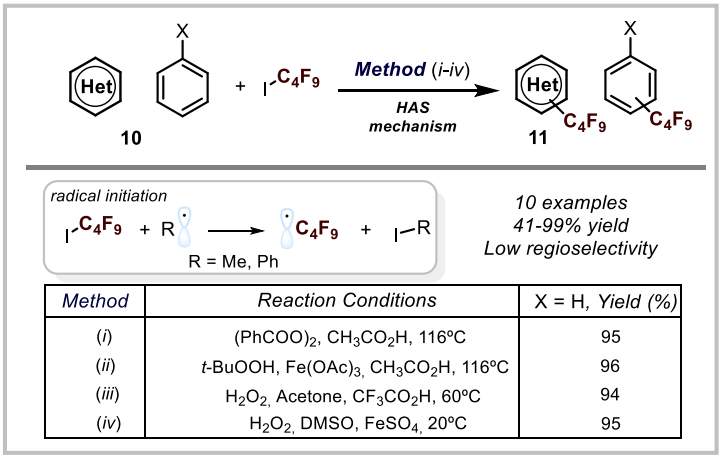

Method	Reaction Conditions	X = H, Yield (%)
(*i*)	$(PhCOO)_2$, CH_3CO_2H, 116ºC	95
(*ii*)	*t*-BuOOH, $Fe(OAc)_3$, CH_3CO_2H, 116ºC	96
(*iii*)	H_2O_2, Acetone, CF_3CO_2H, 60ºC	94
(*iv*)	H_2O_2, DMSO, $FeSO_4$, 20ºC	95

Figure 3.5 Comparison of the four strategies reported by Minisci for the perfluorobutylation of benzene and heteroaromatic compounds.

This reaction (method *i*) is quite general with respect to the nature of the aromatic compound, since both electron-withdrawing (X = CN, NO_2 and Cl) and electron-donating groups (X = OMe and OPh) on the arene ring **10** were tolerated, providing the desired product **11** with moderate to high yields, albeit with low regioselectivity. As mentioned before, the low level of regioselectivity observed is intrinsic to the nature of the HAS reaction manifold.[4]

Later on, a novel approach for the perfluoroalkylation of substituted aromatic and heteroaromatic compounds **12** was reported based on an inexpensive sulfur-containing reductant ($Na_2S_2O_4$) and perfluoroalkyl chlorides **13** as radical sources (Figure 3.6).[15] The dithionite anion ($S_2O_4^{2-}$) undergoes dissociation under thermal activation to yield two equivalents of $SO_2^{\bullet-}$ radical anion. This radical anion then triggers the formation of the electron-deficient radical R_F• through the reductive cleavage of the perfluoroalkyl chloride C-Cl bond *via* a SET mechanism. The electron-donating ability and the relative position of the substituents on the aromatic ring have a key role in dictating both the regioselectivity and the overall yield of the radical addition process. For example,

[15] Huang, X.-T.; Long, Z.-Y.; Chen, Q.-Y. "Fluoroalkylation of aromatic compounds with per(poly) fluoroalkyl chlorides initiated by sodium dithionite in DMSO" *J. Fluorine Chem.* **2001**, *111*, 107.

electron-poor aromatics (X = NO_2, CF_3) do not react at all. This is consonant with the classical HAS reactivity, where the presence of a strongly electron-withdrawing group greatly reduced the efficiency of the reaction, because of the reduced electron density on the aromatic moiety.[4]

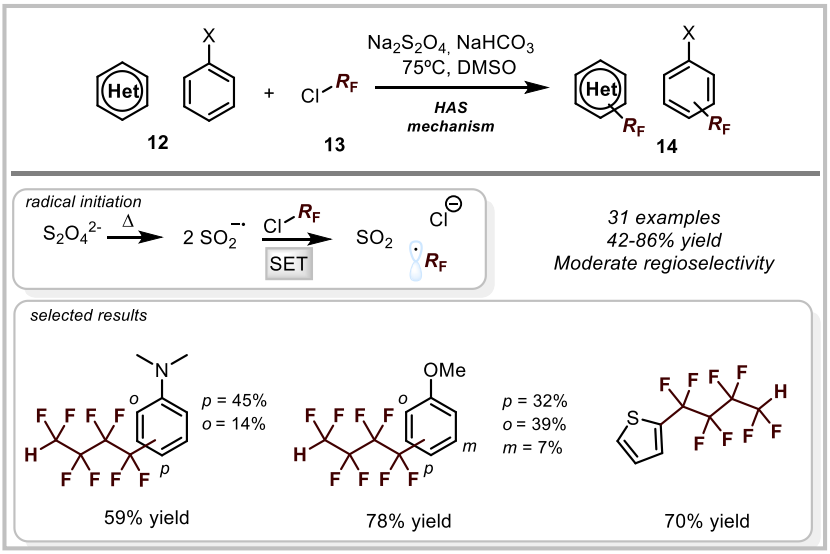

Figure 3.6 An alternative strategy for the perfluoroalkylation of arenes; SET: single-electron transfer.

Organic radical initiators may also be used to generate electrophilic perfluoroalkyl radicals from perfluoroalkyl halides. In 2008, Matsugi and co-workers reported a simple procedure for the direct perfluoroalkylation of substituted phenols **15** using perfluoroalkyl iodides as radical sources (Figure 3.7).[16] The chemistry requires the use of both a stoichiometric amount of an explosive radical initiator (V-70L) to generate the perfluoroalkyl radicals, and a large excess of base (8 equivalents of cesium carbonate) to deprotonate the phenols **15**. The electrophilic radicals (R_F•) selectively react with the two more electron-rich positions of the phenolate anions (*ortho* and *para*), affording the corresponding perfluoroalkylated phenol derivatives **16** in moderate to high yields. Moreover, when the reaction was performed at high temperature (T>100 ºC), the perfluoroalkylation process proceeded without the radical initiator.

[16] Matsugi, M.; Hasegawa, M.; Hasebe, S.; Takai, S.; Suyama, R.; Wakita, Y.; Kudo, K.; Imamura, H.; Hayashi, T.; Haga, S. "Direct perfluoroalkylation of non-activated aromatic C–H bonds of phenols" *Tetrahedron Lett.* **2008**, *49*, 4189.

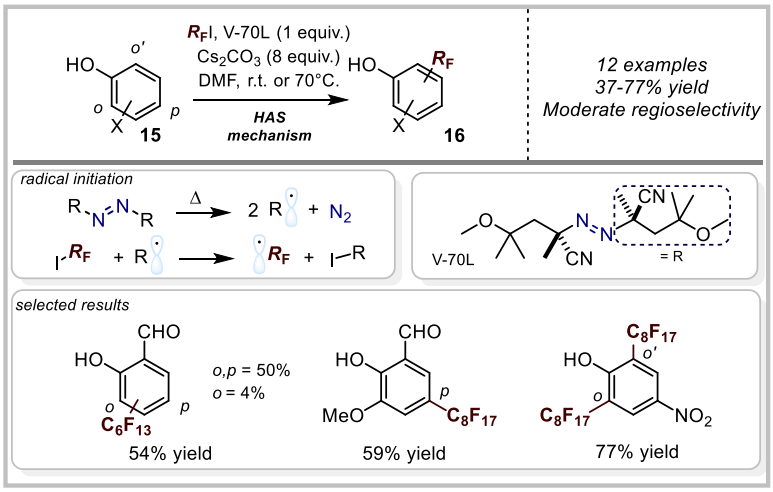

Figure 3.7 Thermal radical perfluoroalkylation of phenols

Recently, Baran developed a C-H trifluoromethylation of heterocycles using a well-known reagent, the Langlois' salt **17** (Figure 3.8).[17]

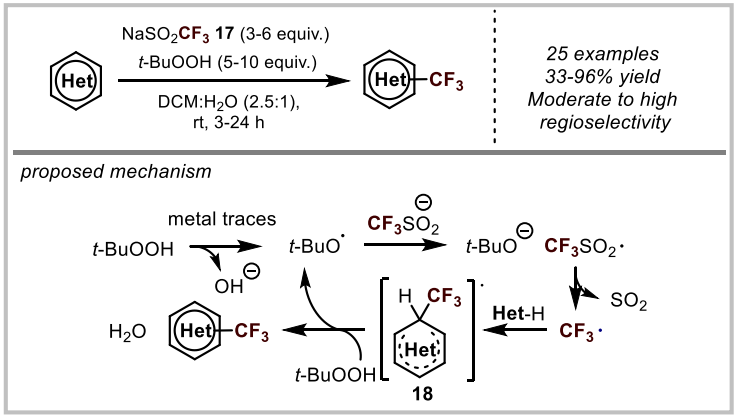

Figure 3.8 Innate C-H trifluoromethylation of heterocycles.

The reaction proceeded at ambient temperature, in aqueous solutions, and under air; however 5-10 equivalents of *tert*-butyl peroxide were needed. The authors proposed a mechanism where adventitious metal traces, present in commercially available CF_3SO_2Na, were responsible of the initial reduction of the peroxide. The resulting *tert*-

[17] Ji, Y.; Brueckl, T.; Baxter, R. D.; Fujiwara, Y.; Seiple, I. B.; Su, S.; Blackmond, D. G.; Baran, P. S. "Innate C-H trifluoromethylation of heterocycles" *Proc. Natl. Acad. Sci. USA* **2011**, *108*, 14411.

butoxy radical was then formed, which could oxidize the trifluoromethanesulfinate ($CF_3SO_2^-$) to the corresponding trifluoromethanesulfinyl radical ($CF_3SO_2\bullet$). Subsequent loss of sulfur dioxide furnished the trifluoromethyl radical ($CF_3\bullet$), which could undergo a HAS chain pathway. Another molecule of *tert*-butyl peroxide was reduced by radical **18** (generated by the attack of the trifluoromethyl radical on the neutral heteroarene, Het-H), therefore starting the radical chain process, and affording the final trifluoromethylated heteroarene upon deprotonation

3.4 Photochemical Radical Perfluoroalkylation of Arenes

The fast-growing field of photoredox catalysis[18] has provided new opportunities for the generation of perfluoroalkyl radicals under mild reaction conditions. In 2011, MacMillan reported an operationally simple strategy for the direct trifluoromethylation of unactivated arenes and heteroarenes **19** through a radical-mediated mechanism.[19] This approach was based on the use of commercially available photocatalysts and a household lightbulb (Figure 3.9).

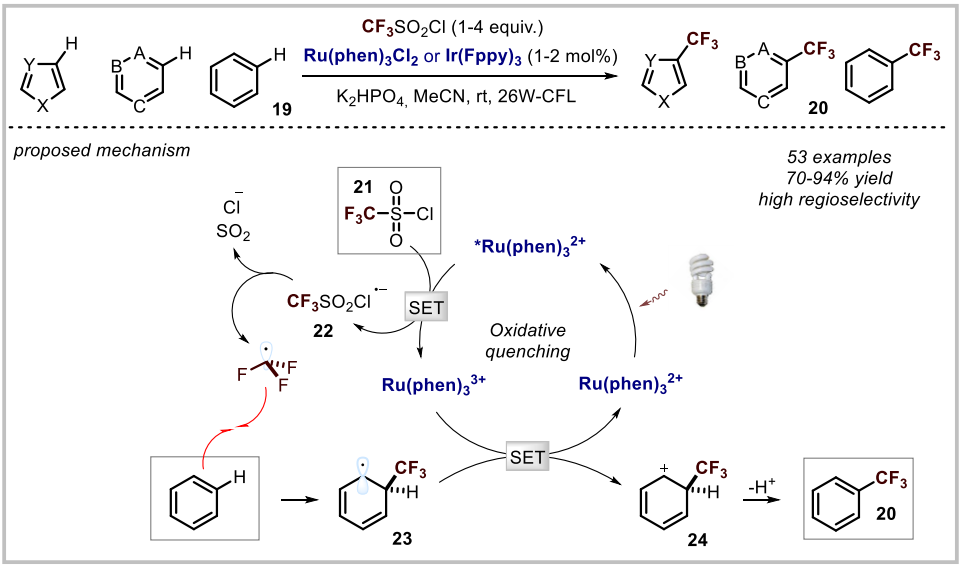

Figure 3.9 Trifluoromethylation of arenes and heteroarenes by means of photoredox catalysis; SET: single-electron transfer.

[18] Shaw, M. H.; Twilton, J.; MacMillan, D. W. C. "Photoredox catalysis in organic chemistry" *J. Org. Chem.* **2016**, *81*, 6898.

[19] Nagib, D. A.; MacMillan, D. W. C. "Trifluoromethylation of arenes and heteroarenes by means of photoredox catalysis" *Nature* **2011**, *480*, 224.

Specifically, under irradiation with visible light the photocatalyst ($Ru(phen)_3^{2+}$) directly reaches an electronically excited-state ($Ru(phen)_3^{2+*}$). The $Ru(phen)_3^{2+*}$ reduces the trifluoromethanosulfonyl chloride **21**, giving the trifluoromethanosulfonyl radical anion **22** and the oxidized Ru(III) complex. The unstable radical anion **22** rapidly undergoes fragmentation to generate the reactive trifluoromethyl radical, along with sulfur dioxide and a chloride anion. The addition of the radical to the aromatic compound provides the cyclohexadienyl radical **23**, which can be easily oxidized by $Ru(phen)_3^{3+}$. The photocatalytic cycle is thus closed. Deprotonation of the positively charged intermediate **24** finally furnishes the trifluoromethylated arenes and heteroarenes **20**.

Later on, Itoh and colleagues reported a direct perfluoroalkylation of arenes and heteroarenes using an organic photoredox catalyst to promote the formation of the perfluoroalkyl radical.[20]

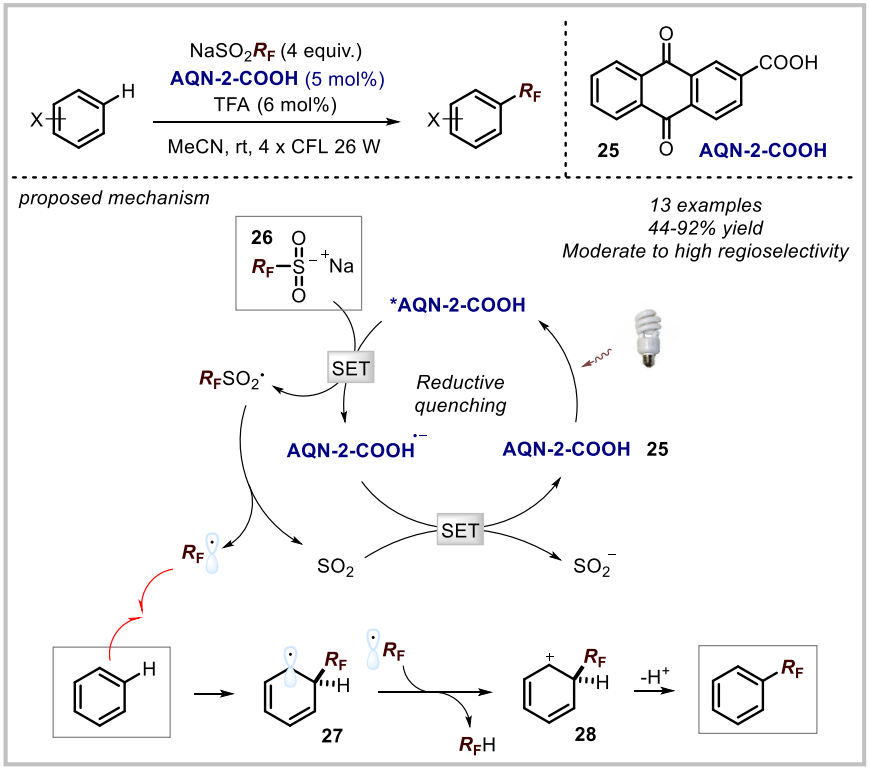

Figure 3.10 Direct C-H perfluoroalkylation of arenes using an organic photoredox catalyst; SET: single-electron transfer.

[20] Cui, L.; Matusaki, Y.; Tada, N.; Miura, T.; Uno, B.; Itoh, A. "Metal-free direct C-H perfluoroalkylation of arenes and heteroarenes using a photoredox organocatalyst" *Adv. Synth. Catal.* **2013**, *355*, 2203.

In this case, an organic molecule, namely anthraquinone-2-carboxylic acid **25**, was used to generate open-shell species from Langlois' salt (Figure 3.10). According to the reported mechanism, the excited-state of anthraquinone **25** oxidizes **26**, providing the corresponding perfluoroalkyl radical R_F• after desulfonative fragmentation of the perfluoroalkylsulfinyl radical (R_FSO_2•) intermediate. The sulfur dioxide then oxidizes the radical anion of the anthraquinone, returning the photocatalyst to the ground-state. At the same time, the perfluoroalkyl radical reacts with the aromatic substrate to yield the cyclohexadienyl radical **27**, which is oxidized to the corresponding cyclohexadienyl cation **28** by a second molecule of perfluoroalkyl radical. Deprotonation provides the desired perfluoroalkylated aromatic compounds.

As briefly mentioned above, in 2014 our research group developed an efficient photochemical protocol for the direct aromatic perfluoroalkylation of α-cyano arylacetates **29** (Figure 3.11).[3] This metal-free process relied on the formation of a photon-absorbing electron donor-acceptor (EDA) complex, generated upon association of perfluoroalkyl iodides **31** (such as $C_6F_{13}I$) with the electron-rich enolate **30**, formed by deprotonating α-cyano arylacetate **29**. Visible light irradiation of the colored EDA complex induced a SET, allowing access to perfluoralkyl radicals **32** under mild conditions. A quantum yield (Φ) of 3.8 was determined (λ = 400 nm), suggesting a radical chain mechanism as the main reaction pathway. Therefore, the perfluoroalkyl radical **32** could react out-of-cage with a second molecule of enolate **30** yielding the corresponding radical-anion **34**. After that, **34** is oxidized by R_FI through a SET mechanism to give the cyclohexadienyl intermediate **35** along with R_F• and the iodide anion. Further deprotonation, followed by an acidic work-up, provided the desired perfluroalkylated aromatic compounds **37**. In 2015, the Maseras group successfully applied DFT methods to elucidate the mechanism of the photochemical aromatic perfluoroalkylation of α-cyano arylacetate.[21] In particular, the observed regioselectivity was explained and the existence of an EDA complex between **30** and **31** was confirmed by calculation. The perfluoroalkylation of **29** with $C_6F_{13}I$ proceeds with good isolated yield (81%), affording the *para* and *ortho* functionalized products **37** in a 2:1 ratio, with a minor amount of the *ortho*-*para* bifunctionalized adduct.[3] The relative Gibbs free energies of activation ($\Delta G^{\ddagger}$) for the radical trapping step were calculated for all possible products, and are $\Delta G^{\ddagger}$= 11.2, 11.7, and 20.8 kcal·mol^{-1} for *para*-**37**, *ortho*-**37** (the HAS products), and for the α-

[21] Fernandez-Alvarez, V. M.; Nappi, M.; Melchiorre, P.; Maseras, F. "Computational study with DFT and kinetic models on the mechanism of photoinitiated aromatic perfluoroalkylations" *Org.Lett.* **2015**, *17*, 2676.

carbonyl-functionalized product (compound **8**, Figure 3.1), respectively.[21] The calculated free energy barriers ($\Delta G^{\ddagger}$) were in good agreement with the experimentally observed regioselectivity.

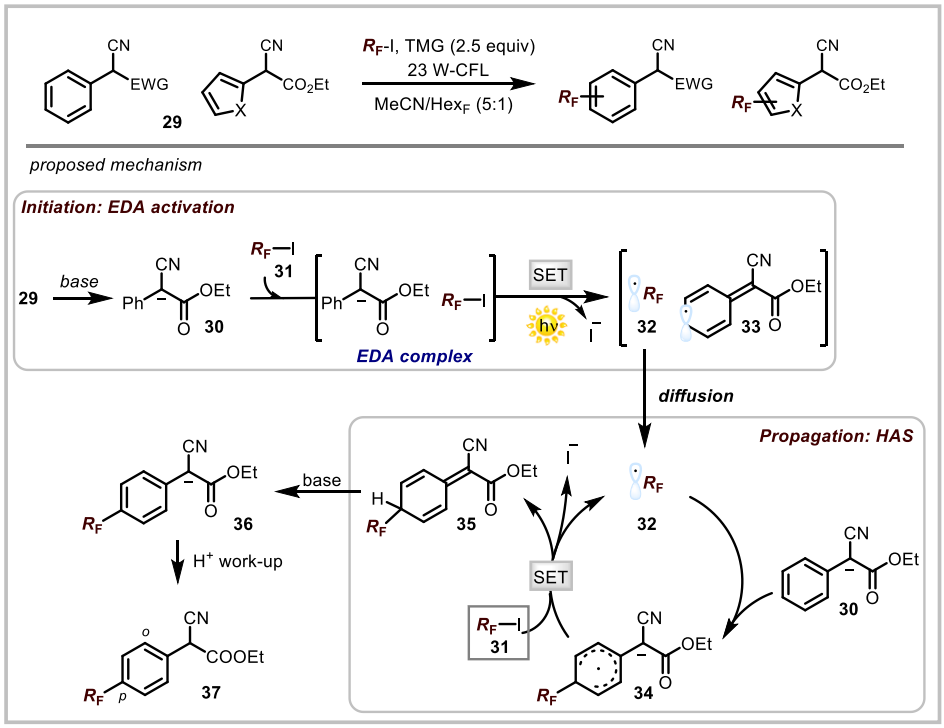

Figure 3.11 Photochemical aromatic perfluoroalkylation of α-cyano arylacetates; Hex_F: perfluorohexane; TMG: 1,1,3,3-tetramethylguanidine; EWG: electron withdrawing group; SET: single-electron transfer.

3.5 Target of the Research Project and Initial Results

As mentioned in the introductive section, we were motivated by the desire to expand the EDA complex activation strategy. In particular, we wondered whether other electron donor substrates than enolates could undergo formation of productive EDA complexes with perfluoroalkyl iodides. We envisioned the possibility of using phenolate anions **42** generated upon facile deprotonation of readily available phenols **41**. Given the electronic similarities to **39**, *in situ* generated phenolate anions **42** were considered as suitable donors (Figure 3.12).

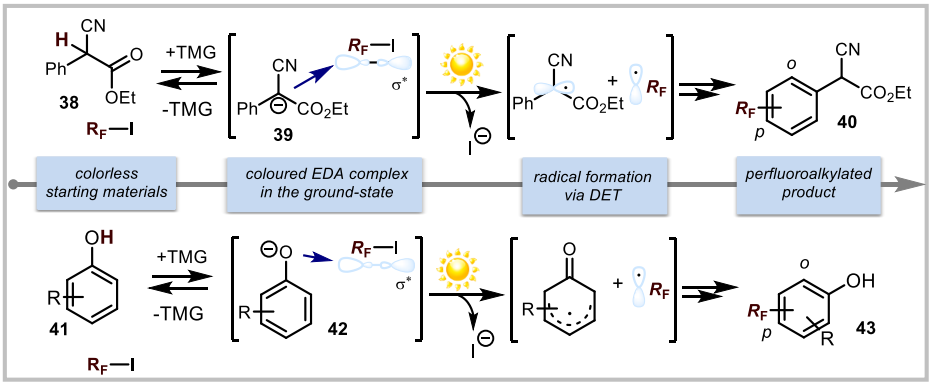

Figure 3.12 Initial idea: using phenolate ions as electron donors for EDA complex formation; DET: dissociative electron transfer. TMG: 1,1,3,3-tetramethylguanidine.

The feasibility of our proposal was tested by reacting salicylaldehyde **41a** with perfluorohexyl iodide **44a** in CH_3CN under irradiation by a 23 W compact fluorescent light (CFL) bulb (Figure 3.13). The reaction was performed in the presence of 1,1,3,3-tetramethyl guanidine (TMG, 1 equiv.) as a base, in order to facilitate the formation of the corresponding phenolate **42a**. The experiment provided both the *ortho* and *para* functionalized products **43a** in a roughly 5:1 ratio, along with the *ortho-para* bifunctionalized adduct *o,p*-**43a** (total yield of 31%).

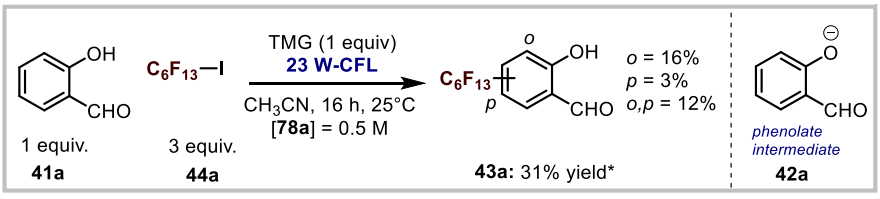

Figure 3.13 The initial experiment; *total yield determined by ^1H and ^{19}F NMR analysis of the crude mixture using 1-fluoro-2-nitrobenzene as the internal standard. TMG: 1,1,3,3-tetramethylguanidine.

3.6 Results and Discussion

After achieving this preliminary indication of the feasibility of the proposed reaction, we tested different inorganic and organic bases in order to improve the reactivity of the perfluoroalkylation of phenols (Table 1). The base was crucial to form the key phenolate anion intermediate **42a** from the phenol **41a**.

Table 1. Base screening and initial control experiments [a]

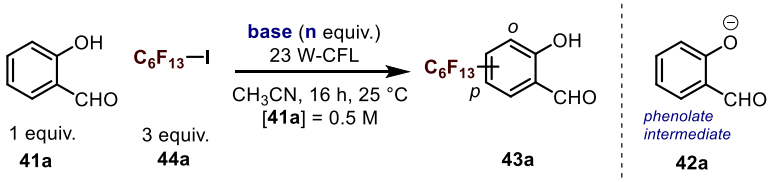

Entry	Base (n)	% Yield[b]	*o*-**43a**[c]	*p*-**43a**[c]	*o*,*p*-**43a**[c]
1	TMG (1.0)	31	52%	9%	39%
2	TMG (2.5)	77	32%	8%	60%
3	TMG (5.0)	78	30%	7%	63%
4[d]	TMG (2.5)	0	-	-	-
5[e]	TMG (2.5)	0	-	-	-
6[f]	TMG (2.5)	0	-	-	-
7	None	0	-	-	-
8	KOH (2.5)	0	-	-	-
9	$NaHCO_3$ (2.5)	0	-	-	-
10	K_2CO_3(2.5)	32	28%	0%	72%
11	Cs_2CO_3 (2.5)	21	5%	0%	95%
12	DBU (2.5)	40	36%	12%	42%
13	DABCO (2.5)	27	35%	27%	38%

[a] Reactions performed on a 0.1 mmol scale using 3 equiv of **44a**, $[\mathbf{41a}]_0$ = 0.5 M, and a 23 W CFL bulb to illuminate the reaction vessel. [b] Total yield determined by ^1H and ^{19}F NMR analysis of the crude mixture using 1-fluoro-2-nitrobenzene as the internal standard. [c] Percent distribution of the *para* (*p*-**43a**), *ortho* (*o*-**43a**) and *ortho*,*para* (*o*,*p*-**43a**) functionalized products. [d] Reaction in the dark. [e] Reaction in air. [f] Reaction performed in the presence of 2 equiv. of TEMPO. TMG: 1,1,3,3-tetramethylguanidine.

Increasing the amount of TMG to 2.5 equivalents (entry 2, Table 1) resulted in a higher reactivity (77% total yield), and the di-perfluorinated adduct *o*,*p*-**43a** was formed as the major product. The use of 5 equivalents of base (TMG) did not bring about any improvement in terms of yield (entry 3, Table 1). At this point, a series of control

experiments were conducted in order to better understand the mechanism of the studied transformation. An experiment showed that the careful exclusion of light completely suppressed the process, thereby proving the photochemical nature of the perfluoroalkylation process (entry 4, Table 1). The inhibition of the reaction was also observed under an aerobic atmosphere, indicating that a radical mechanism was occurring (entry 5, Table 1). This was further corroborated by conducting an experiment in the presence of 2,2,6,6-tetramethylpiperidine 1-oxyl (TEMPO, 2 equiv.), because the final product **43a** was not detected after irradiation with visible light (entry 6, Table 1). In addition, we confirmed that the presence of the phenolate **42a**, formed *in situ* upon deprotonation of **41a**, was essential for reactivity, since the starting materials were completely recovered in the absence of a base (entry 7, Table 1).

Further screening of the bases did not bring any improvement in the efficiency of the model reaction (entries 8-13, Table 1). TMG (2.5 equivalents) turned out to be the best base in the studied transformation (entry 2, Table 1). Recently, the Ritter group found that perfluoroalkyl iodides and TMG form 1:1 halogen bonded adducts.[22] The halogen bond occurs when there is evidence of a net directional attractive interaction between an electrophilic region associated with a halogen atom (also called σ-hole) in a molecular entity and a nucleophilic region in another, or the same, molecular entity.[23] Specifically, the halogen bond between TMG and R_FI can be rationalized as a relatively strong interaction between one of the lone pairs of TMG (electron donor) and the C-I σ*-antibonding orbital (electron acceptor) within the perfluoroalkyl iodide.[22,23] In our system, this interaction may facilitate the carbon-iodine reductive cleavage, thus explaining the high level of reactivity observed with TMG.[24]

We then tested different solvents with the model reaction (entries 2-7, Table 2). Although the use of dichloromethane (DCM), ethyl acetate (EtOAc), dimethylformamide (DMF) and acetone resulted in good reactivity, none of them could rival the performance offered by acetonitrile (CH_3CN). Moreover, variation of the standard reaction parameters, such as temperature, concentration, and stoichiometry, did not afford any improvement to the yield of the model reaction.

---

[22] Sladojevich, F.; McNeill, E.; Borgel, J.; Zheng, S.-L.; Ritter, T. "Condensed-phase, halogen-bonded CF_3I and C_2F_5I adducts for perfluoroalkylation reactions" *Angew. Chem. Int. Ed.* **2015**, *54,* 3712.

[23] Cavallo, G.; Metrangolo, P.; Milani, R.; Pilati, T.; Priimagi, A.; Resnati, G.; Terraneo, G. "The halogen bond" *Chem. Rev.* **2016**, *116,* 2478.

[24] Sun, X.; Metrangolo, P.; Wang, W.; Li, Y.; Yu, S. "Halogen-bond-promoted double radical isocyanide insertion under visible-light irradiation: synthesis of 2-fluoroalkylated quinoxalines" *Org. Lett.* **2016**, *18*, 4638.

Table 2. Solvent screening [a]

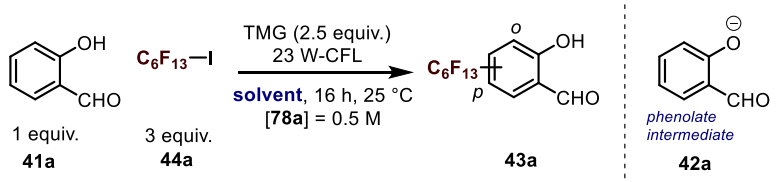

Entry	Solvent	% Yield[b]	*o*-**43a**[c]	*p*-**43a**[c]	*o*,*p*-**43a**[c]
1	CH_3CN	77	32%	8%	60%
2	DCM	62	39%	13%	48%
3	Toluene	36	32%	8%	60%
4	DMF	65	28%	6%	68%
5	MeOH	26	54%	30%	16%
6	Acetone	72	33%	14%	53%
7	EtOAc	70	38%	11%	51%

[a] Reactions performed on a 0.1 mmol scale using 3 equiv. of **44a**, $[\mathbf{41a}]_0$ = 0.5 M, and a 23 W CFL bulb to illuminate the reaction vessel. [b] Total yield determined by ^1H and ^{19}F NMR analysis of the crude mixture using 1-fluoro-2-nitrobenzene as the internal standard. [c] Percent distribution of the *para* (*p*-**43a**), *ortho* (*o*-**43a**) and *ortho*,*para* (*o*,*p*-**43a**) functionalized products.

With the best conditions in hand (CH_3CN and 2.5 equivalents of TMG), we studied the evolution of the product formation over time (Table 3). As shown in Table 3, an induction period was observed in the model reaction. The induction period is defined by IUPAC as the initial slow phase of a chemical reaction which later accelerates.[25] Indeed, after approximately 60 minutes, the reaction rate increased and the total yield of **43a** (purple line) increased rapidly reaching a maximum at about 80% of yield. To account for this initial reactivity profile, we proposed that the presence of trace amounts of molecular oxygen (despite the applied freeze-pump-thaw procedure) retarded the initiation of the reaction by hampering the photo-induced SET processes. This is congruent with the complete loss of reactivity observed when running the reaction in air (entry 4, Table 1).
In addition, the yield of the mono-perfluoroalkylated products *o*-**43a** (blue line) and *p*-**43a** (red line) reached a maximum which then decrease over time. In contrast, the formation of the bifunctionalized adduct *o*,*p*-**43a** (green line) uniformly increased with the reaction progression, indicating that both *o*-**43a** and *p*-**43a** are competent reaction substrates, which were transformed into *o*,*p*-**43a** over time.

[25] McNaught, A. D. "Compendium of chemical terminology" *The Gold Book 2nd Ed.* **1997**, Oxford: Blackwell Science.

Table 3. Evaluation of the total yield and the product distribution over time.

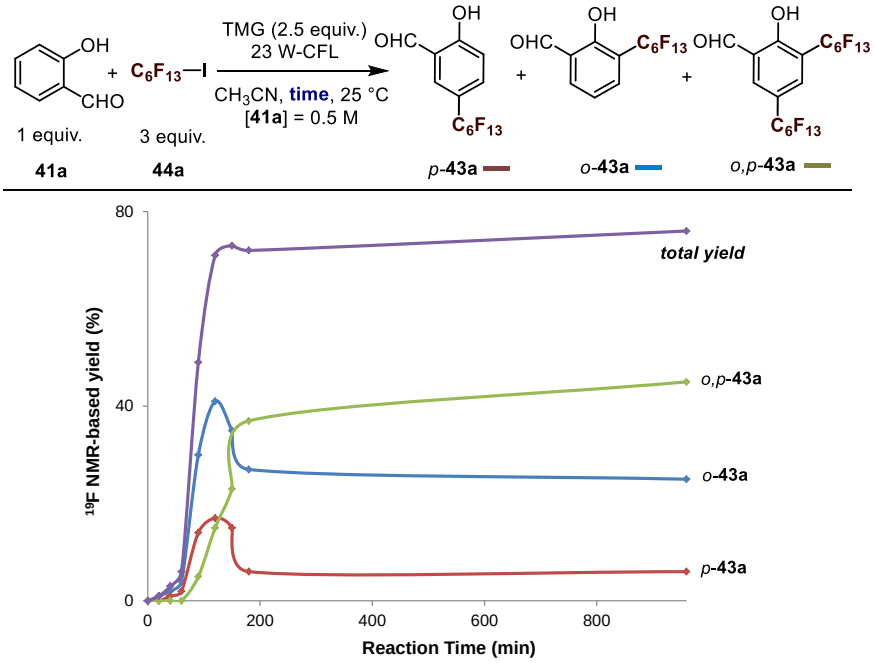

Entry	Time (min)	*o*-**43a** yield[b]	*p*-**43a** yield[b]	*o,p*-**43a** yield[b]	Total yield[b]
1	0	0%	0%	0%	0%
2	20	1%	0%	0%	1%
3	40	2%	1%	0%	3%
4	60	4%	2%	0%	6%
5	90	30%	14%	5%	49%
6	120	41%	17%	15%	71%
7	150	35%	5%	23%	73%
8	180	27%	6%	37%	72%
9	960	25%	6%	46%	77%

[a] Reactions performed on a 0.1 mmol scale using 3 equiv. of **44a**, [**41a**]$_0$ = 0.5 M, and a 23 W CFL bulb to illuminate the reaction vessel. [b] Total yield and distribution of the *para* (*p*-**43a**), *ortho* (*o*-**43a**) and *ortho,para* (*o,p*-**43a**) functionalized products determined by ^{1}H and ^{19}F NMR analysis using 1-fluoro-2-nitrobenzene as the internal standard.

The product distribution and the regioselectivity of the radical process can be rationalized when considering that the phenolate anion intermediate **42a** acts as a strong electron-

donating group. Indeed, the mesomeric effects induce an increase in electronic density at both *ortho* (*o*) and *para* (*p*) positions of the aromatic ring within **42a**. This scenario is supported by the reactivity resonance parameter (σ_R) of the phenolate anion, derived from simple phenol, which is reported to be -0.60[26] (for comparison, an *N*,*N*-dimethyl amino substituent has a σ_R = -0.56).

Next, we evaluated the synthetic potential of the photochemical perfluoroalkylation strategy, reacting differently substituted phenols **41** with perfluorohexyl iodide **44a** (Figure 3.14). As shown in Figure 3.14b, a variety of electron-withdrawing substituents at the *ortho*-position, including aldehyde, ester, bromine, and ketone moieties, were well tolerated under the reaction conditions. The resulting perfluoroalkylation took place with moderate regioselectivity, favoring the formation of the bi-functionalized *ortho*,*para*-adducts *o*,*p*-**43a-d**. Notably, the major isomers could be isolated upon chromatography purification on silica gel, increasing the synthetic utility of the process. Phenols bearing moderate electron-withdrawing group at the *para*-position were also suitable substrates, providing the bifunctionalized *ortho*-adducts *o*,*o'*-**43e-f** in moderate to good yields (Figure 3.14c). The photochemical method was also useful to directly functionalize paracetamol, a widely prescribed pharmaceutical agent used as a mild analgesic. Although paracetamol bears a phenol moiety decorated with a weak electron-donating amide group, the corresponding product *o*,*o'*-**43g** was obtained in 35% yield using a larger excess of **44a** (6 equiv.). An indanone derivative was a suitable substrate, and the resulting adduct *p*-**43h** was isolated in moderate yield (30%).

We also found that the system is amenable to the use of other perfluoralkyl iodides (Figure 3.14d). We focused on a phenol adorned with two electron-withdrawing groups (*o*-ester and *p*-ketone), since the photochemical perfluoroalkylation led to the sole formation of the *ortho*-adducts in high chemical yield. In addition to the perfluorohexyl moiety (product *o*-**43i**), either a shorter or a longer perfluorinated chain were installed in good yield to afford *o*-**43j** and *o*-**43k**, respectively. Interestingly, also a trifluoromethyl fragment could be easily installed starting from gaseous CF_3I (*o*-**43l**).

---

[26] (a) Taft, W. R.; Price, E.; Fox, I. R.; Lewis, I. C.; Andersen, K. K.; Davis, G. T. "Fluorine nuclear magnetic resonance shielding in *p*-substituted fluorobenzenes. The influence of structure and solvent on resonance effects" *J. Am. Chem. Soc.* **1963**, *85,* 3146. (b) Hansch, C.; Leo, A.; Taft, W. R. "A survey of Hammett substituent constants and resonance and field parameters" *Chem. Rev.* **1991**, *9,* 165.

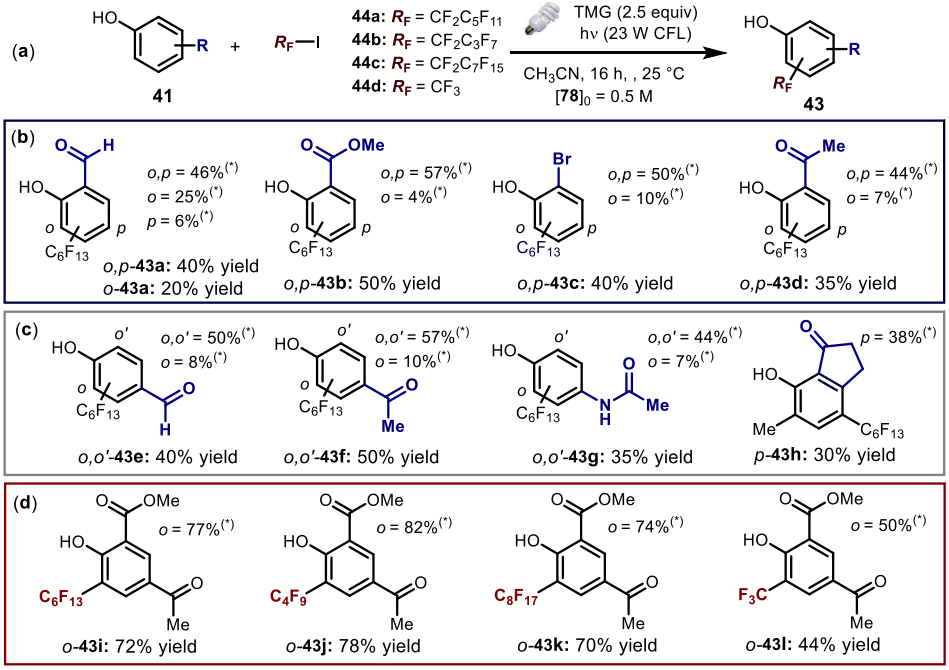

Figure 3.14 Metal-free photochemical aromatic perfluoroalkylation of substituted phenols. The yields refer to the major isolated regioisomeric compounds; [*]^{19}F NMR yields of all the obtained positional isomers, as inferred by analysis of the crude reaction. (**a**) General conditions: reactions performed on a 0.2 mmol scale using 3 equiv. of perfluoroalkyl iodides **44**, 2.5 equiv. of TMG, 0.4 mL of MeCN and a 23 W CFL bulb; an acidic work-up ($HCl_{(aq.)}$, 1M) is required to isolate the products. For the synthesis of compounds **43c**, **43e**, **43f**, and **43g**, 6 equiv. of **44a** have been used. (**b**) Scope of the perfluorohexylation of *o*-substituted phenols. (**c**) Perfluorohexylation of *p*-substituted phenols and of an indanone derivative. (**d**) Scope of the perfluoroalkylating agents.

The limitations of the studied transformation are illustrated in Figure 3.15. In accordance with the classic HAS reactivity, the use of a strong electron-withdrawing substituent, such as a nitro group (NO_2), reduced the yield of the reaction, because of the reduced electron density on the arene (**43m**). Our attempts to react the unsubstituted phenol or a substrate bearing an electron-donating methoxy moiety have met with failure (products **43n** and **43o**). The reason why the presence of an electron withdrawing (EWG) substituent on the phenol ring is essential to ensure a satisfactory level of reactivity will be elucidated in section 3.9 within this Chapter. As expected, the perfluoroalkylation of an *O*-methyl protected phenol did not proceed at all (**43p**), further highlighting the need for the phenolate formation in order to make the photochemical reaction work. The use of phenols substituted at the *ortho*-position with a fluorine atom, an iodine atom, or an amide

group resulted in poor reactivity and regioselectivity (products **43q-s**). Moreover, a heteroaromatic scaffold such as 4-hydroxypyridine was not a suitable substrate (product **43t**). Our attempts to react 2-naphthol, substituted naphthol derivatives, (*R*)-1,1'-Bi-2-naphthol, or a substituted diol met with failure (products **43u-y**).

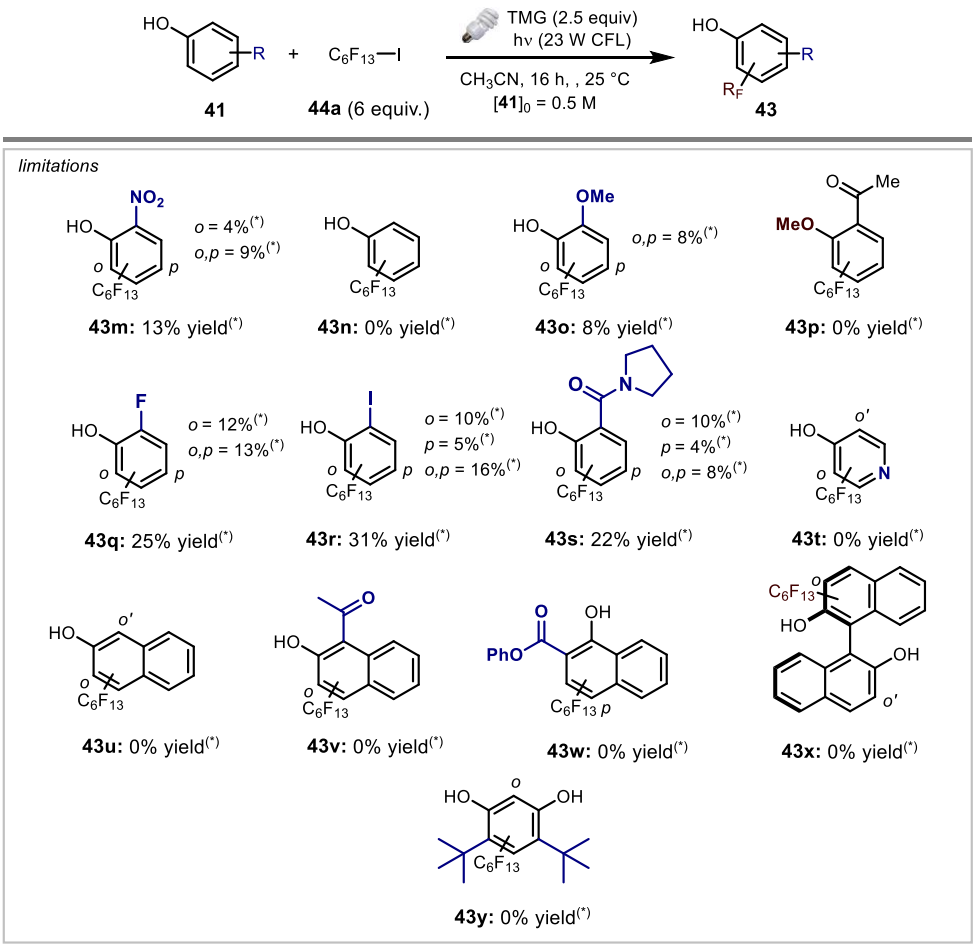

Figure 3.15 Limitations of the photochemical transformation. [*]^{19}F NMR yields of all the obtained positional isomers, as inferred by analysis of the crude reaction.

We then applied our photochemical perfluoroalkylation strategy to *meta*-substituted phenols (Figure 3.16a). The *ortho*-adduct *o*-**45a** was isolated as the major product, while only a minor amount of the *para*-functionalized derivative was formed.

The observed product distribution was likely dictated by steric effects of the *meta*-aryl substituent, which hampered the second perfluoroalkylation event. Interestingly, the

perfluoroalkylated adducts *o*-**45b-d** exhibited axial chirality. This was an unexpected behavior, since open-chain (i.e. non-bridged) bi-*ortho*-substituted biaryl compounds rarely give stable atropisomers at room temperature.[27] The presence of a stable chiral axis was due to the steric interactions between the *ortho*-methyl substituent on the pendant aryl moiety and the perfluoroalkyl fragment, which precluded the possibility for the aryl-aryl single bond to freely rotate.

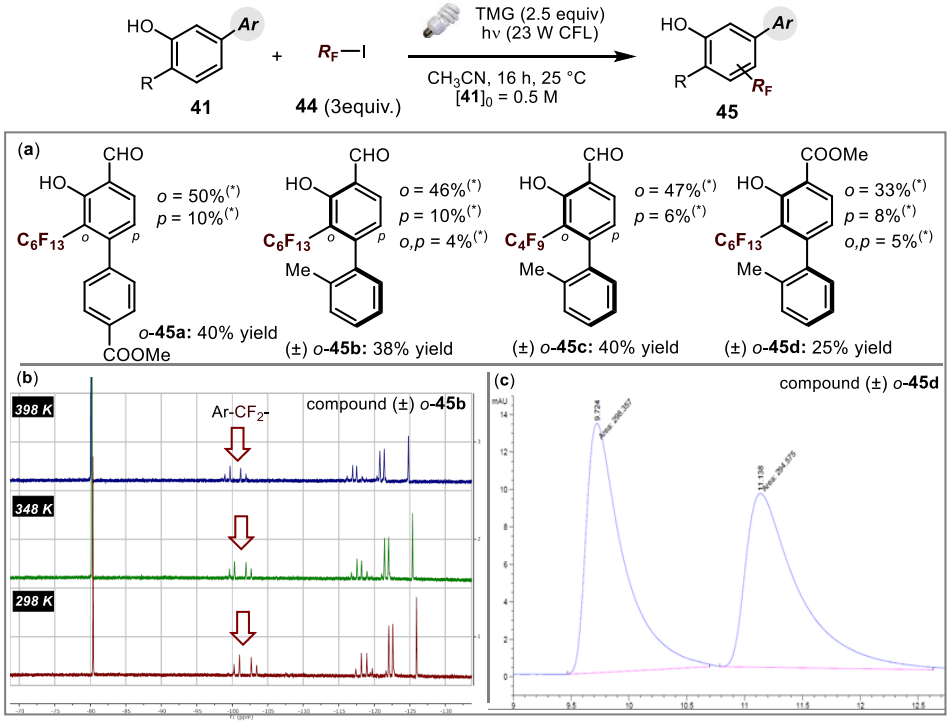

Figure 3.16 (**a**) Metal-free photochemical aromatic perfluoroalkylation of biaryl phenols. The yields refer to the isolated major regioisomeric compounds. (*)^{19}F NMR yields of the minor positional isomers, as inferred by analysis of the crude reaction. (**b**) (VT)-^{19}F NMR studies (376 MHz) of *o*-**45b** in dimethyl sulfoxide-*d6*. Red spectrum: 298 K; green spectrum: 348 K; blue spectrum: 398 K. The red arrows identify the diastereotopic CF_2 signals. (**c**) Chromatographic trace of the two enantiomers of *o*-**45d** (chiral stationary phase column: IC-3; eluent: hexane/dichloromethane 98:2; flow: 0.5 mL/min).

[27] Bringmann, G.; Mortimer, A. J. P.; Keller, P. A.; Gresser, M. J.; Garner, J.; Breuning, M. "Atroposelective synthesis of axially chiral biaryl compounds" *Angew. Chem., Int. Ed.* **2005**, *44*, 5384.

Rotationally hindered biaryl axes are important stereogenic elements found in a large number of natural products, chiral auxiliaries, and catalysts.[28] The configurational stability of the chiral axis in *o*-**45b** was established by means of variable temperature (VT)-^{19}F NMR analyses, conducted in dimethyl sulfoxide-*d6*. The presence of the axial stereogenic element rendered the two fluorine nuclei of the CF_2 group, adjacent to the arene, diastereotopics (Figure 3.16b). Even at a temperature as high as 398 K, we did not observe coalescence of the diastereotopic CF_2 signals, which confirmed the high stability of the chiral axis against rotation. In addition, we found that a perfluorobutyl fragment was bulky enough to block the rotation between the two aromatic systems (product *o*-**45c**). A bi-aryl phenol bearing an ester substituent was also a suitable substrate, since compound *o*-**45d** was isolated in a moderate yield. In this case, the configurational stability of the chiral axis has allowed the separation of the two atropoisomers by HPLC analysis on a chiral stationary phase (Figure 3.16c).

We tried to develop an enantioselective variant of the studied photochemical transformation, capitalizing upon a dynamic kinetic resolution of biaryl atropisomers and using a chiral phase transfer catalyst (PTC in Figure 3.17).

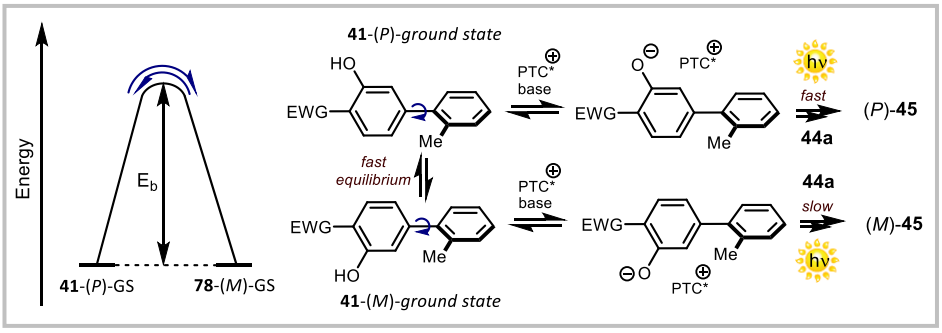

Figure 3.17 Design plan for the photochemical enantioselective variant of the transformation; E_b: rotational energy barrier; PTC: chiral phase transfer catalyst.

Indeed, the biarylic starting material **41** (**o** and **p**) exists in solution as two enantiomeric ground state rotamers (**41**-(*M*)-GS and **41**-(*P*)-GS), which rapidly interconvert via racemization (E_b << 25 Kcal/mol).[27] We surmised that the use of a proper chiral phase transfer catalyst (PTC), along with a suitable base, could lead to an enantio-enriched, axially resolved final product **45** (E_b >25 Kcal/mol) after aromatic perfluoroalkylation by means of a dynamic kinetic resolution. This possibility would require one of the two

[28] Rosini, C.; Franzini, L.; Raffaelli, A.; Salvadori, P. "Synthesis and applications of binaphthylic C_2-symmetry derivatives as chiral auxiliaries in enantioselective reactions" *Synthesis* **1992**, 503.

enantiomers to react much faster than the other, but slower than the rate of interconversion. To test the feasibility of this idea, we focused on the reaction between phenol **41p** (EWG = CO_2Me) and perfluohexyl iodide **44a** (Table 4). All the experiments were conducted over 16 hours, at 25 °C, under irradiation by a 23W CFL. Performing the reaction in the presence of the cinchona derived PTC catalyst **A** and Cs_2CO_3 (2 equiv.), so as to form the corresponding chiral phenolate anion, provided the product *o*-**45d** in very low yield (entry 1, Table 4). Changing the substitution pattern of the benzyl moiety within the PTC had a positive effect on the reactivity (catalyst **B**, entry 2), but either way the target compound was isolated as a racemic mixture. Compound **C** was not a competent catalyst for the studied reaction (entry 3, table 4). The use of **D** as a phase transfer catalyst led to the formation of the desired *ortho*-substituted product (**45d**) in 17% of yield along with detectable enantioselectivity (8% ee, entry 4, Table 4). Using either toluene or chlorobenzene as solvent did not improve the efficiency of the reaction (entries 5-6, Table 4). Other inorganic bases were not suitable for this transformation (entries 7–9, Table 4). We did not observe reactivity using either **E** or **F** as catalysts (entries 10–11, Table 4). The use of the Maruoka-type PTC **G** resulted in the formation of *o*-**45d** in low yield in a racemic form (entry 12, Table 4).[29] Both the chiral guanidinium ion **H** and the chiral tetraaminophosphonium chloride **I** provided *o*-**45d** in moderate chemical yield without any enantioselectivity (entries 13-14, Table 4).

Subsequently, we envisioned the possibility of using a stoichiometric amount of a chiral Brønsted base in order to deprotonate the starting material **41p** (Table 5). The use of 1 equivalent of simple cinchona alkaloids, such as **J** and **K**, led to the formation of the desired product (*o*-**45d**) in very low chemical yield (entries 1-2, Table 5). Increasing the amount of chiral base (**J**) to 2.5 equivalents did not bring about any appreciable improvement in terms of yield (entry 3, Table 5). Using either toluene or acetonitrile as solvent, along with **J** (1 equiv.) as chiral base, did not improve the efficiency of the reaction either (entries 4-5, Table 5). The target *ortho*-substituted product (**45d**) was not obtained using the cinchonine-modified squaramide **L** (entry 6, Table 5). We did not observe satisfactory level of reactivity using either **M** or **N** as chiral bases (entries 7–8, Table 5).

[29] Hashimoto, T.; Maruoka, K. "Recent development and application of chiral phase-transfer catalysts" *Chem. Rev.* **2007**, *107*, 5656.

Table 4. Initial optimization studies: phase transfer catalysis [a]

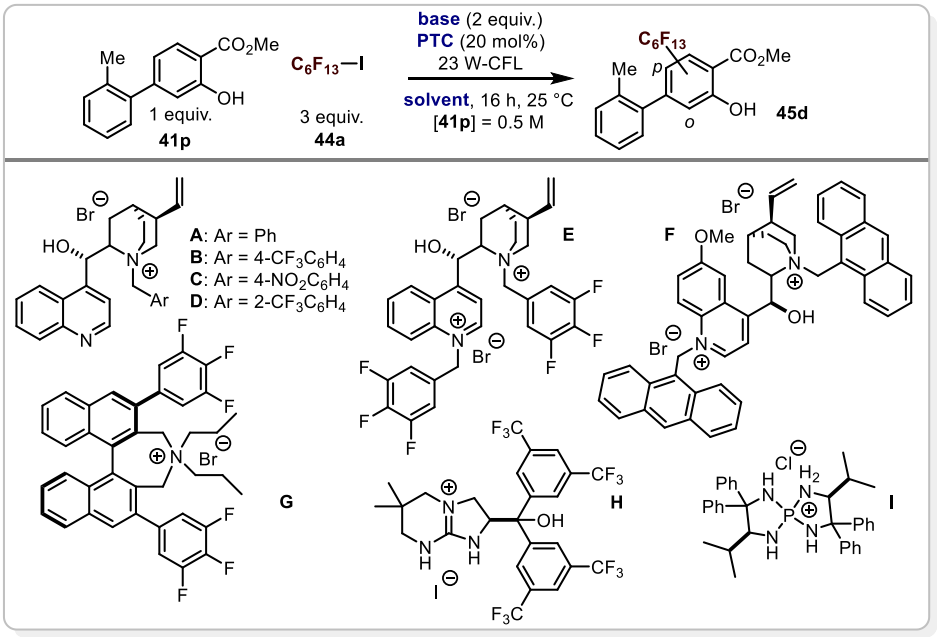

Entry	PTC	solvent	base	*o*-**45d**[b,c]	*p*-**45d**[b,c]	*o*,*p*-**45d**[b,c]	*ee o*-**45d** (%)[d]
1	**A**	DCM	Cs_2CO_3	3%	0%	0%	n.d.
2	**B**	DCM	Cs_2CO_3	16%	3%	0%	0
3	**C**	DCM	Cs_2CO_3	0%	0%	0%	-
4	**D**	DCM	Cs_2CO_3	17%	5%	0%	8
5	**D**	Toluene	Cs_2CO_3	5%	0%	0%	n.d.
6	**D**	C_6H_5Cl	Cs_2CO_3	4%	1%	0%	n.d.
7	**D**	DCM	LiOH	0%	0%	0%	-
8	**D**	DCM	NaOH	0%	0%	0%	-
9	**D**	DCM	K_2CO_3	0%	0%	0%	-
10	**E**	DCM	Cs_2CO_3	0%	0%	0%	-
11	**F**	DCM	Cs_2CO_3	0%	0%	0%	-
12	**G**	DCM	Cs_2CO_3	13%	5%	0%	0
13	**H**	DCM	Cs_2CO_3	30%	9%	2%	0
14	**I**	DCM	Cs_2CO_3	30%	10%	0%	0

[a] Reactions performed on a 0.1 mmol scale [b] Yields determined by ^1H and ^{19}F NMR analysis using 1-fluoro-2-nitrobenzene as the internal standard. [c] Percent distribution of the *para* (*p*-**45d**), *ortho* (*o*-**45d**) and *ortho*,*para* (*o*,*p*-**45d**) functionalized products. [d] Enantiomeric excess determined by HPLC analysis.

Additionally, all our attempts to use **41o** (EWG = CHO) as starting material in the enantioselective variant of the studied photochemical reaction, either under phase transfer catalysis or chiral Brønsted base conditions, have met with failure. Unfortunately, the idea of implementing a dynamic kinetic resolution strategy turned out to be unfeasible.[30]

Table 5. Initial optimization studies: chiral Brønsted bases[a]

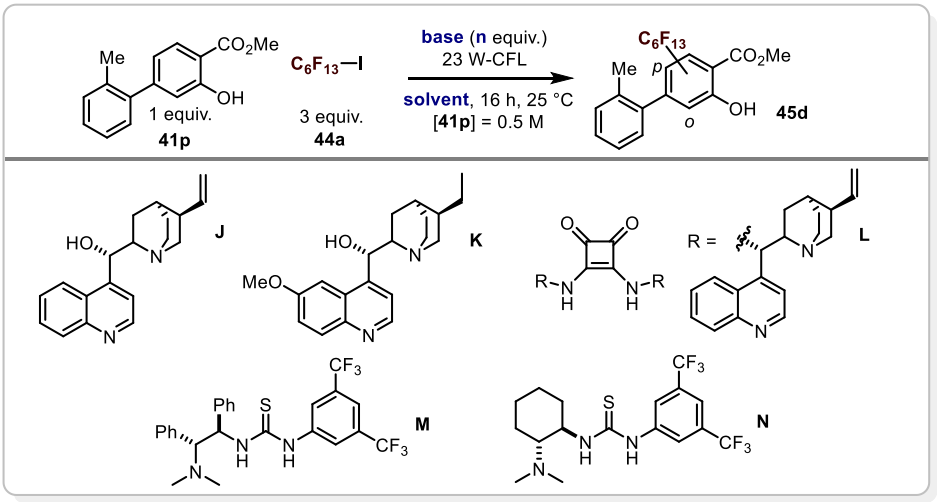

Entry	solvent	base (n)	*o*-**45d**[b,c]	*p*-**45d**[b,c]	*o,p*-**45d**[b,c]	*ee o*-**45d** (%)[d]
1	DCM	**J** (1)	3%	0%	0%	n.d.
2	DCM	**K** (1)	2%	0%	0%	n.d.
3	DCM	**J** (2.5)	5%	0%	0%	n.d.
4	Toluene	**J** (1)	2%	0%	0%	n.d.
5	CH_3CN	**J** (1)	3%	0%	0%	n.d.
6	DCM	**L** (1)	0%	0%	0%	-
7	DCM	**M** (1)	2%	0%	0%	n.d.
8	DCM	**N** (1)	3%	0%	0%	n.d.

[a] Reactions performed on a 0.1 mmol scale [b] Yields determined by ^1H and ^{19}F NMR analysis using 1-fluoro-2-nitrobenzene as the internal standard. [c] Percent distribution of the *para* (*p*-**45d**), *ortho* (*o*-**45d**) and *ortho,para* (*o,p*-**45d**) functionalized products. [d] Enantiomeric excess determined by HPLC analysis.

[30] For recent successful examples, see: a) Gustafson, J. L.; Lim, D.; Miller, S. J. "Dynamic kinetic resolution of biaryl atropisomers via peptide-catalyzed asymmetric bromination" *Science* **2010**, *328*, 1251. b) Barrett, K. T.; Miller, S. J. "Enantioselective synthesis of atropisomeric benzamides through peptide-catalyzed bromination" *J. Am. Chem. Soc.* **2013**, *135*, 2963.

3.7 Mechanistic Investigation

Initially, we recorded the absorption spectra of the reaction components in order to better understand the mechanism of the process (Figure 3.18). While the substrates **41a** (green line), **44a** (purple line), and TMG (grey line) are either slightly colored or colorless, the formation of the phenolate anion **42a**, generated upon TMG addition, induces a strong bathochromic shift (blue line) in the visible region. The addition of the perfluorohexyl iodide **44a** to the phenolate anion **42a** does not lead to any appreciable change of the absorption spectrum (red line perfectly overlays the blue line). According to the latter observation, we could exclude the formation of an EDA complex ground-state association between the phenolate **42a** and the perfluorohexyl iodide **44a**.

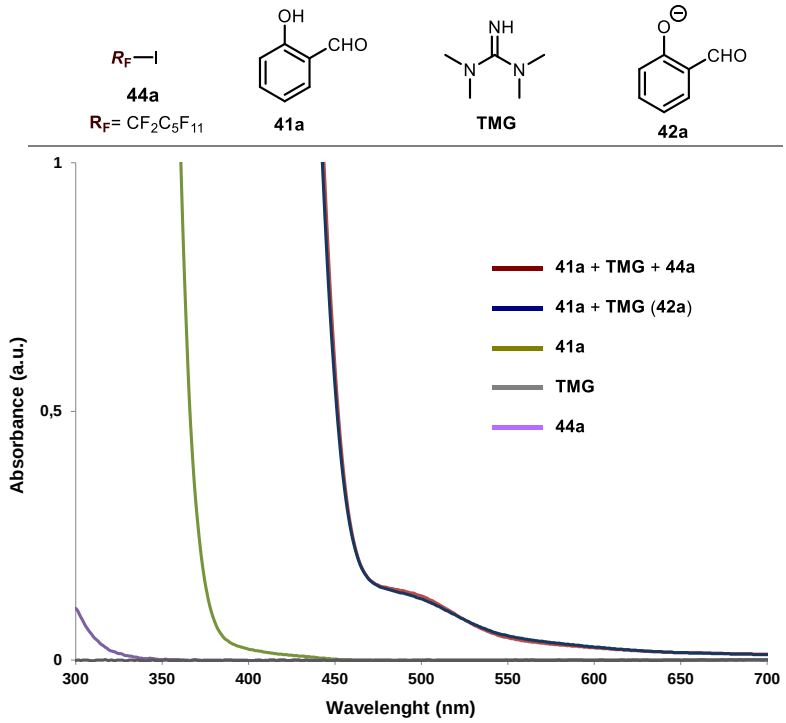

Figure 3.18 Optical absorption spectra recorded in CH_3CN in quartz cuvettes (1 cm path) using a Shimadzu 2401PC UV-visible spectrophotometer. [**44a**] = 0.0025 M, [**41a**] = 0.0075 M; [TMG] = 0.00625 M.

We then performed more mechanistic studies on the model reaction (Table 6). An additional experiment revealed how the use of a 300 W Xenon lamp, equipped with a cut-off filter at 385 nm (irradiation at $\lambda \geq 385$ nm), did not significantly alter the reaction

efficiency (entry 3, Table 6). This result is mechanistically relevant since it excluded a possible homolytic cleavage of the C-I bond in **44a** (not feasible upon irradiation with such low-energy photons) as responsible for the R_F• generation.

Table 6. Mechanistic investigation: source of photons [a]

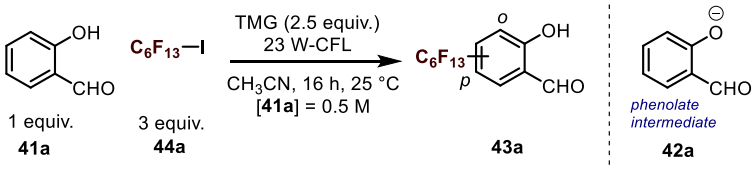

Entry	Deviation from standard conditions	% Yield[b]	*o*-**43a**[c]	*p*-**43a**[c]	*o*,*p*-**43a**[c]
1	none	77	32%	8%	60%
2	dark	0	-	-	-
3[d]	cut off @ 385 nm	68	35%	6%	59%
4[d]	band-pass @ 450 nm	70	33%	7%	60%

[a] Reactions performed on a 0.1 mmol scale using 3 equiv. of **44a**, $[\mathbf{41a}]_0$ = 0.5 M, and a 23 W CFL bulb to illuminate the reaction vessel. [b] Total yield determined by ^{1}H and ^{19}F NMR analysis using 1-fluoro-2-nitrobenzene as the internal standard. [c] Percent distribution of the *para* (*p*-**43a**), *ortho* (*o*-**43a**) and *ortho*,*para* (*o*,*p*-**43a**) functionalized products. [d] Using a 300 W xenon lamp.

A second experiment, conducted using a band-pass filter at 450 nm (irradiation at λ = 450 nm), indicated that the direct photoexcitation of the phenolate **42a** could trigger the radical generation from **44a** (entry 4, Table 2). Indeed, the phenolate anion (**42a**) is the only photo-absorbing species at λ = 450 nm in solution.

To further examine the possible implication of the phenolate within the photochemical regime, we investigated the photoluminescence properties of the intermediate **42a**, prepared by dissolving salicylaldehyde **41a** in freshly distilled TMG (Figure 3.19). The use of neat TMG secured a full deprotonation of the phenol **41a** to the corresponding phenolate anion **42a**.[31] Figure 3.19a shows the absorption spectrum of **42a** in neat TMG. More importantly, we have recorded the emission spectra of **42a** upon excitation at 460 nm (blue line in Figure 3.19b, maximum emission at 490 nm). A series of Stern-Volmer

[31] a) Performing the model reaction in neat TMG ([**41a**] = 0.5 M) over 16 hours did not affect the efficiency of the photochemical perfluoroalkylation, providing a high conversion (about 90%) into the corresponding product **43a**. b) The formation of an EDA complex association between the phenolate **42a** and the perfluorohexyl iodide **44a** in neat TMG was excluded, since the formation of a new absorption band was not observed.

quenching studies was then performed, which revealed that perfluorohexyl iodide **44a** effectively quenched the emission, and therefore the excited state of **42a**.

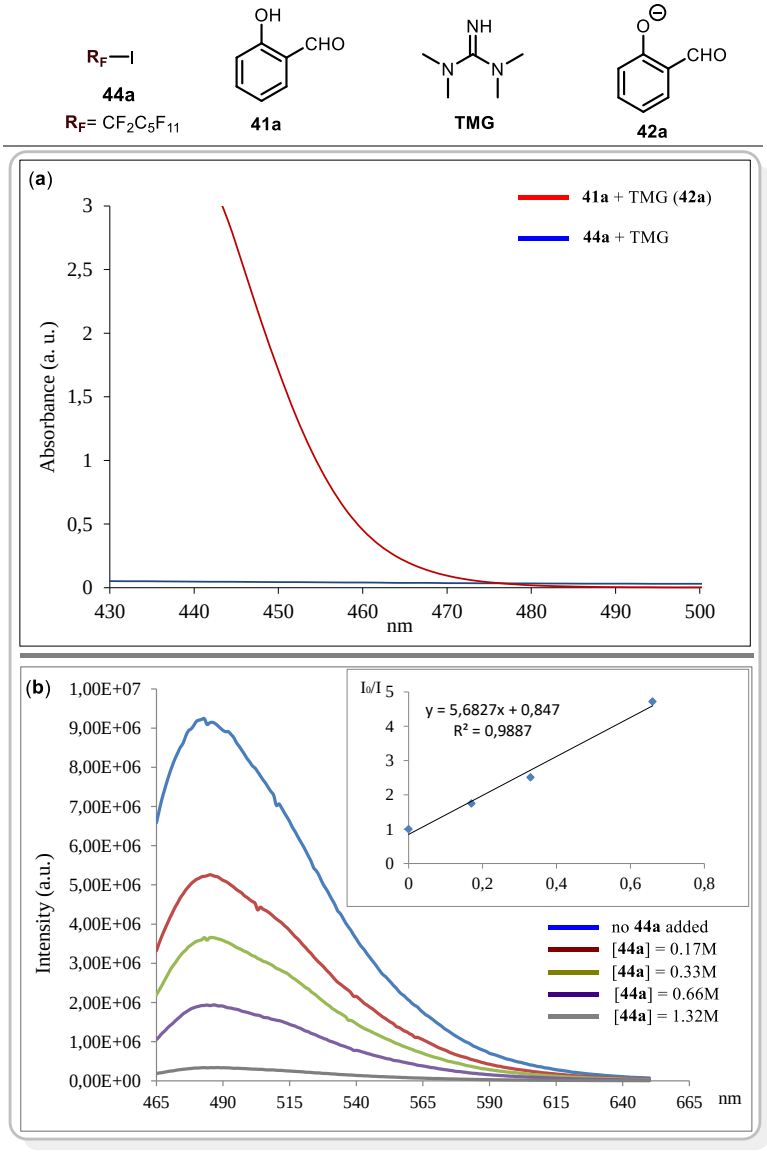

Figure 3.19 (**a**) Optical absorption spectra of **44a** in neat TMG ([**44a**] = 0.021 M, blue line) and of the phenolate **42a** in neat TMG ([**42a**] = 0.007 M, red line). (**b**) Quenching of the phenolate **42a** emission ([**42a**] =7·10^{-3} M in TMG, excitation at 460 nm) in the presence of increasing amounts of perfluorohexyl iodide **44a**.

The data analysis shown in Figure 3.19b revealed a typical linear Stern-Volmer correlation. In general, three types of fluorescence quenching are known (Figure 3.20): (*i*) *inner-filter* effect, (*ii*) dynamic fluorescence quenching, and (*iii*) static fluorescence quenching.[32] *Inner-filter* effect may arise in the case that the quencher compound (Q) absorbs light in the same range of wavelength used for the sample irradiation, thus leading to a less efficient excitation of the fluorophore (F). Dynamic fluorescence quenching arises when the lifetime of the excited states is reduced due to interactions with a quencher, usually caused by electron transfer, energy transfer, or the formation of an excited complex (also known with the term *exciplex*). Static fluorescence quenching may arise in case that an interaction between the fluorophore and the quencher occurs in the ground-state (complex formation, reactions). In our studies, performed in TMG as solvent, both the presence of an *inner-filter* quencher and the possible ground-state aggregation between **42a** and **44a** (static fluorescence quenching) were excluded by recording the absorption spectra of the reaction components (Figure 3.19a).[31] Moreover, a linear Stern-Volmer correlation is observed when only a single type of quenching phenomenon occurs.[32]

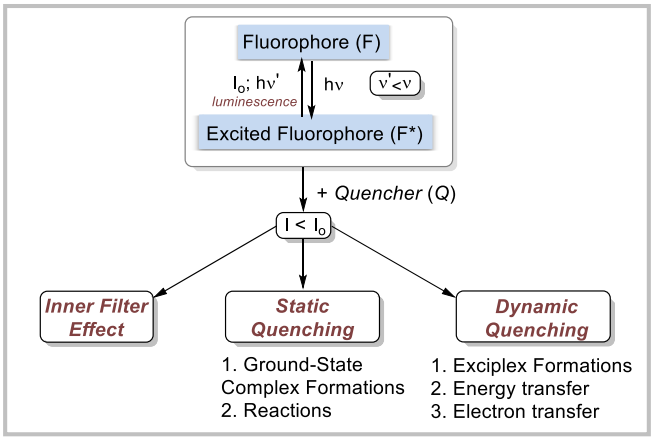

Figure 3.20 Fluorescence quenching mechanisms. F: Fluorophore; I_0: emission intensity of F in the absence of Q; I: emission intensity of F in the presence of Q.

Our mechanistic investigations show the ability of the transiently generated phenolate anion **42a** to directly reach an electronically excited-state upon light absorption while successively triggering the formation of reactive radical species from the perfluorohexyl

[32] Lakowicz, J. R. "Fluorescence quenching" Chapter 9, p. 258 in *Principles of Fluorescence Spectroscopy* **1983**, Premium Press.

iodide **44a**, likely *via* a SET mechanism (dynamic fluorescence quenching). On the basis of our mechanistic studies, we propose a radical chain mechanism for the photochemical perfluoroalkylation of phenols, which follows a classical HAS pathway (Figure 3.21).

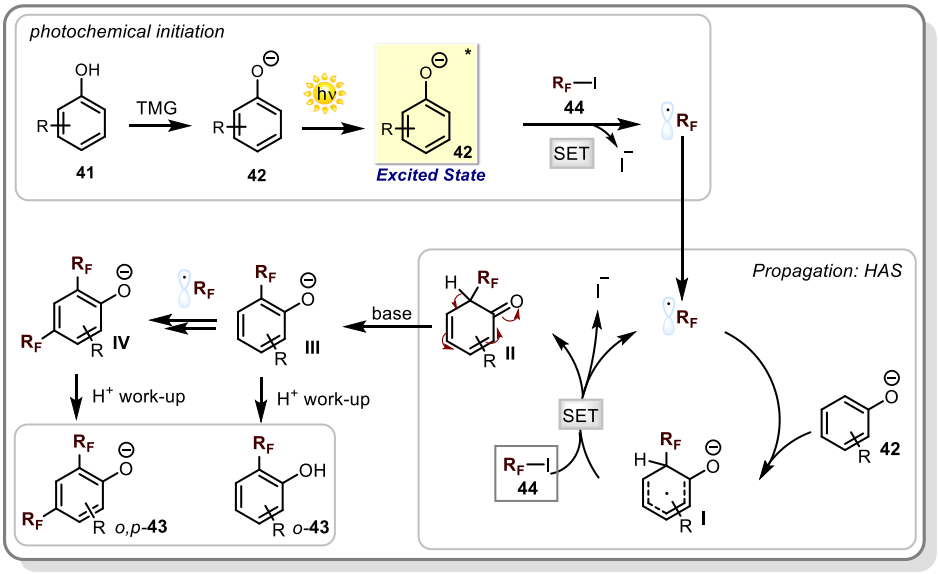

Figure 3.21 Proposed mechanism for the photo-initiated direct perfluoroalkylation of substituted phenols: exploiting the dichotomous reactivity profile of phenolates **42** in the ground- and excited-states. For simplicity, only the pathway that starts with the *ortho*-alkylation is shown.

The reaction is initiated by the photochemical activity of the phenolate anion of type **42**, formed after deprotonation of phenol **41**. Upon light absorption, **42** can directly reach an electronically excited-state (**42***) triggering the formation of the electron-deficient radical R_F• through the reductive cleavage of the perfluorohexyl iodide C-I bond *via* a single electron transfer mechanism. R_F• is then trapped by the ground state phenolate **42** to form the cyclohexadienyl radical anion **I**. We propose that **I** is oxidized by R_FI through a SET mechanism to give the intermediate **II** along with R_F• and the iodide anion. **II** is eventually deprotonated to give the phenolate intermediate **III**. **III** can either undergo a second perfluoroalkylation/deprotonation step, or undergo direct deprotonation to yield the final products upon acidic work-up (*o*-**43** and *o,p*-**43**).

The dichotomous reactivity profile of phenolate anions **42**, which are able to act both as photoinitiators and nucleophiles, allowed the development of a new radical approach for the direct perfluoroalkylation of substituted phenols under very mild reaction conditions.

3.8 Phenolate Anions as Photo-reducing Agents

Phenolate anions of type **42** can directly reach an electronically excited-state **42***, upon light absorption. In the excited-state the arrangement of the electrons are no longer in the lowest energy combination. Indeed, within **42***, one electron populates an antibonding orbital, which is positioned at a greater separation distance from the nucleus (Figure 3.22). For this reason, the ionization potential of the excited phenolate **42*** (IP*) is lower with respect to the ground-state species **42** (IP). In other words, the propensity of excited phenolate **42*** to donate an electron to a suitable acceptor (such as perfluoroalkyl iodide, R_FI) is much higher than the ground-state species **42**. For this reason, **42*** may act as a strong reducing agent.

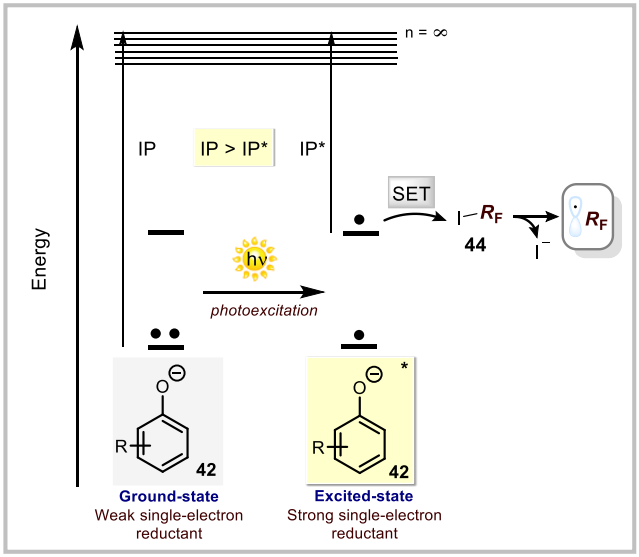

Figure 3.22 Phenolate anions as photo-reducing agents. IP: ionization potential; SET: single-electron transfer.

The propensity of excited phenolates **42*** to undergo ground-state relaxation *via* photo-induced electron ejection has been widely investigated.[33] In fact, studies on electron

[33] a) Ichino, T.; Fessenden, R. W. "Energy requirements for inverted CIDEP in reactions between e_{aq}^- or radical anions and phenoxyl radicals" *J. Phys. Chem. A.* **2003**, *107*, 9257. b) Chen, X.; Larsen, D. S.; Bradforth, S. E. "Broadband spectral probing revealing ultrafast photochemical branching after ultraviolet excitation of the aqueous phenolate anion" *J. Phys. Chem. A.* **2011**, *115*, 3807. c) Wagner, P. J.; Thomas, M. J.; Bradforth, S. E. "Time resolved electron spin resonance spectroscopy. III. Electron spin resonance emission from the hydrated electron. Possible evidence for reaction to the triplet state" *J. Am. Chem. Soc.* **1976**, *98*, 243.

photo-ejection from phenols and phenolates have great biological relevance because of the structural analogies with tyrosine residues contained in proteins.[34] Nonetheless, this photo-induced mechanism has not previously found application in synthetic organic chemistry.

3.9 The Effect of Phenol Substituents on the Photoinitiation Step

The ability of excited-state phenolate anions **42*** to act as reducing agent for the formation of perfluoroalkyl radicals, from R_FI, *via* SET mechanism, has been the key for the development of this transformation. The UV-VIS absorption spectra of some of the phenolate anions (**42 a**,**c**,**g**,**f**,**m**) used in this project, are shown in Figure 3.23a. In all cases, the addition of 2.5 equiv. of TMG to all the phenol (**41**) solutions led to the formation of a new absorption band, indicating the transient formation of the related phenolate anions **42**. The absorption properties of the phenolates **42** depend strongly on the electronic nature of the substituent(s) on the aromatic rings. The phenolate anions bearing EWG(s) (**42a**,**c**,**m)** can reach an electronically excited-state upon irradiation with the 23W-CFL bulb (emission spectrum, Figure 3.23b). This is the reason why compounds **41a**,**c**,**m** are suitable substrates for our photochemical perfluoroalkylation protocol. On the other hand, the lack of reactivity observed with **41g**,**f** is due to the fact that their corresponding phenolate anions (**42g**,**f**) may not absorb the photons emitted by the lamp used, therefore not initiating the radical process. In addition, phenols **41g**,**f** have not been successfully transformed into the corresponding perfluoroalkylated adducts even using a mercury-vapor lamp (irradiation at λ = 254 nm) as photons source because the use of these high energy photons resulted in a complete degradation of the starting materials.

[34] a) Itoh, S.; Taki, M.; Fukuzumi, S. "Active site models for galactose oxidase and related enzymes" *Coord. Chem. Rev.* **2000**, *198*, 3. b) Bent, D. V.; Hayon, E. "Excited state chemistry of aromatic amino acids and related peptides. I. Tyrosine" *J. Am. Chem. Soc.* **1975**, *97,* 2599.

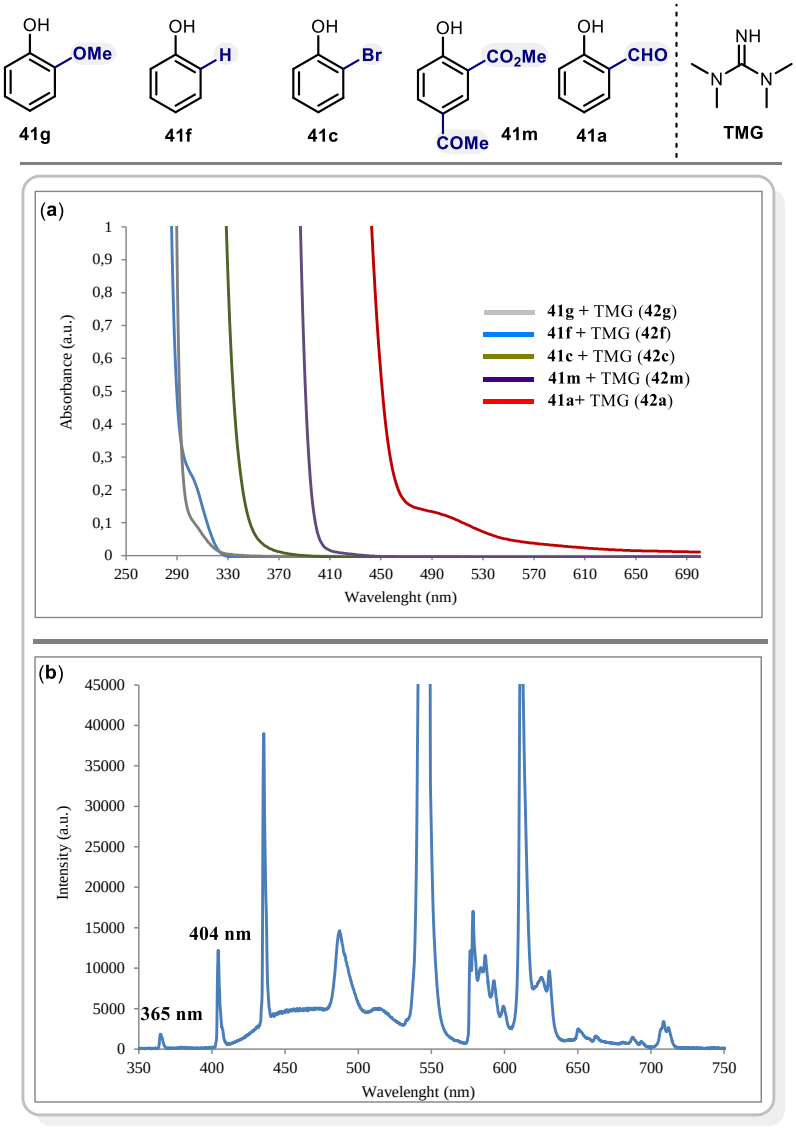

Figure 3.23 (**a**) Optical absorption spectra recorded in CH_3CN in quartz cuvettes (1 cm path) using a Shimadzu 2401PC UV-visible spectrophotometer. [**41**] = 0.0075 M; [TMG] = 0.00625 M. (**b**) Emission spectrum of the 23W-CFL used in our experiments.

3.10 Conclusions

In summary, we have developed a direct and effective strategy to install perfluoroalkyl and trifluoromethyl groups on the aromatic ring of substituted phenols. The reaction protocol is operationally simple, conducted at ambient temperature with readily available

substrates and reagents, and using household CFL bulbs as the light source. The chemistry is driven by the ability of phenolate anions to act as a photo-reducing agents upon visible-light excitation, triggering the formation of perfluoroalkyl radicals *via* SET mechanism under mild conditions.

3.11 Experimental Section

3.11.1. General Information

All reactions were performed under an argon atmosphere in oven dried glassware using standard Schlenk techniques, unless otherwise stated. Synthesis grade solvents were used as purchased and the reaction mixtures were deoxygenated by three cycles of freeze-pump-thaw. Chromatographic purification of products was accomplished using flash chromatography (FC) on silica gel (35-70 mesh). For thin layer chromatography (TLC) analysis throughout this work, Merck precoated TLC plates (silica gel 60 GF_{254}, 0.25 mm) were employed, using UV light as the visualizing agent and an acidic mixture of *para*-anisaldehyde or basic aqueous potassium permanganate ($KMnO_4$) stain solutions, and heat as developing agents. Organic solutions were concentrated under reduced pressure on a Buchi rotatory evaporator. The NMR spectra were recorded at 400 MHz for ^{1}H, 101 MHz for ^{13}C and 376 MHz for ^{1}H decoupled ^{19}F. The chemical shift (δ) for ^{1}H, ^{13}C and ^{1}H decoupled ^{19}F are given in ppm relative to residual signals of the solvents ($CHCl_3$ @ 7.26 ppm ^{1}H NMR and 77.16 ppm ^{13}C NMR, and tetramethylsilane @ 0 ppm). Coupling constants are given in Hertz. The following abbreviations are used to indicate the multiplicity: s, singlet; d, doublet; q, quartet; m, multiplet; bs, broad signal. Mass spectra (high and low resolution) were obtained from the ICIQ High Resolution Mass Spectrometry Unit on a Bruker Maxis Impact (QTOF) or Waters Micromass LCT-Premier (TOF) in Electrospray Ionization (ESI) by direct infusion. UV-VIS measurements were carried out on a Shimadzu UV-2401PC spectrophotometer equipped with photomultiplier detector, double beam optics and D2 and Wlight sources. The emission spectra were recorded in a Fluorolog Horiba Jobin Yvon spectrofluorimeter equipped with photomultiplier detector, double monochromator and 350 W xenon light source. Cut-off and band-pass photochemical experiments have been performed using a 300 W Xenon lamp (Asashi Spectra Co., Ltd.) to irradiate the reaction mixture. Reagents were purchased at the highest commercial quality and used without further purification, unless otherwise stated.

Catalysts **A**, **B**, **C** and **D** were synthetized within the Melchiorre group according to a reported procedure.[35] Catalysts **E** and **F** were synthetized within the Melchiorre group according to a reported procedure.[36] Catalyst **H** was synthetized within the Melchiorre group according to a reported procedure.[37] Catalyst **L** was synthetized within the Melchiorre group according to a reported procedure.[38] Catalysts **M** and **N** were synthetized within the Melchiorre group according to a reported procedure.[39]

^{1}H NMR and ^{13}C NMR spectra of the starting material and the final products are available in the published manuscript[1] and are not reported in the present thesis.

3.11.2. Synthesis of starting materials

General Procedure for **41n-41o**:

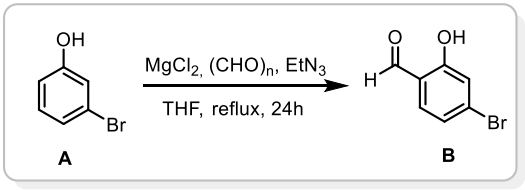

To a stirred solution of phenol derivative **A** (20 mmol) in freshly distilled THF (100 mL) in a 250 mL two neck round bottom flask, was added anhydrous magnesium chloride (30 mmol), paraformaldehyde (135 mmol) and triethylamine (75 mmol) at ambient temperature. The reaction mixture was stirred at reflux for 24 h. After completion of the reaction (monitored by TLC), the mixture was cooled to room temperature and quenched with 1M aqueous HCl solution. The organic layers were separated and the aqueous layer was extracted with ethyl acetate. The combined organics were dried over anhydrous

---

[35] Arai, S.; Hamaguchi, S.; Shioiri, T. "Catalytic asymmetric Horner-Wadsworth-Emmons reaction under phase-transfer-catalyzed conditions" *Tetrahedron Letters* **1998**, *39*, 2997.

[36] Xiang, B.; Belyk, K. M.; Reamer, R. A.; Yasuda, N. "Discovery and application of doubly quaternized cinchona-alkaloid-based phase-transfer catalysts" *Angew. Chem. Int. Ed.* **2014**, *53,* 8375.

[37] Misaki, T.; Takimoto, G.; Sugimura, T. "Direct asymmetric aldol reaction of 5H-oxazol-4-ones with aldehydes catalyzed by chiral guanidines" *J. Am. Chem. Soc.* **2005**, *132*, 6286.

[38] Lee, J. V.; Ryu, T. H.; Oh, J. S.; Bae, H. Y.; Jang, H. B.; Song, C. E. "Self-association-free dimeric cinchona alkaloid organocatalysts: unprecedented catalytic activity, enantioselectivity and catalyst recyclability in dynamic kinetic resolution of racemic azlactones" *Chem.Commun.* **2009**, 7224.

[39] Okino, T.; Hoashi, Y.; Furukawa, T.; Xu, X.; Takemoto, Y. "Enantio-and diastereoselective Michael reaction of 1,3-dicarbonyl compounds to nitroolefins catalyzed by a bifunctional thiourea" *J. Am. Chem. Soc.* **2005**, *127,* 119.

Na_2SO_4, filtered, and concentrated under reduced pressure to afford the crude salicylaldehyde derivative **B**. The crude product was purified by flash chromatography (silica; hex /EtOAc) to give the desired product **B** (isolated yields ranging from 40%).[40]

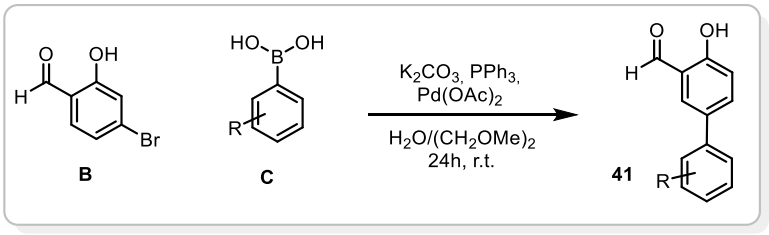

5-Bromosalicylaldehyde **B** (1 g, 4.97 mmol), K_2CO_3 (2.061 g, 14.91 mmol), boronic acid C (5.47 mmol), triphenylphosphine (TPP, 1 mol %), and $Pd(OAc)_2$ (1 mol %) were taken in a 1:1 DME:water mixture (12 mL). The mixture was stirred at room temperature under an atmosphere of nitrogen for 24 h. The reaction mixture was acidified using HCl (1N) on an ice bath, followed by extraction with ethyl acetate. The extracts were combined, dried ($MgSO_4$), and the solvent was removed under vacuum. The crude solid was purified by flash chromatography to isolate the desired salicylaldehyde **41.**[41]

Methyl 4'-formyl-3'-hydroxy-[1,1'-biphenyl]-4-carboxylate (**41n**).

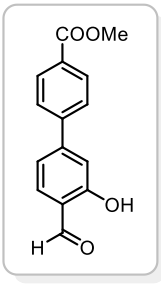

Yield 40%.

^{1}H NMR (400 MHz, $CDCl_3$) δ 11.11 (s, 1H), 9.95 (s, 1H), 8.16-8.11 (m, 2H), 7.71-7.63 (m, 3H), 7.30-7.22 (m, 2H), 3.96 (s, 3H).

^{13}C NMR (101 MHz, CDCl3) δ 196.21, 166.80, 162.04, 148.65, 143.81, 134.34, 130.39, 127.52, 120.18, 119.12, 116.40, 52.44.

[40] Jin, Z.; Yang, R.; Du, Y.; Tiwari, B.; Ganguly, R.; Chi, Y. R. "Enantioselective intramolecular formal [2+4] annulation of acrylates and α,β-unsaturated imines catalyzed by amino acid derived phosphines" *Org. Lett.* **2012**, *14*, 3226.

[41] Das, S. G.; Doshi, J. M.; Tian, D.; Addo, S. N.; Srinivasan, B.; Hermanson, D. L.; Xing, C. "Structure−activity relationship and molecular mechanisms of ethyl 2-amino-4-(2-ethoxy-2-oxoethyl)-6-phenyl-4H-chromene-3-carboxylate (sHA 14-1) and its analogues" *J. Med. Chem.* **2009**, *52*, 5937.

3-hydroxy-2'-methyl-[1,1'-biphenyl]-4-carbaldehyde (**41o**).

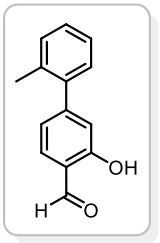

Yield 96%.

^{1}H NMR (400 MHz, $CDCl_3$) δ 11.11 (s, 1H), 9.94 (s, 1H), 7.59 (d, *J* = 7.85 Hz, 1H), 7.36-7.20 (m, 4H), 7.02-6.94 (m, 2H), 2.29 (s, 3H). ^{13}C NMR (101 MHz, $CDCl_3$) δ 196.28, 161.54, 151.44, 140.47, 135.19, 133.51, 130.75, 129.33, 128.36, 126.10, 121.43, 119.49, 118.40, 20.49.

Preparation of **41p**:

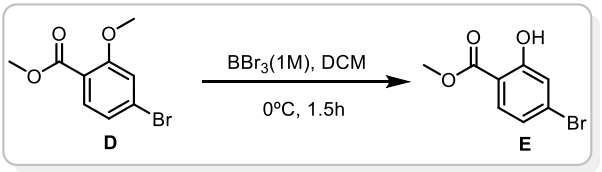

A solution of 1.0 M boron tribromide (44.0 mL, 44 mmol) in DCM (20 mL) was cooled to 0 ºC. **D** (17.4 mmol) dispersed in DCM (120 mL) was slowly added to the tribromide-solution during 20 minutes. The reaction mixture was vigorously stirred for 1.5 h at 0 ºC. Water was added and the organic phase was separated. The aqueous phase was extracted with DCM and EtOAc. The combined organic phases were dried ($MgSO_4$) and evaporated under reduced pressure to give a white powder. The crude solid was purified by flash chromatography to isolate the desired product **E** (yield 94%).

Product **41p** was synthetized from **E** according to the procedure previously described.

Methyl 3-hydroxy-2'-methyl-[1,1'-biphenyl]-4-carboxylate (**41p**).

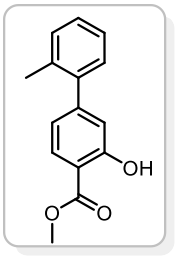

Yield 90%.

^{1}H NMR (400 MHz, $CDCl_3$) δ 10.81 (s, 1H), 7.87 (d, *J* = 8.2 Hz, 1H), 7.31-7.18 (m, 4H), 6.95 (d, *J* = 1.5 Hz, 1H), 6.85 (dd, *J* = 8.2, 1.7 Hz, 1H), 3.98 (s, 3H), 2.28 (s, 3H).

^{13}C NMR (101 MHz, CDCl3) δ 170.69, 161.43, 149.98, 140.75, 135.23, 130.63, 129.70, 129.39, 128.06, 126.00, 120.71, 118.29, 111.04, 52.44, 20.49.

3.11.3. Synthesis of catalyst I

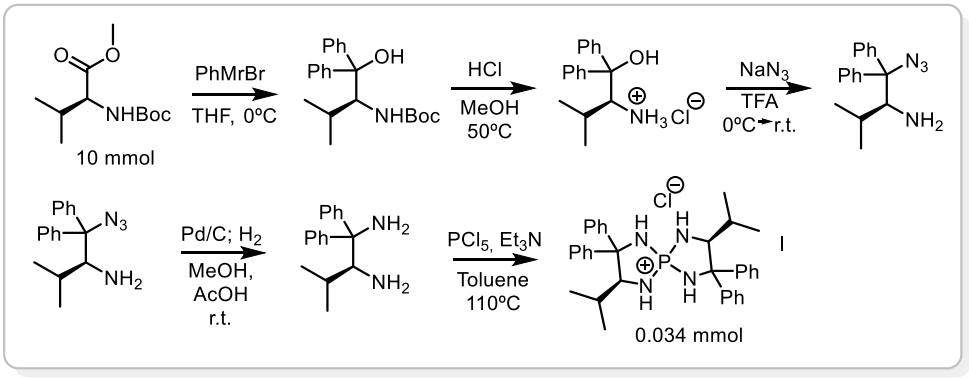

The chiral tetraaminophosphonium chloride **I** was synthesized according to a five-step reported procedure.[42] The characterization of compound **I** matches with the data reported in the literature.

3.11.4. General procedures for the light-driven perfluoroalkylation of phenols

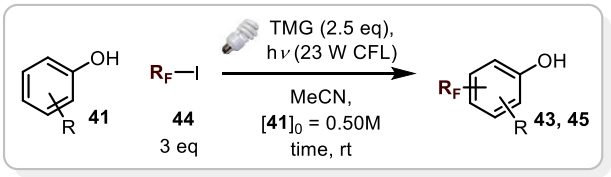

A 10 mL Schlenk tube was charged with the appropriate phenol **41** (0.2 mmol), acetonitrile (0.4 mL, 0.5 M referring to 2), perfluoroalkyl iodide **44** (0.6 mmol, 3 equiv) and *N,N,N',N'*-tetramethylguanidine (0.063 mL, 0.5 mmol, 2.5 equiv). The reaction mixture was thoroughly degassed via 3 cycles of freeze pump thaw, and the vessel was refilled with argon, sealed, and positioned approximately 5 cm away from a household full spectrum 23 W compact fluorescent light (CFL). For the preparation of the trifluoromethylated phenol **43m**, the trifluoroiodomethane (0.6 mmol, 15 mL, gas) was added via gas syringe at -196 ºC (nitrogen bath) after freeze pump thaw of the reaction mixture. After stirring for the indicated time, the reaction was diluted with DCM, quenched with aqueous HCl 1 M solution and extracted 3 times with DCM. The organic phase was then dried and the solvent removed under reduced pressure. The residue was purified by flash column chromatography on silica gel to afford the title compounds **43** and **45**.

---

[42] Uraguchi, D.; Sakaki, S.; Ooi, T. "Chiral tetraaminophosphonium salt-mediated asymmetric direct Henry reaction" *J. Am. Chem. Soc.* **2007**, *129*, 12392.

2-hydroxy-3,5-bis(perfluorohexyl)benzaldehyde (*o,p*-43a)

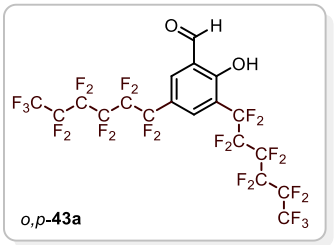

The title compound was isolated in 40% yield (58 mg) as a colorless oil by chromatography using a gradient eluent of hexane/ethyl acetate (*Rf*=0.25 hexane/ethyl acetate 20:1). The characterization of compound (*o,p*-**43a**) matches with the data reported in the literature.[16] ^{1}H NMR (400 MHz, $CDCl_3$) δ 12.20 (s, 1H), 10.02 (s, 1H), 8.03 (d, *J* = 2.28 Hz, 1H), 7.93 (d, *J* = 2.29 Hz, 1H). ^{19}F NMR decoupled ^{1}H (376 MHz, $CDCl_3$) δ -81.00 (m, 6F), -109.42 (t, *J* = 14.61 Hz, 2F), -110.75 (t, *J* = 14.42 Hz, 2F), -121.47 (m, 4F), -121.88 (m, 4F), -122.88 (m, 4F), -126.26 (m, 4F). ^{13}C NMR (101 MHz, $CDCl_3$) δ 195.72, 163.31, 136.70, 134.6, 121.34, 120.65 (t, *J* = 26.26 Hz), 118.56 (t, *J* = 24.13 Hz). HRMS calculated for $C_{19}H_3F_{26}O_2$ (M-H): 756.9723, found: 756.9735.

2-hydroxy-3-(perfluorohexyl)-benzaldehyde (*o*-43a)

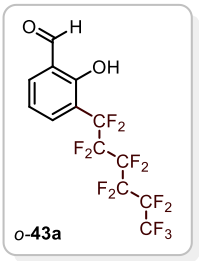

The title compound was isolated in 20% yield (16 mg) as a colorless oil by chromatography using a gradient eluent of hexane/ethyl acetate (*Rf*=0.33 hexane/ethyl acetate 20:1). The characterization of the compound matches with the data reported in the literature.[16] ^{1}H NMR (400 MHz, $CDCl_3$) δ 11.84 (s, 1H), 9.96 (s, 1H), 7.83-7.72 (m, 2H), 7.16 (t, *J* = 7.8 Hz, 1H). ^{19}F NMR decoupled ^{1}H (376 MHz, $CDCl_3$) δ -80.88 (m, 3F), -109.03 (t, *J* = 28.95 Hz, 2F), -121.48 (m, 2F), -121.88 (m, 2F), -122.82 (m, 2F), -126.21 (m, 2F). ^{13}C NMR (101 MHz, $CDCl_3$) δ -196.75, 161.21, 138.49, 136.82 (t, *J* = 8.4 Hz), 121.84, 121.65, 119.82. HRMS calculated for $C_{13}H_4F_{13}O_2$ (M-H): 439.0009, found: 439.0016.

methyl 2-hydroxy-3,5-bis(perfluorohexyl)benzoate (*o,p*-43b)

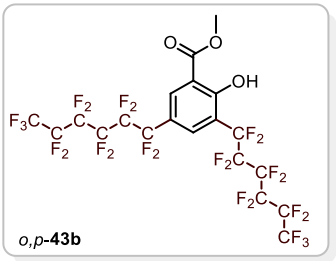

The title compound was isolated in 50% yield (78 mg) as a white solid by chromatography using a gradient eluent of hexane/ethyl acetate (*Rf*=0.30 hexane/ethyl acetate 24:1).^{1}H NMR (400 MHz, $CDCl_3$) δ 12.09 (s, 1H), 8.30 (d, *J* = 2.08 Hz, 1H), 7.87 (d, *J* = 2.00 Hz, 1H), 4.05 (s, 3H). ^{19}F NMR decoupled ^{1}H (376 MHz, $CDCl_3$) δ -80.92 (m, 6F), -109.22 (t, *J* = 14.60 Hz, 2F), -110.68 (t, *J* = 14.30 Hz, 2F), -121.47 (m, 4F), -121.95 (m, 4F), -122.89 (m, 4F), -126.27 (m, 4F). ^{13}C NMR (101 MHz, $CDCl_3$) δ 164.44, 163.29, 133.70, 133.31, 119.59 (t, *J* = 26.04 Hz), 118.12 (t, *J* = 23.87 Hz), 114.36, 53.55. HRMS calculated for $C_{20}H_6F_{26}NaO_3$ (M+Na): 810.9794, found: 810.9824.

2-bromo-4,6-bis(perfluorohexyl)phenol (*o,p*-43c)

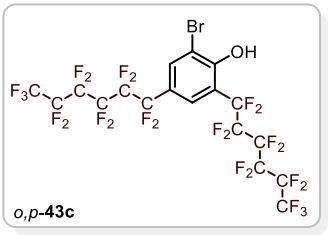

The title compound was isolated in 40% yield (65 mg) as a colorless oil by chromatography using a gradient eluent of hexane/ethyl acetate (*Rf*=0.35 hexane/ethyl acetate 24:1). ^{1}H NMR (400 MHz, $CDCl_3$) δ 7.93 (s, 1H), 7.67 (s, 1H). ^{19}F NMR decoupled ^{1}H (376 MHz, $CDCl_3$) δ -80.96 (m, 6F), -109.15 (t, *J* = 14.67 Hz, 2F), -110.54 (t, *J* = 14.41 Hz, 2F), -121.52 (m, 4F), -121.89 (m, 4F), -122.90 (m, 4F), -126.28 (m, 4F). ^{13}C NMR (101 MHz, $CDCl_3$) δ 154.33, 134.66, 128.13, 122.36 (t, *J* = 25.88 Hz), 116.73 (t, *J* = 24.12 Hz), 113.28. HRMS calculated for $C_{18}H_2BrF_{26}O$ (M-H): 806.8879, found: 806.8883.

1-(2-hydroxy-3,5-bis(perfluorohexyl)phenyl)ethan-1-one (*o,p*-43d)

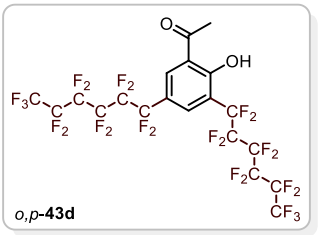

The title compound was isolated in 35% yield (54 mg) as a colorless oil by chromatography using a gradient eluent of hexane/ethyl acetate (*Rf*=0.30 hexane/ethyl acetate 15:1) as a colorless oil. ^{1}H NMR (400 MHz, $CDCl_3$) δ 13.55 (s, 1H), 8.14 (d, *J* = 1.66 Hz, 1H), 7.90 (d, *J* = 1.67 Hz, 1H), 2.75 (s, 3H). ^{19}F NMR decoupled ^{1}H (376 MHz, $CDCl_3$) δ -80.89 (m, 6F), -109.25 (t, *J* = 14.51 Hz, 2F), -110.64 (t, *J* = 14.67 Hz, 2F), -121.38 (m, 4F), -121.87 (m, 4F), -122.86 (m, 4F), -126.25 (m, 4F). ^{13}C NMR (101 MHz, $CDCl_3$) δ 204.26, 164.32, 134.31, 133.61, 120.51, 119.11 (t, *J* = 26.03 Hz), 118.90 (t, *J* = 23.83 Hz). HRMS calculated for $C_{20}H_6F_{26}NaO_2$ (M+Na): 794.9845, found: 794.9878.

4-hydroxy-3,5-bis(perfluorohexyl)benzaldehyde (*o,o'*-43e)

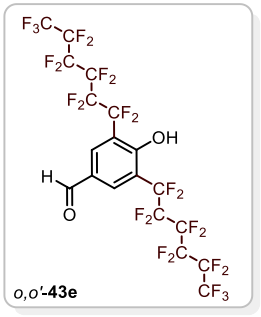

The title compound was isolated in 40% yield as a white solid by chromatography using a gradient eluent of hexane/DCM (*Rf*=0.3 hexane/DCM 2:1). ^{1}H NMR (400 MHz, $CDCl_3$) δ δ 9.98 (s, 1H), 8.22 (s, 2H). ^{19}F NMR decoupled ^{1}H (376 MHz, $CDCl_3$) δ -80.89 (t, *J* = 9.9 Hz, 6F), -108.25 (t, *J* = 14.5 Hz, 4F), -121.38 (m, 4F), -121.74 (m, 4F), -122.79 (m, 4F), -126.21 (m, 4F). ^{13}C NMR (101 MHz, $CDCl_3$) δ 188.16, 158.37, 135.09, 129.46, 118.12 (t, *J* = 23.0 Hz). HRMS calculated for $C_{19}H_3F_{26}O_2$ (M-H): 756.9723, found: 756.9749.

1-(4-hydroxy-3,5-bis(perfluorohexyl)phenyl)ethan-1-one (*o,o'*-43f)

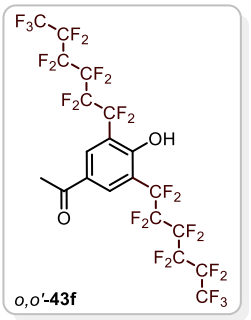

The title compound was isolated in 50% yield (77 mg) as a white solid by chromatography using a gradient eluent of hexane/DCM (*Rf*=0.35 hexane/DCM 2:1). ^{1}H NMR (400 MHz, $CDCl_3$) δ 8.28 (s, 2H), 2.62 (s, 3H). ^{19}F NMR decoupled ^{1}H (376 MHz, $CDCl_3$) δ -80.97 (t, *J* = 10.0 Hz, 6F), -108.19 (t, *J* = 14.6 Hz, 4F), -121.45 (m, 4F), -121.81 (m, 4F), -122.85 (m, 4F), -126.28 (m, 4F). ^{13}C NMR (101 MHz, $CDCl_3$) δ 194.27, 157.50, 133.90 (t, *J* = 8.0 Hz), 130.12, 117.41 (t, *J* = 22.9 Hz), 26.26. HRMS calculated for $C_{20}H_5F_{26}O_2$ (M-H): 770.9880, found: 770.9875.

N-(4-hydroxy-3,5-bis(perfluorohexyl)phenyl)acetamide (*o,o'*-43g)

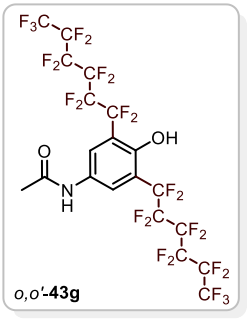

The title compound was isolated in 35% yield (55 mg) as a white solid by chromatography using a gradient eluent of hexane/DCM (*Rf*=0.40 hexane/DCM 2:1). ^{1}H NMR (400 MHz, Acetonitrile-d_3) δ 8.55 (s, 1H), 7.98 (s, 2H), 2.06 (s, 3H). ^{19}F NMR (376 MHz, Acetonitrile-d_3) δ -81.70 (m, 6F), -107.84 (t, *J* = 14.8 Hz, 4F), -121.77 (m, 2F), -122.33 (m, 2F), -123.30 (m, 2F), -126.7 (m, 2F); ^{13}C NMR (101 MHz, Acetonitrile-d_3) δ 170.03, 150.53, 133.85, 126.05-123.98 (m), 119.38 (t, *J* = 22.0 Hz), 24.15; HRMS calculated for $C_{20}H_6F_{26}NO_2$ (M-H): 785.9989, found: 785.9983.

7-Hydroxy-6-methyl-4-(perfluorohexyl)-2,3-dihydro-1H-inden-1-one (*p*-43h)

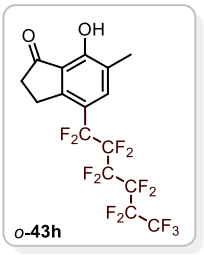

The title compound was isolated in 30% yield (29 mg) as a yellow solid by chromatography using a gradient eluent of hexane/ethyl acetate (*Rf*=0.35 hexane/ethyl acetate 24:1). ^{1}H NMR (400 MHz, $CDCl_3$) δ 9.93 (s, 1H), 7.48 (s, 1H), 3.36 – 3.12 (m, 2H), 2.82–2.70 (m, 2H), 2.29 (s, 3H). ^{19}F NMR decoupled ^{1}H (376 MHz, $CDCl_3$) δ -80.86 (m, 3F), -108.61 (m, 2F), -121.67 (m, 4F), -122.84 (m, 2F), -126.18 (m, 2 F). ^{13}C NMR (101 MHz, $CDCl_3$) δ 209.88, 158.97, 152.17, 137.27 (t, *J* = 7.2 Hz), 124.62, 122.72, 116.86 (t, *J* = 25.0 Hz), 35.85, 25.38, 14.37. HRMS calculated for $C_{16}H_8F_{13}O_2$ (M-H): 479.0322, found: 479.0325.

Methyl 5-acetyl-2-hydroxy-3-(perfluorohexyl)benzoate (*o*-43i)

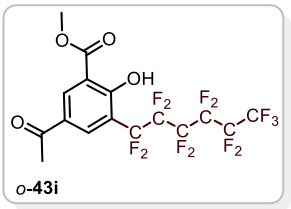

The title compound was isolated in 72% yield (74 mg) as a white solid by chromatography using a gradient eluent of hexane/ethyl acetate (*Rf*=0.3 hexane/ethyl acetate 4:1). ^{1}H NMR (400 MHz, $CDCl_3$) δ 8.68 (s, 1H), 8.31 (s, 1H), 4.04 (s, 3H), 2.61 (s, 3H). ^{19}F NMR decoupled ^{1}H (376 MHz, $CDCl_3$) δ -80.95 (t, *J* = 10.0 Hz, 3F), -108.97 (t, *J* = 14.3 Hz, 2F), -121.18 (m, 2F), -121.90 (m, 2F), -122.85 (m, 2F), -126.22 (m, 2F). ^{13}C NMR (101 MHz, $CDCl_3$) δ 194.74, 169.94, 164.09, 135.43 (t, *J* = 8.4 Hz), 134.89, 128.30, 117.53 (t, *J* = 23.8 Hz), 113.78, 53.39, 26.33. HRMS calculated for $C_{16}H_8F_{13}O_4$ (M-H): 511.0220, found: 511.0218.

Methyl 5-acetyl-2-hydroxy-3-(perfluorobutyl)benzoate (*o*-43j)

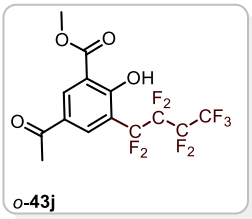

The title compound was isolated in 78% yield (64 mg) as a yellow solid by chromatography using a gradient eluent of hexane/ethyl acetate (*Rf*=0.35 hexane/ethyl acetate 4:1). ^{1}H NMR (400 MHz, $CDCl_3$) δ 12.14 (s, 1H), 8.67 (d, *J* = 2.3 Hz, 1H), 8.30 (d, *J* = 2.3 Hz, 1H), 4.03 (s, 4H), 2.60 (s, 2H). ^{19}F NMR decoupled ^{1}H (376 MHz, $CDCl_3$) δ -81.12 (m, 3F), -109.21 (t, *J* = 13.7 Hz, 2F), -122.11 (m, 2F), -126.06 (m, 2F). ^{13}C NMR (101 MHz, $CDCl_3$) δ 194.72, 169.93, 164.06, 135.37 (t, *J* = 8.4 Hz), 134.88, 128.29, 117.39 (t, *J* = 23.7 Hz), 113.75, 53.35, 26.25. HRMS calculated for $C_{14}H_8F_9O_4$ (M-H): 411.0284, found: 411.0292.

Methyl 5-acetyl-2-hydroxy-3-(perfluorooctyl)benzoate (*o*-43k)

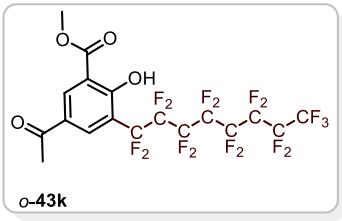

The title compound was isolated in 70% yield (86 mg) as a yellow solid by chromatography using a gradient eluent of hexane/ethyl acetate (*Rf*=0.35 hexane/ethyl acetate 4:1). ^{1}H NMR (400 MHz, $CDCl_3$) δ 12.16 (s, 1H), 8.69 (d, *J* = 2.2 Hz, 1H), 8.31 (d, *J* = 2.2 Hz, 1H), 4.04 (s, 3H), 2.61 (s, 3H). ^{19}F NMR decoupled ^{1}H (376 MHz, $CDCl_3$) δ -80.86 (t, *J* = 10.0 Hz, 3F), -108.92 (t, *J* = 14.1 Hz, 2F), -121.09 (m, 2F), -121.82 (m, 6F), -122.79 (m, 2F), -126.20 (m, 2F). ^{13}C NMR (101 MHz, $CDCl_3$) δ 194.75, 169.94, 164.10, 135.44 (t, *J* = 8.4 Hz), 130.18, 128.43, 128.30, 113.78, 53.40, 26.35; HRMS calculated for $C_{18}H_8F_{17}O_4$ (M-H): 611.0157, found: 611.0167.

Methyl 5-acetyl-2-hydroxy-3-(trifluoromethyl)benzoate (*o*-43l)

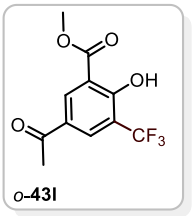

The title compound was isolated in 44% yield (23 mg) as a white solid by chromatography using gradient eluent of hexane/ethyl acetate (*Rf*=0.35 hexane/ethyl acetate 5:1). ^{1}H NMR (400 MHz, $CDCl_3$) δ 12.03 (s, 1H), 8.66 (d, *J* = 2.2 Hz, 1H), 8.38 (d, *J* = 2.7 Hz, 1H), 4.04 (s, 3H), 2.61 (s, 3H). ^{19}F NMR decoupled ^{1}H (376 MHz, $CDCl_3$) δ -63.37 (s, 3F). ^{13}C NMR (101 MHz, $CDCl_3$) δ 194.83, 169.81, 163.20, 134.44, 133.10 (t, *J* = 5.0 Hz), 128.16, 122.77 (q, *J* = 273.1 Hz), 119.37 (q, *J* = 32.5 Hz), 113.63, 53.35, 26.38. HRMS calculated for $C_{11}H_8F_3O_4$ (M-H): 261.0380, found: 261.0384.

Methyl 4'-formyl-3'-hydroxy-2'-(perfluorohexyl)-[1,1'-biphenyl]-4-carboxylate (*o*-45a)

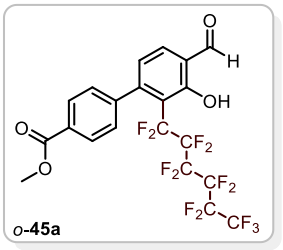

The title compound was isolated in 40% yield (46 mg) as a colorless oil by chromatography using a gradient eluent of hexane/toluene (*Rf*=0.35 hexane/toluene 4:1). ^{1}H NMR (400 MHz, $CDCl_3$) δ 12.17 (s, 1H), 9.98 (s, 1H), 8.05 (d, *J* = 8.5 Hz, 2H), 7.74 (d, *J* = 7.9 Hz, 1H), 7.28 (d, *J* = 8.4 Hz, 2H), 6.87 (d, *J* = 7.9 Hz, 1H), 3.95 (s, 3H). ^{19}F NMR decoupled ^{1}H (376 MHz, $CDCl_3$) δ -80.91 (m, 3F), -100.59 (m, 2F), -118.88 (m, 2F), -122.11 (m, 2F), -122.78 (m, 2F), -126.22 (m, 2F). ^{13}C NMR (101 MHz, $CDCl_3$) δ 195.96, 166.68, 161.97, 151.23, 144.80, 136.25, 129.61, 128.73, 127.76, 123.54, 120.41; HRMS calculated for $C_{21}H_{10}F_{13}O_4$ (M-H): 573.0377, found: 573.0376.

(±) 3-hydroxy-2'-methyl-2-(perfluorohexyl)-[1,1'-biphenyl]-4-carbaldehyde (*o*-45b)

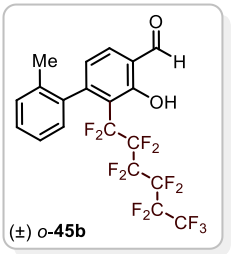

The title compound was isolated in 38% yield (40 mg) as a yellow oil by chromatography using a gradient eluent of hexane/toluene (*Rf*=0.30 hexane/toluene 4:1). ^{1}H NMR (400 MHz, $CDCl_3$) δ 12.20 (s, 1H), 9.99 (s, 1H), 7.75 (d, *J* = 7.9 Hz, 1H), 7.38 – 7.17 (m, 3H), 7.04 (dd, *J* = 7.4, 3.0 Hz, 1H), 6.86 (d, *J* = 7.9 Hz, 1H), 2.08 (s, 3H). ^{19}F NMR decoupled ^{1}H (376 MHz, $CDCl_3$) δ -101.49 (m, 3F), -104.79 (dd, *J* = 722.1, 282.2 Hz 2F), -118.95 (dd, *J* = 581.7, 292.2 Hz, 2F), -122.17 (m, 2F), -122.80 (m, 2F), -126.22 (m, 2F). ^{13}C NMR (101 MHz, $CDCl_3$) δ 196.11, 162.39, 152.25, 139.81 (d, *J* = 3.0 Hz), 136.55,

134.91 (d, *J* = 3.9 Hz), 129.55, 128.04, 127.50, 124.93, 123.81, 120.26, 115.78 (t, *J* = 21.3 Hz), 20.12; HRMS calculated for $C_{20}H_{10}F_{13}O_2$ (M-H): 529.0479, found: 529.0468.

(±) 3-hydroxy-2'-methyl-2-(perfluorobutyl)-[1,1'-biphenyl]-4-carbaldehyde (*o*-45c)

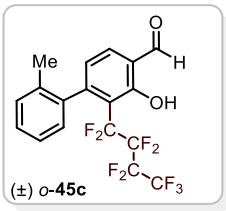

The title compound was isolated in 40% yield (34 mg) as a yellow oil by chromatography using a gradient eluent of hexane/toluene (*Rf* = 0.25 hexane/toluene 4:1). ^{1}H NMR (400 MHz, $CDCl_3$) δ 12.19 (s, 1H), 9.99 (s, 1H), 7.75 (d, *J* = 7.9 Hz, 1H), 7.40 – 7.09 (m, 3H), 7.04 (dd, *J* = 7.4, 2.9 Hz, 1H), 6.86 (d, *J* = 7.9 Hz, 1H), 2.08 (s, 3H). ^{19}F NMR decoupled ^{1}H (376 MHz, $CDCl_3$) δ -81.03 (m, 3F), -102.90 (dd, *J* = 718.5, 286.2 Hz, 2F), -119.45 (dd, *J* = 593.8, 293.0 Hz, 2F), -126.32 (m, 2F). ^{13}C NMR (101 MHz, $CDCl_3$) δ 196.10, 162.32, 152.24, 139.80, 136.54, 134.92, 129.55, 128.03, 127.51, 124.93, 123.80, 120.24, 115.70, 20.15; HRMS calculated for $C_{18}H_{10}F_9O_2$ (M-H): 429.0543, found: 429.0555.

(±) Methyl 3-hydroxy-2'-methyl-2-(perfluorohexyl)-[1,1'-biphenyl]-4-carboxylate (*o*-45d)

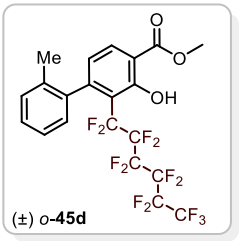

The title compound was isolated in 25% yield (28 mg) as a yellow oil by chromatography using a gradient eluent of hexane/toluene (*Rf*=0.25 hexane/toluene 4:1). ^{1}H NMR (400 MHz, $CDCl_3$) δ 11.91 (s, 1H), 8.02 (d, *J* = 8.2 Hz, 1H), 7.31 – 7.10 (m, 3H), 7.05 – 6.96 (m, 1H), 6.69 (d, *J* = 8.2 Hz, 1H), 4.01 (s, 3H), 2.05 (s, 3H). ^{19}F NMR decoupled ^{1}H (376 MHz, $CDCl_3$) δ -80.92 (t, *J* = 10.0 Hz, 3F), -102.75 (dd, *J* = 693.7, 279.6 Hz, 2F), -119.50 (dd, *J* = 565.0, 287.7 Hz, 2F), -122.18 (m, 2F), -122.76 (m, 2F), -126.25 (m, 2F). ^{13}C NMR (101 MHz, $CDCl_3$) δ 170.41, 162.08, 150.91, 140.27, 135.03, 132.96, 129.44, 127.78, 127.66, 124.85, 122.89, 121.62, 112.57, 52.99, 20.13; HRMS calculated for $C_{21}H_{12}F_{13}O_3$ (M-H): 559.0584, found: 559.0593.

Chapter IV

Enantioselective Formal α-Methylation and α-Benzylation of Aldehydes by Means of Photo-Organocatalysis

Target

Development of a two-step aminocatalytic photochemical strategy for the synthesis of enantioenriched valuable α-methylated and α-benzylated aldheydes.

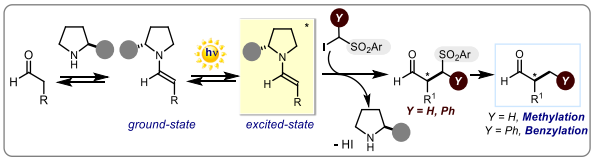

Tool

Ability of enamines, in their excited state, to act as photoreductants for the formation of reactive radical species from α-iodo sulfones.[1]

4.1 Introduction

The ability of some electron-rich substrates to serve, upon light excitation, as reducing agents (see for example the phenolate anions discussed in the previous Chapter)[2] turned out to be an efficient way to generate reactive radicals from suitable acceptors *via* a single-electron transfer (SET) mechanism. Expanding upon this concept, we wondered if other transiently formed electron-rich intermediates could equally act as photoinitiators after direct excitation with visible light. In 2015, our research group demonstrated that chiral tertiary enamines **I**, formed upon condensation of a chiral secondary amine **A** with aldehydes **1**, can, upon light excitation, actively participate in the photoactivation of substrates, triggering the formation of reactive open-shell species from bromo malonates **2** (Figure 4.1a).[3]

[1] The work discussed in this Chapter has been published, see: Filippini, G.; Silvi, M.; Melchiorre, P. "Enantioselective formal α-methylation and α-benzylation of aldehydes by means of photo-organocatalysis" *Angew. Chem. Int. Ed.* **2017**, *56*, 4447.

[2] Filippini, G.; Nappi, M.; Melchiorre P. "Photochemical direct perfluoroalkylation of phenols" *Tetrahedron* **2015**, *71*, 4535.

[3] a) Silvi, M.; Arceo, E.; Jurberg, I. D.; Cassani, C.; Melchiorre, P. "Enantioselective organocatalytic alkylation of aldehydes and enals driven by the direct photoexcitation of enamines" *J. Am. Chem. Soc.*

Meanwhile, the ground-state chiral enamines **I** can efficiently trap these electrophilic radicals in an enantioselective fashion, thus yielding the corresponding enantioenriched α-alkylated derivatives **3**.

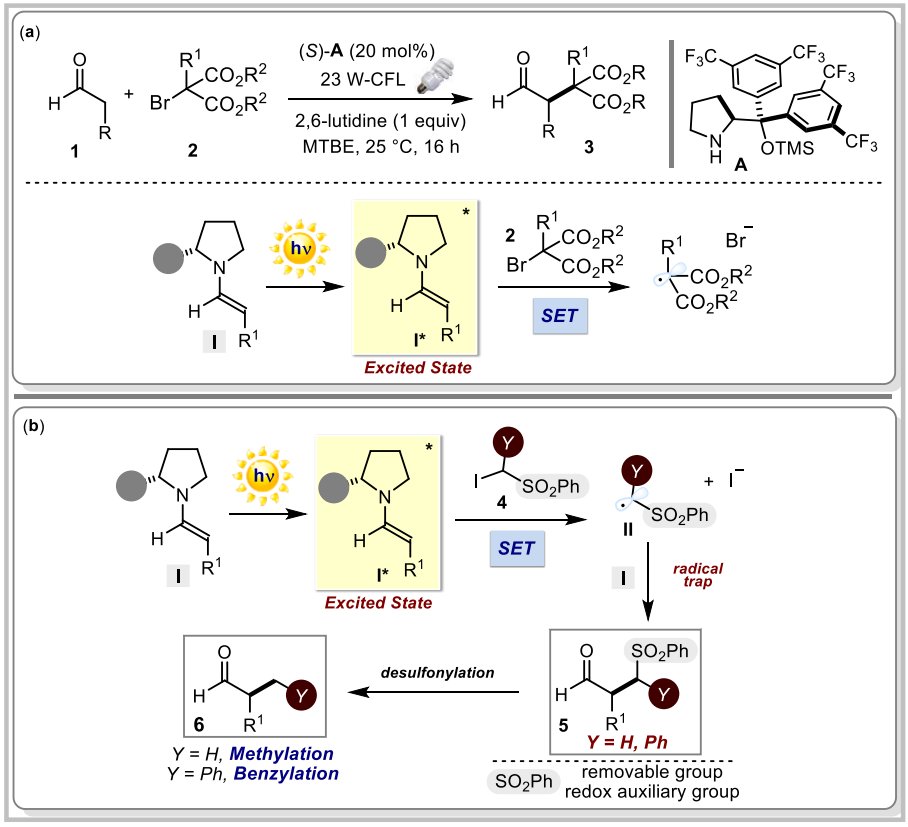

Figure 4.1 (**a**) Enantioselective organocatalytic alkylation of aldehydes with bromomalonates driven by the direct photo-excitation of enamines (**b**) Enantioselective organocatalytic alkylation of aldehydes with α-iodo sulfones: our photochemical two step approach for the catalytic enantioselective α-methylation and α-benzylation of aldehydes. SET: single-electron transfer; the grey circle represents the chiral aminocatalyst scaffold.

In the second part of my PhD, I have further exploited the unique excited-state reactivity of enamines to develop a photochemical enantioselective α-alkylation of aldehydes **1** with α-iodo sulfones **4** (Figure 4.1b). The phenylsulfonyl moiety within substrate **4** plays a dual essential role: it facilitates SET reduction and the generation of radicals **II**, acting as

2015, *137*, 6120. b) Bahamonde, A.; Melchiorre, P. "Mechanism of the stereoselective α-alkylation of aldehydes driven by the photochemical activity of enamines" *J. Am. Chem. Soc.* **2016**, *138*, 8019.

an electron-poor redox auxiliary group;[4] it also serves as a removable moiety, thus unveiling methyl and benzyl groups upon simple desulfonylation of the originally formed adducts **5**. Overall, this is a synthetically useful transformation, since few strategies are available for the catalytic enantioselective α-methylation or benzylation of aldehydes and therefore for the synthesis of products of type **6** (see section 4.4 in this Chapter).[5]
General aspects regarding the reactivity of chiral enamines, both in the ground state and the excited state, and the relevance of methylation and benzylation reactions will be first discussed within this Chapter.

4.2 Ground-State Enamine Chemistry

Catalysis by chiral primary and secondary amines, namely "aminocatalysis", is nowadays an established tool in organic synthesis for the stereoselective functionalization of enolizable carbonyl compounds.[6] While secondary amine-based catalysts (**A**, **B**) provide an effective way of functionalizing linear aldehydes, primary amines (**C**) offer the possibility of expanding enamine-mediated processes to more sterically demanding partners, such as ketones and alpha branched aldehydes (Figure 4.2a). Specifically, the condensation of a chiral secondary amine (**A** or **B**) with an aldehyde **1** produces a tetrahedral intermediate **III**, which afterwards collapses to give an iminium ion **IV** (Figure 4.2b). Subsequently, deprotonation at the α-carbon atom within the iminium ion **IV** generates the corresponding nucleophilic tertiary enamine **I** (4π-electron intermediate). These enamines are nucleophilic intermediates and their reactivity is mainly governed by two factors: (*i*) the HOMO raising effect, due to the donation of the nitrogen lone pair into the C-C double bond; (*ii*) the degree of pyramidalization of the enamine nitrogen atom, which takes into account its percentage of sp^2 character.[7]

---

[4] a) Yoshida, J.-I.; Kataoka, K.; Horcajada, R.; Nagaki, A. "Modern strategies in electroorganic synthesis" *Chem. Rev.* **2008**, *108*, 2265. b) Tyson, E. L.; Farney, E. P.; Yoon, T. P. "Photocatalytic [2 + 2] cycloadditions of enones with cleavable redox auxiliaries" *Org. Lett.* **2012**, *14*, 1110. c) Beatty, J. W.; Douglas, J. J.; Cole, K. P.; Stephenson, C. R. J. "A scalable and operationally simple radical trifluoromethylation" *Nat. Commun.* **2015**, *6*, 7919.

[5] a) Nagib, D. A. "Catalytic desymmetrization by C-H functionalization as a solution to the chiral methyl problem" *Angew. Chem. Int. Ed.* **2017**, *56*, 7354. b) Melchiorre, P. "Light in aminocatalysis: the asymmetric intermolecular α-alkylation of aldehydes" *Angew. Chem. Int. Ed.* **2009**, *48*, 1360.

[6] a) List, B. "Emil Knoevenagel and the roots of aminocatalysis" *Angew. Chem. Int. Ed.* **2010**, *49*, 1730. b) Melchiorre, P.; Marigo, M.; Carlone, A.; Bartoli, G. "Asymmetric aminocatalysis-gold rush in organic chemistry" *Angew. Chem. Int. Ed.* **2008**, *47*, 6138. c) List, B. "The ying and yang of asymmetric aminocatalysis" *Chem. Commun.* **2006**, 819.

[7] Murphy, J. J., Silvi, M., and Melchiorre, P. (**2016**) Enamine-mediated catalysis (n $\longrightarrow \pi^*$), in Lewis base catalysis in organic synthesis (eds E. Vedejs and S. E. Denmark), Wiley-VCH Verlag GmbH & Co. KGaA, Weinheim, Germany. doi: 10.1002/9783527675142.ch17

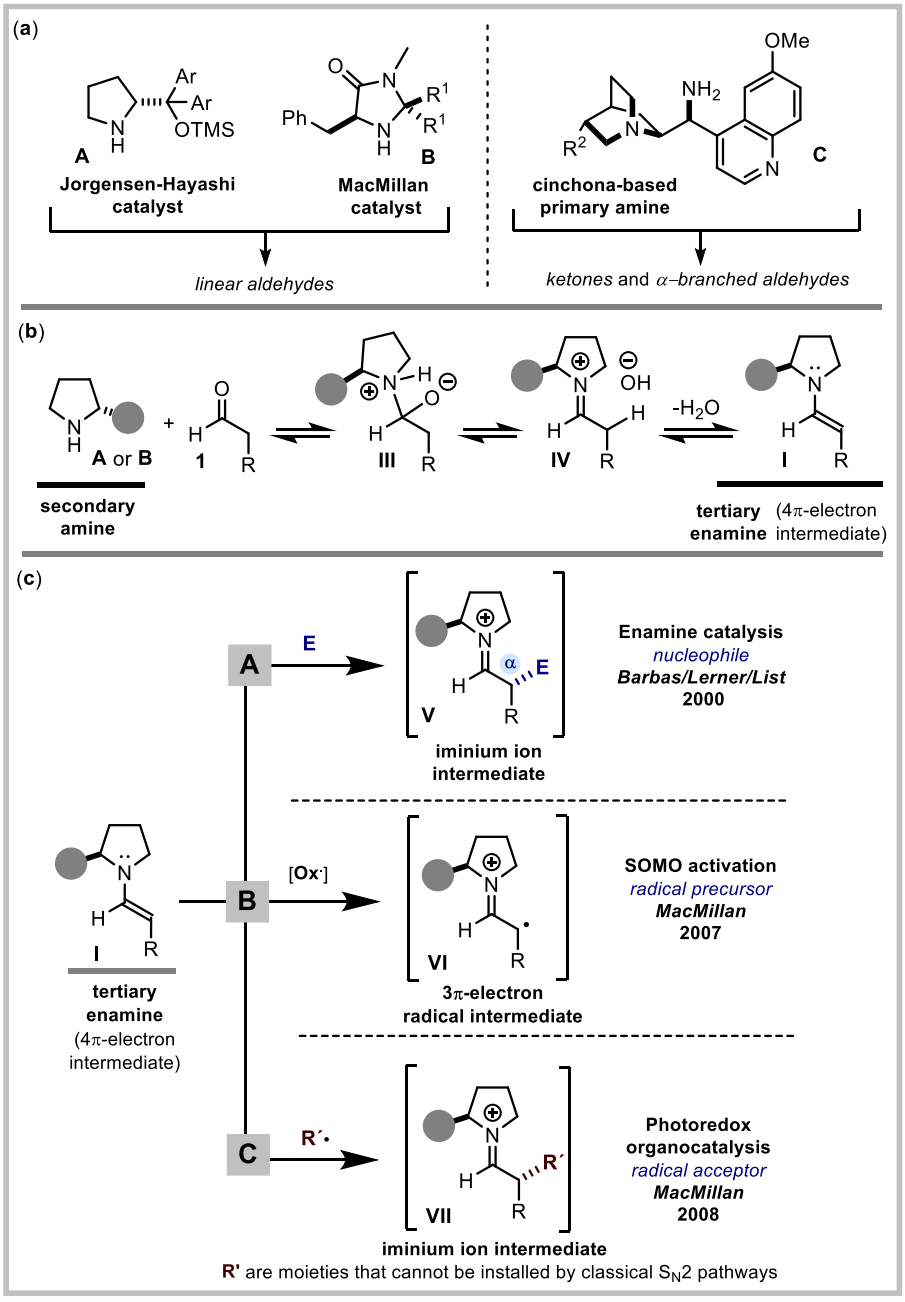

Figure 4.2 (**a**) Privileged chiral secondary and primary amines for enamine activation. (**b**) Formation of a chiral tertiary enamine by condensation of a chiral secondary amine with an enolizable aldehyde. (**c**) Ground-state enamines reactivity. The grey circle represents the bulky group of the secondary amine; E: Electrophile; [Ox·]: single-electron oxidant.

Both the nature of the chiral amine and the carbonyl compound **1** strongly influence these two factors, and therefore also the reactivity of the resulting enamine **I**.[8]

In 2000, a seminal work of List, Lerner, and Barbas III has demonstrated the ability of proline-derived enamines to efficiently catalyze the direct intermolecular asymmetric aldol reaction of acetone and a variety of aldehydes.[9] Since then, the use of chiral enamines to catalyze the stereoselective functionalization of unmodified carbonyl compounds with suitable electrophiles (**E**) at their α-carbon has been growing exponentially (path **A**, Figure 4.2c).[6] In 2007, the MacMillan group expanded the applicability of the enamine activation mode by employing an external single-electron oxidant ([**Ox·**]) to generate a transient radical cation intermediate **VI** from the enamine **I** (path **B**, Figure 4.2c).[10] This 3π-electron radical species has a singly occupied molecular orbital (SOMO) that is activated towards a wide range of enantioselective catalytic transformations, thus establishing the concept of SOMO-activation.[11] In 2008, MacMillan and co-workers have proven the ability of catalytically generated chiral enamines **I** to trap, in an enantioselective manner, photochemically produced electrophilic radicals (path **C**, Figure 4.2c).[12] This last organocatalytic activation mode, termed photoredox organocatalysis, has paved the way for the development of new radical asymmetric carbon-carbon bond-forming transformations under mild reaction conditions.[13]

---

[8] a) Mayr H.; Bug, T.; Gotta, M. F.; Hering, N.; Irrgang, B.; Janker, B.; Kempf, B.; Loos, R.; Ofial, A. R.; Remennikov, G.; Schimmel, H. "Reference scales for the characterization of cationic electrophiles and neutral nucleophiles" *J. Am. Chem. Soc.* **2001**, *123*, 9500. b) Lakhdar S.; Maji B.; Mayr H. "Imidazolidinone-derived enamines: nucleophiles with low reactivity" *Angew. Chem. Int. Ed.* **2012**, *51*, 5739.

[9] List B.; Lerner R. A.; Barbas C. F. III "Proline-catalyzed direct asymmetric aldol reactions" *J. Am. Chem. Soc.* **2000**, *122*, 2395.

[10] Beeson, T. D.; Mastracchio, A.; Hong, J.-B.; Ashton, K.; MacMillan, D. W. C. "Enantioselective organocatalysis using SOMO activation" *Science* **2007**, *316*, 582.

[11] a) Kim, H.; MacMillan, D. W. C. "Enantioselective organo-SOMO Catalysis: the α-vinylation of aldehydes" *J. Am. Chem. Soc.* **2008**, *130*, 398. b) Juy, N. T.; Garber, J. A. O.; Finelli, F. G.; MacMillan, D. W. C. "Enantioselective α-arylation of aldehydes via organo-SOMO catalysis. An ortho-selective arylation reaction based on an open-shell pathway" *J. Am. Chem. Soc.* **2009**, *131*, 11640. c) Juy, N. T.; Garber, J. A. O.; Finelli, F. G.; MacMillan, D. W. C. "Enantioselective organo-SOMO cycloadditions: a catalytic approach to complex pyrrolidines from olefins and aldehydes" *J. Am. Chem. Soc.* **2012**, *134*, 11400.

[12] Nicewicz, D. A.; MacMillan, D. W. C. "Merging photoredox catalysis with organocatalysis: the direct asymmetric alkylation of aldehydes" *Science* **2008**, *322*, 77.

[13] Brimioulle, R.; Lenhart, D.; Maturi, M. M.; Bach, T. "Enantioselective catalysis of photochemical reactions" *Angew. Chem. Int. Ed.* **2015**, *54*, 3872.

4.3 Photochemistry of Enamines

Our research group recently established that the chemistry of enamines is not limited to their ground-state reactivity. Indeed, as described in Chapter II, chiral enamines **I** can be used as photoinitiators to generate reactive radical species after excitation with UV or visible light (Figure 4.3).[3b]

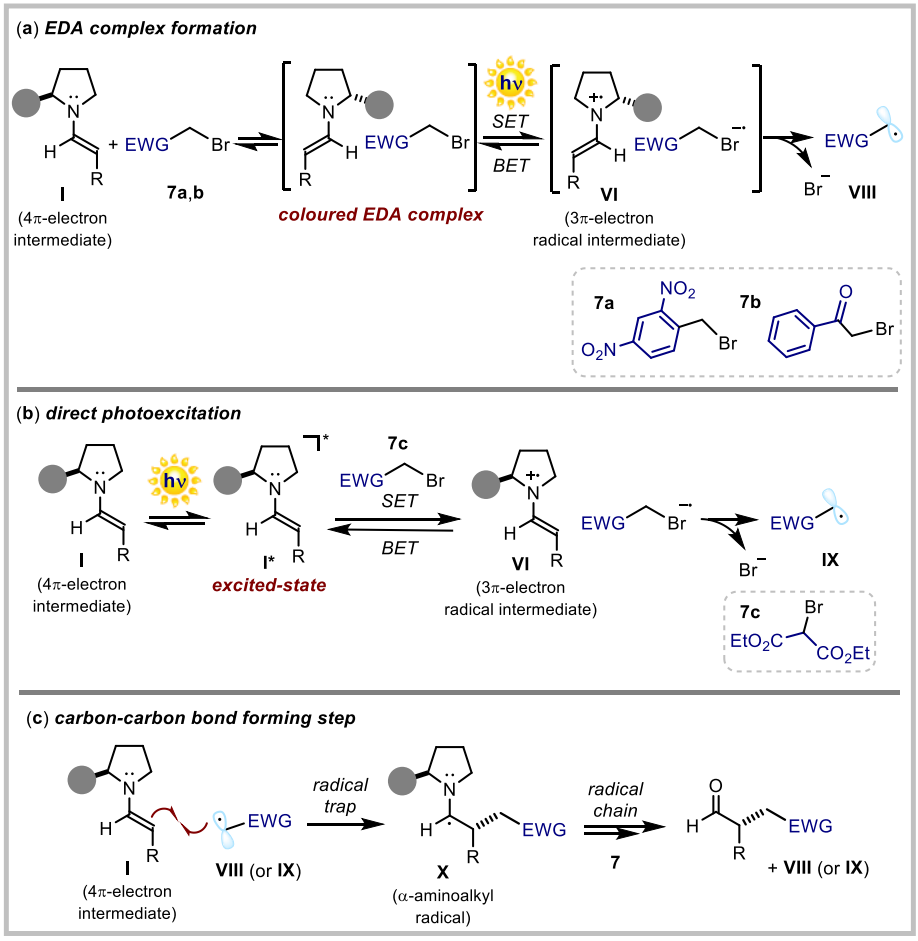

Figure 4.3 Enamines acting as photoinitiators: (**a**) EDA complex formation, (**b**) direct photoexcitation., (**c**) carbon-carbon bond forming step; SET: single-electron transfer, BET: back-electron transfer; EWG: electron withdrawing group.

A radical photoinitiator is a chemical species that undergoes a photoreaction, after light absorption, leading to the formation of reactive radicals from suitable precursors. Depending on the nature of the organic halides **7** used as radical sources, two general

photoinitiation mechanisms have been identified and studied.[3b] The first strategy relies on the formation of a photon-absorbing electron donor-acceptor (EDA) complex, generated in the ground state upon association of the electron-rich tertiary enamine **I** with an electron-deficient organic halide **7a**,**b**.[14] Visible light irradiation of the colored EDA complex induces a SET, allowing the formation of the reactive open-shell intermediates **VIII** (Figure 4.3a). In the second approach, the chiral enamine **I** directly reaches an electronically excited state **I*** upon irradiation, becoming a strong reducing agent. SET reduction of the organic halide **7c** leads to the formation of the electrophilic radical **IX** (Figure 4.3b).[3a] **VI** is an unstable intermediate and a stereocontrolled radical-radical coupling of **VIII** (or **IX**) and **VI** cannot be invoked to account for the formation of the new carbon-carbon bond (see section 4.13 for further details).[3b] On the other hand, in both cases, the nucleophilic ground-state enamine **I** trap the photochemically generated electrophilic radicals to form the corresponding α-amino radicals **X**. (Figure 4.3c). The α-aminoalkyl radicals **X** can then regenerate the chain-propagating radicals **VIII** (or **IX**) while giving the final enantio-enriched α-alkylated products (see Chapter II for more mechanistic details).

4.4 Towards new Applications: Formal Asymmetric Methylation and Benzylation of Aldehydes

In implementing the α-alkylation of aldehydes **1** with α-iodosulfones **4**, we were inspired by our recent studies on the direct photoexcitation of enamines **I** and their potential for generating radicals under mild conditions (Figure 4.4a).[3a]

We demonstrated that chiral enamine **I**, upon light absorption, can reach an excited-state (**I***) becoming a strong reductant, as implied by its reduction potential, that was estimated to be ≈ -2.0 V (vs Ag/Ag^+ in CH_3CN).[3a] Thus, **I*** could trigger the formation of radicals **IX** through SET reduction of bromomalonates (E_p^{red} diethyl bromomalonate = -1.69 V *vs* Ag/Ag^+ in CH_3CN).[3b] We surmised that a similar photochemical mechanism could generate (phenylsulfonyl)alkyl radicals **II** from **4**.[15]

As mentioned above, a critical design element was the phenylsulfonyl moiety, which would act as an electron poor redox auxiliary group facilitating the reductive cleavage of the C−I bond *via* a SET mechanism.[4]

---

[14] Arceo, E.; Jurberg, I. D.; Álvarez-Fernández, A.; Melchiorre, P. "Photochemical activity of a key donor-acceptor complex can drive stereoselective catalytic α-alkylation of aldehydes" *Nat. Chem.* **2013**, *5*, 750.

[15] Liu, F.; Li, P. D. "Visible-light-promoted (phenylsulfonyl)methylation of electron-rich heteroarenes and *N*-arylacrylamides" *Org. Chem.* **2016**, *81*, 6972.

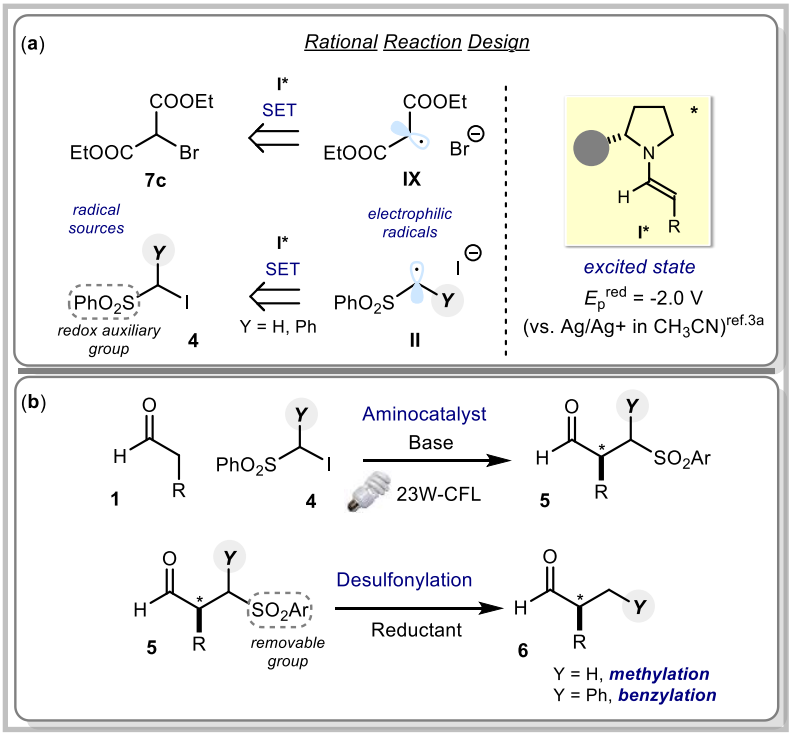

Figure 4.4 (**a**) Rational choice of a suitable substrate. (**b**) Formal asymmetric photochemical α-methylation and α-benzylation of aldehydes with α-iodosulfones. SET: single-electron transfer.

In consonance with this scenario, we measured by cyclic voltammetry a reduction for the iodomethyl phenyl sulfone **4a** (Y = H in Figure 4.4a) as low as -1.49 V (E_p^{red} vs Ag/Ag^+ in CH_3CN). This suggested **4a** as a viable precursor of phenylsulfonyl methyl radicals. The important role played by the iodide, which emerges from the SET mechanism acting as leaving group, will be discussed in section 4.5 of this Chapter. At the same time, the ground state chiral enamines **I** could provide effective stereochemical control over the enantioselective radical-trapping process. The resulting enantio-enriched (phenylsulfonyl)alkylated intermediates **5** could be desulfonylated to reach the target enantio-enriched α-methylated or α-benzylated products **6** (Figure 4.4b).

4.4.1 The Relevance of the Methyl group: α-Methylation of Aldehydes

"*The methyl group, so often considered as chemically inert, is able to alter deeply the pharmacological properties of a molecule.*"

Camille Georges Wermuth

Methylation reactions, and the resulting stereo-electronic changes induced within a molecule upon installation of methyl groups, are directly involved in many biological processes.[16] The concept of methylation plays a key role in epigenetics, as DNA and histone methylation is largely responsible for gene expression without affecting the gene sequence.[17] For example, methylation of the nucleobase cytosine **8** is operated by DNA methyltransferase enzymes, which use *S*-adenosyl methionine (SAM) as an electrophilic methyl source (Figure 4.5).[18] The electrophilic SAM-methylation of the transient intermediate **9** leads to the formation of the 5-methyl cytosine **11**.

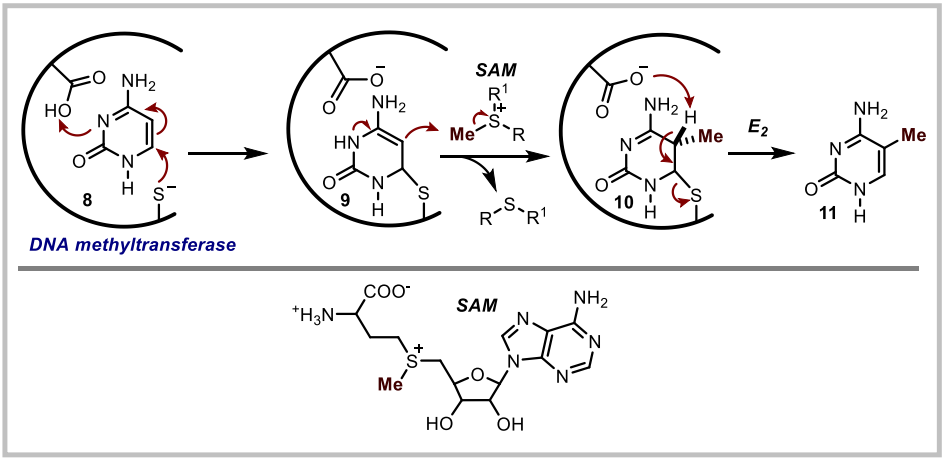

Figure 4.5 SAM-mediated methylation of cytosine; E_2: bimolecular elimination.

[16] Schonherr, H.; Cernak T. "Profound methyl effects in drug discovery and a call for new C-H methylation reactions." *Angew. Chem. Int. Ed.* **2013**, *52*, 12256.

[17] Sasaki, H.; Matsui Y. "Epigenetic events in mammalian germ-cell development: reprogramming and beyond." *Nat. Rev. Genet.* **2008**, *9*, 129.

[18] a) Voet, D.; Voet, J. G. "DNA methylation and trinucleotide repeat expansion" Chapter 30, p. 1246 in *Biochemistry, fourth edition,* **2011**, Wiley. b) Dhe-Paganon, S.; Syeda, F.; Park, L. "DNA methyl transferase 1: regulatory mechanisms and implications in health and disease" *Int. J. Biochem. Mol. Biol.* **2011**, *2*, 58. c) Santi, D. V.; Normant, A.; Garrett, C. E. "Covalent bond formation between a DNA-cytosine methyltransferase and DNA containing 5-azacytosine" *Proc. Natl. Acad. Sci. USA* **1984**, *81*, 6993.

In addition, the methyl group is one of the most prevalent functionality in biologically active compounds.[19] Stereogenic centers bearing methyl groups can be found in several natural products as well as in commercially available drugs and fragrances (Figure 4.6). Despite the so called "*magic methyl effect*", wherein up to 100-fold greater potency can be imparted on a medicinal agent by installation of a simple CH_3 group, only limited methylation tools remain at the synthetic chemist's disposal.[5a] In recent years, the synthetic community has developed a range of new radical transformations in order to install methyl groups on different organic substrates.

These transformations rely on the use of alcohols[20], peroxides[21], and zinc sulfonates[22] as methyl radical precursors.

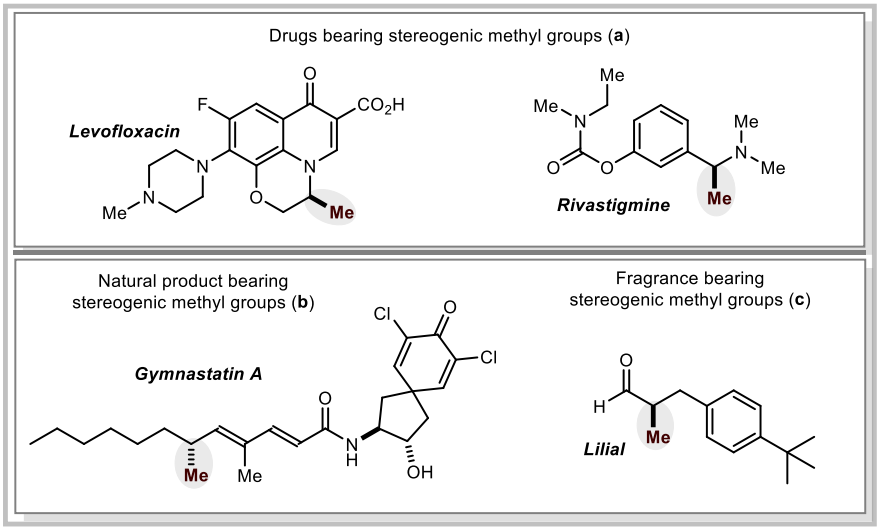

Figure 4.6 Valuable compounds containing a stereogenic center bearing a methyl group: (**a**) commercially available drugs; (**b**) natural product; (**c**) fragrance.

[19] a) Leung, C. S.; Leung, S. S. F.; Tirado-Rives, J.; Jorgensen, W. L. "Methyl effects on protein–ligand binding" *J. Med. Chem.* **2012**, *55*, 4489. b) Barreiro, E. J., Kümmerle, A. E., Fraga, C. A. M. "The methylation effect in medicinal chemistry" *Chem. Rev.* **2011**, *111*, 5215. c) Bartschat, D., Börner, S., Mosandl, A. et al. Z Lebensm Unters Forsch (**1997**) 205: 76. doi:10.1007/s002170050127.

[20] Jin, J.; MacMillan, D. W. C. "Alcohols as alkylating agents in heteroarene C–H functionalization" *Nature* **2015**, *525*, 87.

[21] Zhang, P.-Z.; Li, J.-A.; Zhang, L.; Shoberu, A.; Zou, J.-P., Zhang, W. "Metal-free radical C-H methylation of pyrimidinones and pyridinones with dicumyl peroxide Alcohols as alkylating agents in heteroarene C–H functionalization" *Green Chem.* **2017**, *19*, 919.

[22] Gui, J.; Zhou, Q.; Pan, C.-M.; Yabe, Y.; Burns, A. C.; Collins, M. R.; Ornelas, M. A.; Ishihara, Y.; Baran, P. "C-H methylation of heteroarenes inspired by radical SAM methyl transferase" *J. Am. Chem. Soc.* **2014**, *136*, 4853.

In particular, Baran *et al.* recently reported a remarkable formal methylation of heteroaromatic compounds.[22] Methyl sulfonyl radicals were generated by oxidation of sulfinate salts (**PSMS**) and trapped by heteroaromatic compounds **12**. Cleavage of the sulfonyl moiety of the products **13** under reductive conditions afforded the desired methylated heterocyclic compound **14** (Figure 4.7).

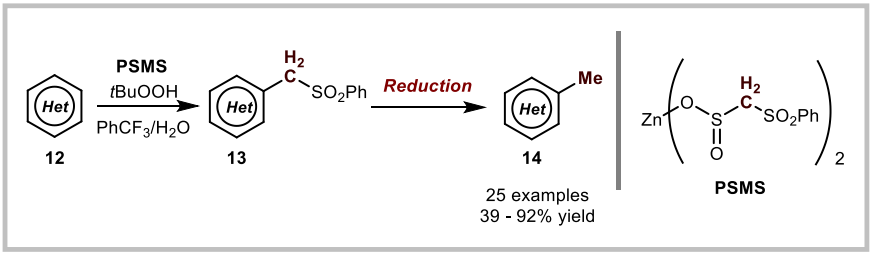

Figure 4.7 Baran's approach for formal methylation of heteroaromatic compounds.

Nevertheless, direct incorporation of a methyl C-C bond *via* catalytic asymmetric α-methylation of carbonyl compounds remains unknown.[5a] Recently, Jin-Quan Yu and co-workers developed a new palladium-catalyzed method for the enantioselective desymmetrization of the prochiral α-isopropyl groups of isobutyramides **15** with compounds **16** (Figure 4.8).[23] This methodology allows for the synthesis of α-methyl stereocenter containing molecules **17** in moderate to good yield with high level of enantioselectivity.

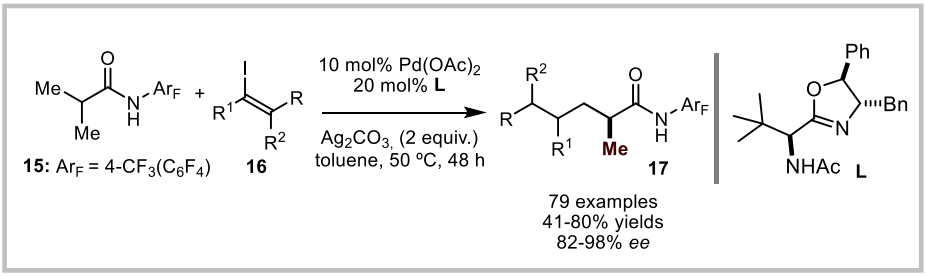

Figure 4.8 Yu's approach for the palladium-catalyzed enantioselective desymmetrization of the prochiral α-isopropyl group of an isobutyramide.

[23] Wu, Q.-F.; Shen, P.-X.; He, J.; Wang, X. B.; Zhang, F.; Shao, Q.; Zu, R.-Y.; Mapelli, C.; Qiao, J. X.; Poss, M. A.; Yu, J.-Q. "Formation of α-chiral centers by asymmetric β-C(sp^3)–H arylation, alkenylation, and alkynylation" *Science* **2017**, *136*, 4853.

In 2011, P. G. Cozzi developed an enantioselective enamine-mediated formal α-methylation of aldehydes **1** using a 1,3-benzodithiolylium moiety as a masked methyl group (Figure 4.9).[24] The 1,3-benzodithiol group in **19** can be easily transformed into a methyl group by using hydrogen in the presence of Raney Ni, to form the valuable α-methylated products of type **20**. Analogous products could be obtained by employing our planned transformation, depicted in Figure 4.4 (when Y = H). Indeed, such a strategy would provide an approach to formally achieve enantioenriched α-methylated derivatives.

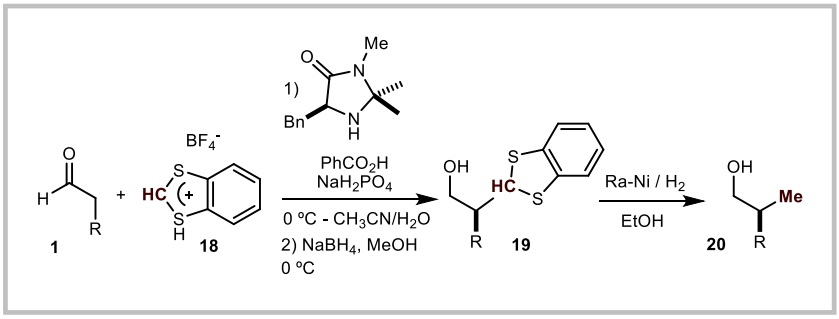

Figure 4.9 Cozzi's approach for the asymmetric formal methylation reaction of aldehydes with benzodithiolium salt.

4.4.2 The Relevance of the Benzyl group: α-Benzylation of Aldehydes

Stereoselective carbonyl α-benzylation, leading to the formation of benzylic stereogenic centers, is a important chemical transformation, since these stereogenic units are present in many natural products, as well as medicinally relevant compounds.[25] Indeed, four of the twenty natural proteinogenic amino acids contain a stereogenic α-carbonyl benzyl moiety, and therefore this moiety appears also in their natural product derivatives. Radical methods for the α-benzylation of aldehydes generally require highly electron-poor benzyl bromides to facilitate the generation of radical intermediates upon SET reduction.[12,14] In 2014, List and co-workers described the first aminocatalyzed α-alkylation of α-branched aromatic-aldehydes **21** with benzyl bromides **22** as alkylating agents, proceeding through

[24] Gualandi, A.; Emer, E.; Capdevilla, M. G.; Cozzi, P. G. "Highly enantioselective α-alkylation of aldehydes with 1,3-benzodithiolylium tetrafluoroborate: a formal organocatalytic α-alkylation of aldehydes by the carbenium ion" *Angew. Chem . Int. Ed.* **2011**, *50*, 7842.

[25] a) Jung, M. E., Lazarova, T. I. "Efficient synthesis of selectively protected L-dopa derivatives from L-tyrosine via Reimer-Tiemann and Dakin reactions" *J. Org. Chem.* **1997**, *62*, 1553. b) Schweizer, U., Steegborn, C. "Thyroid hormones-from crystal packing to activity to reactivity" *Angew. Chem. Int. Ed.* **2015**, *54*, 12856.

a classical S_N2 reaction pathway (Figure 4.10).[26]

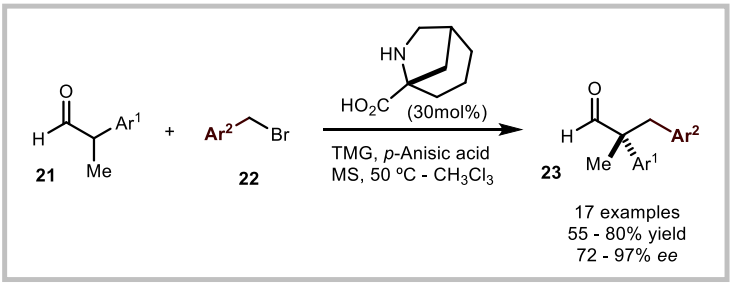

Figure 4.10 List's approach for the asymmetric benzylation reaction of aldehydes with benzyl bromides. TMG: 1,1,3,3-tetramethylguanidine; MS: 4Å Molecular Sieve.

This strategy affords exclusively quaternarized products **23**. The paucity of methodologies for the catalytic enantioselective α-benzylation of linear aldehydes with simple benzyl groups stands in sharp contrast to the prominence of this stereogenic unit. This type of products could be achieved with the planned transformation depicted in Figure 4.4 (when Y = Ph). In fact, our strategy would be a suitable method to formally synthesize enantioenriched α-benzylated aldehydes.

[26] List B., Coric I, Grygorenko O. O., Kaib P. S. J., Komarov I., Lee A., Leutzsch M., Pan S. C., Tymtsunik A. V., Van Gemmeren M. "The catalytic asymmetric α-benzylation of aldehydes" *Angew. Chem. Int. Ed.* **2014**, *53*, 282.

4.5 Initial Results and Preliminary Optimization Studies

The feasibility of our proposal was initially tested by mixing butanal **1a**, the commercially available bromomethyl sulfone **24a**, catalyst **A** and 2,6-lutidine in toluene under irradiation by a 23 W-CFL (compact fluorescent light) bulb (Figure 4.11). This experiment provided only traces of the desired α-alkylated compound **5a**.

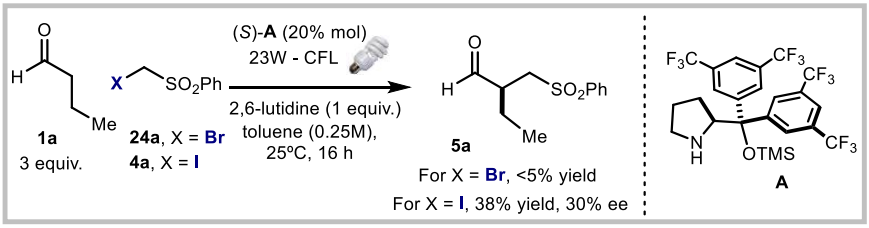

Figure 4.11 α-alkylation reaction of aldehyde **1a** with bromomethyl phenylsulfone **24a** or iodomethyl phenylsulfone **4a**. Yields obtained by ^{1}H NMR analysis of the crude reaction mixture using trichloroethylene as the internal standard. Enantiomeric excess determined by HPLC analysis of the corresponding alcohol after in situ $NaBH_4$ reduction of **5a**.

Interestingly, the use of iodomethyl phenylsulfone **4a**, easily synthesized in a one-step procedure (see experimental part within this Chapter), led to the formation of product **5a** in moderate yield (38%) along with low enantioselectivity. The reason of such increased reactivity is ascribable to the presence of a better leaving group, namely iodide, which facilitates the single-electron transfer event and makes the radical formation step easier.[27] Prior to further optimization studies, we performed a series of control experiments in order to better understand the nature of the studied transformation (Figure 4.12).

Product **5a** was not detected when performing the reaction in the dark, thus ruling out the involvement of a thermal process (Figure 4.12a). Moreover, catalyst **A** was stable under the reaction conditions until 45 ºC, since no byproducts were observed, and full catalyst recovery was inferred by NMR analysis of the crude reaction mixture (using trichloroethylene as the internal standard). The stability of the catalyst in the presence of **4a** (5 equiv.) was further demonstrated by stirring a solution of both species in toluene for 72 hours: no degradation or any sort of side reaction was observed (Figure 4.12b).

[27] Bordwell, F. G.; Clemens, A. H. "Correlation between the basicity of carbanions and their ability to transfer an electron" *J. Org. Chem.* **1981**, *46*, 1035.

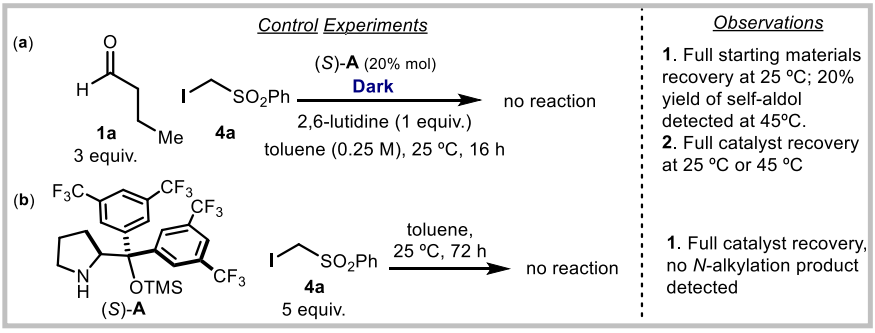

Figure 4.12 Control experiments.

During our optimization studies, we observed that a racemization process was occurring under the reaction conditions, since the enantiomeric excess of product **5a** decreased with increasing reaction time (entries 1-4, Table 1). We observed that the racemization process was completely suppressed by carrying out the reaction at 5 ºC, and in situ reducing ($NaBH_4$ in methanol at 0 ºC) the final product **5a** to the corresponding alcohol prior to workup (entries 5-6, Table 1).

Table 1. Initial optimization studies [a]

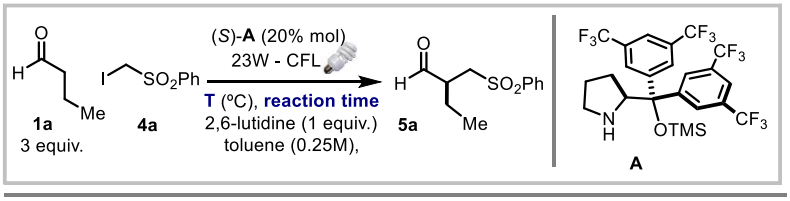

Entry	reaction time (h)	T (ºC)	Yield **5a** (%)[b]	*ee* **5a** (%)[c]
1	6	25	35	60
2	16	25	38	30
3	25	25	40	15
4	116	25	39	0
5	16	5	38	80
6	48	5	36	80
7	16	0	34	80
8[d]	16	5	43	80

[a] Reactions performed on a 0.1 mmol scale [b] Yields determined by ^{1}H NMR analysis using trichloroethylene as the internal standard. [c] Enantiomeric excess determined by HPLC analysis on the corresponding alcohol after in situ $NaBH_4$ reduction of **5a**. [d]Reaction performed under illumination by a 365 nm LED.

Performing the reaction at 0 ºC did not bring about any benefit in terms of enantiomeric excess (entry 7, Table 1). In addition, product **5a** was obtained in slightly better yield (43%) with a satisfactory level of enantioselectivity by using a 365 nm light-emitting diode (LED) as source of photons instead of a CFL lamp (entry 8, Table1). This improvement is likely due to a more efficient excitation of the in situ formed chiral enamine, acting as a photoinitiator. In order to increase the reactivity, we synthesized and tested different radical sources amenable to the photochemical α-alkylation process (Figure 4.13). No reaction was observed using a phenylsulfone bearing a triflate as leaving group (**25a**). The sulfoxide compound **26a** was not a suitable substrate for the studied transformation. The use of a set of α-iodo phenylsulfones bearing different substituents at the *para*-position of the aromatic rings (**4b-e**) did not lead to any improvement in terms of yield or enantioselectivity (0-45% yields, 60-74% ee). In addition, compound **4f** and **4g**, which could have led to the development of a formal asymmetric α-ethylation or α-difluoromethylation process, respectively, did not react at all under the conditions reported in Figure 4.13. The catalytic reactions shown in Figure 4.13, Figure 4.14, and Figure 4.15 were carried out in collaboration with Mrs. Xin Huang.

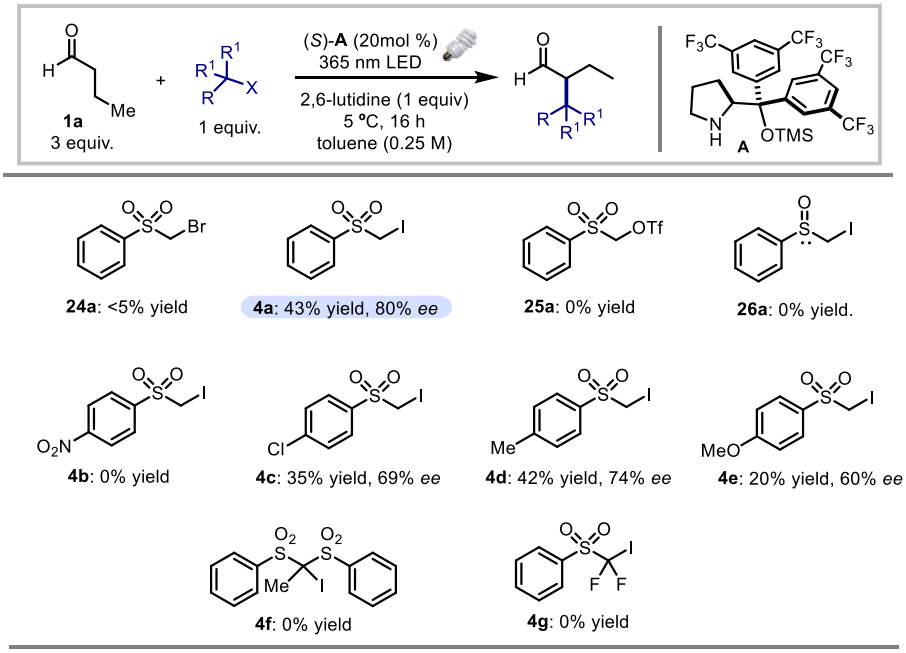

Figure 4.13 Preliminary screening of the radical precursors. Reactions performed on a 0.1 mmol scale. Yields determined by ^{1}H NMR analysis using trichloroethylene as the internal standard. Enantiomeric excess determined by HPLC analysis of the corresponding alcohol after in situ $NaBH_4$ reduction.

We then tested the model reaction with the iodosulfone **4a** in different solvents (entries 1-13, Table 2). These experiments identified toluene as the best reaction solvent (entry 1, Table 2), which was selected for further investigations.

Table 2. Preliminary screening of the solvents [a]

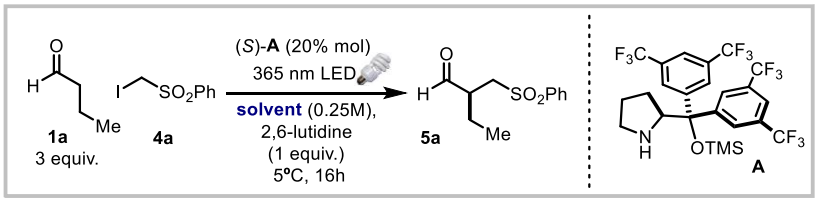

Entry	solvent	Yield **100a** (%)[b]	*ee* **100a** (%)[c]
1	toluene	43	80
2	DCM	40	72
3	MTBE	35	80
4	THF	0	-
5	Et_2O	0	-
6	DCE	20	68
7	$CHCl_3$	42	73
8	$PhCF_3$	20	70
9	PhCl	43	69
10	DMF	25	69
11	MeOH	0	-
12	EtOAc	15	80
13	MeCN	40	72

[a] Reactions performed on a 0.1 mmol scale [b] Yields determined by ^{1}H NMR analysis using trichloroethylene as the internal standard. [c] Enantiomeric excess determined by HPLC analysis on the corresponding alcohol after in situ $NaBH_4$ reduction of **5a**.

A set of different bases was then tested in order to increase the chemical yield of the photochemical transformation (Figure 4.14). The use of 1 equiv. of an acid scavenger is needed to quench hydrogen iodide (HI), which is stoichiometrically formed after the mesolytic cleavage of **4a** to furnish the radical intermediate. In line with this notion, performing the reaction in the absence of a base resulted in a lack of reactivity. Disappointingly, none of the tested bases could rival the performance offered by 2,6-

lutidine. Moreover, the use of an excess of base (2,6-lutidine, 2 equiv.) did not improve the reactivity. It is important to underline that the 2,6-lutidinium iodide is completely insoluble in toluene, and that it precipitates out of solution over the reaction time.

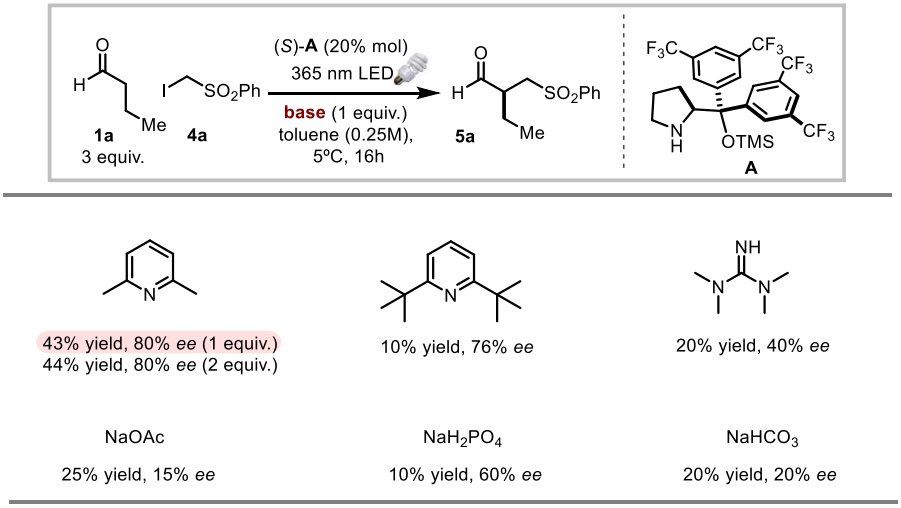

Figure 4.14 Preliminary screening of the bases. Yields determined by ^{1}H NMR analysis using trichloroethylene as the internal standard. Enantiomeric excess determined by HPLC analysis on the corresponding alcohol after in situ $NaBH_4$ reduction.

A screening of catalysts was undertaken to improve both the enantioselectivity and the overall yield of the model transformation (Figure 4.15). First, we studied the effect of different silyl protecting groups on the photochemical transformation, by testing various diarylprolinol silyl ethers as organocatalysts (**A**-**D**).[28] The best result was obtained using catalyst **A**, which bears a trimethylsilyl (TMS) ether as hydroxyl protecting group. Catalyst **E** provided the desired α-alkylated derivative (**5a**) in moderate reactivity (32% yield) along with low enantioselectivity (42% *ee*). In this case, a racemization pathway, which involves the presence of catalyst **E**, was observed even at a temperature as low as 5 ºC. Indeed, compound **5a** was obtained with appreciably higher enantiomeric excess (61%) when performing the reaction over a shorter period of time (6 h). Gilmour type organocatalyst **F** afforded the desired product with promising chemical yield along with

[28] Donslund, B. S.; Johansen, T. K.; Poulsen, P. H.; Halskov, K. S.; Jørgensen K. A. "The diarylprolinol silyl ethers: ten years after" *Angew. Chem. Int. Ed.* **2015**, *54*, 13860.

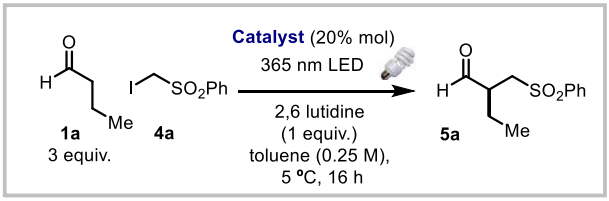

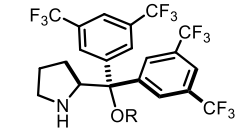

A, R = TMS: 43% yield, 80% *ee*.
B, R = TBDMS: 38% yield, 78% *ee*.
C, R = TIPS: 15% yield, 76% *ee*.
D, R = $SiPh_3$: 9% yield, n.d.

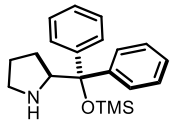

E: 32% yield, 42% *ee*.
15% yield, 61% *ee*.*
(6 h)*

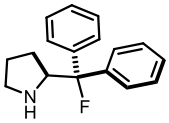

F: 48% yield, 31% *ee*.

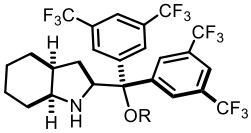

G: R = TMS: 10% yield, 92% *ee*.
H: R =TBDMS: 12% yield, 93% *ee*.

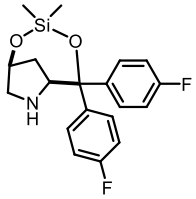

I: 26% yield, 70% *ee*.

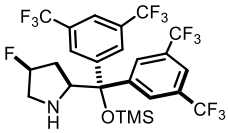

J: 11% yield, 88% *ee*.

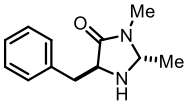

K: 0% yield.

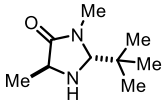

L: 0% yield.

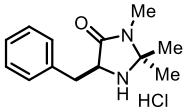

M: 0% yield.[a]

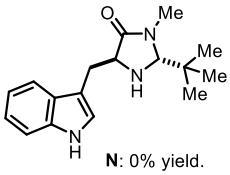

N: 0% yield.

Figure 4.15 Preliminary screening of the catalysts. Yields determined by ^{1}H NMR analysis using trichloroethylene as the internal standard. Enantiomeric excess determined by HPLC analysis on the corresponding alcohol after in situ $NaBH_4$ reduction. [a] Reaction performed using 2 equivalents of 2,6-lutidine.

poor enantiocontrol (31%).[29] A racemization pathway was probably operative in this case too. Bicyclic chiral amines **G** and **H** yielded the final compound (**5a**) in high enantioselectivity along with poor yields. Chiral amine **I** was an inefficient catalyst in the studied photochemical transformation. A similar lack of reactivity was observed using catalyst **J**, since product **5a** was obtained in low NMR yield but with good enantioselectivity. Imidazolidinones **K**-**N** (also called MacMillan organocatalysts) were not competent catalysts for the studied reaction. Overall, and despite extensive experimentation, we could not increase the yield of the photochemical alkylation, which reached a standstill at about 40% and could not evolve any further.

We believed that this could have been a perfect situation to exploit the synthetic benefits of flow chemistry in photochemical transformations. We expected that the use of flow conditions could lead to an improvement of the overall yield of the reaction. This idea led to a four-month collaboration with Professor Oliver Kappe (University of Graz, Austria), an expert in the application of flow techniques. For this reason, general aspects regarding the implementation of photochemical transformations under flow regime will be discussed.

4.6 Acceleration of Photochemical Transformations in Continuous-Flow Reactors

In recent years, continuous-flow photochemistry has been used increasingly by researchers, both in academia and industry, to facilitate photochemical transformations and their subsequent scale-up.[30] The implementation of photochemistry in the large-scale production of chemicals has been largely neglected for a variety of reasons.[31] The main issue is associated with the reactor design and its modeling. Indeed, if light can be considered a reactant, a proper geometry of the photo-reactor, securing a uniform photon distribution, is required. Continuous-flow irradiation of the reaction mixture is highly advantageous compared to the irradiation achievable under batch conditions. One of the main limitations of batch reactors is that light penetration within the solution is limited

[29] Tanzer, E.-M.; Zimmer, E. L.; Schweizer, W. B.; Gilmour, R. "Fluorinated organocatalysts for the enantioselective epoxidation of enals: molecular preorganisation by the fluorine-iminium ion gauche effect." *Chem. Eur. J.* **2012**, *18*, 11334

[30] a) Su, Y.; Straathof, M. J. W.; Hessel V.; Noel T. "Photochemical transformations accelerated in continuous-flow reactors: basic concepts and applications" *Chem. Eur. J.* **2014**, *20,* 10562. b) Gutmann, B.; Cantillo, D.; Kappe C. O. "Continuous-flow technology-a tool for the safe manufacturing of active pharmaceutical ingredients" *Angew. Chem. Int. Ed.* **2015**, *54,* 6688.

[31] Fischer M. "Industrial applications of photochemical syntheses" *Angew. Chem. Int. Ed. Engl.* **1978**, *17,* 16.

by the absorption of the substrates and diminishes rapidly with distance from the lamp.[32] Essentially, the reaction solution nearest the lamp "screens" the bulk of the reaction solution from photons. Starting materials, products, photosensitizers, and photocatalysts can all act as filters reducing the light intensity available for the rest of the reaction mixture.[33] This effect is also amplified if the reaction solution is concentrated. On the other hand, a more efficient irradiation of a reaction mixture can be achieved under flow condition, due to the large surface-to-volume ratios typical of flow reactors (Figure 4.16).[34]

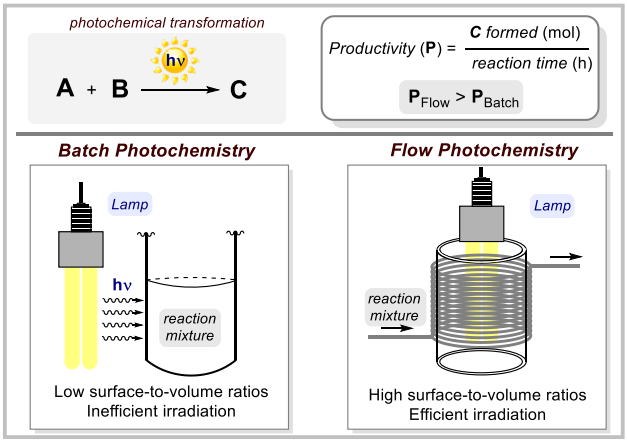

Figure 4.16 Batch photochemistry *vs* flow photochemistry

In addition, under flow reaction conditions both the time of light exposure and the reaction temperature may be precisely controlled.[35] This typically translates in a higher chemical productivity (**P** = moles of product formed per hour, Figure 4.16) with respect to batch conditions.[32,33] It is for these reasons that the combination of visible light photoredox catalysis with flow chemistry is highly desirable both to accelerate and facilitate photochemical transformations.

---

[32] Knowles, J. P.; Elliot, L. D.; Booker-Milburn K. I. "Flow photochemistry: old light through new windows" *Beilstein J. Org. Chem.* **2012,** *8,* 2025.

[33] Plutschack, M. B.; Pieber, B.; Gilmore, K.; Seeberger, P. H. "The Hitchhiker's guide to flow chemistry" *Chem. Rev.* **2017**, DOI: 10.1021/acs.chemrev.7b00183

[34] Gilmore, K.; Seeberger, P. H. "Continuous flow photochemistry" *Chem. Rec.* **2014**, *14,* 410.

[35] Manson, B. P.; Price, K. E. Steinbache J. L.; Bogdan A. R.; McQuade D. T. "Greener approaches to organic synthesis using microreactor technology" *Chem. Rev.* **2007**, *107,* 2300.

As an example, in 2012, Zeitler and co-workers studied under a flow regime a variant of the reaction described by MacMillan.[36] In particular, the photochemical α-alkylation of octanal **1c** with diethyl bromomalonate **7c**, catalyzed by an imidazolidinone catalyst **L** and Eosin Y **27** (an organic photoredox catalyst), had been performed both under batch and flow reaction conditions (Figure 4.17). The reaction proved to be high yielding under both conditions. However, the reaction performed under flow conditions was much faster, providing the desired enantioenriched α-alkylated product **3a** with comparable optical purity but with higher productivity.

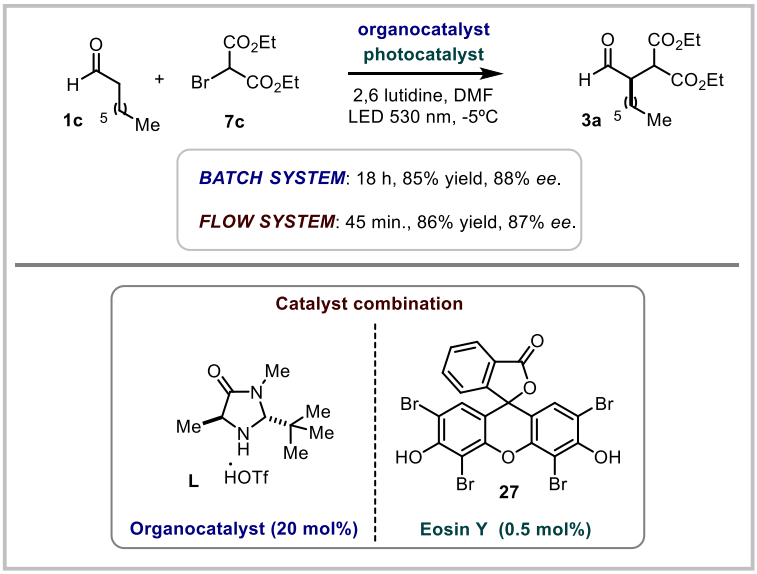

Figure 4.17 Comparison of batch and flow regime for the enantioselective photochemical alkylation of octanal with diethyl bromomalonate.

4.7 Towards the Application in Flow

Initially, we studied the reaction under batch conditions laying the foundation for the following flow experiments (Table 3). Firstly, we decided to use acetonitrile as reaction solvent because of the following reasons: (*i*) it provides appreciable reactivity along with good enantioselectivity in the studied reaction (40% yield, 72% ee; entry 13, Table 2); (*ii*) it is able to dissolve polar substrates, for both starting materials and reaction products

[36] Neumann, M.; Zeitler, K. "Application of microflow conditions to visible light photoredox catalysis" *Org. Lett.* **2012**, *14*, 2658.

are completely soluble in acetonitrile, which is extremely important under flow conditions;[33] (*iii*) it does not absorb above 200 nm; (*iv*) it is easy to remove on a rotary evaporator; (*v*) it is economical; (*vi*) it can be used at relatively low reaction temperatures. In addition, we decided to carry out our experiments at 0 ºC, using an ice-water bath as cooling system. Indeed, in our previous experiments (results in Table 1), we observed that a racemization mechanism was operative when the reaction was performed at temperature higher than 5 ºC. Another key requirement to run reactions under flow conditions is to have relatively fast transformations.[33] Therefore, in order to better understand the behavior of the model photochemical transformation, we decided to run further batch experiments over a relatively short period of time (3-5 hours) using high-intensity illumination devices (Table 3).

Table 3. Testing the model reaction under batch conditions[a]

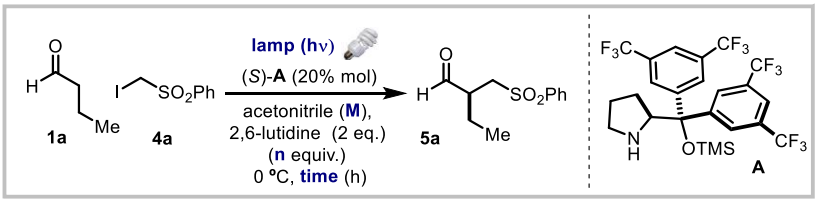

Entry	**1a**/**4a**	lamp (hv)	reaction time (h)	[**M**]	Yield **5a** (%)[b]	*ee* **5a** (%)[c]
1	3:1	105W-BLB	3	0.20	32	nd
2	2:1	105W-BLB	3	0.20	34	nd
3	5:1	105W-BLB	3	0.20	30	nd
4	2:1	105W-BLB	5	0.20	43	72
5	1:2	105W-BLB	5	0.20	25	nd
6	2:1	105W-BLB	5	0.50	20	nd
7	2:1	105W-BLB	5	0.10	15	nd
8	2:1	100W-CFL	5	0.20	33	nd
9[d]	2:1	105W-BLB	5	0.20	0	-

[a] Reactions performed on a 0.2 mmol scale. [b] Yields determined by HPLC analysis at 215 nm on the corresponding alcohol after in situ $NaBH_4$ reduction of **5a** using trichloroethylene as the internal standard. [c] Enantiomeric excess determined by HPLC analysis on the corresponding alcohol after in situ $NaBH_4$ reduction of **5a**. CFL = compact fluorescence lamp. BLB = black lamp bulb. [d] Reaction performed in the presence of air.

The desired product (**5a**) was obtained in moderate yield (32%) by irradiating the reaction mixture with a 105 W black lamp bulb (BLB) over 3 hours (entry 1). Performing the

reaction with a lower excess of **1a** (2 instead 3 equiv.) brought about the formation of the final product **5a** with slightly better chemical yield (entry 2, Table 3). The use of 5 equiv. of **1a** did not lead to any benefit in terms of reactivity (entry 3, Table 3). We obtained the enantioenriched α-alkylated product **5a** in 43% yield with good enantioselectivity (72% ee) carrying out the reaction over 5 hours (entry 4, Table 3). Variation of the standard reaction parameters, such as concentration, stoichiometry, and source of photons, did not afford any improvement on the reaction yield (entries 5-8, Table 3). In addition, the reaction did not work in the presence of air (entry 9, Table 3). It was not possible to measure the enantiomeric excesses of all the entries in Table 3, since a HPLC-CSP (chiral stationary phase) machine was not available in the Kappe's laboratory. Some of the ee (%) measurements have been performed in the laboratory of Prof. Kurt Faber (Biocatalysis Department-University of Graz).

4.8 Building up the Flow Reactor

The continuous flow reactor was thought and designed on the basis of the length of the photo-emitting part of the lamp (around 20 cm) available. Indeed, the studied reaction works only in the presence of a proper photon-flux and it immediately shuts down in the dark. We, together with the glass-blowing unit of the institute of chemistry within Graz University, initially made a cooling jacket by combining two suitable beakers, leaving an empty space, an input and an output in order to efficiently circulate the cooling liquid through it (Figure 4.18a).

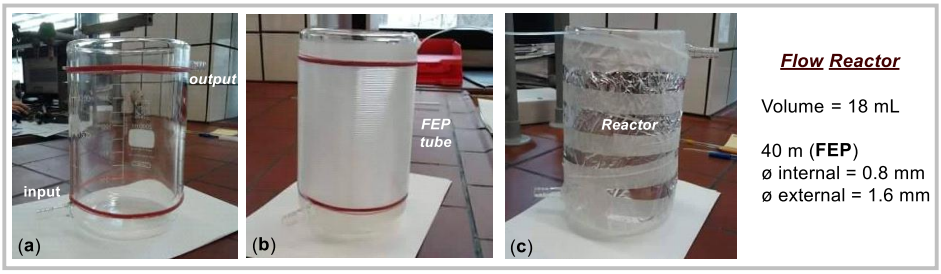

Figure 4.18 Design and construction of the photo-reactor for the flow experiments. FEP: fluorinated ethylene propylene copolymer; Ø: capillary diameter.

After that, UV-transparent fluorinated ethylene propylene (FEP) copolymer capillary (40 m; volume = 18 mL; $Ø_{internal}$ = 0.8 mm; $Ø_{external}$ = 1.6 mm) was tightly wrapped around the cooling jacket (Figure 4.18b). Lastly, we covered the reactor with a layer of cotton

and aluminum foil in order to minimize the heat transfer with the environment (Figure 4.18c).

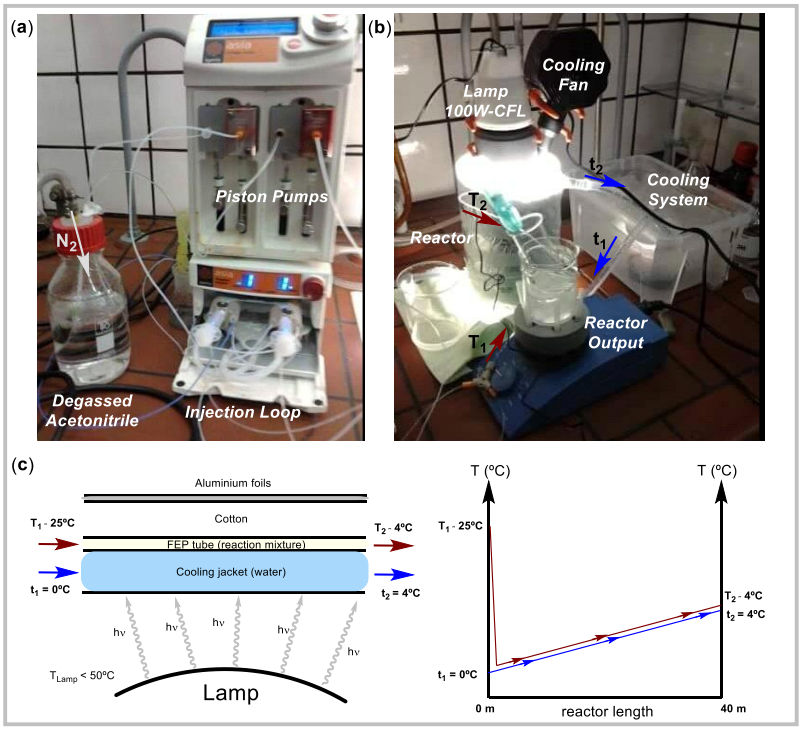

Figure 4.19 Reaction setup for the experiments under flow conditions.

The reactor was then connected with an injection system, needed to introduce the reaction mixture into the apparatus (Figure 4.19a). Two piston pumps were continuously pumping degassed acetonitrile towards an injection-loop (2 mL). The system was equipped with six-port valves, so that the reaction crude could be injected using a plastic syringe into the flow path at continuous pressure. The lamp (105 W-BLB or 100 W-CFL) was placed inside the cooling jacket in order to capture the maximum number of photons, and hence maximise the productivity (Figure 4.19b). It has been connected with a temperature indicator, which was linked to a cooling fan in order to maintain the temperature of the lamp under 50 ºC. Water at 0 ºC was used as cooling fluid, and it was pumped continuously inside the cooling jacket for the entire duration of the experiments. The input ($\mathbf{t_1}$) and output ($\mathbf{t_2}$) temperature of the water in the cooling jacket were measured after allowing the lamp to reach the regime temperature and were found to be 0 ºC and 4 ºC

respectively. Considering this and the high surface-to-volume ratio of the flow reactor, it is reasonable to assume that the incoming reaction mixture ($\mathbf{T_1}$ of approximately 25 ºC) immediately reached a temperature slightly higher than 0 ºC, and then going through the length of the reactor gradually increased to about 4 ºC ($\mathbf{T_2}$, Figure 4.19c). Finally, the reactor output was collected into a mechanically stirred flask, which contained a large excess of $NaBH_4$ (5 equiv.) dissolved in methanol at 0 ºC, in order to reduce the aldehydic moiety of the final product **5** to the corresponding alcohol **28**. The complete schematic representation of the flow apparatus is shown in Figure 4.20a-b.

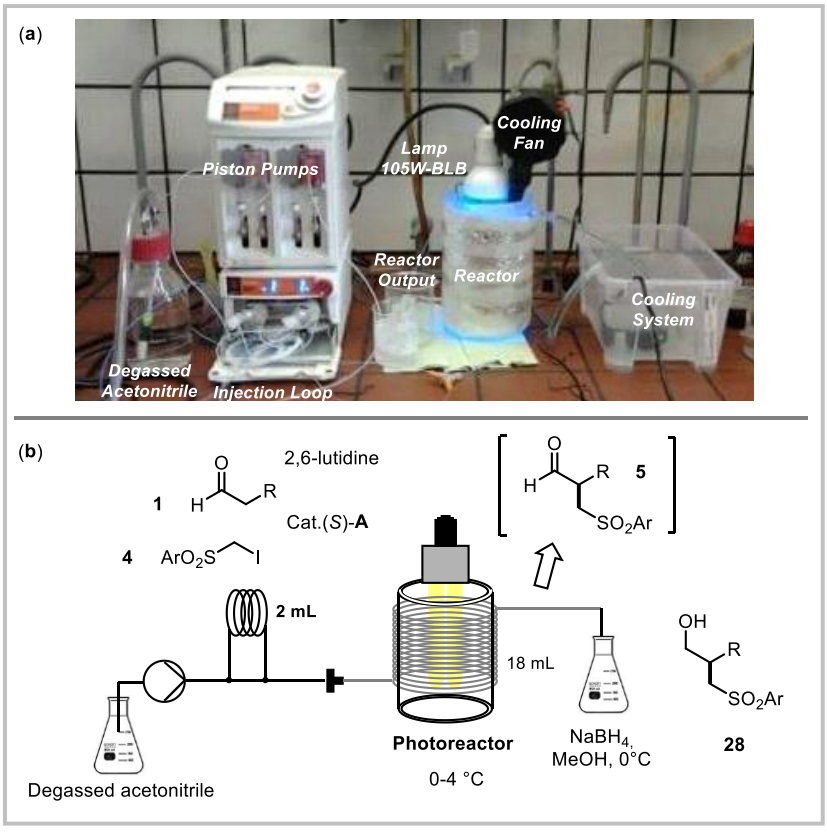

Figure 4.20 (**a**) Experimental apparatus for flow experiments. (**b**) Schematic representation of the apparatus.

4.9 Flow Experiments

A series of flow reactions were then carried out to establish the optimal flow conditions (Table 4).

Table 4. Reaction optimization under flow conditions [a]

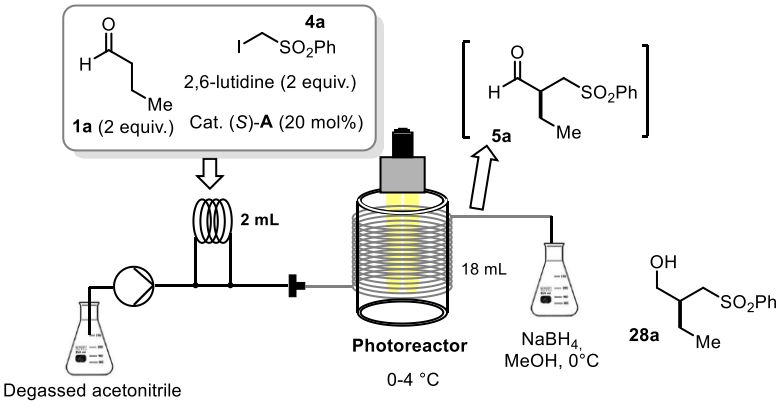

Entry	**1a**/**4a**	lamp (hν)	residence time (h)	photocatalyst (mol%)	yield **28a** (%)[b]	*ee* **28a** (%)[c]
1	2:1	105W-BLB	1	none	48	nd
2	2:1	105W-BLB	2	none	55	72
3	2:1	105W-BLB	3	none	54	nd
4	4:1	105W-BLB	2	none	46	nd
5	1:2	105W-BLB	2	none	36	nd
6	2:1	100W-CFL	2	none	35	nd
7	2:1	100W-CFL	2	$Ru(bpy)_3Cl_2$ (1)	54	nd
8	2:1	100W-CFL	2	*fac*-$Ir(ppy)_3$ (1)	40	nd
9	2:1	100W-CFL	2	Rose Bengal (1)	42	nd

[a] Reactions performed on a 0.4 mmol scale. [b] Yields determined by HPLC analysis at 215 nm on the corresponding alcohol obtained after in situ $NaBH_4$ reduction of **5a** using trichloroethylene as the internal standard. [c] Enantiomeric excess determined by HPLC analysis on the corresponding alcohol after in situ $NaBH_4$ reduction of **5a**. CFL: compact fluorescent lamp. BLB: black light bulb.

Gratifyingly, under continuous flow conditions the productivity of the studied process (mol**5a** h^{-1}) was improved compared to the batch reaction (entry 1, Table 4). Increasing the residence time to 2 h (flow rate of 0.150 mL min^{-1}) led to better results, since the product **5a** was obtained in moderate yield and good enantiomeric excess (entry 2, Table

4). Unfortunately, further increasing the residence time did not lead to any improvements (entry 3, Table 4). The yield dropped both working with a larger excess of **1a** (4 equiv.) and using an excess of **4a** (2 equiv., entries 4-5, Table 4). The 105 W black lamp bulb (BLB) was confirmed as a better source of light, since the use of a 100 W CFL led to a lower reactivity (entry 6, Table 4). The results in entries 7, 8, and 9 indicate that the addition of external photosensitizers did not increase the chemical yield of the photochemical transformation.

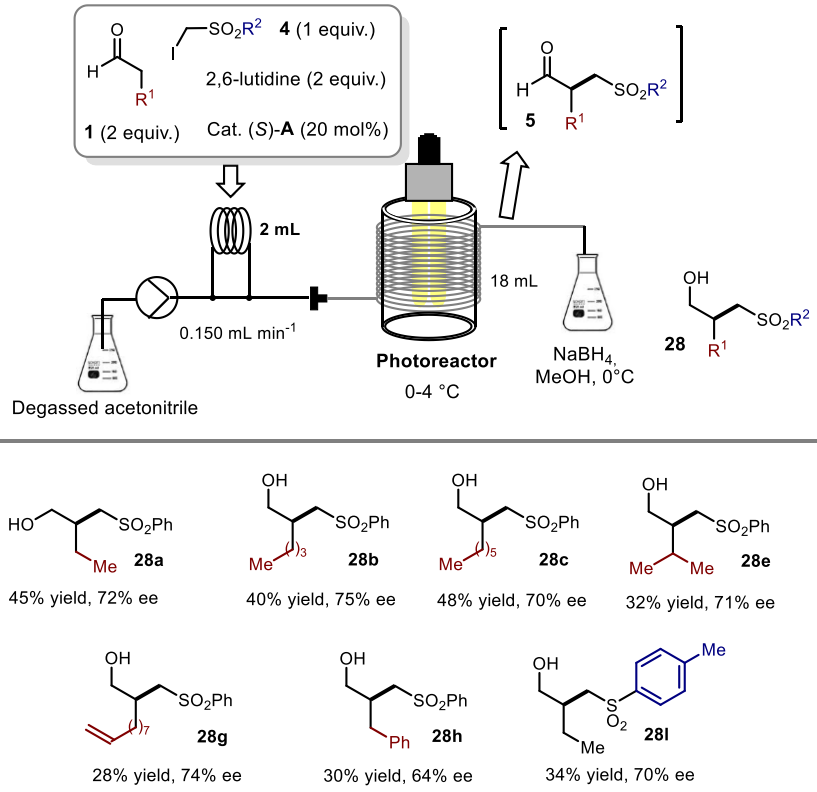

Figure 4.21 Photo-organocatalytic enantioselective alkylation of aldehydes under flow conditions. Yields and enantiomeric excesses of the isolated alcohols **28** are indicated below each entry.

We then evaluated the synthetic potential of the photo-organocatalytic strategy (Figure 4.21). Using the optimized reaction conditions (entry 2, Table 4), a diverse set of aldehydes **1** were transformed into the corresponding α-alkylated derivatives **5** using the continuous-flow regime. Aldehydes bearing alkyl chains were alkylated stereoselectively

to afford **28a-e** in moderate isolated yield (32-48%) and good enantiomeric excess (70-75%). 10-Undecenal, bearing a long alkyl fragment with a terminal olefin, was also alkylated stereoselectively to afford **28g** in a moderate isolated yield (28%) with good stereocontrol (74%). Hydrocinnamaldehyde**,** bearing a β-aromatic group, is also a suitable starting material for this transformation affording the final product **28h** in moderate isolated yield (30%) and enantiomeric excess (64%). Iodo sulfone bearing an aromatic moiety decorated with a *para*-methyl group effectively participated in the enantioselective alkylation of butanal (product **28l**, 34% yield, 70% *ee*).

In conclusion, we found that the studied photochemical reaction was faster under flow conditions with respect to the batch version (higher productivity), even though the isolated yields of the final compounds (**28**) were not sufficient from a methodological point of view. After that, I moved back to Spain (Tarragona, ICIQ), and we proceeded with a second cycle of optimization studies under batch conditions.

4.10 The Reactivity Conundrum: the Iodine Formation

We focused on a more detailed study of the reaction mechanism in order to increase the chemical yield of the model photochemical process. The absorption spectra of the reaction components were recorded (Figure 4.22a). First, the absence of any photo-absorbing ground state EDA complex between **4a** and **Ia** was confirmed, as the absorption spectrum of the reaction mixture (orange line in Figure 4.22a) overlapped with the absorption spectrum of the enamine (light blue line in Figure 4.22a), formed upon condensation of **1a** with catalyst (*S*)-**A**. We then observed that the α-iodo sulfone **4a** absorbs light up to 390 nm. The emission spectrum of the 365nm LED (blue line in Figure 4.22b), used in the preliminary experiments, shows an emission peak in the range of wavelength between 350-400 nm. This observation pointed out that both the enamine **Ia** and **4a** could absorb light under the reaction conditions. For this reason, we decided to investigate the photochemical stability of **4a** under 365 nm irradiation (Figure 4.23). A solution of **4a** in toluene, which appears colorless, was irradiated at 365 nm using a LED for 16 hours (Figure 4.23-(*i*)). Following irradiation, the solution turned to a yellow color, and only 95% of the initial amount of **4a** could be recovered (Figure 4.23-(*ii*)).

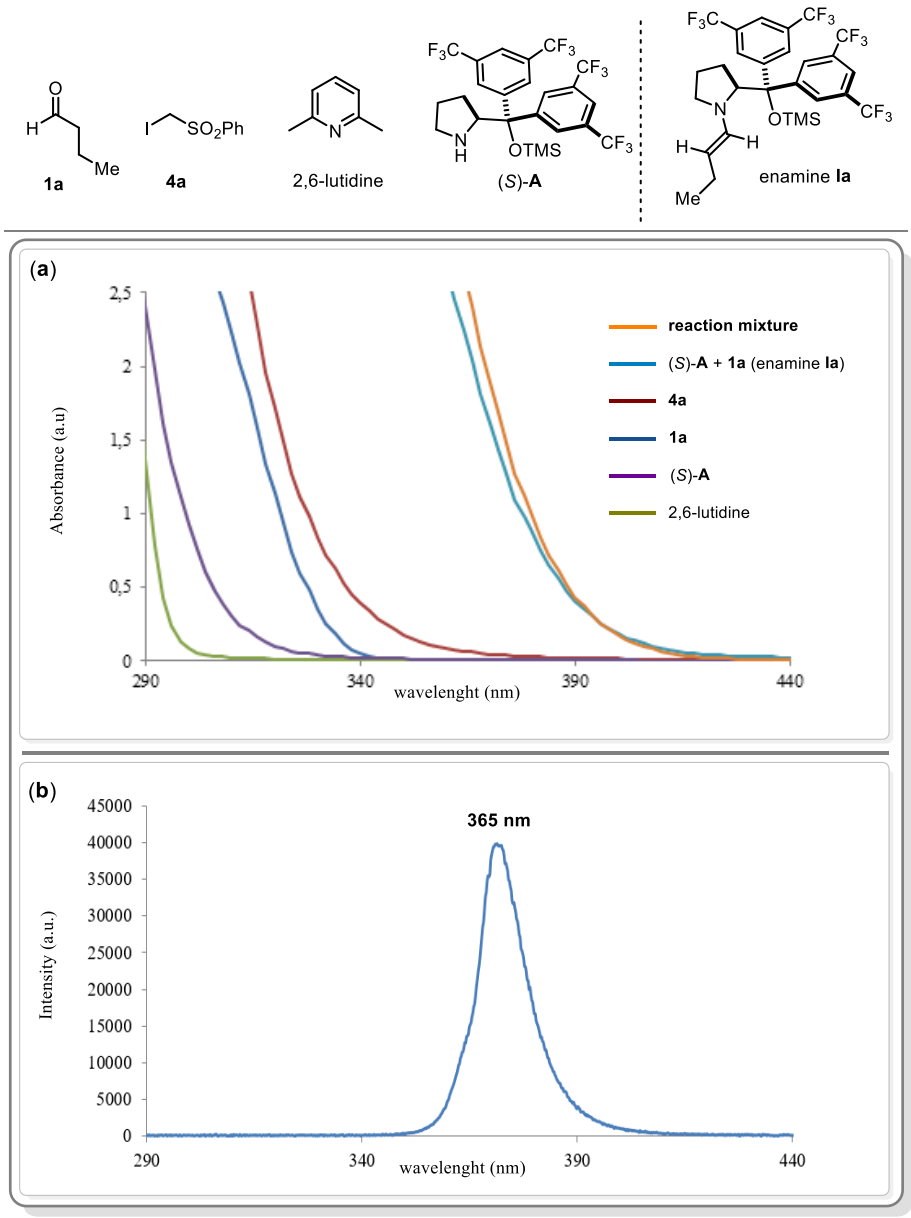

Figure 4.22 (**a**) Optical absorption spectra recorded in toluene in quartz cuvettes (1 cm path) using a Shimadzu 2401PC UV-visible spectrophotometer: [**1a**] = 1.5 M; [**4a**] = 0.5 M; [2,6-lutidine] = 0.5 M; (*S*)-**A** = 0.1 M (**b**) Emission spectrum of the single black-light-emitting diode (black LED, λ_{max} = 365 nm) used in our experiments.

This observation suggested the possibility that **4a** could undergo photo-induced homolytic cleavage of the C-I bond forming molecular iodine, which could be responsible for the yellow color of the solution ($2I\cdot \rightarrow I_2$).

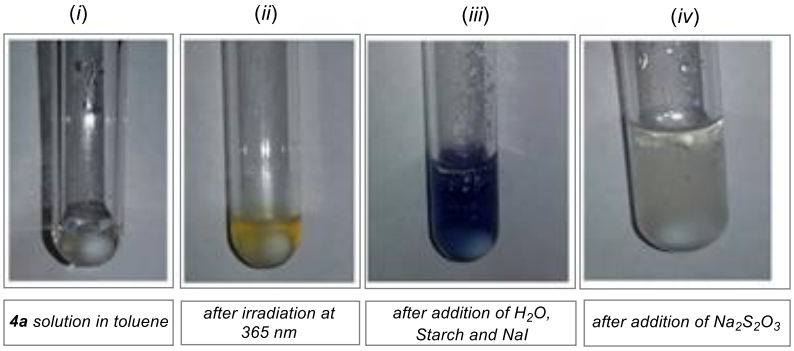

Figure 4.23 Evaluating the photostability of **4a**: (*i*) aspect of a 0.25 M solution of **4a** in degassed toluene; (*ii*) the same solution after black LED irradiation at 365 nm for 16 hours; (*iii*) the same solution after the addition of water, starch, and NaI; (*iv*) final aspect of the solution after the addition of $Na_2S_2O_3$.

Molecular iodine, even in traces, is a well-known inhibitor of radical chain reactions.[37] In fact, both atomic and molecular iodine may trap carbon centered radicals (both electrophilic and nucleophilic) at very high rates (rate constants of about 10^9 $M^{-1}s^{-1}$)[37c] suppressing radical chain propagation manifolds. Moreover, the intense light absorption of molecular iodine may also interfere with the photolytic initiation steps by means of an *inner-filter* effect.[37] In order to confirm our hypothesis, a standard iodine detection test was performed.[38] The addition of a commercially available starch solution, sodium iodide and water resulted in the formation of a blue coloration, thus confirming the presence of iodine (Figure 4.23-(*iii*)). Finally, the solution switched back to achromatic when adding solid sodium thiosulfate ($Na_2S_2O_3$, E_p^{red} = +0.28 vs Ag/Ag^+ in H_2O),[38a] which can easily reduce I_2 to iodide (Figure 4.21-(*iv*)).

[37] a) Curran, D. P.; Chang, C. T. "Evidence that palladium(0)-promoted cyclizations of unsaturated α-iodocarbonyls occur by an atom transfer mechanism" *Tetrahedron Lett.* **1990**, *31*, 933. b) Curran, D. P.; Chen, M.-H.; Kim D. "Atom transfer cyclization reactions of hex-5-ynyl iodides: synthetic and mechanistic studies" *J. Am. Chem. Soc.* **1989**, *111*, 6265. c) Studer, A.; Curran, D. P. "Catalysis of radical reactions: a radical chemistry perspective" *Angew. Chem. Int. Ed.* **2016**, *55*, 58.

[38] a) Jeffery, G. H.; Bassett, J.; Mendham, J.; Denney, R. C. *Vogel's Quantitative Chemical Analysis*, 5th ed., Longman Scientific & Technical, Harlow Essex, **1989** b) Ono, S.; Tsuchihashi, T.; Kuge, T. "On the starch-iodine complex" *J. Am. Chem. Soc.* **1953**, *75*, 3601.

These experiments confirmed that I_2 is photochemically formed in the reaction mixture and conditions to remove any iodine were investigated (Table 5).

Table 5. Optimization studies on the model reaction [a]

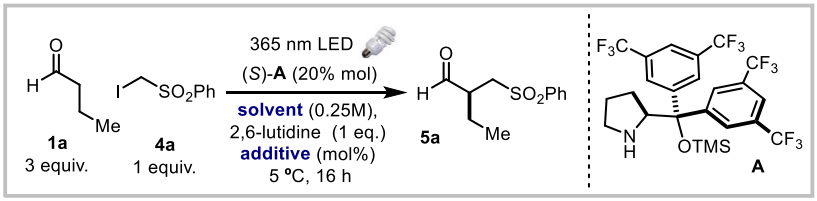

Entry	Solvent	Additive (mol%)	Conversion (%)[b]	Yield **5a** (%)[b]	*ee* **5a** (%)[c]
1	toluene	none	77	43	80
2	toluene	I_2 (10)	20	13	80
3	toluene	$Na_2S_2O_3$ (10)	55	50	81
4	toluene:H_2O (1:1)	$Na_2S_2O_3$ (10)	71	65	78
5	toluene:H_2O (1:1)	$Na_2S_2O_3$ (50)	99	99	78
6	toluene:hexane:H_2O (1:1:2)	$Na_2S_2O_3$ (50)	99	99	82
7[d]	toluene:hexane:H_2O (1:1:2)	$Na_2S_2O_3$ (50)	5 <	0	nd
8[e]	toluene:hexane:H_2O (1:1:2)	$Na_2S_2O_3$ (50)	5 <	0	nd
9[f]	toluene:hexane:H_2O (1:1:2)	$Na_2S_2O_3$ (50)	5 <	0	nd
10[g]	toluene:hexane:H_2O (1:1:2)	$Na_2S_2O_3$ (50)	5 <	0	nd
11[h]	toluene:hexane:H_2O (1:1:2)	$Na_2S_2O_3$ (50)	99	92	82

[a] Reactions performed on a 0.1 mmol scale. [b] Yields and conversions determined by ^{1}H NMR analysis using trichloroethylene as the internal standard. [c] Enantiomeric excess determined by HPLC analysis on the corresponding alcohol after in situ $NaBH_4$ reduction of **5a**. [d] Reaction performed in the dark. [e] Reaction performed in the presence of TEMPO (1 equiv.). [f] Reaction performed in the presence of O_2. [g] Reaction performed using a cut-off filter at 450 nm. [h] Reaction performed using a band pass filter at 400 nm.

The overall yield of the process significantly dropped adding an additional amount of I_2 (10 mol%) to the reaction mixture, confirming iodine's ability to inhibit the model transformation (entry 2, Table 5). On the other hand, the addition of sodium thiosulfate (10 mol%) led to an increased chemical yield (entry 3, Table 5). The desired product **5a** was obtained in acceptable yield (65%) and good enantioselectivity by performing the reaction in a toluene/H_2O mixture (1:1) as solvent (entry 4, Table 5). The use of a higher amount of $Na_2S_2O_3$ (50 mol%) led to the formation of **5a** in quantitative yield (entry 5,

Table 5). Finally, we found that the use of a biphasic mixture of solvents (toluene/hexane/water 1:1:2) in addition to a substoichiometric amount of sodium thiosulfate (50 mol%) resulted in the formation of the desired enantioenriched α-alkylated derivatives **5a** in excellent yield with good enantioselectivity (99% yield, 82% ee; entry 6, Table 5). Final control experiments indicated how the complete exclusion of light, adding 1 equiv. of TEMPO, or the presence of air completely suppressed the reactivity, confirming both the photochemical and the radical nature of the process (entries 7-9, Table 5). The fact that direct excitation of enamine **Ia** is involved in the photochemical initiation step of the process was demonstrated by using a xenon lamp equipped with a cut-off filter at 450 nm, which resulted in a complete inhibition of the reaction (entry 10, Table 5). This was further confirmed by carrying out a control experiment using a band-pass filter at 400 nm, a wavelength that could be absorbed only by the enamine **Ia** (see Figure 4.22). This result is mechanistically relevant since it excluded a possible homolytic cleavage of the C-I bond in **4a** (not feasible upon irradiation with such low-energy photons) as responsible for the radicals generation (entry 11, Table 5).

Afterwards, in order to improve the enantioselectivity of the process, a screening of catalysts was undertaken under the optimal reaction conditions (Figure 4.24). First of all, we tried to decrease the organocatalyst loading. Product **5a** was obtained in 61% NMR yield with good enantioselectivity (82% ee) using 10 mol% of catalyst **A**. The use of an even lower loading of secondary amine **A** (5 mol%) led to the formation of the desired product **5a** in moderate NMR yield (41%) along with identical stereocontrol (82% ee). In these last two experiments, we did not observe any remaining catalyst **A**, by NMR analysis of the reaction crude after 16 hours. This underlines the need for a relatively large catalyst **A** loading (20 mol%) in order to ensure quantitative yield of product **5a** over a reasonable reaction time (16 hours). Bicyclic chiral amines **G** and **H** yielded **5a** in high enantioselectivity but with poor yields. Even under the optimal reaction conditions, imidazolidinones **K**-**N** were found to be incompetent catalysts. Low reactivity was observed using catalysts **P**-**O**, since product **5a** was obtained in low NMR yield, albeit with excellent enantioselectivity. Diarylprolinol silyl ethers organocatalysts **Q** and **R** resulted in moderate reactivity and lower enantioselectivity. Catalyst **S**, decorated with two geminal fluorine atoms, did not provide the desired compound **5a**.

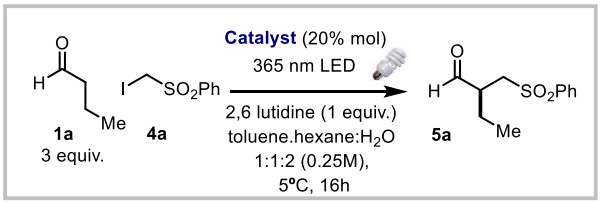

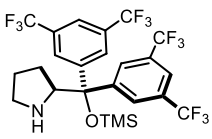

A: 99% yield, 82% *ee*.
A: 61% yield, 82% *ee*.[a]
A: 41% yield. 82% *ee*.[b]

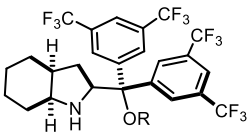

G: R = TMS: 10% yield, 89% *ee*.
H: R =TBDMS: 15% yield, 87% *ee*.

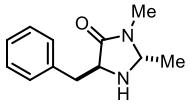

K: 0% yield.

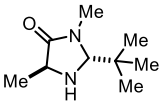

L: 0% yield.

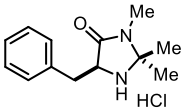

M: 0% yield.[c]

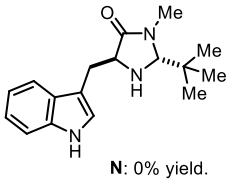

N: 0% yield.

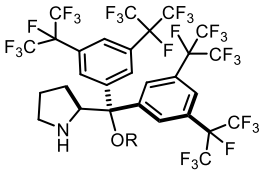

P: R = TMS: 8% yield, 93% *ee*.
O: R =TBDMS: 9% yield, 92% *ee*.

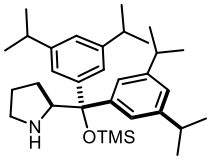

Q: 54% yield, 73% *ee*.

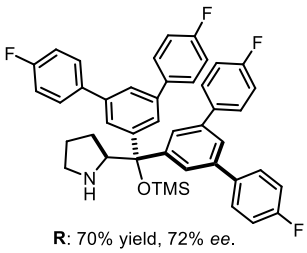

R: 70% yield, 72% *ee*.

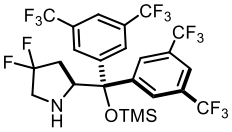

S: 0% yield

Figure 4.24 Screening of the catalysts. Yields determined by ^{1}H NMR analysis using trichloroethylene as the internal standard. Enantiomeric excess determined by HPLC analysis on the corresponding alcohol after in situ $NaBH_4$ reduction. [a] Reaction performed using 10 mol% of catalyst **A**. [b] Reaction performed using 5 mol% of catalyst **A**. [c] Reaction performed using 2 equivalents of 2,6-lutidine.

With the best conditions in hand (entry 6, Table 5), we studied the evolution of the product formation during time (Figure 4.25). The yield of **5a** increased rapidly reaching a full conversion after 16 hours (light blue line, Figure 4.25). Racemization of **5a** was not observed under the reaction conditions (5 ºC and 1 equiv. of 2,6-lutidine).

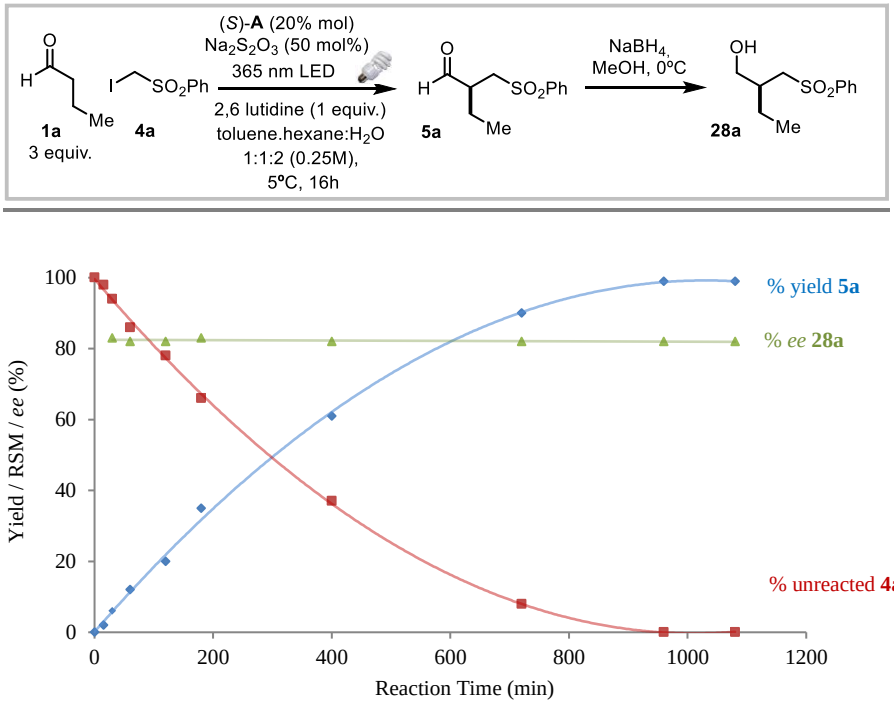

Figure 4.25 Reaction profile during the time. RMS: remaining starting material

4.11 Scope of the Reaction

We then studied the generality of the photochemical alkylation protocol. Using the optimized reaction conditions, a diverse set of aldehydes **1** were transformed into the corresponding α-alkylated derivatives **28** (Figure 4.26). Aldehydes **1a-f** bearing alkyl chains were stereoselectively alkylated to afford the corresponding alcohols **28a-f** in moderate to high isolated yield (50-95%) and good enantiomeric excess (82-96%). Compound **5a** was isolated in 76% yield with 80% *ee* (see experimental part for details). Aldehydes **1g-j** bearing a terminal olefin, an aromatic group, or a heteroatom moiety were also alkylated under the reaction conditions to afford **28g-j**.

The process is amenable to scale up (1 mmol, product **5a**), but with a slightly reduced yield. Moreover, α-iodo sulfones containing a tosyl group (**4d**), or a mesyl group (**4h**)

actively participated in the enantioselective alkylation of aldehydes (products **28k-l**). In addition, our attempts to react phenylacetaldehyde and benzyloxyacetaldehyde met with failure (products **28m-n**).

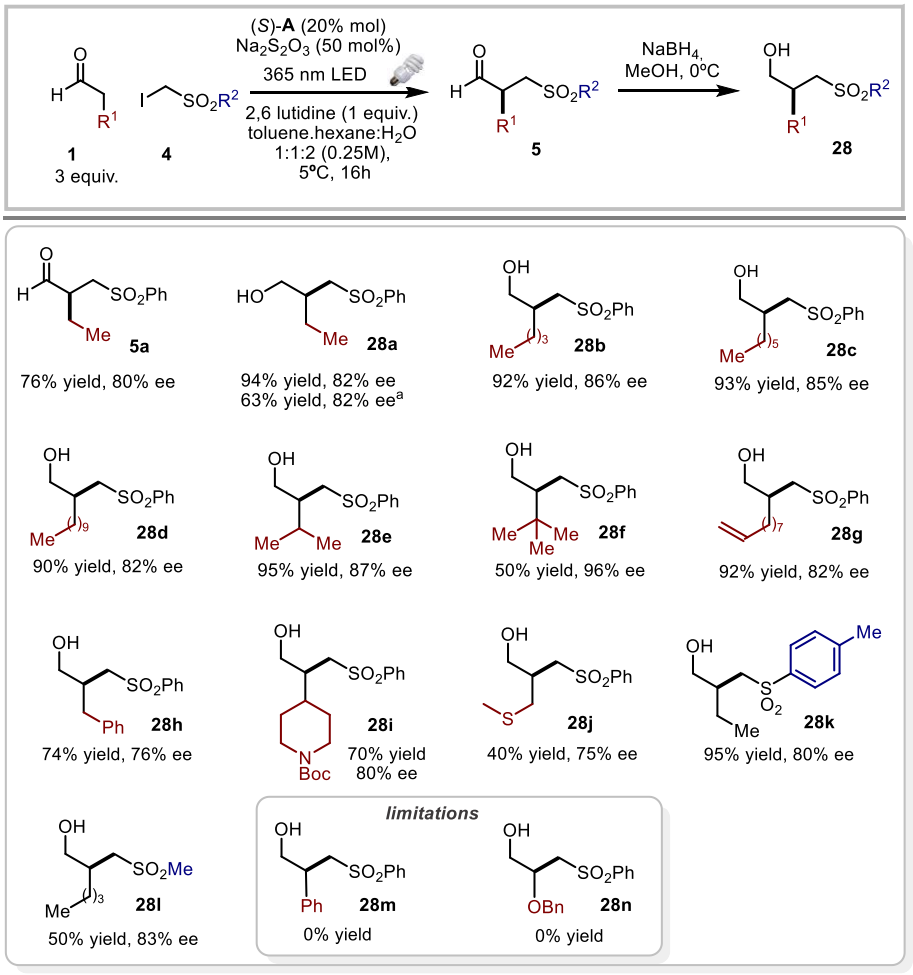

Figure 4.26 Scope of the enantioselective α-alkylation of aldehydes with α-iodo sulfones (Y=H).[a] Reaction performed in 1 mmol scale.

We then evaluated the possibility of applying our strategy to α-aryl substituted iodo sulfones **29** (Table 6), in order to develop a formal α-benzylation of aldehydes **1**.

To test the feasibility of our design plan, we focused on the reaction between butanal **1a** and the α-iodo sulfone **29a** (Table 6).

Table 6. Optimization studies on the formal benzylation reaction [a]

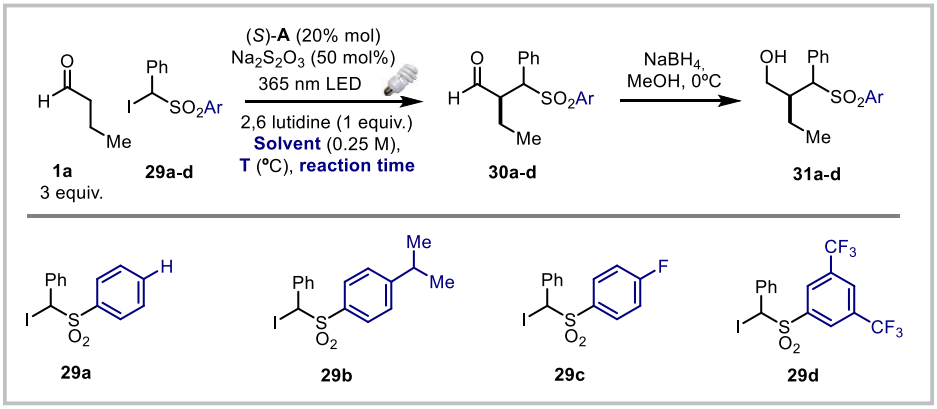

Entry	**29**	Solvent [M]	reaction time (h)	T (ºC)	yield **31** (%)[b]
1	**29a**	toluene:hexane:H_2O (1:1:2)	16	5	0
2	**29a**	Toluene:H_2O (1:1)	16	5	0
3	**29a**	CH_3CN:H_2O (1:1)	16	5	0
4	**29a**	DMSO:H_2O (1:1)	16	5	0
5	**29a**	EtOH:H_2O (1:1)	16	5	0
6	**29a**	DMF:H_2O (1:1)	16	5	0
7	**29a**	EtOAc:H_2O (1:1)	16	5	0
8	**29a**	$CHCl_3$:H_2O (1:1)	16	5	5<
9	**29a**	CH_2Cl_2:H_2O (1:1)	16	5	12
10	**29a**	CH_2Cl_2:H_2O (1:1)	16	25	7
11	**29a**	CH_2Cl_2:H_2O (1:1)	16	35	<5
12	**29a**	CH_2Cl_2:H_2O (1:1)	48	5	21
13	**29a**	CH_2Cl_2:H_2O (1:1)	120	5	33
14	**29b**	CH_2Cl_2:H_2O (1:1)	48	5	20
15	**29c**	CH_2Cl_2:H_2O (1:1)	48	5	64
16	**29c**	CH_2Cl_2:H_2O (1:1)	70	5	70
17[c]	**29c**	CH_2Cl_2:H_2O (1:1)	70	5	0
18[d]	**29c**	CH_2Cl_2:H_2O (1:1)	70	5	0
19	**29d**	CH_2Cl_2:H2O (1:1)	48	5	32

[a] Reactions performed on a 0.1 mmol scale. [b] Yields determined by ^{1}H NMR analysis using trichloroethylene as the internal standard. [c] Reaction performed in the dark. [d] Reaction performed in the presence of O_2.

Disappointingly, no product formation was observed under the optimal reaction conditions (entry 1, Table 6). We observed that compound **29a** was poorly soluble in the used solvent mixture (toluene/hexane/H_2O 1:1:2), and this prompted us to test different biphasic mixtures (H_2O/organic media 1:1) as solvent systems (entries 2-9, Table 6). The formation of product **31a** (12% NMR yield) was only observed when performing the reaction in a mixture of CH_2Cl_2/H_2O (entry 9, Table 6). Increasing the reaction temperature up to 25 ºC or 35 ºC did not lead to any benefit in terms of reactivity (entries 10-11, Table 6). On the other hand, product **31a** was obtained in a slightly better NMR yield (21%) by carrying out the reaction over 48 hours (entry 12, Table 6). A further increase of the reaction time to 120 hours led to the formation of the desired product **31a** in moderate yield (33% yield; entry 13).

In order to increase the solubility of the α-iodo sulfone, we synthesized **29b** containing a *para*-isopropyl substituent, since an alkyl chain could increase the solubility of the starting material. Gratifyingly, compound **29b** was completely soluble in CH_2Cl_2 and the reaction mixture appeared as a homogeneous solution (entry 14, Table 6). Unfortunately, no improvement was achieved in terms of reactivity, since the product **31b** was obtained in moderate NMR yield after 48 hours (20% yield). This experiment clearly pointed out that the low solubility of the starting material (**29a**) was not the main problem in the studied reaction. We thought that the corresponding carbon centered radical of **29a**, formed upon a SET mechanism, could be stabilized by the presence of the vicinal phenyl group, thus decreasing its electrophilicity and reactivity. In addition, the steric effect of the phenyl substituent could also reduce the reactivity of the radical. With this in mind, we prepared **29c**, since the presence of an electron withdrawing group (*para*-fluorine atom) could both make the α-iodo sulfone more prone to reduction while increasing the electrophilicity of the corresponding radical. Gratifyingly, after 48 hours product **31c** was obtained in 64% NMR yield (entry 15, Table 6). Increasing the reaction time to 70 hours led to the formation of the desired product **31c** in 70% NMR yield (entry 16, Table 6). Control experiments indicates that the reaction did not proceed either in the dark or in the presence of oxygen (entries 17-18, Table 6).

We then synthesized **29d** bearing an aromatic moiety decorated with two strong electron-withdrawing -CF_3 groups. Unfortunately, the use of **29d** as source of radicals did not improve the chemical yield of the process (entry 19, Table 6).

With the best conditions in hand (entry 16, Table 6) we studied the evolution of the product formation over time (Table 7). Under the optimal conditions, the total yield of **31c** increased slowly reaching a maximum at about 70% after 70 hours. The desired compound **31c** was obtained as a mixture of two diastereoisomers (d.r = 3.2:1) with

excellent enantioselectivity. Appreciable degradation of the final compound (**31c**) was observed by performing the reaction over a longer period of time (> 70 hours).

Table 7. Evaluation of the total yield and the product distribution over time [a]

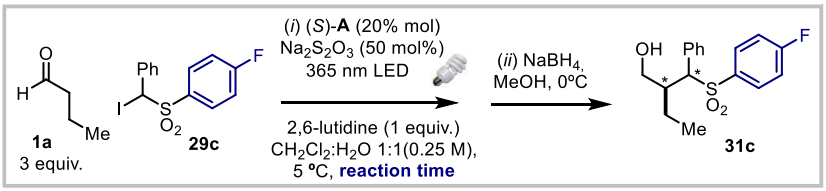

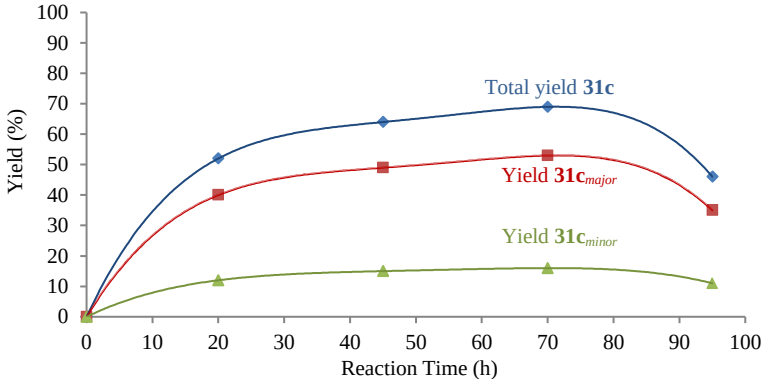

Entry	reaction time (h)	yield **31c** (%)[b]	d.r.[c]	*ee*major **31c** (%)[d]	*ee*minor **31c** (%)[d]
1	0	0	-	-	-
2	20	52	3.2:1	97	80
3	48	64	3.2:1	96	80
4	70	70	3.2:1	97	80
19	95	46	3.2:1	97	80

[a] Reactions performed on a 0.1 mmol scale. [b] Yields determined by ^{1}H NMR analysis using trichloroethylene as the internal standard. [c] Determined by ^{1}H NMR analysis of the crude reaction mixture. [d] Enantiomeric excess determined by HPLC analysis.

The scope of this catalytic transformation was evaluated under the optimized conditions (entry 16, Table 6). Aldehydes containing alkyl chains, or a terminal olefin were well tolerated under the reaction conditions (Figure 4.27). The corresponding enantioenriched α-alkylated derivatives **31c-g** were isolated in moderate yields (43-60%) and low diastereoselectivity but with good enantiomeric excess (74-97%). In addition, compound **31h**, bearing a *para*-methyl substituent, was obtained in moderate isolated yield (35%) as a mixture of two diastereoisomers with good enantioselectivity.

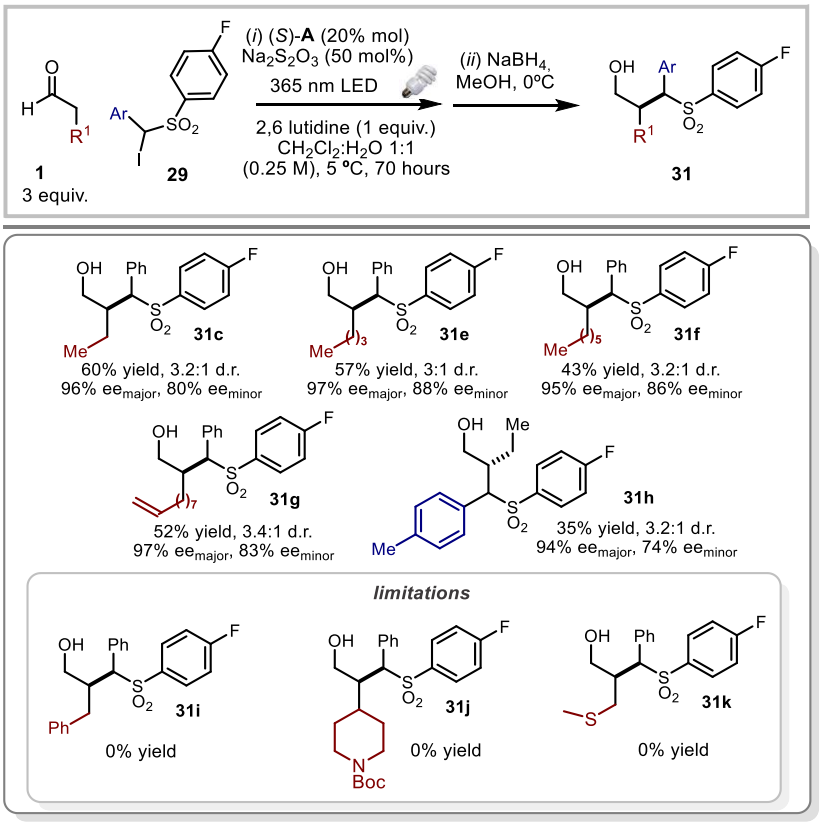

Figure 4.27 Scope of the enantioselective α-alkylation of aldehydes with α-iodo sulfones (Y=Ar).

As a limitation of this photochemical process, we found that hydrocinnamaldehyde, 2-(1-methyl-4-piperidinyl) acetaldehyde and methional were not suitable substrates (products **31i**, **31j**, **31k** respectively). Furthermore, the use of **32a** led to the formation of product **33a** in 51% isolated yield (Figure 4.28). In this case too, the presence of the methyl group adjacent to the carbon centered radical decreased its reactivity for both steric and electronic reasons. The use of a α-iodo sulfone bearing a more electron withdrawing *para*-fluoro phenyl substituent (**32a**) was found to be essential to increase the reactivity of the studied reaction. Unfortunately the d.r. (1.5:1.0) and the enantioselectivity ($ee_{\mathbf{major}}$ = 66%, $ee_{\mathbf{minor}}$ = 61%) remained low.

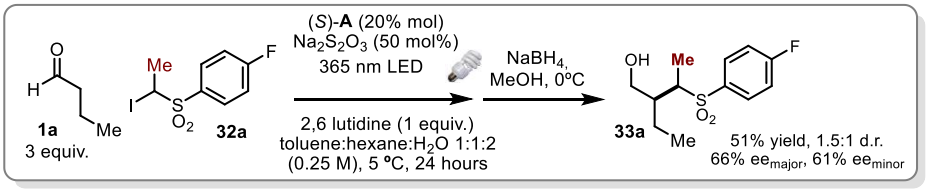

Figure 4.28 α-alkylation reaction of aldehydes **1a** with compound **32a**.

4.12 Desulfonylation Strategies

The main goal of our studies was to provide an efficient method for stereoselectively installing either a methyl or a benzyl group at the α-position of aldehydes **1**. To achieve this goal, we used the synthetic versatility of the phenylsulfonyl moiety. Indeed, products of type **28** may be easily desulfonylated under reducing conditions to give the corresponding valuable enantioenriched methylated derivatives **20** (Figure 4.29).

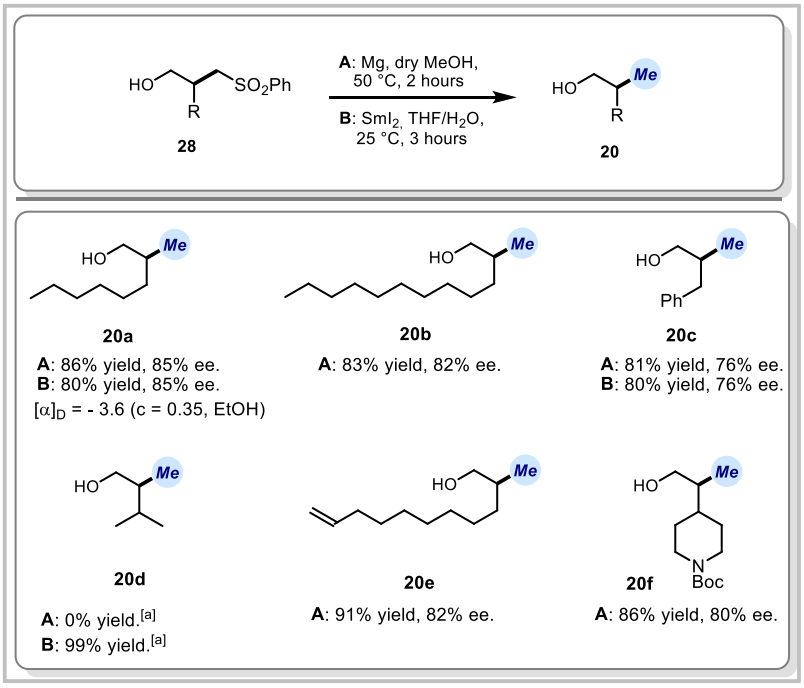

Figure 4.29 Desulfonylation which reveals the methyl group [a] NMR yield of **20d** determined using 1,1,2-trichloroethene as the internal standard.

Two different reported conditions were identified[22]: activated Mg in dry MeOH at 50 ºC (method **A**) or SmI_2 in H_2O/THF (method **B**).

Method **A** (activated Mg in dry MeOH at 50 ºC) was found to be compatible with products **28** bearing long alkyl chains, an aromatic moiety, a terminal olefin and heteroatoms, since compounds **20a**, **20b**, **20c**, **20e** and **20f** were isolated in high chemical yields (80-91%) without any erosion of the enantiomeric excesses. The absolute configuration of **20a** was assigned by comparison with reported optical rotation value (see the experimental section for details).[24] On the other hand, method **A** was found not to be compatible with products bearing short alkyl chains (such as compound **28e**), where complete conversion of the starting material was achieved but the final product (**20d**) was not observed by ^{1}H NMR analysis of the crude reaction mixture.

By contrast, method **B** (SmI_2 in H_2O/THF at 25 ºC) afforded the desired compound **20d** in high ^{1}H NMR based yield. Compound **20d** was found to be highly volatile, therefore its isolation by flash column chromatography was not possible. Method **B** works well with products **28** bearing long and short alkyl chains and an aromatic moiety, since compounds **20a**, **20c** and **20d** were isolated in high yields without any erosion of the enantiomeric excesses. In a similar way, products of type **31** can be easily desulfonylated under reductive conditions to reveal the corresponding enantioenriched benzylated derivatives **34** (Figure 4.30).[22]

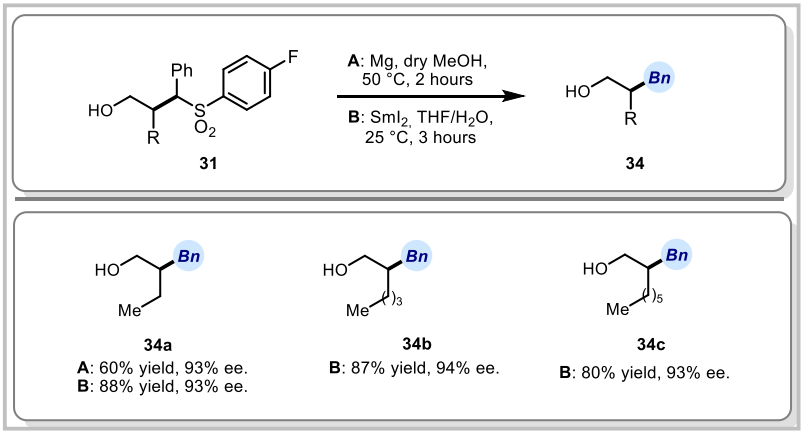

Figure 4.30 Desulfonylation which reveals the benzyl group.

Method **A** (activated Mg in dry MeOH at 50 ºC) did not afford the desired product **34a** efficiently; indeed the model compound was isolated only in moderate yield and without erosion of enantioenrichment. On the other hand, method **B** (SmI_2 in H_2O/THF at 25 ºC) provided compound **34a** in high isolated yield (88%) without any erosion of the enantiomeric excess. Furthermore, method **B** was extended to compounds **31e** and **31f** furnishing the corresponding benzylated derivatives **34b-c** in high yields and good enantioselectivity.

4.13 Mechanistic Investigations

Our initial experiments, detailed in Table 5, indicates that the direct photoexcitation of the enamine **Ia**, formed *in situ* upon condensation of the chiral secondary amine **A** and aldehyde **1a**, triggers the radical generation from **4a**. The photo-excited enamine **Ia*** (E_p^{red} (**Ia***) ≈ -2 V vs Ag/Ag^+ in CH_3CN)[3a] may induce the reductive cleavage of the C–I bond in **4a** (E_p^{red} (**4a**) = -1.49 V vs Ag/Ag^+ in CH_3CN) *via* SET mechanism, affording the electrophilic radical **IIa** and the intermediate **VI** (Figure 4.31). In a similar manner, enamine **Ia** can be used to generate electrophilic radicals from compound **29c** (E_p^{red} (**29c**) = -1.02 V vs Ag/Ag^+ in CH_3CN).

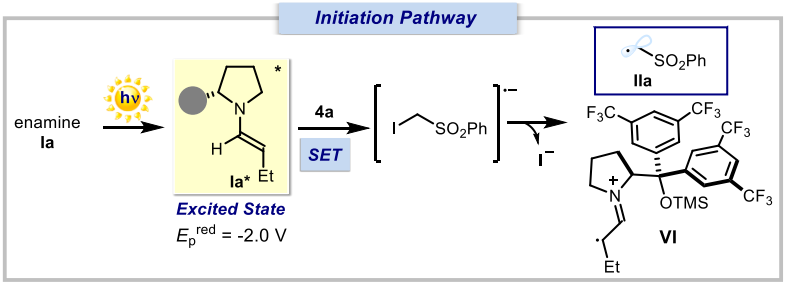

Figure 4.31 Radical formation strategy based on the direct photoexcitation of the chiral enamine. SET: single-electron transfer; the grey circle represents a bulky substituent.

Furthermore, a quantum yield (Φ) of 3.9 (λ = 400 nm) was determined for the model reaction (aldehyde **1a** and α-iodosulfone **4a**) corroborating a radical chain mechanism as the main pathway, thus discarding the possibility of a radical-radical combination of **IIa** and **VI** within the solvent cage. Intermediate **VI** is an unproductive species, since it lies outside of the chain propagation manifold which converts substrates into products. We have obtained evidence that **VI** is an unstable intermediate which cannot be reduced back to the progenitor enamine **Ia**. Instead, the α-iminyl radical cation **VI** collapses to give a variety of degradation products that, despite our efforts, have remained unidentified so

far.[3b] In the determination of the quantum yield, the model reactions were performed in acetonitrile at room temperature in the absence of sodium thiosulphate (see experimental section for details). Indeed, our attempts to determine the quantum yield under the optimal reaction conditions were complicated by the heterogeneity of the reaction mixture, which precluded a homogeneous illumination, which is a crucial requirement for a reliable quantum yield determination.[3b] According to a quantum yield of 3.9, two possible radical propagation manifolds are possible, both of which exploit the intermediacy of the electron-rich α-amino radical **X** to regenerate the propagating radical **IIa** (Figure 4.32a). An electron-transfer from **X** to the electron-poor alkyl iodide **4a**, which regenerates the chain-propagating radical **IIa** while giving the iodine-iminium ion pair **VII**. Alternatively, an atom-transfer mechanism can be envisaged, where the α-aminoalkyl radical **X** would abstract an iodine atom from **4a**, regenerating the radical **IIa** while affording an unstable α-iodo amine adduct **XI. XI** would eventually evolve to the iminium ion **VII**.

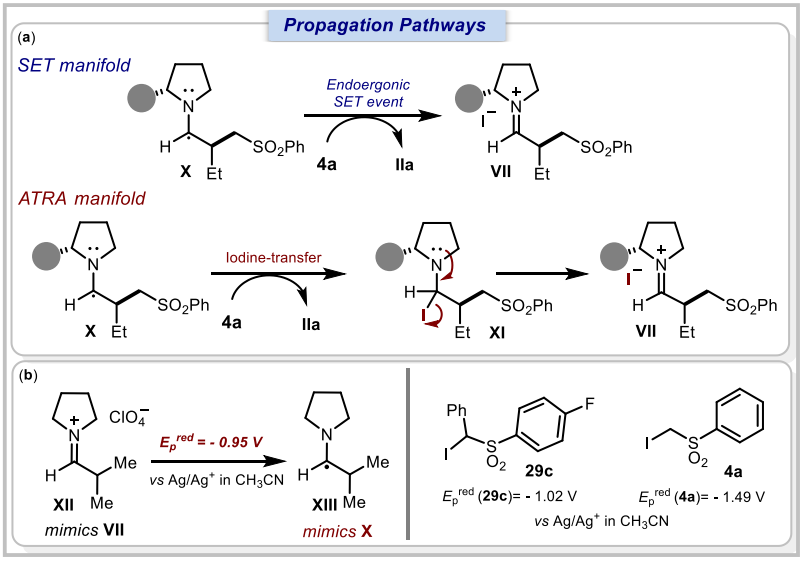

Figure 4.32 (**a**) Possible propagation pathways. (**b**) Estimating the redox properties of the α-amino radical intermediates

In order to discriminate between the two possible propagation pathways, we prepared and isolated the iminium ion **XII**, derived from the condensation of pyrrolidine and isobutyraldehyde (see experimental part for further details), which mimics the actual iminium ion intermediate **VII** involved in the catalytic cycle (Figure 4.32b).[3b] **VII** could

not be synthesized because of the steric hindrance of catalyst **A** hampering a facile condensation with the aldehydic compound **5a**. Evaluating the redox properties of **XII** is pertinent, since its electrochemical reduction provides access to α-aminoalkyl radical of type **XIII**, which is the key intermediate of the radical chain propagation. We measured, by cyclic voltammetry, a reduction potential (E_p^{red} of **XII**) of -0.95 V *vs* Ag/Ag^+ in CH_3CN. This value means that the α-amino radical of type **X** is incapable of reducing **4a** (E_p^{red} of **4a** = -1.49 V *vs* Ag/Ag^+ in CH_3CN) by a direct SET mechanism, which would be a highly endergonic step, indicating that an iodine-transfer mechanism (ATRA type mechanism)[39] is likely operative instead. In contrast, a SET reduction of **29c** (E_p^{red} (**29c**) = -1.02 V vs Ag/Ag^+ in CH_3CN) from **X** may not be excluded. On the basis of all these observations, we propose the following reaction mechanism (Figure 4.33).

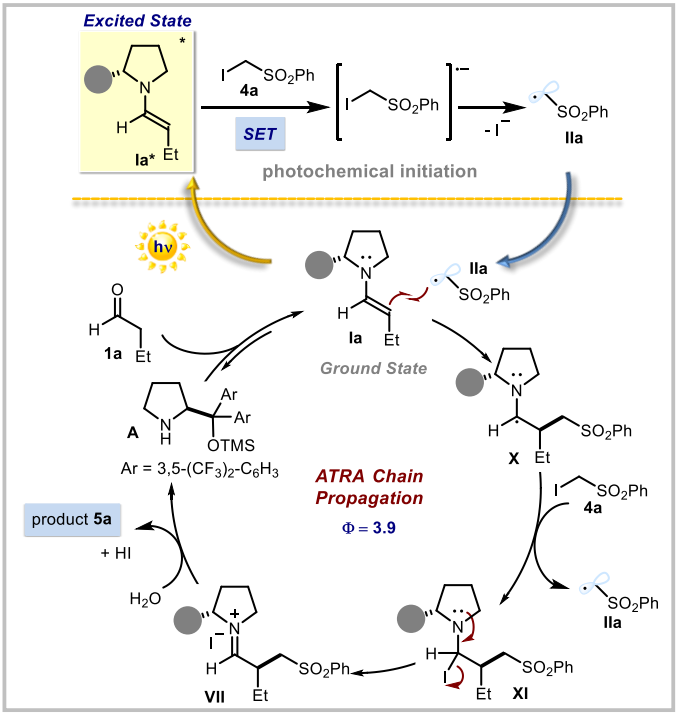

Figure 4.33 Proposed mechanism

[39] a) Kharasch, M. S.; Jensen, E. V.; Urry, W. H. "Addition of carbon tetrachloride and chloroform to olefins" *Science* **1945**, *102*, 128. b) Pintauer, T.; Matyjaszewski, K. "Encyclopedia of radicals" **2012**, Volume 4, p. 1851, Wiley.

The chiral enamine **Ia**, formed upon condensation of **A** and butanal **1a**, directly reaches an electronically excited state **Ia*** after light absorption, triggering the formation of the electron-deficient radical **IIa** through the reductive cleavage of the iodo sulfone C−I bond *via* a SET mechanism. The ground-state chiral enamine **Ia** then stereoselectively intercepts the radical (**IIa**) affording the electron-rich α-aminoalkyl radical **X**. The α-aminoalkyl radical **X** then abstracts an iodine atom from **4a**, thereby regenerating radical **IIa**. The resulting adduct **XI** is not stable and evolves to an iodine-iminium ion pair **VII**, which eventually hydrolyzes to release the product **5a** and the aminocatalyst **A** Overall, this chemistry can be considered as an example of an enantioselective catalytic atom transfer radical addition (ATRA), explaining well the striking effect of iodine, which is a powerful inhibitor of iodine atom transfer chains.[37c]

4.14 Conclusions

In summary, we have reported a photochemical strategy for the enantioselective catalytic formal α-methylation and α-benzylation of aldehydes. This two-step method uses mild conditions and easily available substrates and catalysts to provide compounds that are difficult to synthesize with other catalytic approaches. The chemistry exploits the phenylsulfonyl moiety within the radical precursor to facilitate the generation of open-shell species, acting as a redox auxiliary group, while unveiling the methyl and benzyl groups upon desulfonylation of the alkylation products. Key for reaction development was the ability of chiral enamines to generate radicals upon light excitation and then trap them in a stereocontrolled fashion.

4.15 Experimental Section

4.15.1. General Information

The NMR spectra were recorded at 400 MHz for ^{1}H, 101 MHz for ^{13}C and 376 MHz for ^{1}H decoupled ^{19}F. The chemical shift (δ) for ^{1}H, ^{13}C and ^{1}H decoupled ^{19}F are given in ppm relative to residual signals of the solvents ($CHCl_3$ @ 7.26 ppm ^{1}H NMR and 77.16 ppm ^{13}C NMR, and tetramethylsilane @ 0 ppm). Coupling constants are given in Hertz. The following abbreviations are used to indicate the multiplicity: s, singlet; d, doublet; q, quartet; m, multiplet; bs, broad signal. High resolution mass spectra (HRMS) were obtained from the ICIQ HRMS unit on Waters GCT gas chromatograph coupled time-of-flight mass spectrometer (GC/MS-TOF) with electrospray ionization (ESI). Optical rotations were measured on a Polarimeter Jasco P-1030 and are reported as follows: $[\alpha]_D$ r.T. (c in g per 100 mL, solvent). Cyclic voltammetry studies were carried out on a

Princeton Applied Research PARSTAT 2273 potentiostat offering compliance voltage up to ± 100 V (available at the counter electrode), ± 10 V scan range and ± 2 A current range. UV-vis measurements were carried out on a Shimadzu UV-2401PC spectrophotometer equipped with photomultiplier detector, double beam optics and D_2 and W light sources. Cut-off and band-pass photochemical experiments have been performed using a 300 W xenon lamp (*Asashi* Spectra Co., Ltd.) to irradiate the reaction mixture.

General Procedures. All reactions were performed under an argon atmosphere in oven-dried glassware using standard Schlenk techniques, unless otherwise stated. Synthesis grade solvents were used as purchased, anhydrous solvents were taken from a commercial SPS solvent dispenser. Chromatographic purification of products was accomplished using force-flow chromatography (FC) on silica gel (35-70 mesh). For thin layer chromatography (TLC) analysis throughout this work, Merck pre-coated TLC plates (silica gel 60 GF_{254}, 0.25 mm) were employed, using UV light as the visualizing agent and an acidic mixture of *para*-anisaldehyde or basic aqueous potassium permangante ($KMnO_4$) stain solutions, and heat as developing agents. Organic solutions were concentrated under reduced pressure on a Büchi rotatory evaporator.

Determination of Enantiomeric Purity: HPLC analysis on chiral stationary phase was performed on an Agilent 1200-series instrument, employing Daicel Chiralpak IA, IB, ID, IC and IC-3 columns, or a Waters ACQUITY® UPC^2 instrument, using Trefoil IC, AMY1, CEL1, and CEL2 chiral columns. The exact conditions for the analyses are specified within the characterisation section. HPLC traces were compared to racemic samples prepared performing the reactions in the presence of a racemic mixture of catalyst **A**.

Materials. Commercial grade reagents and solvents were purchased from Sigma-Aldrich, Fluka, Alfa Aesar, Fluorochem, SynQuest and used as received, without further purifications. Reagents were purchased at the highest commercial quality from Sigma Aldrich, Fluka, and Alfa Aesar and used as received, without further purification, unless otherwise stated. The chiral secondary amine catalyst *(S)*-**A** is commercially available; catalyst *(R)*-**A** was purified by flash column chromatography prior to use and stored at 4 °C under argon to avoid undesired desilylation that would affect the catalytic potential of the amine. Sodium thiosulfate anhydrous (extra pure, 98.5%) was purchased from Acros Organic and used as received. Reagents were purchased at the highest commercial quality and used without further purification, unless otherwise stated. Catalysts **G** and **H** were synthesized within the Melchiorre group according to a reported procedure.[14] Catalyst **P**, **O** and **S** were synthesized within the Melchiorre group according to a reported

procedure.[40] Catalysts **Q** and **R** were synthesized within the Melchiorre group according to a reported procedure.[41]

HPLC, UPC2, ^{1}H NMR and ^{13}C NMR traces and spectra are available in the published manuscript[1] and are not reported in the present thesis.

4.15.2. Synthesis of the Starting Materials

General Procedure 1: Synthesis of α-iodo sulfones (**4a**), (**4d**) and (**4h**)

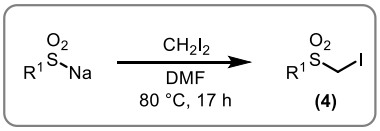

Using a modified literature procedure[42], a solution of sodium sulfinate (1.0 equiv.) in dimethylformamide (0.25 mL) was stirred at room temperature for 15 minutes. Diiodomethane (1.2 equiv.) was added dropwise and the solution was stirred for 17 hours at room temperature. The reaction was quenched by the addition of water (100 mL). The solution was then transferred to a separatory funnel and extracted with ethyl acetate (3 x 50 mL). The organic phases were combined and washed with brine (50 mL), saturated solution of sodium thiosulfate (50 mL) and then dried over magnesium sulfate before concentration *in vacuo*. The residue was purified by flash column chromatography to afford the desired α-iodo-sulfone (**4**).

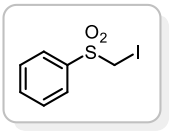

((Iodomethyl)sulfonyl)benzene (4a) was prepared according to the General Procedure **1** using sodium benzenesulfinate (10.0 g, 60.9 mmol, 1.0 equiv.) The residue was purified by flash column chromatography (*n*-hexane: ethyl acetate = 3:1) affording the desired iodo-sulfone (**4a**) as a white solid (12.0 g, 70% yield).

^{1}H NMR:(400 MHz, $CDCl_3$) δ 8.03 – 7.94 (m, 2H), 7.72 (tt, *J* = 6.9, 1.2 Hz, 1H), 7.66 – 7.58 (m, 2H), 4.48 (s, 2H). **^{13}C NMR**:(101 MHz, $CDCl_3$) δ 135.9, 134.6, 129.4, 129.0, 16.9.

---

[40] Silvi, M.; Verrier, C.; Rey, P. Y.; Buzzetti, L.; Melchiorre, P. "Visible-light excitation of iminium ions enables the enantioselective catalytic β-alkylation of enals" *Nat. Chem.* **2017**,DOI: 10.1038/nchem.2748.
[41] Shi, L.; Tao, C.; Yang, Q.; Liu, Y. E.; Chen, J.; Tian, J.; Liu, F.; Li, B.; Du, Y.; Zhao, B. "Chiral pyridoxal-catalyzed asymmetric biomimetic transamination of α-keto acids" *Org. Lett.* **2015**, *17,* 5784.
[42] Pospíšil, J.; Robiette, R.; Sato, H.; Debrus, K. "Practical synthesis of β-oxo benzo[d]thiazolyl sulfones: scope and limitations" *Org. Biomol. Chem.* **2012**, *10,* 7708.

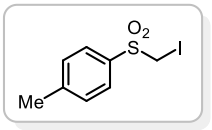

1-((Iodomethyl)sulfonyl)-4-methylbenzene (4d) was prepared according to the General Procedure **1** using sodium 4-methylbenzenesulfinate (10.80 g, 60.0 mmol, 1.0 equiv.) The residue was purified by flash column chromatography (*n*-hexane:ethyl acetate = 3:1) affording the desired iodo-sulfone (**4d**) as a white solid (11.6 g, 65% yield). **^{1}H NMR**:(400 MHz, $CDCl_3$) δ 7.85 (d, *J* = 8.3 Hz, 2H), 7.39 (d, *J* = 8.0 Hz, 2H), 4.44 (s, 2H), 2.48 (s, 3H). **^{13}C NMR**:(101 MHz, $CDCl_3$) δ 145.89 , 133.18 , 130.12 , 129.20 , 21.89 , 17.07.

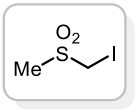

1-((Iodomethyl)sulfonyl)-4-methylbenzene (4h) was prepared according to General Procedure **1** using sodium methanesulfinate (6.0 g, 60.0 mmol, 1.0 equiv.) The residue was purified by flash column chromatography (*n*-hexane:ethyl acetate = 3:1) affording the desired iodo-sulfone (**4h**) as a white solid (6.6 g, 50% yield). **^{1}H NMR**:(400 MHz, $CDCl_3$) δ 4.38 (q, *J* = 0.8 Hz, 2H), 3.18 (d, *J* = 0.9 Hz, 3H). **^{13}C NMR**:(101 MHz, $CDCl_3$) δ 38.54 , 13.59.

Compounds **4b**, **4c**, **4e** were synthesized within the Melchiorre group according to a reported procedure.[42] Compound **4f** was synthesized within the Melchiorre group according to a reported procedure.[43] Compound **4g** was synthesized within the Melchiorre group according to a reported procedure.[44]

[43] Gogonas, E. P.; Nyxas, I.; Hadjiarapoglou, L. P. "The reaction of phenyliodonium bis(phenylsulfonyl)methylide with alkyl iodides" *Synlett* **2004**, *14, 2563.*
[44] Yagupolski, L. M.; Matsnev, A. V. "Aryliododifluoromethylsulfides, sulfoxides and sulfones: the first optically active compounds with polyfluoroalkyliodo groups" *Mendeleev Commun.* **2006**, *3, 132.*

General Procedure 2: Synthesis of α-iodo sulfones (**29c**) and (**29e**)

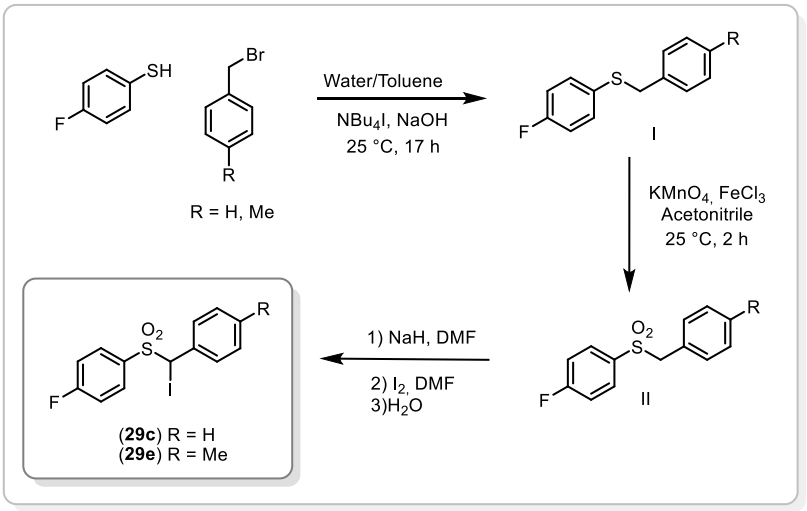

STEP 1: A solution of 4-fluorobenzenethiol (45 mmol, 5.8 g) and the appropriate benzyl bromide (48 mmol, 1.06 equiv) in toluene (20 mL) was added to a solution containing NaOH (75 mmol, 3 g) and Bu_4NI (1.4 mmol, 0.5 g) in H_2O (20 mL). The biphasic system was stirred vigorously during 16 hours. The aqueous phase was extracted with Et_2O (3 x 20 mL), the combined organic phases were washed with NaOH (20 mL, 1M) and brine (50 mL) and then dried over magnesium sulfate before concentration *in vacuo*. The residue (**I**) was used without any further purification (R = H: 95% yield; R = Me: 97% yield).

STEP 2, according to a modified literature procedure[45]: A solution of **I** (25 mmol), $FeCl_3$ (0.9 mmol, 0.15 g) and $KMnO_4$ (95 mmol, 15 g) in acetonitrile (100 mL, 0.25 m) was stirred at room temperature for 2 hours. The crude reaction mixture was filtered over celite before concentration *in vacuo*. The residue was purified by flash column chromatography (*n*-hexane:ethyl acetate = 6:4) affording the desired product (**II**) as a white solid (R = H: 82% yield, R = Me: 80% yield).

STEP 3, according to a modified literature procedure[46]: Compound **II** (17 mmol) was placed in a two-necked round-bottom flask and dissolved with 85 mL of dry DMF at room temperature under argon. To this solution was added 1.6 g of sodium hydride (60% dispersion in mineral oil). A temperature of 25 ºC was maintained constant while stirring

[45] Lai, S.; Lee, D. G. "Lewis acid assisted permanganate oxidations" *Tetrahedron* ***2002****, 58, 9879.*
[46] Jarvis, B. B.; Saukaitis J. C. "Nucleophilic displacements on halogen atoms. II. Kinetic study of the reactions of alpha.-Halo sulfones with triphenylphosphine" *J. Am. Chem. Soc.* **1973**, *95,* 4853.

the solution. In the meanwhile, the color changed from colorless to yellow. After 10 minutes, the solution was transferred via cannula to a solution of 4.2 g of iodine in 25 mL of dry DMF under argon. The resulting mixture was poured into 500 mL of water and the precipitate was collected and recrystallized from acetone to give the final compound **29** (R = H: 40% yield, R= Me: 13% yield).

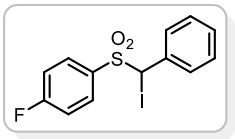

1-fluoro-4-((iodo(phenyl)methyl)sulfonyl)benzene (29c) was prepared according to the General Procedure **2** using benzyl bromide (8.2 g, 48 mmol, 1.06 equiv). **^{1}H NMR**: (400 MHz, Chloroform-*d*) δ 7.62 – 7.53 (m, 2H), 7.37 – 7.27 (m, 3H), 7.25 – 7.18 (m, 2H), 7.11 – 6.99 (m, 2H), 5.90 (s, 1H). **^{13}C NMR**: (101 MHz, Chloroform-*d*) δ 166.20 (d, *J* = 257.8 Hz), 133.33, 132.70 (d, *J* = 9.8 Hz), 130.60, 130.22, 129.97 (d, *J* = 3.2 Hz), 128.88, 116.33 (d, *J* = 22.7 Hz), 43.35. **^{1}H decoupled ^{19}F NMR:** (376 MHz, Chloroform-*d*) δ -102.28 (s, 1F). **HRMS**: Calculated for $C_{13}H_{10}FINaO_2S$ 398.9322, found 398.9328.

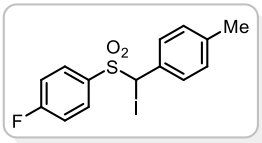

1-fluoro-4-((iodo(p-tolyl)methyl)sulfonyl)benzene (29e) was prepared according to general Procedure **2** using 4-methylbenzyl bromide (8.9 g, 48 mmol, 1.06 equiv). **^{1}H NMR**: (400 MHz, Chloroform-*d*) δ 7.71 – 7.50 (m, 2H), 7.25 – 7.15 (m, 2H), 7.12 – 6.94 (m, 4H), 5.88 (s, 1H), 2.32 (s, 3H). **^{13}C NMR**: δ 166.18 (d, *J* = 257.5 Hz), 140.55, 132.74 (d, *J* = 9.7 Hz), 130.44, 130.28, 129.57, 116.30 (d, *J* = 22.7 Hz), 43.36, 21.44. **^{1}H decoupled ^{19}F NMR:** (376 MHz, Chloroform-*d*) δ -102.45 (1F). **HRMS**: Calculated for $C_{14}H_{12}FINaO_2S$ 412.9479, found 412.9485.

Compounds **29a**, **29b** and **29d** were synthetized according to "General Procedure 2".
The characterization of compound **29a** matches with the data reported in the literature.[46]
The characterizations of compounds **29b** and **29d** are not reported due to the paucity of materials.

Procedure 3: Synthesis of α-iodo sulfone **32a**

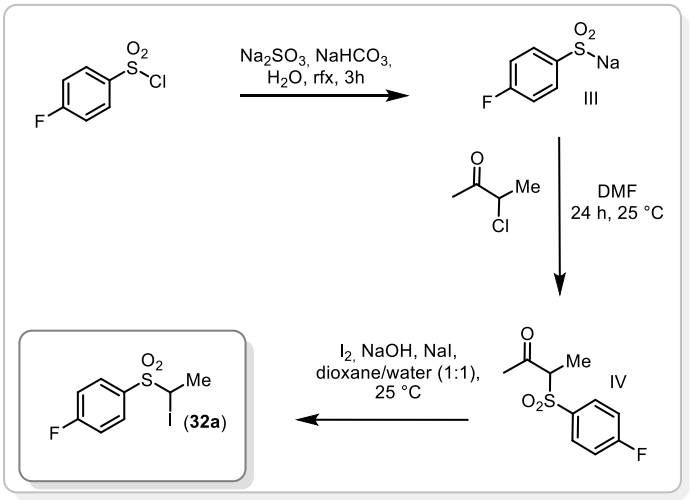

STEP 1, according to a reported procedure[47]: Commercially available 4-fluorobenzenesulfonyl chloride (1 equiv, 5 mmol, 0.98 g) was dissolved in 15 mL of water. Sodium sulfite (8 mmol, 1.0 g) and sodium bicarbonate (8 mmol, 0.7 g) were added and the reaction mixture was refluxed for 3 hours. Water was evaporated and ethanol was added to the residue. The suspension was heated for 10 minutes, cooled and filtered. This procedure was repeated twice using the residue of the filtration. The ethanol fractions were combined and the solvent was evaporated *in vacuo*. Adduct **III** was used without any further purification (95% yield).

STEP 2, according to a modified literature procedure[48]: To a solution of commercially available 3-chloro butanone (1 equiv, 5 mmol, 0.5 g) in DMF (10 mL, 0.5 M) was added **III** (1 equiv, 5 mmol) in one portion. The reaction mixture was stirred at room temperature for 24 hours. The reaction was quenched by the addition of water (50 mL), the mixture was extracted with DCM (3 x 35 mL), dried over $MgSO_4$ and the solvent was removed under reduced pressure. Product **IV** was used without any further purification (92% yield).

---

[47] Skillinghaug, B.; Skold, C.; Rydfjord, J.; Svensson, F.; Behrends, M.; Savmarker, J.; Sjoberg, P. J. R.; Larhed, M. "Palladium(II)-catalyzed desulfitative synthesis of aryl ketones from sodium arylsulfinates and nitriles: scope, limitations, and mechanistic studies" *J. Org. Chem.* **2014**, *79,* 12018.

[48] Enders, D.; Grossmann, A.; Huang, H.; Raabe, G. "Dual secondary amine/*N*-heterocyclic carbene catalysis in the asymmetric Michael/cross-benzoin cascade reaction of β-oxo sulfones with enals" *Eur. J. Org. Chem.* **2011**, 4298.

STEP 3, according to a reported procedure[49]: To a dioxane-water (1:1, 0.5 M) solution of **IV** (4.7 mmol, 1.0 g) and iodine (18.8 mmol, 4.8 g) in the presence of potassium iodide (37.6 mmol, 6.2 g), 1 M solution of NaOH is added under stirring at room temperature until decoloration of the excess of iodine occurred. After 20 minutes stirring, the reaction mixture was diluted with water and extracted with DCM (3 x 20 mL). The final α-iodo sulfone **32a** was used without any further purification (45% yield).

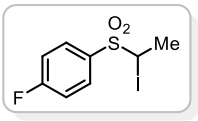

1-fluoro-4-((1-iodoethyl)sulfonyl)benzene (32a)
^{1}H NMR: (400 MHz, Chloroform-*d*) δ 8.04 – 7.95 (m, 2H), 7.34 – 7.22 (m, 2H), 5.00 (q, *J* = 7.1 Hz, 1H), 2.11 (d, *J* = 7.1 Hz, 3H). **^{13}C NMR**: (101 MHz, Chloroform-*d*) δ 166.47 (d, *J* = 257.8 Hz), 133.09 (d, *J* = 9.8 Hz), 130.38 (d, *J* = 3.3 Hz), 116.69 (d, *J* = 22.7 Hz), 34.78, 22.41. **^{1}H decoupled ^{19}F NMR:** (376 MHz, Chloroform-*d*) δ -102.04 (s, 1F). **HRMS**: Calculated for $C_8H_8FINaO_2S$ 336.9166, found 336.9168.

4.15.3. General Procedure for the Enantioselective Photo-organocatalytic (Phenylsulfonyl)methylation of Aldehydes with α-Iodo-Sulfone 4a

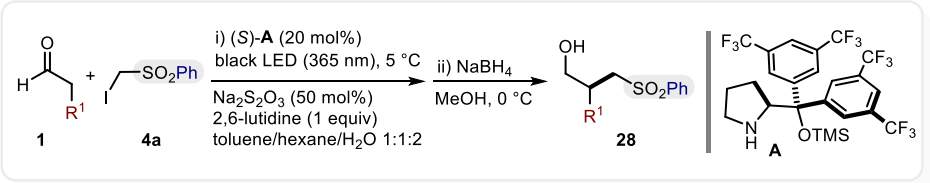

A 10 mL Schlenk tube was charged with the α-iodomethyl phenyl sulfone **4a** (0.1 mmol, 28.2 mg), the chiral secondary amine catalyst (*S*)-**A** (0.02 mmol, 20 mol%), sodium thiosulfate (0.05 mmol, 50 mol%), 2,6-lutidine (0.1 mmol, 1 equiv) and the appropriate aldehyde **1** (0.3 mmol, 3 equiv). To this mixture was then added hexane, toluene, and water in a 1:1:2 ratio (100μL, 100μL, 200μL, respectively; [**4a**]$_0$= 0.25 M). The reaction mixture was thoroughly degassed via 3 cycles of freeze pump thaw, and the vessel was refilled with argon, sealed with parafilm and placed into a single black LED plate (λ = 365 nm, intensity of emission = 100 μA, as controlled by an external power supply). The temperature was kept at 5 ºC with a chiller connected to the irradiation plate (the setup is

[49] Del Buttero, P.; Maiorana, S. "Haloform reaction on β-sulphonyl methylketones" *Gazzetta Chimica Italiana* **1973**, *103*, 809.

detailed in Figure 4.34). In order to avoid condensation of moisture on the plate, a flux of nitrogen was blown over the plate for the entire duration of the experiments by means of a bell-shaped glass. Stirring was maintained for the indicated time (generally 20 hours), and then the irradiation was stopped. The reaction was then diluted with methanol (2 mL) and the aldehyde product was reduced with sodium borohydride (5 equiv) at 0 ºC. The reaction was quenched after 15 minutes by addition of a satured solution of ammonium chloride (5 mL). The crude mixture was extracted with dichloromethane (3 x 5 mL). The volatiles were removed *in vacuo* and the residue was purified by column chromatography to give the alcohols products **28** in the stated yield and optical purity. The light source used for illuminating the reaction vessel consisted of a single black LED (3.6 W, EOLD-365-525 LED, UV, 5 mm, 365 nm) produced by OSA OPTO Light and purchased from Farnell.

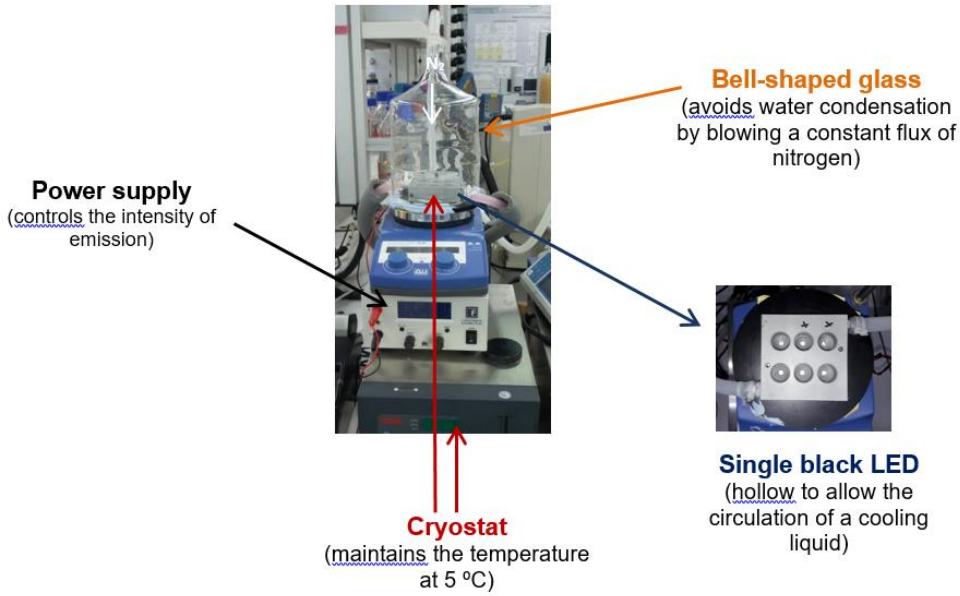

Figure 4.34 The reaction set-up of the photochemical organocatalytic of (phenylsulfonyl)methylation of aldehydes.

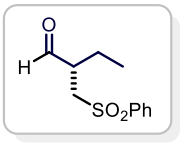

(*S*)-2-((phenylsulfonyl)methyl)butanal (5a). Prepared according to the general procedure using butyraldehyde (0.3 mmol, 27 µL). Time of irradiation: 16 hours. The crude mixture was not reduced but instead it was directly purified by rapid (total elution time < 2 minutes) flash column chromatography at 5 ºC (hexane/ethyl acetate 6:4) to afford the product as a colourless oil (17 mg, 75% yield). The enantiomeric excess was determined to be 80% by UPC^2 analysis on a Acquity Trefoil IC column with a gradient 100% CO_2 to 60:40 CO_2/Isopropanol over 4 minutes, 20 ºC, flow rate 3 mL/min, λ = 215 nm: τ_{Major} = 3.72 min, τ_{Minor} = 3.94 min. $[\alpha]_D^{26}$ = +22.2 (c = 0.20, $CHCl_3$, 80% *ee*). **^{1}H NMR**:(400 MHz, $CDCl_3$) δ 9.62 (d, *J* = 1.1 Hz, 1H), 7.91 (dt, *J* = 8.2, 1.1 Hz, 2H), 7.74 – 7.63 (m, 1H), 7.61 – 7.44 (m, 2H), 3.70 (dd, *J* = 14.2, 6.8 Hz, 1H), 3.06 (dd, *J* = 14.2, 5.1 Hz, 1H), 2.99 (ddd, *J* = 6.5, 5.3, 1.2 Hz, 1H), 1.94 – 1.68 (m, 2H), 0.94 (t, *J* = 7.5 Hz, 3H). **^{13}C NMR**:(101 MHz, $CDCl_3$) δ 200.12, 139.41, 134.13, 129.58, 128.15, 53.87, 47.10, 22.11, 10.60. **HRMS**: Calculated for $C_{11}H_{14}NaO_3S$: 249.0556, found: 249.0557.

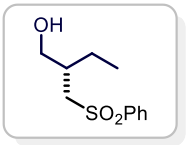

(*S*)-2-((phenylsulfonyl)methyl)butan-1-ol (28a). Prepared according to the general procedure using butyraldehyde (0.3 mmol, 27 µL). Time of irradiation: 16 hours. The crude mixture was purified by flash column chromatography (hexane/ethyl acetate 6:4) to afford the product as colourless oil (22 mg, 94% yield). The enantiomeric excess was determined to be 82% by HPLC analysis on a Daicel Chiralpak IC-3 column: 60:40 hexane/IPA, flow rate 0.8 mL/min, λ = 254 nm: τ_{Major} = 22.6 min, τ_{Minor} = 18.4 min. $[\alpha]_D^{26}$ = -7.4 (c = 0.90, $CHCl_3$, 82% *ee*). **^{1}H NMR**:(400 MHz, $CDCl_3$) δ 8.02 – 7.87 (m, 2H), 7.72 – 7.63 (m, 1H), 7.58 (dd, *J* = 8.3, 6.9 Hz, 2H), 3.86 (dt, *J* = 10.5, 5.1 Hz, 1H), 3.63 (dt, *J* = 11.3, 5.7 Hz, 1H), 3.31 (dd, *J* = 14.2, 7.6 Hz, 1H), 3.05 (dd, *J* = 14.2, 4.7 Hz, 1H), 2.19 – 2.01 (m, 1H), 1.93 (t, *J* = 5.9 Hz, 1H), 1.67 – 1.37 (m, 2H), 0.88 (t, *J* = 7.4 Hz, 3H). **^{13}C NMR**:(101 MHz, $CDCl_3$) δ 140.0, 133.9, 129.5, 127.9, 63.7, 57.6, 37.9, 24.4, 11.2. **HRMS**: Calculated for $C_{11}H_{16}NaO_3S$: 251.0712, found: 251.0718.

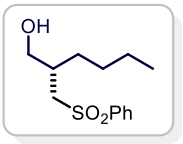

(*S*)-2-((phenylsulfonyl)methyl)hexan-1-ol (28b). Prepared according to the general procedure using hexanal (0.3 mmol, 38 µL). Time of irradiation: 20 hours. The crude mixture was purified by flash column chromatography (hexane/ethyl acetate 6:4) to afford the product as a colourless oil (24 mg, 92% yield). The enantiomeric excess was determined to be 86% by HPLC analysis on a Daicel Chiralpak IC-3 column: 60:40 hexane/IPA, flow rate 0.8 mL/min, λ = 254 nm: τ_{Major} = 21.3 min, τ_{Minor} = 18.0 min. $[\alpha]_D^{26}$= -5.2 (c = 1.2, $CHCl_3$, 86% *ee*). **^{1}H NMR**:(400 MHz, $CDCl_3$) δ 8.02 – 7.85 (m, 2H), 7.76 – 7.62 (m,

1H), 7.62 – 7.49 (m, 2H), 3.94 – 3.73 (m, 1H), 3.60 (dt, *J* = 11.1, 5.4 Hz, 1H), 3.32 (dd, *J* = 14.2, 7.6 Hz, 1H), 3.04 (dd, *J* = 14.3, 4.6 Hz, 1H), 2.30 – 2.08 (m, 1H), 2.04 (t, *J* = 6.0 Hz, 1H), 1.58 – 1.32 (m, 2H), 1.38-1.20 (m, 4H), 0.97 – 0.70 (m, 3H). **^{13}C NMR**:(101 MHz, $CDCl_3$) δ 140.0, 133.9, 129.5, 127.9, 64.1, 57.9, 36.3, 31.2, 28.9, 22.7, 14.0. **HRMS**: Calculated for $C_{13}H_{20}NaO_3S$: 279.1025; found: 279.1031.

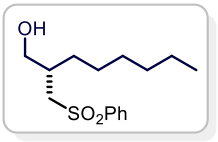

(*S*)-2-((phenylsulfonyl)methyl)octan-1-ol (28c). Prepared according to the general procedure using octanal (0.3 mmol, 48 µL). Time of irradiation: 20 hours. The crude mixture was purified by flash column chromatography (hexane/ethyl acetate 7:3) to afford the product as a colourless oil (27 mg, 93% yield). The enantiomeric excess was determined to be 85% by HPLC analysis on a Daicel Chiralpak IC-3 column: 60:40 hexane/IPA, flow rate 0.8 mL/min, λ = 254 nm: τ_{Major} = 19.2 min, τ_{Minor} = 16.7 min. $[\alpha]_D^{26}$= -7.0 (c = 1.0, $CHCl_3$, 85% *ee*). **^{1}H NMR**:(400 MHz, $CDCl_3$) δ 8.00 – 7.87 (m, 2H), 7.72 – 7.63 (m, 1H), 7.62-7.54 (m, 2H), 3.86 (dd, *J* = 11.3, 4.3 Hz, 1H), 3.61 (dd, *J* = 11.3, 5.7 Hz, 1H), 3.32 (dd, *J* = 14.2, 7.7 Hz, 1H), 3.04 (dd, *J* = 14.2, 4.5 Hz, 1H), 2.16 (t, *J* = 6.3 Hz, 1H), 1.96 (t, *J* = 6.0 Hz, 1H), 1.41 (dt, *J* = 14.3, 7.1 Hz, 2H), 1.34 – 1.12 (m, 8H), 0.86 (t, *J* = 6.9 Hz, 3H). **^{13}C NMR**:(101 MHz, $CDCl_3$) δ 140.0, 133.9, 129.5, 128.0, 64.1, 57.9, 36.3, 31.8, 31.6, 29.3, 26.7, 22.7, 14.2. **HRMS**: Calculated for $C_{15}H_{24}NaO_3S$: 307.1338, found: 307.1349.

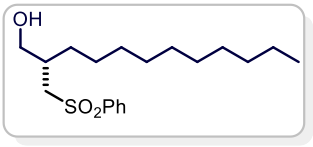

(*S*)-2-((phenylsulfonyl)methyl)dodecan-1-ol (28d). Prepared according to the general procedure using dodecanal (0.3 mmol, 67 µL). Time of irradiation: 16 hours. The crude mixture was purified by flash column chromatography (hexane/ethyl acetate 7:3) to afford the product as colourless oil (31 mg, 90% yield). The enantiomeric excess was determined to be 82% by UPC^2 analysis on a Acquity Trefoil IC column with a gradient (100% CO_2 to 60:40 CO_2/CH_3CN over 4 minutes, curve 6), flow rate 3 mL/min, λ = 270 nm: τ_{Major} = 4.61 min, τ_{Minor} = 4.36 min. $[\alpha]_D^{26}$= -5.0 (c = 0.68, $CHCl_3$, 82% *ee*). **^{1}H NMR**:(400 MHz, $CDCl_3$) δ 7.99 – 7.92 (m, 2H), 7.72 – 7.65 (m, 1H), 7.60 (dd, *J* = 8.4, 7.1 Hz, 2H), 3.87 (dt, *J* = 10.2, 4.7 Hz, 1H), 3.63 (dt, *J* = 10.9, 5.2 Hz, 1H), 3.34 (dd, *J* = 14.2, 7.6 Hz, 1H), 3.06 (dd, *J* = 14.2, 4.5 Hz, 1H), 2.23 – 2.13 (m, 1H), 2.07 (t, *J* = 5.9 Hz, 1H), 1.48-1.40 (m, 2H), 1.34-1.16 (m, 16H), 0.90 (t, *J* = 7.0 Hz, 3H). **^{13}C NMR**:(101 MHz, $CDCl_3$) δ 140.0, 133.8, 129.5, 128.0, 64.1, 57.9, 36.4, 32.0, 31.6, 29.7, 29.7, 29.6, 29.6, 29.4, 26.7, 22.8, 14.2. **HRMS**: Calculated for $C_{19}H_{32}NaO_3S$: 363.1964, found: 363.1969.

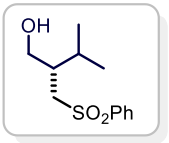

(*S*)-3-methyl-2-((phenylsulfonyl)methyl)butan-1-ol (28e). Prepared according to the general procedure using isovaleraldehyde (0.3 mmol, 32 µL). Time of irradiation: 20 hours. The crude mixture was purified by flash column chromatography (hexane/ethyl acetate 6:4) to afford the product as a colourless oil (23 mg, 95% yield). The enantiomeric excess was determined to be 87% by HPLC analysis on a Daicel Chiralpak IC-3 column: 60:40 hexane/IPA, flow rate 0.8 mL/min, λ = 254 nm: τ_{Major} = 27.4 min, τ_{Minor} = 17.7 min. $[\alpha]_D^{26}$= -13.0 (c = 0.68, $CHCl_3$, 87% *ee*). **^{1}H NMR**:(400 MHz, $CDCl_3$) δ 8.01 – 7.88 (m, 2H), 7.71 – 7.64 (m, 1H), 7.63 – 7.54 (m, 2H), 3.85 (ddd, *J* = 11.0, 5.9, 4.9 Hz, 1H), 3.70 (dt, *J* = 11.5, 5.8 Hz, 1H), 3.25 (dd, *J* = 14.3, 8.5 Hz, 1H), 3.08 (dd, *J* = 14.3, 3.3 Hz, 1H), 2.21 (t, *J* = 6.0 Hz, 1H), 2.10 – 1.97 (m, 1H), 1.92-1.84 (m, 1H), 0.84 (dd, *J* = 6.8, 4.1 Hz, 6H). **^{13}C NMR**:(101 MHz, $CDCl_3$) δ 139.7, 133.9, 129.5, 128.1, 63.0, 55.9, 41.9, 29.4, 19.7, 19.2. **HRMS**: Calculated for $C_{12}H_{18}NaO_3S$: 265.0869, found: 265.0868.

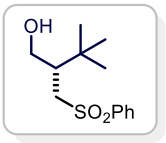

(*S*)-3,3-dimethyl-2-((phenylsulfonyl)methyl)butan-1-ol (28f). Prepared according to the general procedure using 3,3-dimethylbutyraldehyde (0.3 mmol, 38 µL). Time of irradiation: 20 hours. The crude mixture was purified by flash column chromatography (dichloromethane/ethyl acetate 85:15) to afford the product as a colourless oil (13 mg, 50% yield). The enantiomeric excess was determined to be 96% by UPC^2 analysis on a Acquity Trefoil IC column with a gradient (100% CO_2 to 60:40 CO_2/CH_3CN over 4 minutes, curve 6), flow rate 3 mL/min, λ = 216 nm: τ_{Major} = 4.37 min, τ_{Minor} = 4.03 min. $[\alpha]_D^{26}$= -15.2 (c = 0.31, $CHCl_3$, 96% *ee*). **^{1}H NMR**:(400 MHz, $CDCl_3$) δ 7.99 – 7.90 (m, 2H), 7.72 – 7.64 (m, 1H), 7.62 – 7.55 (m, 2H), 4.01 (ddd, *J* = 11.6, 5.5, 4.6 Hz, 1H), 3.66 (dt, *J* = 11.5, 6.6 Hz, 1H), 3.34 (dd, *J* = 14.3, 8.8 Hz, 1H), 3.18 (dd, *J* = 14.2, 2.2 Hz, 1H), 2.50 (dd, *J* = 6.9, 5.5 Hz, 1H), 2.00 (ddt, *J* = 6.4, 4.2, 2.2 Hz, 1H), 0.87 (s, 9H). **^{13}C NMR**:(101 MHz, $CDCl_3$) δ 139.7, 133.9, 129.5, 128.2, 62.2, 55.6, 45.2, 33.2, 27.9. **HRMS**: Calculated for $C_{13}H_{20}NaO_3S$: 279.1025, found: 279.1024.

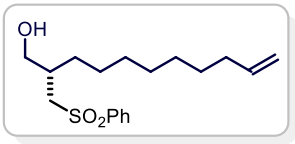

(*S*)-2-((phenylsulfonyl)methyl)undec-10-en-1-ol (28g). Prepared according to the general procedure using 10-undecenal (0.3 mmol, 61 µL). Time of irradiation: 24 hours. The crude mixture was purified by flash column chromatography (hexane/ethyl acetate 6:4) to afford the product as a colourless oil (30 mg, 92% yield). The enantiomeric excess was determined to be 82% by HPLC analysis on a Daicel Chiralpak IC-3 column: 60:40 hexane/IPA, flow rate 0.8 mL/min, λ = 254 nm: τ_{Major} = 19.0 min, τ_{Minor} = 16.8 min. $[\alpha]_D^{26}$= -4.30 (c = 1.9, $CHCl_3$, 82% *ee*). **^{1}H**

NMR:(400 MHz, $CDCl_3$) δ 8.01 – 7.86 (m, 2H), 7.74 – 7.62 (m, 1H), 7.62 – 7.52 (m, 2H), 5.91 – 5.66 (m, 1H), 5.09 – 4.79 (m, 2H), 3.85 (dd, *J* = 10.7, 5.2 Hz, 1H), 3.61 (dt, *J* = 10.8, 5.6 Hz, 1H), 3.31 (dd, *J* = 14.2, 7.6 Hz, 1H), 3.04 (dd, *J* = 14.2, 4.5 Hz, 1H), 2.25 – 2.09 (m, 1H), 2.08 – 1.91 (m, 2H), 1.57 – 1.02 (m, 12H). **^{13}C NMR**:(101 MHz, $CDCl_3$) δ 140.0, 139.3, 133.9, 129.5, 128.0, 114.3, 64.1, 57.9, 36.4, 33.9, 31.6, 29.6, 29.4, 29.1, 28.9, 26.7. **HRMS**: Calculated for $C_{18}H_{28}NaO_3S$: 347.1651, found: 347.1651.

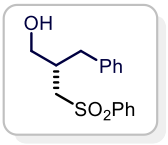

(*S*)-2-benzyl-3-(phenylsulfonyl)propan-1-ol (28h). Prepared according to general procedure using hydrocinnamaldehyde (0.3 mmol, 40 µL). Time of irradiation: 24 hours. The crude mixture was purified by flash column chromatography (hexane/ethyl acetate 6:4) to afford the product as a colourless oil (22 mg, 74% yield). The enantiomeric excess was determined to be 76% by HPLC analysis on a Daicel Chiralpak IC-3 column: 60:40 hexane/IPA, flow rate 0.8 mL/min, λ = 254 nm: τ_{Major} = 25.7 min, τ_{Minor} = 20.3 min. $[\alpha]_D^{26}$= -13.4 (c = 0.60, $CHCl_3$, 76% *ee*). **^{1}H NMR**:(400 MHz, $CDCl_3$) δ 7.93 – 7.81 (m, 2H), 7.73 – 7.63 (m, 1H), 7.62 – 7.51 (m, 2H), 7.32 – 7.18 (m, 3H), 7.15 – 7.06 (m, 2H), 3.89 (ddd, *J* = 11.3, 5.9, 4.3 Hz, 1H), 3.66 (dt, *J* = 11.0, 5.4 Hz, 1H), 3.33 (dd, *J* = 14.3, 7.6 Hz, 1H), 3.09 (dd, *J* = 14.3, 4.7 Hz, 1H), 2.88 – 2.73 (m, 2H), 2.54 – 2.37 (m, 1H), 2.01 (t, *J* = 5.9 Hz, 1H). **^{13}C NMR**:(101 MHz, $CDCl_3$) δ 139.7, 138.5, 133.8, 129.5, 129.2, 128.7, 127.9, 126.7, 63.4, 56.6, 38.2, 37.5.
HRMS: Calculated for $C_{16}H_{18}NaO_3S$: 313.0869, found: 313.0873.

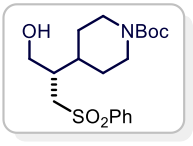

***tert*-butyl (*S*)-4-(1-hydroxy-3-(phenylsulfonyl)propan-2-yl) piperidine-1-carboxylate (28i)**. Prepared according to the general procedure using *tert*-butyl 4-(2-oxoethyl)piperidine-1-carboxylate (0.3 mmol, 23 µL). Time of irradiation: 24 hours. The crude mixture was purified by flash column chromatography (hexane/ethyl acetate 6:4) to afford the product as a colourless oil (27 mg, 70% yield). The enantiomeric excess was determined to be 80% by UPC^2 analysis on a Acquity Trefoil IC-3 column with a gradient (100% CO_2 to 60:40 CO_2/EtOH over 4 minutes, curve 6), flow rate 3 mL/min, λ = 264 nm: τ_{Major} = 5.0 min, τ_{Minor} = 4.9 min. $[\alpha]_D^{26}$= -5.8 (c = 1.0, $CHCl_3$, 80% *ee*). **^{1}H NMR**:(400 MHz, $CDCl_3$) δ 7.99 – 7.88 (m, 2H), 7.72 – 7.64 (m, 1H), 7.59 (dd, *J* = 8.3, 6.9 Hz, 2H), 4.11 (s, 1H), 3.91 (dt, *J* = 10.8, 5.1 Hz, 1H), 3.74 (dt, *J* = 11.2, 5.6 Hz, 1H), 3.29 (dd, *J* = 14.2, 8.3 Hz, 1H), 3.08 (dd, *J* = 14.2, 3.6 Hz, 1H), 2.62-2.50 (m, 2H), 2.17 – 1.98 (m, 2H), 1.80 – 1.62 (m, 1H), 1.65-1.53 (m, 1H), 1.44 (s, 9H), 1.18-1.10 (m, 2H), 0.93-0.85 (m, 1H). **^{13}C NMR**:(101 MHz, $CDCl_3$) δ 155.0, 140.0, 134.3, 129.8, 128.3, 79.9, 62.4, 55.7, 40.9, 38.0, 29.4, 28.8. **HRMS**: Calculated for $C_{19}H_{29}NNaO_5S$: 406.1659, found: 406.1660.

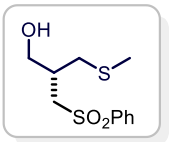

(*R*)-3-(methylthio)-2-((phenylsulfonyl)methyl)propan-1-ol (28j). Prepared according to the general procedure using methional (0.3 mmol, 30 µL). Time of irradiation: 24 hours. The crude mixture was purified by flash column chromatography (hexane/ethyl acetate 6:4) to afford the product as colourless oil (11 mg, 40% yield). The enantiomeric excess was determined to be 75% by UPC^2 analysis on a Acquity Trefoil AMY-1 column with a gradient (100% CO_2 to 60:40 CO_2/CH_3CN over 4 minutes, curve 6), flow rate 2 mL/min, λ = 220 nm: τ_{Major} = 4.68 min, τ_{Minor} = 4.82 min. $[\alpha]_D^{26}$= -26.9 (c = 0.4, $CHCl_3$, 75% *ee*). **^{1}H NMR**:(400 MHz, $CDCl_3$) δ 8.08 – 7.87 (m, 2H), 7.78 – 7.67 (m, 1H), 7.65 – 7.55 (m, 2H), 3.95 (d, *J* = 11.4 Hz, 1H), 3.88 – 3.71 (m, 1H), 3.40 (dd, *J* = 14.2, 5.0 Hz, 1H), 3.32 (dd, *J* = 14.2, 7.3 Hz, 1H), 2.72 (dd, *J* = 13.5, 6.7 Hz, 1H), 2.64 (dd, *J* = 13.5, 7.3 Hz, 1H), 2.48-2.40 (m, 1H), 2.10-2.00 (m, 4H). **^{13}C NMR**:(101 MHz, $CDCl_3$) δ 139.6, 133.9, 129.4, 127.9, 63.5, 56.1, 36.0, 35.5, 15.6. **HRMS**: Calculated for $C_{11}H_{16}NaO_3S_2$: 283.0433, found: 283.0435.

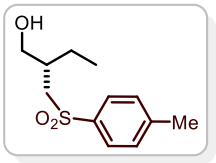

(S)-2-(tosylmethyl)butan-1-ol (28k). Prepared according to the general procedure using butyraldehyde (0.3 mmol, 27 µL) and 1-((iodomethyl)sulfonyl)-4-methylbenzene **4d** (0.1 mmol, 30 mg). Time of irradiation: 16 hours. The crude mixture was purified by flash column chromatography (hexane/ethyl acetate 6:4) to afford the product as colourless oil (23 mg, 95% yield). The enantiomeric excess was determined to be 80% by HPLC analysis on a Daicel Chiralpak IC-3 column: 60:40 hexane/IPA, flow rate 0.8 mL/min, λ = 254 nm: τ_{Major} = 27.3 min, τ_{Minor} = 22.9 min. $[\alpha]_D^{26}$= -8.0 (c = 1.3, $CHCl_3$, 80% *ee*). **^{1}H NMR**:(400 MHz, $CDCl_3$) δ 7.80 (d, *J* = 8.3 Hz, 2H), 7.36 (d, *J* = 8.0 Hz, 2H), 3.83 (ddd, *J* = 10.6, 6.0, 4.3 Hz, 1H), 3.61 (dt, *J* = 11.4, 5.7 Hz, 1H), 3.28 (dd, *J* = 14.2, 7.6 Hz, 1H), 3.02 (dd, *J* = 14.2, 4.7 Hz, 1H), 2.45 (s, 3H), 2.17-1.98 (m, 1H), 1.59 – 1.30 (m, 2H), 0.87 (t, *J* = 7.4 Hz, 3H). **^{13}C NMR**: (101 MHz, $CDCl_3$) δ 144.7, 137.0, 130.1, 127.9, 63.7, 57.7, 37.9, 24.4, 21.8, 11.2. **HRMS**: Calculated for $C_{12}H_{18}NaO_3S$: 265.0869, found: 265.0865.

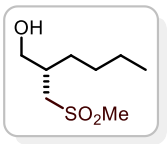

(*S*)-2-((methylsulfonyl)methyl)hexan-1-ol (28l). Prepared according to the general procedure using hexanal (0.3 mmol, 38 µL) and 1-((iodomethyl)sulfonyl)-4-methylbenzene **4h** (0.1mmol, 22 mg). Time of irradiation: 24 hours. The crude mixture was purified by flash column chromatography (hexane/ethyl acetate 1:1) to afford the product as colourless oil (10 mg, 50% yield). The enantiomeric excess was determined upon esterification of the alcohol moiety with 3,5-dinitrobenzoyl chloride (see procedure detailed below). **^{1}H**

NMR:(400 MHz, $CDCl_3$) δ 3.87 (dt, *J* = 9.5, 4.2 Hz, 1H), 3.69 – 3.52 (m, 1H), 3.26 (dd, *J* = 14.0, 7.7 Hz, 1H), 3.09 – 2.90 (m, 4H), 2.33 – 2.15 (m, 1H), 2.10 (s, 1H), 1.55-1.45 (m, 2H), 1.35-1.26 (m, 4H), 1.01 – 0.80 (m, 3H). **^{13}C NMR**:(101 MHz, $CDCl_3$) δ 64.0, 56.4, 41.2, 36.2, 31.4, 29.0, 22.8, 14.1. **HRMS**: Calculated for $C_8H_{18}NaO_3S$: 217.0869, found: 217.0870.

Derivatization to evaluate the enantiomeric excess of compound **28l**.

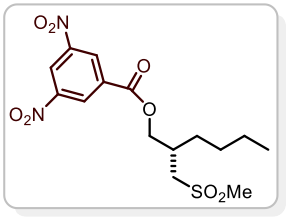

(*S*)-2-((methylsulfonyl)methyl)hexyl 3,5-dinitrobenzoate (34a) was prepared from (*S*)-2-((methylsulfonyl)methyl)hexan-1-ol (**28l**) (0.1 mmol, 19.4 mg) adding 3,5-dinitrobenzoyl chloride (0.15 mmol, 36 mg), 4-(dimethylamino)pyridine (0.02 mmol, 3mg) and trimethylamine (0.15 mmol, 20 µL) to a dry dichloromethane solution of **28l**. Reaction Time: 7 hours. The crude product was purified by flash column chromatography (hexane/ethyl acetate 3:7) to afford **34a** as yellow oil (35 mg, 90% yield). The enantiomeric excess was determined to be 83% by UPC^2 analysis on a Acquity Trefoil AMY-1 column with a gradient (100% CO_2 to 60:40 CO_2/MeOH over 4 minutes, curve 6), flow rate 2 mL/min, λ = 208 nm: τ_{Major} = 5.7 min, τ_{Minor} = 6.0 min. $[\alpha]_D^{26}$= -5.9 (c = 1.0, $CHCl_3$, 83% *ee*). **^{1}H NMR**: (400 MHz, Chloroform-*d*) δ 9.24 (t, *J* = 2.1 Hz, 1H), 9.16 (d, *J* = 2.2 Hz, 2H), 4.63 (dd, *J* = 11.3, 4.8 Hz, 1H), 4.54 (dd, *J* = 11.3, 5.9 Hz, 1H), 3.22 (dd, *J* = 14.0, 7.5 Hz, 1H), 3.12 (dd, *J* = 14.0, 4.5 Hz, 1H), 2.98 (s, 3H), 2.75-2.62 (m, 1H), 1.70 – 1.58 (m, 2H), 1.50 – 1.31 (m, 4H), 0.94 (t, *J* = 7.0 Hz, 3H). **^{13}C NMR:** (101 MHz, Chloroform-*d*) δ 162.6, 148.9, 133.7, 129.6, 122.7, 67.9, 56.2, 42.3, 32.9, 31.6, 28.7, 22.7, 14.0. **HRMS**: Calculated for $C_{15}H_{20}N_2NaO_8S$: 411.0833, found: 411.0828.

4.15.4. General Procedure for the Enantioselective Photo-organocatalytic (Arylsulfonyl)Benzylation of Aldehydes

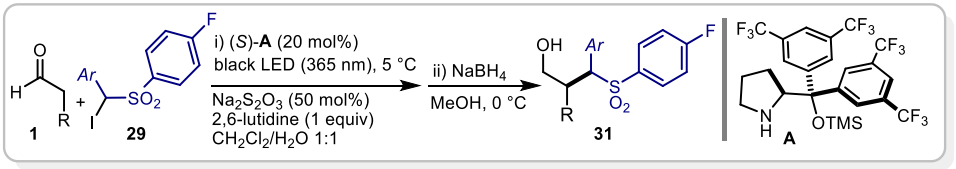

A 10 mL Schlenk tube was charged with the α-iodo sulfone (0.1 mmol, 1 equiv), the chiral secondary amine catalyst (*S*)-**A** (0.02 mmol, 20 mol%), sodium thiosulfate (0.05 mmol, 50 mol%), 2,6-lutidine (0.1 mmol, 1 equiv) and the appropriate aldehyde **1** (0.3 mmol, 3 equiv). To this mixture was then added dichloromethane and water in a 1:1ratio (200 µL each, for a total of 400µL; [**29**]$_0$= 0.25 M). The reaction mixture was thoroughly degassed via 3 cycles of freeze pump thaw, and the vessel was refilled with argon, sealed with parafilm and placed into a single black LED plate (λ = 365 nm, intensity of emission = 100 µA, as controlled by an external power supply). The temperature was kept at 5 ºC with a chiller connected to the irradiation plate (the setup is detailed in Figure 4.34). In order to avoid condensation of moisture on the plate, a flux of nitrogen was blown over the plate for the entire duration of the experiments by means of a bell-shaped glass. Stirring was maintained for the indicated time, and then the irradiation was stopped. The reaction was then diluted with methanol (2 mL) and the aldehyde product was reduced with sodium borohydride (5 equiv) at 0 ºC. The reaction was quenched after 15 minutes by addition of a sutured solution of ammonium chloride (5 mL). The crude mixture was extracted with dichloromethane (3 x 5 mL). The volatiles were removed *in vacuo* and the residue was purified by column chromatography to give the alcohols products **31** in the stated yield and optical purity. The light source used for illuminating the reaction vessel consisted of a single black LED (3.6 W, EOLD-365-525 LED, UV, 5 mm, 365 nm).

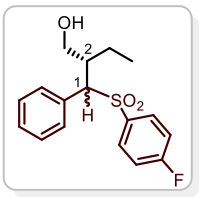

(2*S*)-2-(((4-fluorophenyl)sulfonyl)(phenyl)methyl)butan-1-ol (31c). Prepared according to the general procedure using butyraldehyde (0.3 mmol, 27 µL), 1-fluoro-4-((iodo(phenyl)methyl)sulfonyl)benzene **29c** (0.1 mmol, 37.6 mg) and a mixture of dichloromethane:water 1:1 as solvent. Time of irradiation: 70 hours. The crude mixture was purified by flash column chromatography (dichloromethane/ethyl acetate 20:1) to afford the product as colourless oil (20 mg, 62% yield, 3.3:1.0 d.r., 96% ee_{major}, 80% $ee_{\mathbf{minor}}$). The enantiomeric

excesses were determined by UPC^2 analysis on a Acquity Trefoil CEL-1 column with a gradient (100% CO_2 to 60:40 CO_2/EtOH over 4 minutes, curve 6), flow rate 2 mL/min, λ = 212 nm: Major diastereoisomer (96% ee): τ_{Major} = 3.53 min, τ_{Minor} = 3.64 min; Minor diastereoisomer (80% ee): τ_{Major} = 3.29 min, τ_{Minor} = 3.35 min. $[\alpha]_D^{26}$= +33.7 (c = 0.47, $CHCl_3$, 3.2:1 dr, 96% ee_{Major}, 80% ee_{minor}). **^{1}H NMR**: (400 MHz, Chloroform-*d*) δ 7.56 – 7.47 (m, 2H *major*), 7.47 – 7.41 (m, 2H *minor*), 7.27 – 7.06 (m, 5H *major* +5H *minor*), 7.02 – 6.91 (m, 2H *major* +2H *minor*), 4.52 – 4.38 (m, 1H *minor*), 4.35 – 4.23 (m, 1H *major* +1H *minor*), 3.89 (dt, *J* = 11.5, 4.5 Hz, 1H *major*), 3.86 – 3.79 (m, 1H *minor*), 3.43 (ddd, *J* = 11.4, 6.9, 4.3 Hz, 1H *major*), 2.76 – 2.59 (m, 1H *major* +1H *minor*), 2.53 (ddd, *J* = 9.7, 6.4, 3.2 Hz, 1H *minor*), 1.97 (dtd, *J* = 14.8, 7.4, 5.2 Hz, 1H *major*), 1.80 (ddt, *J* = 14.2, 8.4, 7.3 Hz, 1H *major*), 1.72 (dd, *J* = 7.0, 4.5 Hz, 1H *major*), 1.48 – 1.34 (m, 1H *minor*), 1.07 (t, *J* = 7.4 Hz, 3H *major*), 0.90 (t, *J* = 7.4 Hz, 3H *minor*). **^{13}C NMR**: (101 MHz, Chloroform-*d*) δ 165.5 (d, *J* = 256.0 Hz, *minor*), 165.9 (d, *J* = 256.0 Hz, *major*), 135.0 (d, *J* = 3.2 Hz, *major*), 134.6 (d, *J* = 2.9 Hz, *minor*), 133.1 (*minor*), 132.4 (*major*), 131.5 (d, *J* = 9.5 Hz, *minor*), 131.4 (d, *J* = 9.6 Hz, *major*), 130.4 (*major*), 130.2 (*major*), 128.9 (*major*), 128.8 (*major*), 115.9 (d, *J* = 22.6 Hz, *major*), 73.4 (*major*), 72.7 (*minor*), 61.6 (*major*), 60.7 (*minor*), 43.5 (*minor*), 43.1 (*major*), 22.6 (*minor*), 22.3 (*major*), 11.7 (*major*), 11.6 (*minor*). **^{1}H decoupled ^{19}F NMR:** (376 MHz, Chloroform-*d*) δ -104.03 (s, 1F*minor*), -104.27 (s, 1F*major*). **HRMS**: Calculated for $C_{17}H_{19}FNaO_3S$:345.0931, found: 345.0944.

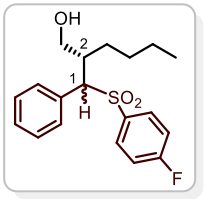

(2*S*)-2-(((4-fluorophenyl)sulfonyl)(phenyl)methyl)hexan-1-ol (31e) Prepared according to the general procedure using hexanal (0.3 mmol, 38 µL) and 1-fluoro-4-((iodo(phenyl)methyl)sulfonyl)benzene **29c** (0.1 mmol, 37.6 mg). Time of irradiation: 70 hours. The reaction mixture was purified by flash column chromatography (hexane/ethyl acetate 7:3) to afford the product as colourless oil (19 mg, 57% yield, 3.1:1.0 d.r., 97% ee_{major}, 88% ee_{minor}). The enantiomeric excesses were determined by UPC^2 analysis on a Acquity Trefoil CEL-1 column with a gradient (100% CO_2 to 60/40 CO_2/Isopropanol over 4 minutes, curve 6), flow rate 2 mL/min, λ = 220 nm: Major diastereoisomer (97% ee): τ_{Major} = 3.82 min, τ_{Minor} = 3.90 min; minor diastereoisomer (88% ee): τ_{Major} = 3.53 min, τ_{Minor} = 3.64 min. $[\alpha]_D^{26}$= +43.0 (c = 0.80, $CHCl_3$, 3:1 dr, 97% ee_{Major}, 88% ee_{minor}). **^{1}H NMR**: (400 MHz, Chloroform-*d*) δ 7.55 – 7.46 (m, 2H *major*), 7.45 – 7.37 (m, 2H *minor*), 7.25 – 7.12 (m, 5H *major* +5H *minor*), 7.02 – 6.87 (m, 2H *major* +2H *minor*), 4.40 (d, *J* = 12.3 Hz, 1H *minor*), 4.32 – 4.14 (m, 1H *major* +1H *minor*), 3.87 (dd, *J* = 11.5, 4.8 Hz, 1H *major*), 3.77 (d, *J* = 12.9 Hz, 1H *minor*), 3.40 (dd, *J* = 11.5, 4.3 Hz, 1H *major*), 2.79 – 2.64 (m,

1H *major* +1H *minor*), 2.58 (d, *J* = 2.9 Hz, 1H *minor*), 1.83 (ddt, *J* = 15.2, 10.9, 5.2 Hz, 2H *major*), 1.72 – 1.60 (m, 1H *major* +1H *minor*), 1.49 – 1.27 (m, 4H *major* +4H *minor*), 0.92 (t, *J* = 7.0 Hz, 3H *major*), 0.76 (t, *J* = 7.1 Hz, 3H *minor*). **^{13}C NMR**: (101 MHz, Chloroform-*d*) δ 165.4 (d, *J* = 256.3 Hz, *minor*), 165.3 (d, *J* = 256.0 Hz, *major*), 134.9 (d, *J* = 3.2 Hz, *major*), 134.5 (d, *J* = 3.2 Hz, *minor*), 132.9 (*minor*), 132.1 (*major*), 131.3 (d, *J* = 9.6 Hz, *major*), 130.3 (*major*), 130.0 (*minor*), 128.7 (*major*), 128.65 (*major*), 128.62 (*major*), 115.8 (d, *J* = 22.6 Hz, *major*), 115.7 (d, *J* = 22.6 Hz, *minor*), 73.5 (*major*), 72.6 (*minor*), 61.9 (*major*), 61.0 (*minor*), 41.7 (*minor*), 41.4 (*major*), 29.3 (*major*), 29.0 (*minor*), 29.0 (*major*), 28.9 (*minor*), 22.7 (*major*), 22.4 (*minor*), 14.0 (*major*), 13.8 (*minor*). **^{1}H decoupled ^{19}F NMR:** (376 MHz, Chloroform-*d*) δ -104.05 (s, 1F*minor*), -104.25 (s, 1F*major*). **HRMS**: Calculated for $C_{19}H_{23}FNaO_3S$: 373.1244, found: 373.1227.

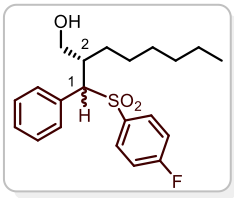

(2*S*)-2-(((4-fluorophenyl)sulfonyl)(phenyl)methyl)octan-1-ol (31f) Prepared according to the general procedure using octanal (0.3 mmol, 48 µL) and 1-fluoro-4-((iodo(phenyl)methyl)sulfonyl)benzene **29c** (0.1 mmol, 37.6 mg). Time of irradiation: 70 hours. The crude mixture was purified by flash column chromatography (dichloromethane/ethyl acetate 20:1) to afford the product as colourless oil (16 mg, 43% yield, 3.3:1.0 d.r., 95% *ee*$_{\mathbf{major}}$, 86% *ee*$_{\mathbf{minor}}$). The enantiomeric excesses were determined by UPC^2 analysis on a Acquity Trefoil AMY-1 column with a gradient (100% CO_2 to 60/40 CO_2/ethanol over 4 minutes, curve 6), flow rate 2 mL/min, λ = 220 nm: Major diastereoisomer (95% ee): τ_{Major} = 4.52min, τ_{Minor} = 4.83 min; minor diastereoisomer (86% ee): τ_{Major} = 3.87 min, τ_{Minor} = 3.95 min. $[\alpha]_D^{26}$= +38.7 (c = 0.57, $CHCl_3$, 3.2:1 dr, 95% *ee*$_{\mathbf{major}}$, 86% *ee*$_{\mathbf{minor}}$). **^{1}H NMR**: (400 MHz, Chloroform-*d*) δ 7.58 – 7.49 (m, 2H *major*), 7.47 – 7.40 (m, 2H *minor*), 7.29 – 7.08 (m, 5H *major* +5H *minor*), 7.05 – 6.87 (m, 2H *major* +2H *minor*), 4.49 – 4.36 (m, 1H *minor*), 4.34 – 4.20 (m, 1H *major* +1H *minor*), 3.93 – 3.84 (m, 1H *major*), 3.79 (ddd, *J* = 11.9, 8.1, 3.3 Hz, 1H *minor*), 3.43 (dt, *J* = 10.9, 5.4 Hz, 1H *major*), 2.81 – 2.65 (m, 1H *major* +1H *minor*), 2.65 – 2.53 (m, 1H *minor*), 1.92 – 1.78 (m, 2H *major*), 1.71 (ddt, *J* = 14.1, 9.9, 6.7 Hz, 1H *major*), 1.55 – 1.01 (m, 8H *major* + 8H *minor*), 0.95 – 0.87 (t, *J* = 7.0 Hz, 3H *major*), 0.83 (t, *J* = 7.1 Hz, 3H *minor*). **^{13}C NMR**: (101 MHz, Chloroform-*d*) δ 165.6 (d, *J* = 256.3 Hz, *minor*), 165.5 (d, *J* = 256.0 Hz, *major*), 135.1 (d, *J* = 3.1 Hz, *major*), 134.6 (d, *J* = 3.3 Hz, *minor*), 133.0 (*minor*), 132.3 (*major*), 131.5 (d, *J* = 9.6 Hz, *major*), 130.5 (*major*), 130.2 (*minor*), 128.9 (*major*), 128.8 (*major*), 128.7 (*major*), 115.9 (d, *J* = 22.6 Hz, *major*), 115.8 (d, *J* = 22.6 Hz, *minor*), 73.6 (*major*), 72.8 (*minor*), 62.1 (*major*), 61.1 (*minor*), 41.8 (*minor*), 41.6 (*major*), 31.9 (*major*), 31.7 (*minor*), 29.4 (*major*), 29.2 (*minor*), 27.3 (*major*), 26.9

(*minor*), 22.8 (*major*), 22.6 (*minor*), 14.2 (*major*), 14.1 (*minor*).**^{1}H decoupled ^{19}F NMR:** (376 MHz, Chloroform-*d*) δ -104.06 (s, 1F*minor*), -104.25 (s, 1F*major*). **HRMS**: Calculated for $C_{21}H_{27}FNaO_3S$: 401.1557, found: 401.1556.

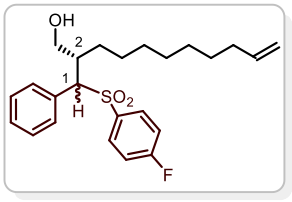

(2*S*)-2-(((4-(fluorophenyl)sulfonyl)(phenyl)methyl) undec-10-en-1-ol (31g) Prepared according to the general procedure using 10-undecenal (0.3 mmol, 61 µL) and 1-fluoro-4-((iodo(phenyl)methyl)sulfonyl)benzene **29c** (0.1 mmol, 37.6 mg). Time of irradiation: 20 hours. The crude mixture was purified by preparative TLC (hexane/ethyl acetate 9:1) to afford the product as colourless oil (22 mg, 52% yield, 3.4:1.0 d.r., 97% ee_{major}, 83% ee_{minor}). The enantiomeric excesses were determined by UPC^2 analysis on a Acquity Trefoil CEL-2 column with a gradient (100% CO_2 to 60/40 CO_2/MeOH over 4 minutes, curve 6), flow rate 2 mL/min, λ = 212 nm: major diastereoisomer (97% ee): τ_{Major} = 4.27 min, τ_{Minor} = 4.08 min; ninor diastereoisomer (83% ee): τ_{Major} = 3.96 min, τ_{Minor} = 4.45 min. $[\alpha]_D^{26}$= +29.3 (c = 0.33, $CHCl_3$, 3.4:1 dr, 97% ee_{Major}, 83% ee_{minor}). **^{1}H NMR**: (400 MHz, Chloroform-*d*) δ 7.54 – 7.46 (m, 2H *major*), 7.47 – 7.41 (m, 2H *minor*), 7.26 – 7.03 (m, 5H *major* +5H *minor*), 7.02 – 6.88 (m, 2H *major* +2H *minor*), 5.90-5.70 (m, 1H *major* +1H *minor*), 5.07 – 4.86 (m, 2H *major* +2H *minor*), 4.46 – 4.35 (m, 1H *minor*), 4.30 – 4.18 (m, 1H *major* +1H *minor*), 3.87 (dd, *J* = 11.6, 4.7 Hz, 1H *major*), 3.81 – 3.72 (m, 1H *minor*), 3.48 – 3.35 (m, 1H *major*), 2.77 – 2.63 (m, 1H *major* +1H *minor*), 2.62 – 2.51 (m, 1H *minor*), 2.12 – 1.91 (m, 2H *major* +2H *minor*), 1.92 – 1.61 (m, 3H *major* +1H *minor*), 1.53 – 1.19 (m, 10H *major* +10H *minor*). **^{13}C NMR**: (101 MHz, Chloroform-*d*) δ 165.5 (d, *J* = 256.1 Hz, *major*), 139.3 (*major*), 139.3 (*minor*), 135.0 (d, *J* = 3.2 Hz, *major*), 134.6 (d, *J* = 3.1 Hz, *minor*), 133.1 (*minor*), 132.3 (*minor*), 131.5 (d, *J* = 9.6 Hz, *major*), 130.4 (*major*), 128.9 (*major*), 128.81 (*major*), 128.78 (*major*), 115.80 (d, *J* = 22.7 Hz, *major*), 115.76 (d, *J* = 22.5 Hz, *minor*) 114.31 (*major*), 114.27 (*minor*), 73.6 (*major*), 72.9 (*minor*), 62.1 (*major*), 61.1 (*minor*), 41.8 (*minor*), 41.5 (*major*), 33.9 (*major*), 33.8 (*minor*), 29.8 (*minor*), 29.7 (*major*), 29.5 (*major*), 29.4 (*major*), 29.34 (*minor*), 29.32 (*minor*), 29.2 (*major*), 29.1 (*minor*), 29.0 (*major*), 28.9 (*minor*), 27.3 (*major*), 26.9 (*minor*). **^{1}H decoupled ^{19}F NMR:** (376 MHz, Chloroform-*d*) δ -104.04 (s, 1F*minor*), -104.23 (s, 1F*major*). **HRMS**: Calculated for $C_{24}H_{31}FNaO_3S$: 441.1870, found: 441.1870.

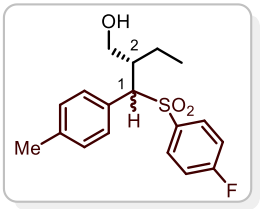

(2S)-2-(((4-fluorophenyl)sulfonyl)(p-tolyl)methyl)butan-1-ol (31h) Prepared according to the general procedure using butyraldehyde (0.3 mmol, 27 µL) and 1-fluoro-4-((iodo(p-tolyl)methyl)sulfonyl)benzene **29e** (0.1 mmol, 39.0 mg). Time of irradiation: 70 hours. The reaction mixture was purified by flash column chromatography (hexane/ethyl acetate 6:4) to afford the product as colourless oil (11 mg, 35% yield, 3.4:1.0 d.r., 94% ee_{major}, 74% ee_{minor}). The enantiomeric excesses were determined by UPC^2 analysis on a Acquity Trefoil CEL-1 column with a gradient (100% CO_2 to 60/40 CO_2/EtOH over 4 minutes, curve 6), flow rate 2 mL/min, λ = 212 nm: Major diastereoisomer (94% ee): τ_{Major} = 3.47 min, τ_{Minor} = 3.52 min; minor diastereoisomer (74% ee): τ_{Major} = 3.25 min, τ_{Minor} = 3.35 min. $[\alpha]_D^{26}$= +77.4 (c = 0.25, $CHCl_3$, 3.2:1 dr, 94% ee_{Major}, 74% ee_{minor}). **^{1}H NMR**: (400 MHz, Chloroform-*d*) δ 7.55 – 7.47 (m, 2H *major*), 7.46 – 7.39 (m, 2H *minor*), 7.11 – 6.85 (m, 6H *major* + 6H *minor*), 4.45 – 4.28 (m, 1H *minor*), 4.31 – 4.10 (m, 1H *major* + 1H *minor*), 3.86 (dt, *J* = 11.6, 4.0 Hz, 1H *major*), 3.79 (ddd, *J* = 11.9, 8.0, 3.3 Hz, *minor*), 3.42 (dt, *J* = 11.2, 5.1 Hz, 1H *major*), 2.76 – 2.54 (m, 1H *major* + 1H *minor*), 2.47 (ddt, *J* = 13.0, 9.6, 3.6 Hz, 1H *minor*), 2.28 (s, 3H *major*), 2.27 (s, 3H *minor*), 1.98 – 1.67 (m, 3H *major*), 1.46 – 1.18 (m, 3H *minor*), 1.02 (t, *J* = 7.4 Hz, 3H *major*), 0.86 (t, *J* = 7.4 Hz, 3H *minor*). **^{13}C NMR**: (101 MHz, Chloroform-*d*) δ 165.53 (d, *J* = 256.1 Hz, *minor*), 165.48 (d, *J* = 255.8 Hz, *major*), 138.86 (*major*), 138.78 (*minor*), 135.1 (d, *J* = 3.0 Hz, *major*), 134.7 (d, *J* = 3.3 Hz, *minor*), 131.5 (d, *J* = 9.5 Hz, *minor*), 131.4 (d, *J* = 9.5 Hz, *major*), 130.3 (*major*), 130.1 (*minor*), 129.8 (*minor*), 129.5 (*major*), 129.4 (*minor*), 129.0 (*major*), 115.74 (d, *J* = 22.6 Hz, *major*), 115.70 (d, *J* = 22.6 Hz, *minor*), 73.1 (*major*), 72.4 (*minor*), 61.7 (*major*), 60.7 (*minor*), 43.5 (*minor*), 43.1 (*major*), 22.5 (*minor*), 22.4 (*major*), 21.2 (*major*), 11.7 (*major*), 11.6 (*minor*). **^{1}H decoupled ^{19}F NMR:** (376 MHz, Chloroform-*d*) δ -104.20 (s, 1F*minor*), -104.38 (s, 1F*major*). **HRMS**: Calculated for $C_{18}H_{21}FNaO_3S$:359.1088, found: 359.1090.

4.15.5. Procedure for the Enantioselective Photo-organocatalytic Formal α-ethylation of butanal.

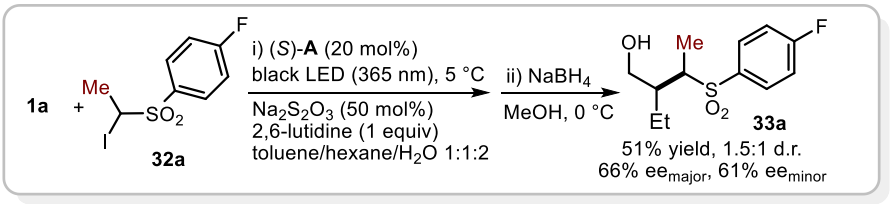

A 10 mL Schlenk tube was charged with the α-iodomethyl methyl sulfone **32a** (0.1 mmol, 31.4 mg), the chiral secondary amine catalyst (*S*)-**A** (0.02 mmol, 20 mol%), sodium thiosulfate (0.05 mmol, 50 mol%), 2,6-lutidine (0.1 mmol, 1 equiv) and butanal **1a** (0.3 mmol, 27 µL). To this mixture was then added hexane, toluene, and water in a 1:1:2 ratio (100µL, 100µL, 200µL, respectively; [**32a**]$_0$= 0.25 M). The reaction mixture was thoroughly degassed via 3 cycles of freeze pump thaw, and the vessel was refilled with argon, sealed with parafilm and placed into a single black LED plate (λ = 365 nm, intensity of emission = 100 µA, as controlled by an external power supply). The temperature was kept at 5 ºC with a chiller connected to the irradiation plate (the setup is detailed in Figure 4.34). In order to avoid condensation of moisture on the plate, a flow of nitrogen was blown over the plate for the entire duration of the experiments by means of a bell-shaped glass. Stirring was maintained for 24 hours, and then the irradiation was stopped. The reaction was then diluted with methanol (2 mL) and the aldehyde product was reduced with sodium borohydride (5 equiv) at 0 ºC. The reaction was quenched after 15 minutes by addition of a satured solution of ammonium chloride (5 mL). The crude mixture was extracted with dichloromethane (3 x 5 mL). The volatiles were removed *in vacuo* and the residue was purified by column chromatography to give the alcohols products **33a** in the stated yield and optical purity.

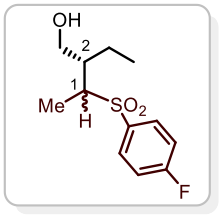

(2S)-2-ethyl-3-((4-fluorophenyl)sulfonyl)butan-1-ol (33a) Prepared according to the general procedure using butyraldehyde (0.3 mmol, 27 µL), 1-fluoro-4-((1-iodoethyl)sulfonyl)benzene (0.1 mmol, 31.4 mg) and a hexane/toluene/water mixture (1:1:2). Time of irradiation: 24 hours. The crude mixture was purified by flash column chromatography (hexane/ethyl acetate 7:3) to afford the product as colourless oil (13 mg, 51% yield, 1.5:1.0 d.r., 66% *ee*$_{\mathbf{major}}$, 61% *ee*$_{\mathbf{minor}}$). The enantiomeric excesses were determined by UPC^2 analysis on a Acquity Trefoil IC-3

column with a gradient (100% CO_2 to 60/40 CO_2/CH_3CN over 4 minutes, curve 6), flow rate 3 mL/min, λ = 219 nm; major diastereoisomer (66% ee): τ_{Major} = 3.62 min, τ_{Minor} = 3.50 min; minor diastereoisomer (61% ee): τ_{Major} = 3.94 min, τ_{Minor} = +3.85 min. $[\alpha]_D^{26}$= +8.6 (c = 0.34, $CHCl_3$, 1.5:1 dr, 66% ee_{Minor}, 61% ee_{major}). **^{1}H NMR**: (400 MHz, Chloroform-*d*) δ 7.99 – 7.86 (m, 2H *major* + 2H *minor*), 7.33 – 7.18 (m, 2H *major* + 2H *minor*), 3.90-3.85 (m, 1H *major* + 1H *minor*), 3.64 (dd, *J* = 11.6, 4.8 Hz, 1H *minor*), 3.54 – 3.34 (m, 2H *major*), 3.21 (qd, *J* = 7.2, 2.3 Hz, 1H *minor*), 2.53 (s, 1H *minor*), 2.25-2.15 (m, 1H *major* + 1H *minor*), 1.76 (dtd, *J* = 15.2, 7.6, 3.1 Hz, 2H *minor*), 1.72 – 1.49 (m, 3H *major*), 1.28 (d, *J* = 7.2 Hz, 3H *minor*), 1.22 (d, *J* = 7.1 Hz, 3H *major*), 0.95 (t, *J* = 7.4 Hz, 3H *major*), 0.89 (t, *J* = 7.4 Hz, 3H *minor*). **^{13}C NMR**: (101 MHz, Chloroform-*d*) δ 166.0 (d, *J* = 256.6 Hz, *minor*), 165.9 (d, *J* = 256.2 Hz, *major*), 134.7 (d, *J* = 3.2 Hz, *major*), 134.2 (d, *J* = 3.2 Hz, *minor*), 131.7 (d, *J* = 9.6 Hz, *minor*), 131.6 (d, *J* = 9.5 Hz, *major*), 116.7 (d, *J* = 22.6 Hz, *minor*), 116.6 (d, *J* = 22.6 Hz, *major*), 62.3 (*major*) , 62.1 (*minor*), 62.0 (*minor*), 60.1 (*major*), 41.9 (*minor*), 41.6 (*major*), 23.1 (*minor*), 19.4 (*major*), 12.4 (*major*), 12.1 (*minor*), 9.6 (*major*), 9.5 (*minor*). **^{1}H decoupled ^{19}F NMR:** (376 MHz, Chloroform-*d*) δ -104.40 (s, 1F*minor*), -103.95 (s, 1F*major*). **HRMS**: Calculated for $C_{12}H_{17}FNaO_3S$: 283.0775, found: 283.0777.

Characterization data adducts **20**

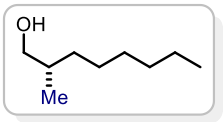

(*S*)-2-methyloctan-1-ol (20a). Prepared according to a reported procedure.[22] To a solution of (*S*)-2-((methylsulfonyl)methyl)hexan-1-ol (**28c**, 0.1 mmol, 28 mg, 85% *ee*) in dry methanol (2 mL) was added freshly activated magnesium (40 equiv) at 50 ºC. After 1.5 hours stirring, the reaction was quenched by adding an aqueous solution of HCl (0.1 M, 5 mL). The crude mixture was then transferred to a separatory funnel and extracted with dichloromethane (3 x 10 mL). The organic phases were combined and dried over magnesium sulfate before concentration *in vacuo*. The mixture was purified by flash column chromatography (hexane/ethyl acetate 8:2) to afford the product **20a** as colourless oil (13 mg, 86% yield). The enantiomeric excess was determined to be 85% by GC analysis on an Beta DEX column 120 (30m x 0.25mm, 0.25µm, isotherm 70 ºC, FID detector, carrier gas: He): τ_{Major} = 230.1 min, τ_{Minor} = 221.7 min. $[\alpha]_D^{25}$= -3.6 (c = 0.35, EtOH, 85% *ee*). An (*S*) absolute configuration was inferred by comparison of the optical rotation with the value reported in the literature ($[\alpha]_D^{25}$ = -9.8, c = 1.00, EtOH, 96% ee for (*S*)-**5c**).[24] The characterization of the compound matches with the data reported in the literature.[24]

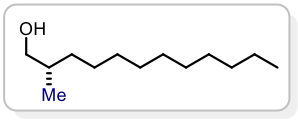

(*S*)-2-methyldodecan-1-ol (20b) Prepared according to a reported procedure.[22] To a solution of (*S*)-2-((phenylsulfonyl)methyl)dodecan-1-ol (**28d**) (0.05 mmol, 17 mg, 82% *ee*) in dry methanol (3 mL) was added freshly activated magnesium (40 equiv) at 50 ºC. After 2 hours stirring, the reaction was quenched by adding an aqueous solution of HCl (0.1 M, 5 mL). The crude mixture was then transferred to a separatory funnel and extracted with dichloromethane (3 x 10 mL). The organic phases were combined and dried over magnesium sulfate before concentration *in vacuo*. The mixture was purified by flash column chromatography (hexane/ethyl acetate 8:2) to afford the product **20b** as a colourless oil (8.3 mg, 83% yield, 82% *ee*). Although it was not possible to measure the *ee* of compound **20b**, the experiments conducted demonstrated that the reductive desulfonylation generally proceeds without eroding the enantiomeric purity of the alcohol precursor **28**. $[\alpha]_D^{25}$= -8.3 (c = 0.25, EtOH). An (*S*) absolute configuration was inferred by comparison of the optical rotation with the value reported in the literature ($[\alpha]_D^{25}$ = -10.0, c = 0.50, EtOH, 99% ee for (*S*)-**20b**).[50] The characterization of the compound matches with the data reported in the literature.[50]

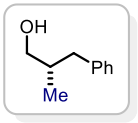

(*S*)-2-methyl-3-phenylpropan-1-ol (20c). Prepared according to a reported procedure.[22] To a solution of (*S*)-2-benzyl-3-(phenylsulfonyl)propan-1-ol (**28h**, 0.2 mmol, 58 mg, 76% *ee*) in dry methanol (4 mL) was added freshly activated magnesium (40 equiv) at 50 ºC. After 1.5 hours stirring, the reaction was quenched by adding an aqueous solution of HCl (0.1 M, 5 mL). The crude mixture was then transferred to a separatory funnel and extracted with dichloromethane (3 x 15 mL). The organic phases were combined and dried over magnesium sulfate before concentration *in vacuo*. The mixture was purified by flash column chromatography (hexane/ethyl acetate 8:2) to afford the product **20c** as a colourless oil (24 mg, 81% yield). The enantiomeric excess was determined to be 76% by UPC[2] analysis on a Acquity Trefoil CEL-1 column with a gradient (100% CO_2 to 60:40 CO_2/Methanol over 4 minutes, curve 6), flow rate 2 mL/min, λ = 208 nm: τ_{Major} = 2.53 min, τ_{Minor} = 2.59 min. $[\alpha]_D^{25}$= -2.8 (c = 0.5, $CHCl_3$, 76% *ee*). An (*S*) absolute configuration was inferred by comparison of the optical rotation with the value reported

[50] Wakabayashi, T.; Mori, K.; Kobayashi, S. *J.* "Total synthesis and structural elucidation of Khafrefungin" *J. Am. Chem. Soc.* **2001**, *123*, 1372.

in the literature ($[\alpha]_D^{25}$ = -3.0, c = 0.67, $CHCl_3$, 99% ee for (*S*)-**20c**).[51] The characterization of the compound matches with the data reported in the literature.[51]

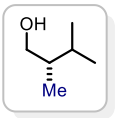

(*S*)-2,3-dimethylbutan-1-ol (20d). Prepared according to a reported procedure.[22] (*S*)-3-methyl-2-((phenylsulfonyl)methyl)butan-1-ol (**28e**, 0.15 mmol, 36 mg, 87% *ee*) was dissolved in a 10:1 solution of THF/H_2O (2.6 mL). The solution was thoroughly degassed via 3 cycles of freeze pump thaw, and the vessel was refilled with argon. Then, a solution of SmI_2 (0.1 M in THF, 8 mL, 6 equiv) was added at 25 ºC. After stirring for 3 hours, the reaction was quenched with saturated $NaHCO_3$ solution (10 mL) and extracted with cold diethyl ether (3 x 10 mL). The combined organic phase was washed with brine (15 mL) and dried over magnesium sulfate before concentration *in vacuo* at low temperature (5ºC). The yield of **20d** was determined by ^1H NMR spectroscopy to be 99%, in reference to 1,1,2-trichloroethylene (0.15 mmol, δ 6.5 (s, 1H)). The characterization of the compound matches with the data reported in the literature.[52] The compound cannot be isolated by by flash column chromatography due to its volatility.

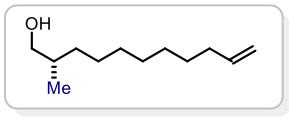

(*S*)-2-methylundec-10-en-1-ol (20e) Prepared according to a reported procedure.[22] To a solution of (*S*)-2-((phenylsulfonyl)methyl)undec-10-en-1-ol (**28g**) (0.2 mmol, 65 mg, 82% *ee*) in dry methanol (4 mL) was added freshly activated magnesium (40 equiv) at 50 ºC. After 1.5 hours stirring, the reaction was quenched by adding an aqueous solution of HCl (0.1 M, 5 mL). The crude mixture was then transferred to a separatory funnel and extracted with dichloromethane (3 x 15 mL). The organic phases were combined and dried over magnesium sulfate before concentration *in vacuo*. The mixture was purified by flash column chromatography (hexane/ethyl acetate 8:2) to afford the product **20e** as a colourless oil (33 mg, 91% yield, 82% *ee*). Although it was not possible to measure the *ee* of compound **20e**, the experiments conducted demonstrated that the reductive desulfonylation generally proceeds without eroding the enantiomeric purity of the alcohol precursor **28**. $[\alpha]_D^{25}$= -5.1 (c = 0.85, $CHCl_3$). An (*S*) absolute configuration was inferred by comparison of the

[51] Kita, Y.; Hida, S.; Higashihara, K.; Jena, H. S.; Higashida, K.; Mashima, K. "Chloride-bridged dinuclear rhodium(III) complexes bearing chiral diphosphine ligands: catalyst precursors for asymmetric hydrogenation of simple olefins" *Angew. Chem. Int. Ed.* **2016**, *55*, 8299.
[52] Gonzales, A. Z.; Roman, J. G.; Gonzales, E.; Martinez, J.; Medina, J. R.; Matos, K.; Soderquist, J. A. "9-borabicyclo[3.3.2]decanes and the asymmetric hydroboration of 1,1-disubstituted alkenes" *J. Am. Chem. Soc.* **2008**, *130*, 9218.

optical rotation with the value reported in the literature ($[\alpha]_D^{25}$ = +8.4, c = 0.85, $CHCl_3$, 99% ee for (*R*)-**20e**).[53] The characterization of the compound matches with the data reported in the literature.[53]

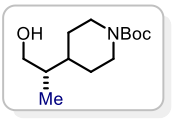

tert-butyl (*S*)-4-(1-hydroxypropan-2-yl)piperidine-1-carboxylate (20f) Prepared according to a reported procedure.[22] To a solution of *tert*-butyl (*S*)-4-(1-hydroxy-3-(phenylsulfonyl)propan-2-yl)piperidine-1-carboxylate (**28i**) (0.12 mmol, 46 mg, 80% *ee*) in dry methanol (3 mL) was added freshly activated magnesium (40 equiv) at 50 ºC. After 2 hours stirring, the reaction was quenched by adding water (10 mL). The crude mixture was then transferred to a separatory funnel and extracted with dichloromethane (3 x 15 mL). The organic phases were combined and dried over magnesium sulfate before concentration *in vacuo*. The mixture was purified by flash column chromatography (hexane/ethyl acetate 8:2) to afford the product **20i** as a colourless oil (25 mg, 86% yield, 80% *ee*). The enantiomeric excess was determined to be 80% by UPC^2 analysis on a AMY-1 column with a gradient (100% CO_2 to 60:40 CO_2/Isopropanol over 4 minutes, curve 6), flow rate 2 mL/min, λ = 215 nm: τ_{Major} = 3.71 min, τ_{Minor} = 3.65 min. $[\alpha]_D^{25}$= +1.50 (c = 0.25, $CHCl_3$, 80% *ee*).[54] The characterization of the compound matches with the data reported in the literature.[54]

Characterization data adducts **34**

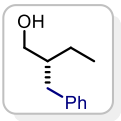

(*R*)-2-benzylbutan-1-ol (34a). Prepared according to a reported procedure.[22] ((2*S*)-2-(((4-fluorophenyl)sulfonyl)(phenyl)methyl)butan-1-ol (**31c**, 0.13 mmol, 41.2 mg, d.r.=3.2:1.0, 96% ee_M, 80% ee_m) was dissolved in a 10:1 solution of THF/H_2O (2.6 mL). The solution was thoroughly degassed via 3 cycles of freeze pump thaw, and the vessel was refilled with argon. Then, a solution of SmI_2 (0.1 M in THF, 8 mL, 6 equiv) was added at 25 ºC. After stirring for 3 hours, the reaction was quenched with saturated $NaHCO_3$ solution (10 mL) and extracted with ethyl acetate (3 x 10 mL). The combined organic phase was washed with brine (15 mL) and dried over magnesium sulfate before concentration *in vacuo*. The

[53] Kovalenko, V. N.; Mineeva, I. V. "Cyclopropane intermediates in the synthesis of chiral alcohols with methyl-branched carbon skeleton. Application in the synthesis of insect pheromones" *Russian Journal of Organic Chemistry* **2014**, *50*, 934.
[54] Sato, K.; Sugimoto, H.; Rikimaru, K.; Imoto, H.; Kamaura, M.; Negoro, N.; Tsujihata, Y.; Miyashita, H., Odani, T.; Murata T. "Discovery of a novel series of indoline carbamate and indolinylpyrimidine derivatives as potent GPR119 agonists" *Bioorganic & Medicinal Chemistry* **2014**, *22*, 1649.

crude mixture was purified by flash column chromatography (hexane/ethyl acetate 8:2) to afford the benzylated product **34a** as colourless oil (20 mg, 88% yield). The enantiomeric excess was determined to be 93% by by UPC^2 analysis on a Acquity Trefoil CEL-1 column with a gradient (100% CO_2 to 60:40 CO_2/Isopropanol over 4 minutes, curve 6), flow rate 2 mL/min, λ = 220 nm: τ_{Major} = 3.14 min, τ_{Minor} = 3.03 min. $[\alpha]_D^{25}$= -6.02 (c = 0.50, $CHCl_3$, 93% *ee*). An (*R*) absolute configuration was inferred by comparison of the optical rotation with the value reported in the literature (Lit. $[\alpha]^{25}_D$ = +6.2 (c = 24, $CHCl_3$, 95% *ee* for (*S*)-compound).[55] The characterization of the compound matches with the data reported in the literature.[55]

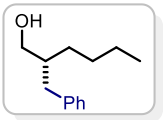

(*R*)-2-benzylhexan-1-ol (34b). Prepared according to a reported procedure.[22] (2*S*)-2-(((4-fluorophenyl)sulfonyl)(phenyl)methyl)hexan-1-ol (**31e**, 0.05 mmol, 17 mg, d.r.= 3.1:1.0, 97% ee_M, 88% ee_m) was dissolved in a 10:1 solution of THF/H_2O (1.5 mL). The solution was thoroughly degassed via 3 cycles of freeze pump thaw, and the vessel was refilled with argon. Then, a solution of SmI_2 (0.1 M in THF, 4 mL, 6 equiv) was added at 25 ºC. After stirring for 3 hours, the reaction was quenched with saturated $NaHCO_3$ solution (5 mL) and extracted with ethyl acetate (3 x 10 mL). The combined organic phase was washed with brine (5 mL) and dried over magnesium sulfate before concentration *in vacuo*. The crude mixture was purified by flash column chromatography (hexane/ethyl acetate 8:2) to afford the benzylated product **34b** as colourless oil (8.5 mg, 87% yield). The enantiomeric excess was determined to be 94% by by UPC^2 analysis on a Acquity Trefoil CEL-1 column with a gradient (100% CO_2 to 60:40 CO_2/Ethanol over 4 minutes, curve 6), flow rate 2 mL/min, λ = 213 nm: τ_{Major} = 2.87 min, τ_{Minor} = 2.73 min. $[\alpha]_D^{25}$= +3.5 (c = 0.25, CH_2Cl_2, 94% *ee*). An (*R*) absolute configuration was inferred by comparison of the optical rotation with the value reported in the literature (Lit. $[\alpha]^{25}_D$ = -4.0 (c = 0.5, CH_2Cl_2, 90% *ee* for (*S*)-compound).[56] The characterization of the compound matches with the data reported in the literature.[56]

[55] Landa, A.; Maestro, M.; Masdeu, C.; Puente, A.; Vera, S.; Oiarbide, M.; Palomo C. "Highly enantioselective conjugate additions of aldehydes to vinyl sulfones" *Chem. Eur. J.* **2009**, *15*,1562.
[56] Hodgson, D. M.; Kaka, N. S. "Asymmetric synthesis of α-alkylated aldehydes using terminal epoxide-derived chiral enamines" *Angew. Chem. Int. Ed.* **2008**, *47*, 9958.

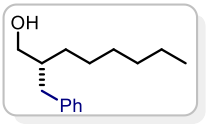

(*R*)-2-benzyloctan-1-ol (34c). Prepared according to a reported procedure.[22] (2*S*)-2-(((4-fluorophenyl)sulfonyl)(phenyl)methyl) octan-1-ol (**31f**, 0.050 mmol, 19 mg, d.r.= 3.2:1.0, 95% ee_M, 86% ee_m) was dissolved in a 10:1 solution of THF/H_2O (1.5 mL). The solution was thoroughly degassed via 3 cycles of freeze pump thaw, and the vessel was refilled with argon. Then, a solution of SmI_2 (0.1 M in THF, 4 mL, 6 equiv) was added at 25 ºC. After stirring for 3 hours, the reaction was quenched with saturated $NaHCO_3$ solution (5 mL) and extracted with ethyl acetate (3 x 10 mL). The combined organic phase was washed with brine (5 mL) and dried over magnesium sulfate before concentration *in vacuo*. The crude mixture was purified by flash column chromatography (hexane/ethyl acetate 8:2) to afford the benzylated product **34c** as colourless oil (9.2 mg, 80% yield). The enantiomeric excess was determined to be 93% by by UPC^2 analysis on a Acquity Trefoil CEL-1 column with a gradient (100% CO_2 to 60:40 CO_2/Isopropanol over 4 minutes, curve 6), flow rate 2 mL/min, λ = 215 nm: τ_{Major} = 3.45 min, τ_{Minor} = 3.23 min. $[\alpha]_D^{25}$= +1.5 (c = 0.25, $CHCl_3$, 93% *ee*). An (*R*) absolute configuration was inferred by comparison of the optical rotation with the value reported in the literature (Lit. $[\alpha]^{25}_D$ = -0.076 (c = 0.15, $CHCl_3$, 95% *ee* for (*S*)-compound).[57] The characterization of the compound matches with the data reported in the literature.[57]

[57] Bartoli, G.; Bellucci, M. C.; Bosco, M.; Dalpozzo, R.; De Nino, A.; Sambri, L.; Tagarelli "Mechanism and extensibility of the reaction" Eur. *J. Org. Chem.* **2000**, 99.

4.15.6. Determination of the Absolute Configuration

The stereochemical outcome of the photochemical alkylation of aldehydes (**1**) with α-iodo-sulfone derivatives has been established by cleaving the sulfone moiety of compounds **28c, 28g, 28h**, **31c** and **31e** under reductive conditions, as shown in Figure 4.35a-b (note that the (*S*)-enantiomer of the aminocatalyst **A** was used in the photochemical alkylations).

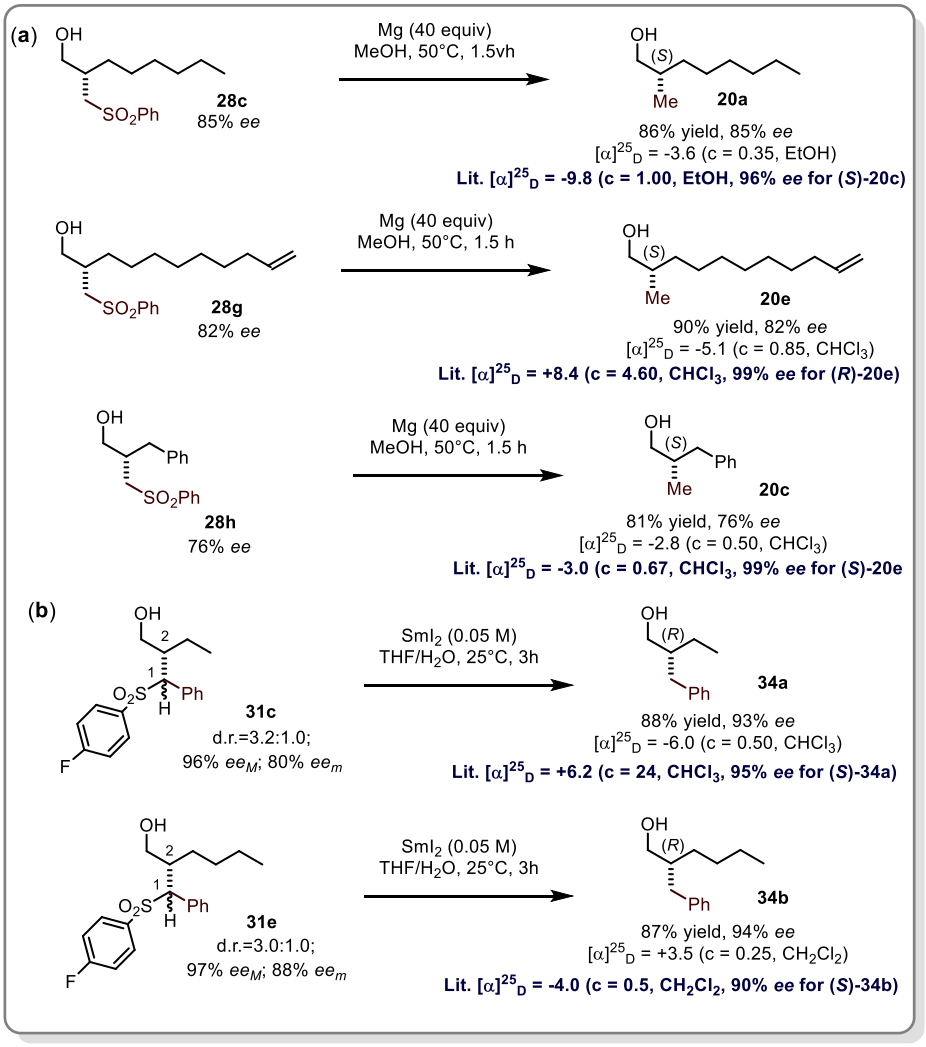

Figure 4.35 Establishing the stereochemical outcome of the photochemical asymmetric catalytic alkylation of aldehydes with α-iodo sulfones.

4.15.7. Cyclic Voltammetry

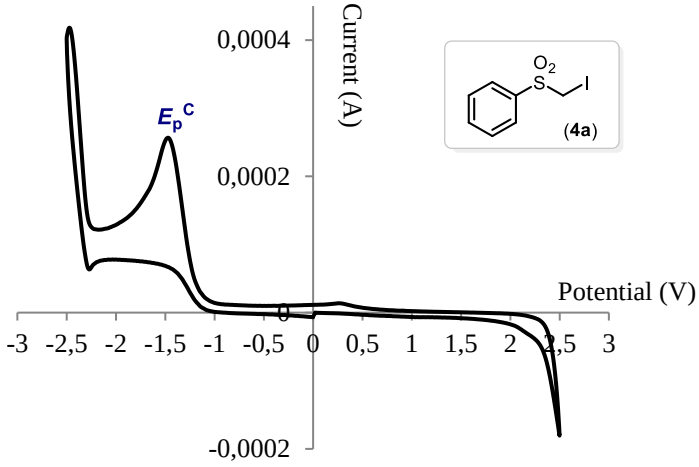

Figure 4.36 Cyclic voltammogram of **4a** [0.01 M] in [0.1 M] $TBAPF_6$ in CH_3CN. Sweep rate: 100 mV/s. Graphite electrode working electrode, Ag/AgCl (KCl saturated) reference electrode, Pt wire auxiliary electrode. Irreversible reduction. $E_p^C = E_{red}$ (**4a**/**4a**$^{\bullet-}$) = -1.49 V; E_p^C is the cathodic peak potential, while E_{red} value describes the electrochemical properties of **4a**.

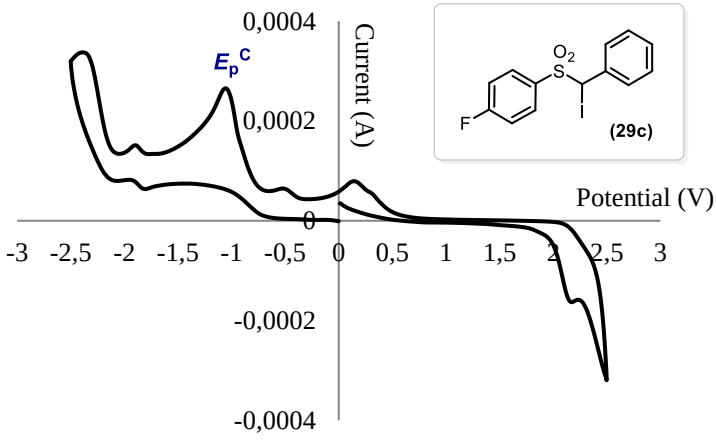

Figure 4.37 Cyclic voltammogram of **29c** [0.01 M] in [0.1 M] $TBAPF_6$ in CH_3CN. Sweep rate: 100 mV/s. Graphite electrode working electrode, Ag/AgCl (KCl saturated) reference electrode, Pt wire auxiliary electrode. Irreversible reduction. $E_p^C = E_{red}$ (**29c**/**29c**$^{\bullet-}$) = -1.02 V; E_p^C is the cathodic peak potential, while E_{red} value describes the electrochemical properties of **29c**.

4.15.8. Estimating the Redox Properties of the α-Amino Radical Intermediates

Compound **XII** was synthesized by Dr Ana Bahamonde from pyrrolidine, perchloric acid and isobutyraldehyde according to a reported procedure.[58] The pyrrolidine perchlorate salt was prepared by adding 3 mmol of pyrrolidine (0.025 mL) to a solution of 3 mmol of perchloric acid (0.026 mL of a 70% solution) in 1 mL of ether. A slightly yellow precipitate formed, which was filtered and washed with dry ether. The pyrrolidinium perchlorate salt was used for the following step without further purification. Pyrrolidinium perchlorate (0.23 mmol, 40 mg) was suspended in 2 mL of dry ether and freshly distilled *iso*butryladehyde (1 mmol, 0.91 mL) was added. After the addition, the precipitate dissolved while the slow precipitation of a white solid was observed. The reaction was stirred overnight at room temperature. The precipitate was washed with dry hexane (10 mL) under argon and then dried using high vacuum pump. The iminium ion **XII** was obtained in a 23% yield (12 mg) as a white solid. **^{1}H NMR** (400 MHz, CD_3CN): δ 8.16 (d, *J* = 9.2 Hz, 1H), 4.07 (t, *J* = 7.0 Hz, 2H), 3.94 (t, *J* = 7.0 Hz, 2H), 2.93 (dh, *J* = 9.2, 6.6 Hz, 1H), 2.13 (m, 4H), 1.24 (d, *J* = 6.6 Hz, 6H). **^{13}C NMR** (101 MHz, CD_3CN) δ 180.90, 58.62, 52.25, 32.33, 23.98, 23.63, 17.10.

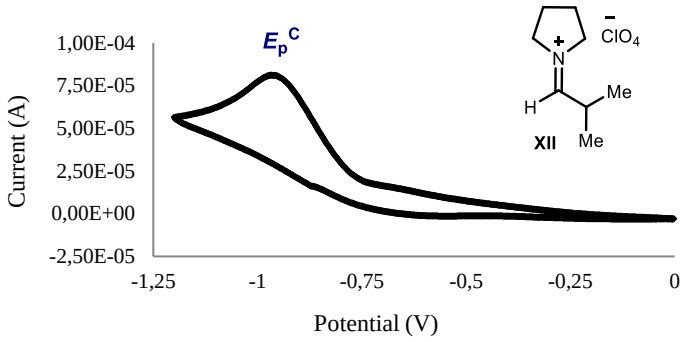

Figure 4.38 Cyclic voltammogram of the iminium ion **XII** [0.02 M] in [0.1 M] $TBAPF_6$ in CH_3CN. Sweep rate: 10 mV/s. Pt electrode working electrode, Ag/AgCl (NaCl saturated) reference electrode, Pt wire auxiliary electrode. Irreversible reduction. $E_p^C = E_{red}$ (**XII**/**XIII**) = -0.95 V; E_p^C is the cathodic peak potential, while E_{red} value describes the electrochemical properties of **XII**.

[58] Leonard, N. J.; Paukstelis, J. V. "Direct Synthesis of Ternary Iminium Salts by Combination of Aldehydes or Ketones with Secondary Amine Salts" *J. Org. Chem.* **1963**, *28*, 3021.

Dr Ana Bahamonde measured by cyclic voltammetry a reduction potential (E_p^{red} of **XII**) of -0.95 V *vs* Ag/Ag^+ in CH_3CN (irreversible reduction to give the α-aminoalkyl radical **XIII**, see Figure 4.39).[3b]

4.15.9. Quantum Yield Measurement

The quantum yield measurement of the model reaction, depicted in Table 1 of the main manuscript, was performed in acetonitrile, where the reaction mixture is completely soluble. This choice was motivated by the need to avoid the presence of biphasic solvent systems with water, in order to elude any scattering of the irradiating light which would preclude a reliable measurement. A ferrioxalate actinometer solution was prepared following the Hammond variation of the Hatchard and Parker procedure outlined in the *Handbook of Photochemistry*.[59] The ferrioxalate actinometer solution measures the decomposition of ferric ions to ferrous ions, which are complexed by 1,10-phenanthroline and monitored by UV/Vis absorbance at 510 nm. The moles of iron-phenanthroline complex formed are related to moles of photons absorbed.

The following solutions were prepared and stored in a dark laboratory (red light):

1. Potassium ferrioxalate solution: 294.8 mg of potassium ferrioxalate (commercially available from Alfa Aesar) and 139 μL of sulfuric acid (96%) were added to a 50 mL volumetric flask, and filled to the mark with water (HPLC grade).
2. Phenanthroline solution: 0.2% by weight of 1,10-phenanthroline in water (100 mg in 50 mL volumetric flask).
3. Buffer solution: 2.47 g of NaOAc and 0.5 mL of sulfuric acid (96%) were added to a 50 mL volumetric flask, and filled to the mark with water (HPLC grade).
4. Model reaction solution: α-iodo sulfone **4a** (0.4 mmol), butanal **1a** (1.2 mmol), amine catalyst **A** (0.08 mmol) and 2,6-lutidine (0.4 mmol) were dissolved in acetonitrile (1 mL).

[59] Murov, S. "Handbook of photochemistry" Marcel Dekker, New York, **1973**.

The actinometry and the model reaction solution measurements were done as follows:

1. 1 mL of the actinometer solution was added to a Schlenk tubes (*diameter* = 12 mm). The Schlenk tube was placed 10 cm away from the light source. It was irradiated with a 300 W Xenon Lamp operating at 100% of light intensity with a high transmittance bandpass filter of 400 ± 5 nm without stirring. This procedure was repeated 4 times, quenching the reaction after different time intervals: 45 sec, 60 sec, 75 sec and 90 sec.
2. After irradiation, the actinometer solution was removed and placed in a 10 mL volumetric flask containing 0.5 mL of 1,10-phenanthroline solution and 2 mL of buffer solution. This flask was filled to the mark with water (HPLC grade).
3. The UV-Vis spectra of the complexed actinometer samples were recorded for each time interval. The absorbance of the complexed actinometer solution was monitored at 510 nm.
4. 1 mL of the model reaction (α -alkylation of **1a** with **4a** catalyzed by amine **A**) was added to a Schlenk tubes (diameter = 12 mm). The Schlenk tube was placed 10 cm away from the light source. It was irradiated with a 300 W Xenon Lamp operating at 100% of light intensity with a high transmittance bandpass filter of 400 ± 5 nm without stirring. This procedure was repeated 4 times, quenching the reaction after different time intervals: 7.5 min, 15 min, 30 min and 60 min.

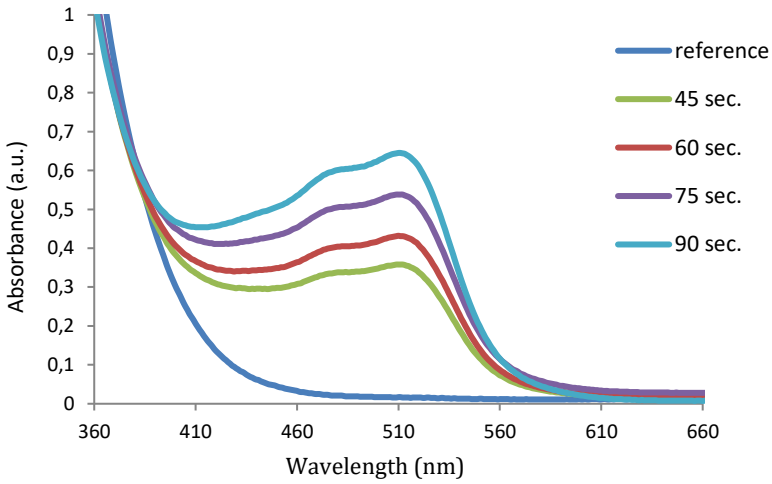

The moles of Fe^{2+} formed for each sample is determined using Beers' Law (Eq. S1):

$$\text{Mols of Fe(II)} = \frac{V_1 \times V_3 \times \Delta A(510\text{ nm})}{10^3 \times V_2 \times l \times \varepsilon(510\ nm)} \text{ (Eq. S1)}$$

where V_1 is the irradiated volume (1 mL), V_2 is the aliquot of the irradiated solution taken for the determination of the ferrous ions (1 mL), V_3 is the final volume after complexation with phenanthroline (10 mL), l is the optical path-length of the irradiation cell (1 cm), ΔA(510 nm) is the optical difference in absorbance between the irradiated solution and the one stored in the dark, ε(510 nm) is the extinction coefficient the complex $Fe(phen)_3^{2+}$ at 510 nm (11100 L mol^{-1} cm^1).The moles of Fe^{2+} formed (x) are plotted as a function of time (t). The slope of this line was correlated to the moles of incident photons by unit of time ($q^0_{n,p}$) by the use of the following Equation S2:

$$\Phi(\lambda) = \frac{dx/dt}{q^0_{n,p}\left[1-10^{-A(\lambda)}\right]} \quad \text{(Eq. S2)}$$

where dx/dt is the rate of change of a measurable quantity (spectral or any other property), the quantum yield (Φ) for Fe^{2+} at 400 nm is 1.13 (*53*), $[1\text{-}10^{-A(\lambda)}]$ is the ratio of absorbed photons by the solution, and $A(\lambda)$ is the absorbance of the actinometer at the wavelength used to carry out the experiments (400 nm). The absorbance at 400 nm $A(400)$ was measured using a Shimadzu 2401PC UV-Vis spectrophotometer in a 10 mm path quartz cuvette, obtaining an absorbance of 2.819.

$q^0_{n,p}$, which is the photon flux, was determined to be 5.32×10^{-9} einstein s^{-1}.

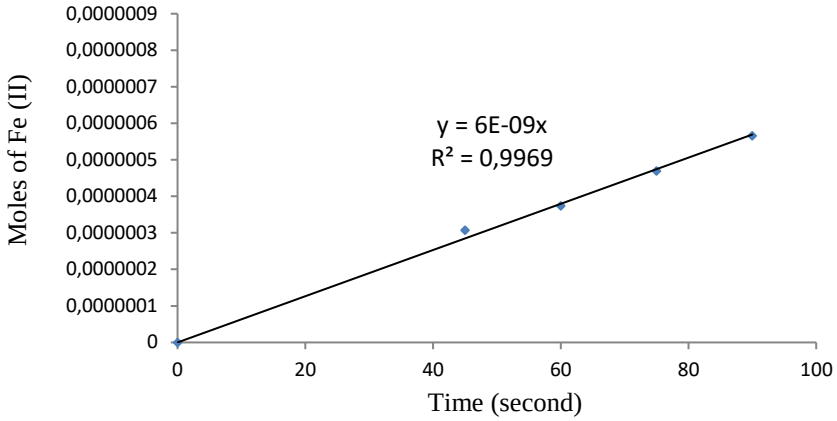

The moles of product **5a** formed for the model reaction were determined by GC measurement using trichloroethylene as internal standard.

The moles of product per unit of time are related to the number of photons absorbed. The photons absorbed are correlated to the number of incident photons by the use of Equation S2. According to this, when plotting the moles of product (x) versus the moles of incident photons ($q^0_{n,p}\cdot dt$), the slope is equal to: $\mathbf{\Phi\cdot(1-10^{-A(400\ nm)})}$, where Φ is the quantum yield to be determined and *A*(400 nm) is the absorption of the reaction under study.

A(400 nm) was measured using a Shimadzu 2401PC UV-Vis spectrophotometer in 10 mm path quartz. An absorbance of 0.86 was determined for the model reaction mixture.

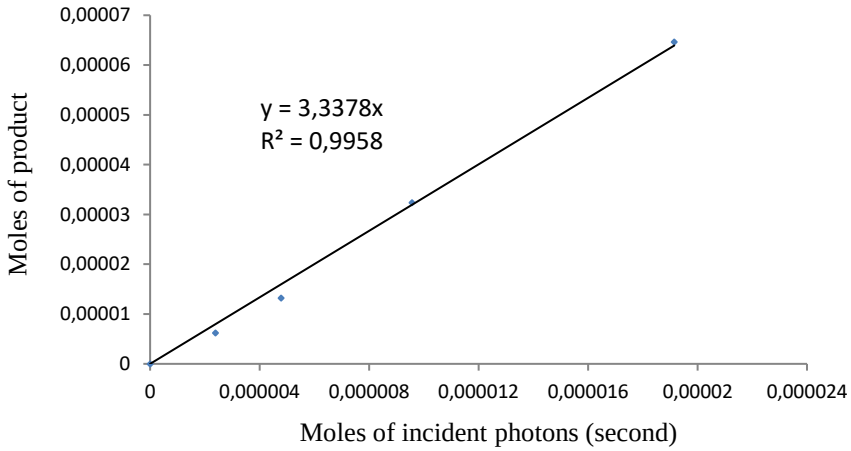

The quantum yield (Φ) of the photochemical alkylation of butanal **1a** with α-iodo sulfone **4a** catalyzed by **A** was calculated to be **3.9**.

UNIVERSITAT ROVIRA I VIRGILI
DEVELOPMENT OF RADICAL PROCESSES TRIGGERED BY THE PHOTOCHEMICAL ACTIVITY OF TRANSIENT ORGANIC INTERMEDIATES
Giacomo Filippini

UNIVERSITAT ROVIRA I VIRGILI
DEVELOPMENT OF RADICAL PROCESSES TRIGGERED BY THE PHOTOCHEMICAL ACTIVITY OF TRANSIENT ORGANIC INTERMEDIATES
Giacomo Filippini